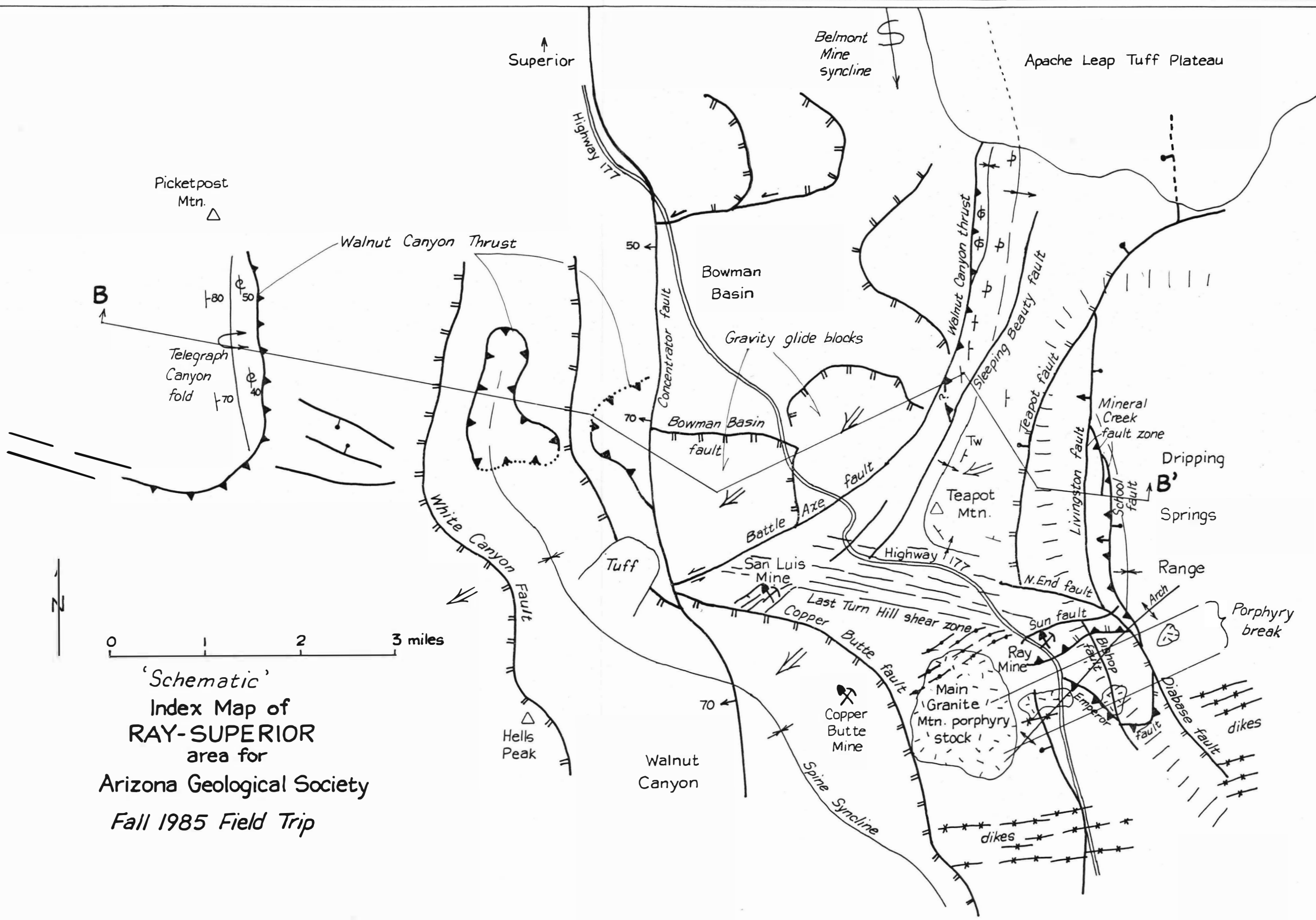


LARAMIDE, GALIURO, AND SAN ANDREAS OROGENIES
RAY-SUPERIOR AREA, PINAL COUNTY, ARIZONA

by
Stanley B. Keith



ARIZONA GEOLOGICAL SOCIETY
1985 FALL FIELD TRIP



'Schematic'
 Index Map of
RAY-SUPERIOR
 area for
 Arizona Geological Society
Fall 1985 Field Trip



LARAMIDE, GALIURO, AND SAN ANDREAS OROGENIES
RAY-SUPERIOR AREA, PINAL COUNTY, ARIZONA

by
Stanley B. Keith



ARIZONA GEOLOGICAL SOCIETY
1985 FALL FIELD TRIP

Table of Contents

	Page
INTRODUCTION.....	1
ROCKS.....	2
Quaternary Geomorphic Units.....	3
Quaternary Rock Units.....	3
Rocks of the San Andreas Orogeny.....	5
Rocks of the Galiuro Orogeny.....	5
Rocks of the Laramide Orogeny.....	12
Paleozoic Rocks.....	20
Younger Precambrian Rocks.....	25
Older Precambrian Rocks.....	30
Explanation of Structures.....	36
STRUCTURAL GEOLOGY.....	41
STRUCTURES OF THE SAN ANDREAS OROGENY.....	41
High-Angle Normal Faults.....	41
Concentrator Fault.....	41
Livingston Fault.....	42
Diabase Fault.....	42
Bishop Fault.....	43
Folds.....	43
Northeast-Southwest Trending Folds.....	43
Regional Significance.....	43
STRUCTURES OF THE GALIURO OROGENY.....	44
Low-Angle Normal Faults.....	44
Copper Butte Fault.....	44
White Canyon Fault.....	45
Bowman Basin Fault System.....	45
Emperor Fault.....	45
Teapot Mountain Fault.....	46
Sleeping Beauty Fault.....	47
Reverse Faults.....	48
Mineral Creek Fault Zone.....	48
Sun Fault.....	48
Reverse Movement on Normal Faults.....	49
Folds.....	50
Spine Syncline.....	50
School Fold.....	50
Texas Zone Structures.....	50
Last Turn Hill Shear Zone.....	50
General Description.....	50
Galiuro-age Movement.....	51
Regional Significance.....	52

STRUCTURES OF THE LATE LARAMIDE OROGENY.....	52
West- to Southwest-Directed Reverse Faults.....	52
Sleeping Beauty Fault.....	52
Southwest-Directed Folds.....	53
Belmont Mine Fold.....	53
STRUCTURES OF THE MID-LARAMIDE OROGENY.....	53
Intrusions and Mineralization.....	53
Dike Swarms.....	53
Porphyry Break.....	54
Ray Porphyry Copper Deposit.....	54
High-Angle Strike-Slip Faults.....	55
Last Turn Hill Shear Zone.....	55
STRUCTURES OF THE EARLY LARAMIDE OROGENY.....	55
Low-Angle Thrust Faulting.....	55
Walnut Canyon Thrust.....	55
Emperor Thrust Fault.....	57
Folds.....	57
Telegraph Canyon Fold.....	57
Drag Folds on the Walnut Canyon Thrust.....	58
SUMMARY OF LARAMIDE, GALIURO, AND SAN ANDREAS OROGENIES IN THE RAY-SUPERIOR REGION.....	58
References.....	61
Appendices.....	65

List of Figures

	Page
Figure 1 Tentative Correlation of Tertiary Rocks, Superior to Aravaipa Canyon, Arizona.....	6
Figure 2 Schematic Correlation of Late Cretaceous, Early Tertiary Intrusives, Ash Creek to Superior, Arizona.....	13
Figure 3 Schematic Correlation of Precambrian, Paleozoic, and Mesozoic Rocks, Ash Creek to Superior, Arizona.....	21
Figure 4 Correlation of Older Precambrian Rocks, Ash Creek to Superior, Arizona.....	32

List of Tables

	Page
Table 1 Chronology of Late Cretaceous-Early Tertiary Igneous Rocks from Saddle Mountain to Ray.....	14
Table 2 Age Data for Madera Diorite.....	33

List of Appendices

Appendix I	Historical Notes and Discussion
Appendix II	"The Ray Ore Body" by Donald S. Fountain
Appendix III	"Hydrothermal Alteration, Mineralization, and Zoning in the Ray Mine Deposit" by C.H. Phillips, et al
Appendix IV	"Late Cretaceous and Cenozoic Orogenesis of Arizona and Adjacent Regions: A Stratotectonic Approach" by S.B. Keith and J.C.Wilt

INTRODUCTION

The Ray-Superior area contains some of the most complicated supracrustal geology in southeast Arizona. The geology and metallogeny is interpreted here as the product of three major orogenies that affected the Ray-Superior region from Late Cretaceous (circa 85 Ma) through Tertiary time (to circa 5 Ma). Stratigraphy and structural geology related to each orogeny is excellent, and although the geology is abundantly complex, a generally coherent story is decipherable.

This communication will summarize the overall geology of the region and place particular emphasis on the Late Cretaceous rocks, structures, and mineral deposits that are attributed to the Laramide, Galiuro, and San Andreas orogenies. For an overview of the definition and characteristics of each orogeny, see Keith and Wilt (1985; reproduced at the back of this guidebook).

Most of the geological discussion is based on geologic mapping in the Ray-Superior area done by S.B. Keith in 1976 for Kennecott Copper Corporation. Portions of the maps are reproduced for critical pieces of the geologic puzzle that we will visit during this field trip. Also, the maps and accompanying text are available from the Arizona Bureau of Geology as open-file report 83-14.

Note: The 1974 Phillips, Gambel, Fountain article "hydrothermal Alteration, Mineralization, and Zoning in the Ray Deposit" is reprinted with permission from the Society of Economic Geologists."

ROCKS

Rock units on the accompanying maps for this guidebook are summarized below. Additional comments on the regional context, and significance of the San Andreas, Galiuro, and Laramide orogenic periods are also provided.

DESCRIPTION OF ROCK UNITS

<u>Map Symbol</u>	<u>Description of Map Unit</u>
QUATERNARY GEOMORPHIC UNITS*	
Qs	Geomorphic surface--low relief, low gradient surfaces which may be erosionally cut on beveled bedrock (pediments) and beveled, non-indurated, valley fill alluviums or, represent depositional heights of alluvial valley fills. Age determined by height (oldest = highest) above present-day stream channels. Surfaces of slope $<5^{\circ}$ were mapped as Qs.
Qc	Colluvium or hillwash overlying bedrock in hillslopes. Locally continuous with Qs. Surfaces of slope $>5^{\circ}$ but $<12^{\circ}$ were mapped as Qc.
Qtl	Talus or debris material resting on steeper slopes $>12^{\circ}$. Locally continuous with Qc.
Qld	Landslide deposits containing boulders consistently larger than 5 x 5 x 5' were mapped as Qld regardless of slope angle.
Qm	Landslide deposits which contain structurally coherent blocks of bedrock. That is, the blocks within the slide have not been internally rotated with respect to each other, and the original preslide lithology can be mapped within the slide at the map scale. The preslide lithologies are designated by the appropriate letter symbols enclosed by parentheses, e.g., (Me).
QUATERNARY ROCK UNITS	
Qd	Mine dumps and tailings; road fill.
Qs ₅	Modern alluviums (Holocene) within present-day stream channels; younger than 10,000 years.
Qs ₄	Floodplain surface cut on alluviums adjacent to modern stream channels 2 to 10 feet above present-day stream base levels. Does not contain red soils.

*All Quaternary geomorphic units are tentatively considered younger than the upper Saint Davids formation in the upper San Pedro Valley. The upper Saint David formation at Curtis Range has a magnetostratigraphy which probably contains Brunhes-Matuyama boundary dated at 0.69 m. y. (Johnson, et al., 1975). If so, alluviums deposited during and after Qs₁ time are younger than about 600,000 years.

- Qs₃ Surface 15 to 18 feet above present-day stream base levels. Present along or at confluences of major streams. Red soils, if present, are poorly developed compared to those on Qs₁ and Qs₂ surfaces. On streams with greater than ~2° gradients, "boulder terraces and levys" were mapped as Qs₃.
- Qw Winkleman formation (10 to 100 feet). Gravels which underlie Qs₃ surface but are younger than gravels related to Qs₂. Formation named for exposures in Highway 77 roadcuts along north side of Gila River at Winkleman, Arizona. Generally an unconsolidated coarse gravel containing well-rounded pebbles, cobbles, and boulders of older rocks; contains fine-grained light yellow lenses of silty material locally.
- Qc₃ Colluvium graded to Qs₃ surface. Mapped in the Saddle Mountain area of Winkleman 7½ minute quadrangle and Teapot Mountain area of Teapot 7½ minute quadrangle.
- Qtl₃ Talus graded to Qc₃ and Qs₃ surface. Deposits overlie Qtl₂ and are distinguished by lack of soil development. Fine-grained material between rock fragments has been washed away. May represent debris flows.
- Qs₂ Widespread surface 15 to 80 feet above present-day stream base levels. Contains well-developed red soils. A mature soil exposure in a haulage roadcut 1 mile north of the Ray mine has 2 feet of dense red clay at the B2T horizon and 2 to 3 feet of calcareous C horizon.
- Qc₂ Colluvium graded to Qs₂ surface.
- Qlt₂ Talus graded to Qc₂ and Qs₂.
- Qm₂ Megabreccia masses stratigraphically related to Qs₂ surfaces.
- Qld₂ Landslides graded to Qs₂ surface.

- Qtr Travertine. Especially well developed along Highway 177 near Walnut Spring in the Teapot Mountain quadrangle.
- Qs₁ Surface 100 to 250 feet above present-day stream base levels; contains well-developed red soils. Generally on alluvial facies of Quiburis formation; questionably cut on alluviums of Sacaton age. In the Tortilla Mountains veneer, gravels of possible Sacaton age rest on an extensive pediment surface cut on Oracle quartz monzonite. This pediment surface is believed equivalent to the Rillito pediment surface in the Tucson area defined by Pashley (1966). Qs₁ and Qs₂ surfaces merge downward with the pediment surfaces in the upper reaches of streams in the Tortilla Mountains. The pediment surface is therefore inferred to be older than Qs₁ and Qs₂. Qs₁ is poorly preserved in the valley fill areas and more common in pedimented bedrock areas.
- Qm₁ Megabreccia graded to Qs₁ surface. The megabreccias north of Ray in White Canyon north of Hells Peak and south of Walnut Gap are inferred to be related to Qs₁ base levels.
- MID TO LATE MIOCENE ROCKS
(ROCKS OF THE SAN ANDREAS OROGENY)
- Trt Bedded rhyolitic tuff (50-100 feet) which overlies Qtb and contains fragments of Qtb in the northcentral Teapot Mountain quadrangle.
- Tby Aphanitic dense basalt (300 feet ±) possibly basaltic andesite which overlies Big Dome-equivalent gravels in the northcentral Teapot Mountain quadrangle.
- Tbyi Aphanitic dense basalt which intrudes a normal fault in the Wood Canyon area of Teapot Mountain quadrangle.
- MID-MIOCENE TO OLIGOCENE ROCKS
(ROCKS OF THE GALIURO OROGENY)
Miocene Conglomerates
- Tbd Big Dome formation (2,000 feet ±). Alluvial deposits named by Krieger, et al. (1973) for exposures at Big Dome, Sonora quadrangle. Biotite and hornblende from a quartz latite ash flow tuff below the middle of the formation gave ages of 14 and 17 m. y., respectively (Banks, et al. 1972). Big Dome equivalents are considered to be conglomerate in the Superior area, Apsay conglomerate (Krieger, 1968a, 1968b) in the Galiuro Mountains, and Hellhole conglomerate in the Klondyke quadrangle (Simmons, 1964).

*See Figure 1 for northwest-southeast distribution and correlation of Tertiary rocks.

Tentative Correlation of Tertiary Rocks,
 Superior to Aravaipa Canyon, Arizona

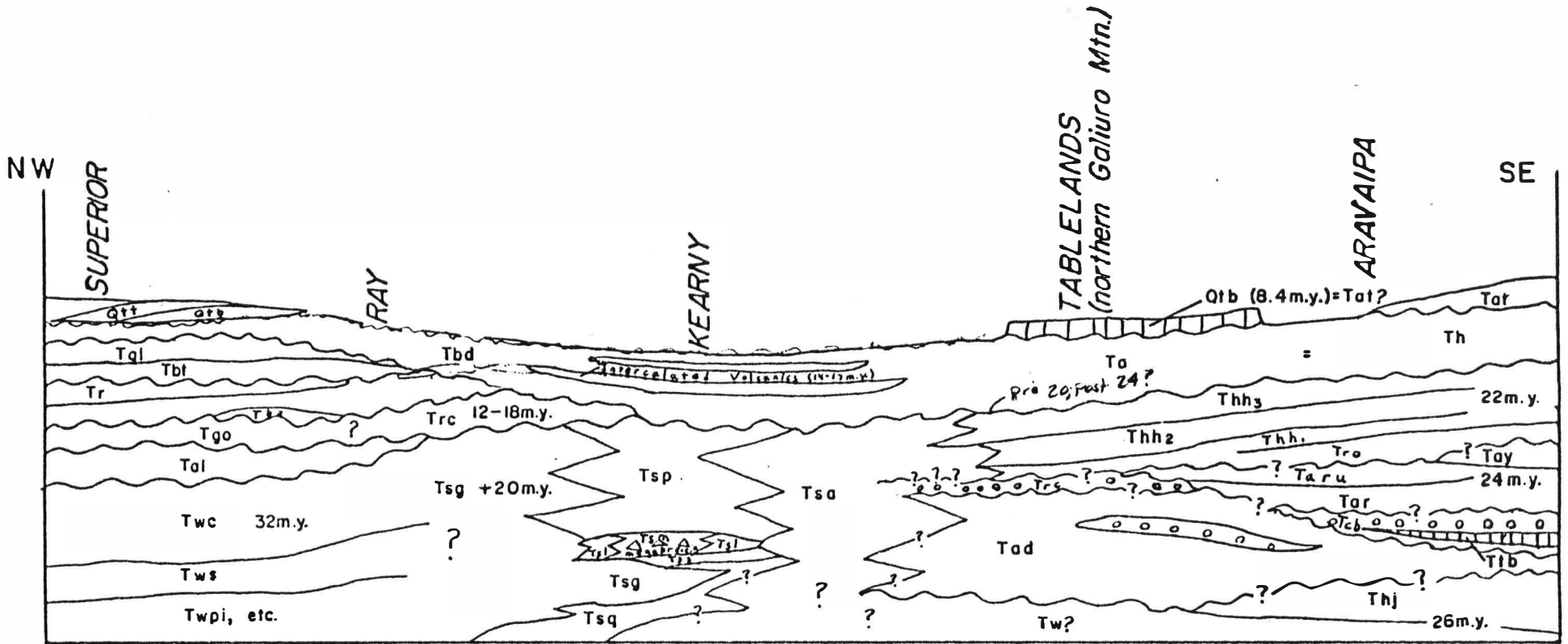


Fig. 1

- Tbdc Big Dome formation; mixed conglomerate facies (500-1,000 feet).
- Tbdql Quartz latite ash flow tuff (0-40 feet) embedded in Big Dome formation near Kearny, Arizona. The 14 and 17 m. y. ages are from this flow (see Cornwall and Krieger, 1975a).
- Tbdlt Thinly laminated to massive rhyolite lapilli tuff (0-40 feet) contains abundant pumice shards (see Cornwall and Krieger, 1975a).
- Tbdl Big Dome formation; limestone conglomerate (1,000 feet \pm); see Cornwall and Krieger (1975a).
- Tbds Big Dome formation; sandstone and conglomerate (1,000 feet \pm); see Cornwall and Krieger (1975a).
- Tbdwc Big Dome formation. Conglomerate containing clasts of Williamson Canyon volcanics (1,000 feet \pm) present along southwest margin of Dripping Spring Mountains in Hayden quadrangle.
- Tbdpi Big Dome formation; Pinal schist bearing conglomerate (400 feet \pm).

Picketpost Mountain Volcanics

An extensive sequence of dominantly rhyolitic volcanic rocks unconformably underlie the Miocene conglomerates and overlie older conglomerates and Apache Leap tuff northwest of Ray and southwest of Superior. These rocks are named the Picketpost Mountain volcanics for a thick section exposed at Picketpost Mountain 4 miles west-southwest of Superior, Arizona. Creasey (1975) has mapped many of these units in the Teapot Mountain 7 $\frac{1}{2}$ minute quadrangle.

- Tql Quartz latite flows showing basal vitrophyre as a cross-hatched band (250 feet \pm).
- Tqli Intrusive quartz latite (intrusive equivalent of quartz latite flows).
- Trd Rhyodacite porphyry. Medium to medium coarse-grained biotite rhyodacite porphyry contains biotite, resorbed quartz, and plagioclase within a light pink groundmass. Forms a prominent north- to northwest-trending dike south of Telegraph Canyon in the Mineral Mountain

- quadrangle. Intrudes Tri. Phenocrysts are 40% of rock. Equals coarse-grained rhyolite porphyry in reports of Lyon and Clayton.
- Trp Rhyolite porphyry. Rhyolite porphyry with biotite and quartz "eye" phenocrysts set in a white groundmass. Phenocrysts are approximately 20% of rock. Forms numerous pluglike masses south and west of Telegraph Canyon in the Mineral Mountain quadrangle.
- Tbt₁₋₄ Bedded cream-colored rhyolite tuffs, probably in part waterlain. A sequence of four units intercalated with Tp and Tr. Contact between Tbt₁ and Tbt₃ in the White Canyon area is very approximately located on topographic criteria. Approximate thicknesses as follows: Tbt₁, 100-250 feet; Tbt₂, 100 feet ±; Tbt₃, 100-250 feet; Tbt₄, 100-200 feet. Tbt north of Ray mine is tentatively correlated with more extensive Tbt in Teapot Mountain quadrangle. Creasey (oral communication) has dated Tbt₁(?) at 17 m. y.
- Tmt Massive rhyolitic lithic tuff (100-250 feet) thick, well exposed in Wood Canyon area of Teapot Mountain quadrangle. Lithic fragments are of Tr + Tp 70% ± and pi 30% ±.
- Tr₁₋₄ Massive fine-grained rhyolite flow breccia, a sequence of four yellowish-white flow units intercalated with Tp and Tbt. Brecciation is probably due to autobrecciation during extrusion of flow. Approximate thicknesses as follows: Tr, 50-75 feet; Tr₂, 50-100 feet; Tr₃, 50 feet ±, Tr₄, 50-100 feet. Creasey (oral communication) has dated one of these flows at 16 m. y.
- Tri Massive fine-grained flow-banded rhyolite (intrusive equivalent of Tr). Cross-hatched band is vitrophyre which commonly occurs at the contacts of Tr and its host rock.
- Tp Perlite flows: A sequence of two flows intercalated in Tbt and Tr; pygmatic flow banding and associated b lination are common. Rock has a glassy, ropey outcrop texture and is light gray in color. Flows are 100 to 200 feet thick.

- Tpt Bedded to massive pink lithic tuff (15-30 feet). Lithic fragments in tuff are mostly Pinal schist. Generally present below Tbt and above Tgo. However, in the Telegraph Canyon a pink lithic tuff occurs at the base of Tgo.
- Tbo Dark purplish aphanitic vesicular basalt flows (0-75 feet), may be basaltic andesite.
- — — — —
- Tgo Older gravel (50 to +300 feet). Alluvium above Apache Leap tuff and below Tpt. Consists of coarse gravel alluviums dominated by rounded clasts of Oracle quartz monzonite. In the vicinity of Hells Peak, Tgo consists of finer grained sediments. As unit is traced northwest, clast's proportion becomes progressively more Pinal schist-rich. Unit may be an equivalent of the Ripsey Wash sequence (Schmidt, 1971) in the Kearny and Grayback quadrangles farther south. Gravel unit which rests between rhyolite tuff and Apache Leap tuff north of Ray mine is tentatively correlated with Tgo. Age is between 20 and 18 m. y. based on radiometric dates in the underlying Apache Leap tuff and overlying bedded rhyolite tuffs.
- Txg Sedimentary breccia (0-250 feet ±). Unbedded aggregate of silt, sand, pebbles, cobbles, and boulder-sized clasts. Clast composition is predominantly Oracle quartz monzonite with some Grayback granodiorite. Unit is a mud flow or megabreccia derived from a source area to the south in the Grayback quadrangle(?).
- Tal Apache Leap tuff (averages 200-500 feet in mapped area, 2,000 feet at type section in Superior quadrangle (Peterson, 1968, 1969)). A nonwelded white tuff 0 to 5 feet thick at base is commonly overlain by a 10- to 30-foot densely welded black vitrophyre (cross-hatched band). Black vitrophyre grades upward into a less densely welded brownish weathering tuff commonly with flattened pumice shards. Vapor phase crystallization increases near top. K-Ar ages are 20 m. y. (Creasey and Kistler, 1962) and 19.8 m. y. (Damon and Bickerman, 1964). Outcrops extensively in northwest Sonora quadrangle and entire Teapot Mountain quadrangle.

Tw Whitetail conglomerate (0-6,000 feet thick). Named by Ransome (1903) for exposures in the Globe quadrangle Conglomerate units which rest beneath mid-Tertiary volcanics above pre-Tertiary rocks and contain no mid-Tertiary volcanic clasts are generally assigned to the Whitetail conglomerate. One exception is in the Telegraph Canyon area where the basal conglomerate can be traced southeast where it is found to rest on Tal.

The Whitetail is divisible into three members which are lithologically and stratigraphically distinct. The lowest member consists of conglomerates with multiple monolithologic lithologies which grade and interfinger laterally and appear to have local sources (for example, see Phillips, 1976). The middle member is comprised of sandstone and siltstone, some of which is of lacustrine origin. In Walnut Canyon 0.5 mile upstream from its confluence with White Canyon gypsum is interlayered with siltstones of the middle member. The upper member consists of coarse conglomerate with clasts of variable lithology. North of Ray this unit contains sizeable masses of megabreccia. A tuff from the upper Whitetail at Ray is dated at 32.4 ± 0.6 m.y. (Banks, et al., 1972).

Whitetail Conglomerate, Upper Member

Twc Conglomerate (50 to 4,500+ feet thick). Coarse conglomerate with subrounded to angular clasts of variable composition. North of Ray this unit contains several large megabreccia masses.

Twm Megabreccia (0-300 feet thick). Found in Twc north of Ray. Lithologies mapped within the megabreccia are designated by the appropriate symbol enclosed in parentheses.

Whitetail Conglomerate, Middle Member

Twss Sandstone and siltstone (50-400 feet thick). Thin- to medium-bedded sands and silts, some conglomerate interbeds. Unit in Walnut Canyon contains intercalated gypsum beds; very soft; equals Twss of Phillips (1976).

Whitetail Conglomerate, Lower Member

- Twpi Conglomerate containing gray to grayish-brown angular clasts of unmineralized schist (0-300 feet thick) found west of Teapot Mountain and in Walnut Canyon area; equals TwS of Phillips (1976).
- Twpim Conglomerate containing angular clasts of metamorphosed Pinal schist. Clasts are gray to silverish and commonly contain numerous folds (0-300 feet thick) mapped northwest of Teapot Mountain.
- Twq Conglomerate containing angular clasts of quartzite derived from Dripping Spring and Troy quartzite. Diabase, Mescal limestone, and basalt clasts are less common (0-300 feet thick); mapped northwest of Teapot Mountain.

LATE CRETACEOUS-EARLY TERTIARY IGNEOUS ROCKS* (ROCKS OF THE LARAMIDE OROGENY)

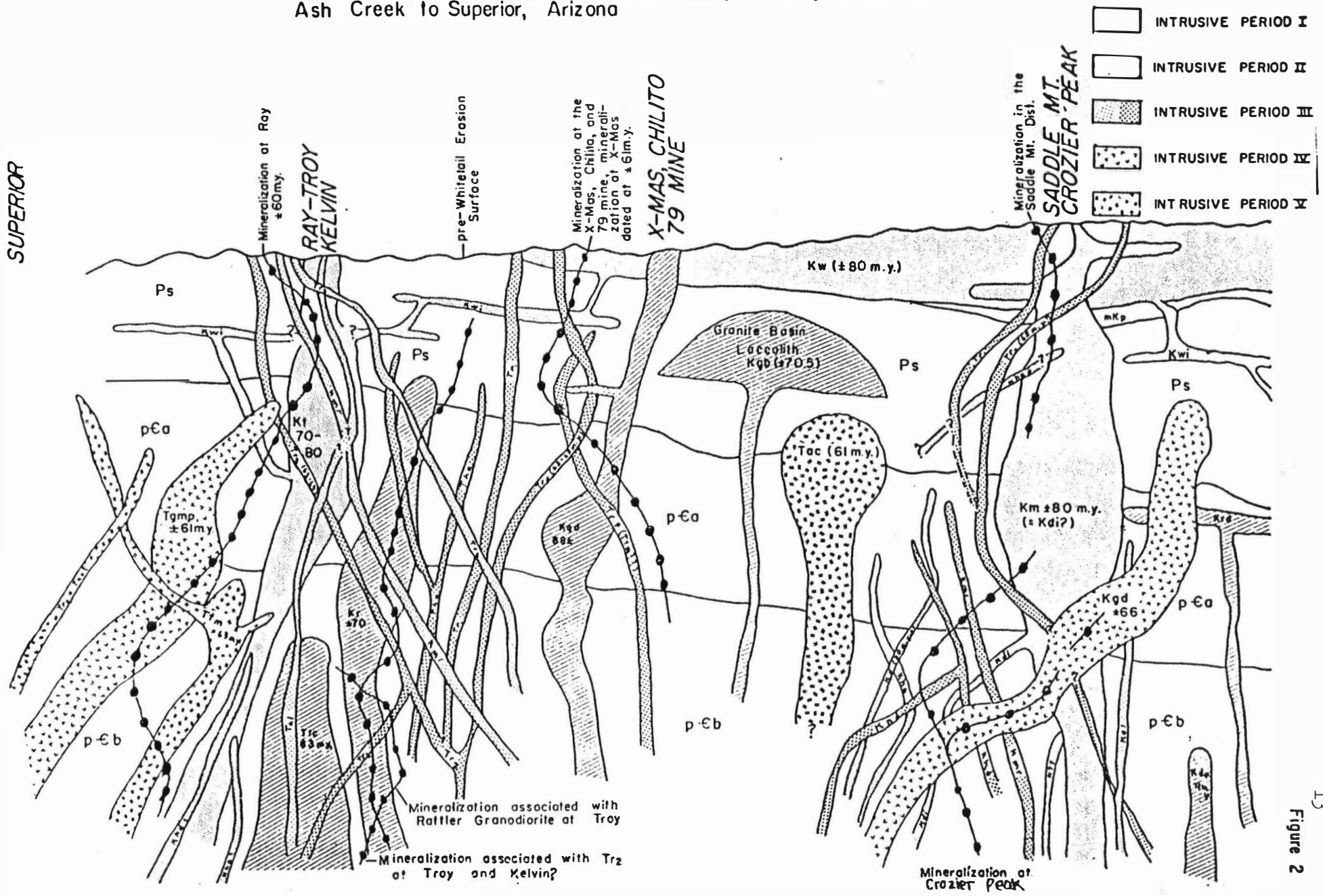
Numerous late Cretaceous-early Tertiary igneous rocks have been mapped (dikes, stocks, and sills). Based on relative ages established by crosscutting relationships, five principal stages of intrusions are defined on a regional basis (Table 1). Fifty-four age determinations are summarized in Table 1. In general, rocks of intrusive period I are more mafic than those of intrusive period II which in turn is more mafic than those in intrusive periods III and IV. Age data are commonly erratic with single rock bodies and numerous inconsistencies with respect to relative ages occur. Nevertheless rocks of intrusive period I are generally older (average of 75.9 for 18 dates) than periods II (average 68.6 for 11 dates), III (average of 61.9 for 5 dates), IV (62.8 for 8 dates), and V (61.3 for 3 dates). Using the current radiometric definition of Laramide magmatism (Damon and Mauger, 1966; Damon, 1968, 1970) in Arizona and New Mexico (75-50 m. y.), rocks of intrusive period I in general are pre-Laramide. Tectonic considerations too lengthy to develop here are also consistent with this definition.

The microdiorite (Km in Saddle Mountain area), diorite (Kdi in Crozier Peak area), and Tortilla quartz diorite (Kt in northern Tortilla and central Dripping Springs Mountains) are similar petrographically, chemically, and geochronologically and have the same relative ages. It is possible that these bodies are comagmatic and should be included under the same name (not done in this mapping). Relationships in the Saddle Mountain area suggest that the microdiorite and Williamson Canyon volcanics may be related. The volcanic pile is intruded by microdiorite, but within the pile lithic fragments of a rock petrographically identical to the microdiorite are found within lithic lapilli tuff flows.

Dike rock types which have regional extent are those of intrusive period III. In order of decreasing abundance the rocks are Tr₁-Tr₂, Kmr, Tkha, and Tql. Figure 2 is a correlation diagram for early T-late K intrusions based on crosscutting relationships observed in the field.

*See Figure 2 and Table 1.

Schematic Correlation of Late Cretaceous, Early Tertiary Intrusives
Ash Creek to Superior, Arizona



13
Figure 2

TABLE I
 CHRONOLOGY OF LATE CRETACEOUS-EARLY TERTIARY IGNEOUS ROCKS
 FROM SADDLE MOUNTAIN TO RAY, ARIZONA

Rock	W. R.	K-Ar						Fission Track	
		Biotite	Hornblende	K-Spar	Sphene	Zircon	Apatite		
Intrusive Period I 22 dates, average age 75.9 m. y.									
Kw		75.6 ± 1.4 ⁽¹⁾							
			74.3 ± 2.6 ⁽²⁾						
Kwi									
Km			79.7 ± 1.8 ⁽²⁾						
			81.7 ± 1.9 ⁽¹⁾						
Kdi			65.6 ± 2.0 ⁽⁴⁾						
Kt		71.5 ± 1.4 ⁽⁵⁾	83.1 ± 1.7 ⁽⁵⁾			69.8 ± 2.5 ⁽³⁾	69.5 ± 6.1 ⁽³⁾		
		70.6 ± 1.4 ⁽⁵⁾				69.8 ± 4.0 ⁽³⁾	72.4 ± 8.4 ⁽³⁾		
		71.3 ± 2.1 ⁽⁵⁾							
		68.7 ± 1.7 ⁽⁶⁾							
		80.0 ± 1.4 ⁽⁵⁾							
			285 ± 10 ⁽⁵⁾						
			110 ± 2 ⁽⁵⁾						
			93.7 ± 1.9 ⁽⁵⁾						
Kha ₁			128 ± 3(?) ⁽⁵⁾						
			74.3 ± 1.3 ⁽²⁾						
			79.3 ± 1.4 ⁽¹⁾						
Kha ₂									
Kd	80.6 ± 1.8 ⁽¹⁾								
Khd									
Ktt									
Intrusive Period II 11 dates, average age 68.6 m. y.									
Kv									
Kda			71.3 ± 2.1 ⁽⁷⁾						
Kqd			68.0 ± 0.9 ⁽²⁾						
Kgb			70.5 ± 1.6 ⁽²⁾						
Kr		68.5 ± 1.4 ⁽⁵⁾							
		71.1 ± 3.2 ⁽⁸⁾							
		69.7 ± 1.4 ⁽⁵⁾	74.4 ± 1.5 ⁽⁵⁾			68.3 ± 2.3 ⁽³⁾	68.5 ± 4.2 ⁽³⁾		
Mineralization associated with Kr									
Itc		62.9 ± 1.3 ⁽⁶⁾				61.4 ± 3.4	(garnet) ⁽³⁾		

TABLE 1 (Continued)

Rock	W.R.	Biotite	Hornblende	K-Spar	Sphene	Zircon	Apatite
Intrusive Period III 5 dates, average age 61.9 m. y.							
Kr							
Tkha							
Tr ₁ -Tr ₂		63.1 ± 1.3 ⁽⁶⁾					
		62.1 ± 1.2 ⁽⁵⁾					
		62 ± 2 ⁽⁹⁾					
mineralization associated with Tr ₂ at Christmas							
		61.0 ± 1.0	(sericite) ⁽²⁾				
		61.4 ± 1.1	(hydrothermal biotite) ⁽²⁾				
Kmr							
Tql							
Intrusive Period IV 8 dates, average age 62.8 m. y.							
Kgd		68.0 ⁽¹²⁾					
		66.0 ± 2.0 ⁽⁴⁾					
		65.7 ± 2.0 ⁽⁴⁾					
Tgm		59.5 ± 1.2 ⁽⁵⁾				61.0 ± 2.1 ⁽³⁾	
		63.0 ± 2 ⁽⁹⁾					
		60 ⁽¹⁰⁾					
		59.5 ± 1.8 ⁽¹¹⁾					
Intrusive Period V 3 dates, average age 61.3 m. y.							
Ttm							63.0 ± 0.7 ⁽⁵⁾
mineralization at Ray and Crozier Peak							
		65.6 ± 1.1 hydrothermal	biotite	60.0 ± 6.0		61.4 ± 3.2 (garnet)	
		65.1 ± 1.1 at Ray					60.0 ± 6 ^(*)
Tr ₃		69.7 ± 1.4					
Tac		61.0 ± 2					

- (1) Keith and Damon (unpub.)
(2) Koski (written communication, 1976)
(3) Banks and Stuckless (1973)
(4) Krieger (1974a)
(5) Banks, et al. (1972)
(6) Damon, et al. (1970)
(7) Krieger (1974b)
(8) Damon and Mauger (1966)
(9) Creasey and Kistler (1962)
(10) Rose and Cook (1966)
(11) McDowell (1971)
(12) Damon, et al. (1964)
(13) Krieger (1968d)
(*) Reset apatite from 1150 m. y. diabase in Ray deposit

Intrusive Period V

- Tr₃ Rhyodacite dikes, fine-grained, orangish, weathering, east- to west-trending dikes that cut Teapot Mountain porphyry northeast of Ray, Rattler granodiorite at Troy, central Dripping Springs Mountains, and Williamson Canyon volcanics west of Saddle Mountain. Equals Tr₃ (Cornwall, et al., 1972) and Tr₃ (Cornwall and Krieger, 1975b). Banks, et al. (1972) reports a 69.7 ± 1.4 m. y. date on chloritized biotite from the dikes which cut the Troy intrusion. The date is anomalously old and was interpreted by Banks, Cornwall, Siberman, and Marvin (1972) to represent extraneous radiogenic argon introduced by late-stage magmatic or hydrothermal fluids.
- Tac Ash Creek rhyolite. A 1-square-mile stock intruding Pinal schist and Paleozoic rocks and overlain by Whitetail conglomerate 1.5 miles east of Saddle Mountain. Yellowish-white, very fine-grained rhyolite with flow foliation. Contains sparse phenocrysts of euhedral thin biotite books to 3 mm and K-spar(?). The biotite has yielded a K-Ar age of 61 ± 2 m. y. (Krieger, 1968c). This rock may be related to Tr₃ on the basis of its texture and proximity to Tr₃ dikes 1 mile to the west.
- Ttm Teapot Mountain porphyry. White to light yellow porphyry containing large euhedral phenocrysts of K-spar and euhedral to slightly resorbed quartz eyes 3 to 12 mm in diameter. Banks, et al. (1972) reports a 63.0 ± 0.7 m. y. date on orthoclase. The date is older than the granite porphyry which it intrudes on Granite Mountain. The porphyry crops out in the Ray area (see also Cornwall, et al., 1971).

Intrusive Period IV

- Tgm Granite Mountain porphyry. Medium-grained biotite granodiorite. Comprises large stock west of Ray and small stocks at Ray mine. Average of five dates from four sources (Table 1) is 60.6 m. y. (see also Cornwall, et al., 1971). Truncates Tr₂ dikes.
- Kgd Medium-grained biotite hornblende granodiorite porphyry stocks and dikes in Crozier Peak area. Forms a small stock and subsidiary dikes on Ripsey Ridge at boundary of Kearny and Crozier Peak $7\frac{1}{2}$ minute quadrangles. Average of their K-Ar ages on biotite (Table 1) is 66.6 m. y.

Intrusive Period III

- Tq1 Quartz latite porphyry dikes in Crozier Peak, Kearny, and Winkleman 7½ minute quadrangles. Equals Tq1 of Cornwall and Krieger (1975a, 1975b), Trp of Schmidt (1971), and Tkly of Krieger (1974b, 1974c). Tal near Crozier Peak is intruded by Kgd and is therefore older and not younger than Kgd as indicated by Krieger (1974a, 1974b).
- Kmr Melanocratic rhyodacite porphyry. Phenocrysts of plagioclase, resorbed quartz (to 10 mm), biotite, and accessory hornblende in a medium dark greenish-gray groundmass. Equals Kmr of Cornwall, et al. (1971), Krieger (1974b, 1974c), and Cornwall and Krieger (1975a, 1975b). In areas mapped by S. Keith intrudes Tr₂ which is consistent with existing literature above.
- Tr₁-Tr₂ Rhyodacite porphyry dikes. East-northeast- to east-west-striking dike swarms. Probably the most common dike type.
- Tr₁ Rhyodacite porphyry which contains phenocrysts of andesine, biotite, minor hornblende, and no quartz set in a tan to light greenish-gray groundmass.
- Tr₂ Rhyodacite porphyry. Same as above except contains resorbed quartz grains (5-13%) about 5 mm in diameter.

Both varieties were mapped separately. Individual dikes may or may not contain quartz. No crosscutting relationships between these dikes were observed. Rock type is identical except for presence or absence of quartz. Similar positions in relative age sequence suggest these two dike types are comagmatic. Analogous observations have been made by other workers (Tkd and Tkq of Barrett, 1972, and Tkr-Tkrq of Krieger, 1974a, 1974b). Tr₁-Tr₂ is also equivalent to Tkr₂ of Cornwall, et al. (1971), Tr₂ of Cornwall and Krieger (1975a, 1975b), Tqmp of Schmidt (1971), and Tkfm of Willden (1964). An average of three K-Ar ages on biotite from three dikes in this series is 62.4 m. y.

Intrusive Period II

- Krp Rhyodacite porphyry. Porphyritic (plagioclase) medium to light gray with a greenish, brownish, or olive cast rhyodacite. Contains smaller euhedral phenocrysts of hornblende and biotite; accessory magnetite; visible quartz is rare. Forms dikes and a large sill in Apache group east of Crozier Peak. Questionably assigned to intrusive period II on the basis of its sill-like nature.
- Ttc Teacup granodiorite (see Cornwall and Krieger, 1975b). Equals Grayback granodiorite of Schmidt (1971); not on S. Keith maps. Average of two dates (Table 1) is 62.2 m.y. Large pluton in Grayback and North Butte quadrangles. Cut by dikes of intrusive period III.
- Kr Rattler granodiorite (see Ransome, 1923; Cornwall, et al., 1971). Equals granodiorite of Troy (Ransome, 1923); referred to informally as Troy granodiorite by Schmidt (1971) and others. Main phase is a medium-grained biotite hornblende granodiorite. Average of six dates from three sources (Table 1) is 70.1 m.y. Forms a 2-square-kilometer stock at Troy in central Dripping Spring Mountains.
- Kgb Granodiorite of Granite Basin (see Willden, 1964). Forms large laccolithic intrusion into Naco group 5 miles east of Christmas mine. Biotite hornblende granodiorite included by Willden (1964) as Tkfm. K-Ar date on hornblende is 70.5 ± 1.6 m.y. (Koski, written communication, 1976). Not on S. Keith maps. Rock closely resembles Rattler granodiorite (Koski, personal communication).
- Kqd Quartz diorite. Medium-grained biotite hornblende quartz diorite. Comprises small stock southeast of 79 mine in southern Dripping Springs and MacDonald stock 1 mile east of Christmas. K-Ar age of hornblende is 68.0 ± 1.6 m.y. (Koski, written communication) from MacDonald stock. MacDonald stock not on S. Keith maps.
- Kda Dacite (see Krieger, 1974c). Consists of a sill in Apache group rocks in central Crozier Peak quadrangle. K-Ar age on hornblende is 71.3 ± 2.1 m.y. (Krieger, 1974c). Not on S. Keith maps.
- Kv Volcanics on east side of Ripsey Ridge in Crozier Peak quadrangle (see Krieger, 1974c). Not on S. Keith maps.

Intrusive Period I

- Ktt** Turkey Track porphyry. Large (to 15 mm) plagioclase laths poikilitically enclosed in a dark gray groundmass exhibiting Turkey Track texture. Only one east-west striking dike mapped northwest of Crozier Peak. Dike appeared to be truncated by Kdi.
- Khd** Hornblende diorite porphyry. Medium gray to greenish or olive-gray fine- to medium coarse-grained hornblende diorite or andesite. Phenocrysts are almost entirely hornblende (2-10 mm) with rare plagioclase. Equals Kh of Krieger (1974b, 1974c). Forms east- to northeast-trending dikes in Crozier Peak and Winkleman quadrangles.
- Kd** Fine-grained light green quartz diorite (see Krieger, 1974b). North- to south-trending dike which intrudes Romero Wash fault yielded a K-Ar whole rock age of 80.6 m. y. (Keith and Damon, unpublished). Forms numerous east- to northeast-striking dikes south of Crozier Peak. Some of Krieger's Tku in this area is probably this rock.
- Kha** Hornblende andesite. Light brown andesite dikes containing phenocrysts of hornblende (2-5 mm) and tabular white plagioclase "squares" (2-4 mm) scattered in a light brownish-gray groundmass. Intrudes Kdi, Kd, and Khd. Forms numerous east- to northeast-striking dikes south of Crozier Peak. Some of Krieger's (1974b, 1974c) Tku south of Crozier Peak is of this rock. Could be equivalent to Tka and Tkrh in Kearny quadrangle (Cornwall and Krieger, 1975a) and Tkr and Tkha in Sonora quadrangle (Cornwall, et al., 1971).
- Khap** Hornblende andesite. Large (to 3 cm in diameter) hornblende phenocrysts set in a medium gray groundmass. Dikes which intrude Kw in Saddle Mountain area. Dikes appear to cut and be cut by Km and therefore are interpreted to be comagmatic with Km₁. Dated dike in Ray area Kha of Cornwall, et al. (1971) and hornblende andesite in Crozier Peak quadrangle (Kha of Krieger, 1974c) may be equivalent(?). Average of two dates from Christmas and Saddle Mountain areas (Table 1) is 76.8 m. y.).
- Kt** Tortilla quartz diorite (see Cornwall, et al., 1971). Equals Sonora diorite of Schmidt (1971). Consists of a number of small stocks in the Kearny, Grayback, and Sonora quadrangles. The largest stock is west of Kelvin, Grayback,

and Sonora quadrangles. Composition ranges from pyroxene-hornblende diorite through biotite-hornblende diorite. Typically medium-grained hypidiomorphic granular rock, although local porphyritic patches with pyroxene and hornblende phenocrysts to 3 cm across are common. Average of 10 selected ages from 3 sources (Table 1) is 72.65 m.y. Banks, Cornwall, Silberman, and Marvin (1972) interpret the anomalously old hornblende ages to reflect extraneous or excess radiogenic argon introduced by late stage magmatic fluids.

PALEOZOIC ROCKS*

IPs

IPn

Naco group. Name given by Ransome (1904) to a series of rocks above Mississippian Escabrosa limestone in the Naco Hills, southwest Mule Mountains, Cochise County, Arizona. Since Ransome, rocks in the unit have been subdivided by numerous workers into many formations. Only the lowest formation (Horquilla

formation) is recognized in the Saddle Mountain to Superior area. All previous mapping in this area has referred this unit under the name of Naco formation.

IPh

Horquilla formation (500 to 1,500 feet thick \pm). Light grayish weathering alternating carbonates and clastics. Basal contact with IPb is variable. At Superior the contact is marked by a quartzite pebble conglomerate. At Ray it is a chert breccia. At Eskiminzin Wash it is a chert breccia and sandstone. The basal 150 feet of IPh is predominantly slope forming pinkish and reddish siltstones and shales interbedded with micrite. Resistant carbonate lithologies (100 feet \pm) are encountered about 150 feet above base

*See Figure 3 for northwest-southeast distribution and correlation of Paleozoic rocks.

interbedded with clastics (20%). Above the ledge-forming carbonate sequence, IPh is a monotonous sequence of interbedded carbonates (65%) and clastics (35%) at regular intervals. In general the IPh carbonates (mostly crinoidal and fusilinid limestone with numerous chert lenses) have more grayish outcrop colors than Black Prince. IPh clastics (mostly pinkish to maroon siltstones and shales) form slopes so that a conspicuous regular-shaped ribbing or banding is observed when viewing IPh from a distance. Fossils common in IPh are crinoids, echinoid spines, composita productid, and spirifer brachiopods. Guide fossils in central Arizona are fusilinids, *Caninia rugose* coral, and *prisma pora* bryozoa. IPh in general forms slopes. See Ross (1973) and Reid (1969) for more detail on IPh.

- IPb Black Prince formation (100-150 feet thick). Basal unit is commonly a maroon shale or siltstone and forms topographic recesses. Basal bed is locally a chert breccia. Upper unit is a thick-bedded ledge to cliff-forming white crinoidal limestone (biosparite) with chert pods and lenses. Black Prince contains no fusilinids. *Chaetetes* "brain" coral is common in the upper limestone unit. See Ross (1973) and Berry (1975) for more detail on IPb.
- Mes Eskiminzin formation (new; 0-110 feet thick) named for exposures in Eskiminzin Wash, Saddle Mountain quadrangle (Keith and Purvis, unpublished). Conodonts collected from this unit place the unit as Chester in age (Purvis, unpublished data). Formation consists of pink to yellowish-orange unfossiliferous fine-grained to aphanitic dolomite. Base of unit is a sedimentary breccia resting unconformably on a karst surface developed in underlying Escabrosa limestone. Sinkholes in this surface penetrate to 60 feet into Escabrosa and contain angular brecciated material of Eskiminzin which has collapsed into the void space. The karst is spectacularly exposed in a road cut on the north side of Highway 177 where it passes through Me in the core of an anticlinal fold 2 miles northeast of Winkleman, Arizona. Contact with Naco formation in other mapping is inconsistently placed above and below this unit (e. g. , Krieger, 1968c).
- Me Escabrosa formation (approximately 500 feet thick). Unit forms prominent cliffs of massive bluish-gray crinoidal limestone (biosparite). Contains a series of conspicuous

white marker beds about 200-300 feet above base (Mew). Base of formation is a banded (light to dark bluish-gray bands) cliff-forming crinoidal biosparite (40-50 feet thick) with black chert bands locally at its base (referred to colloquially as the "zebra stripe" unit). Intervals between cliff-forming units are medium-bedded orangish-brown aphanitic dolomite with a few white chert pods and lenses. Two white marker beds were mapped in exposures in Saddle Mountain 7½ minute quadrangle and are designated Mew1 and Mewu. An unconformity about 350 feet above base was mapped in Me exposures along Ash Creek. Fossils are ostracods (oolites) crinoids, spirifer and composita brachiopods, and syringopora "organ pipe" coral. Zaphrenthis rugose coral are guides to Me. See Huddle and Dobrovolny (1952) for more information on Escabrosa formation in central Arizona.

- Dp Percha formation (30-150 feet). Recently recognized in central Arizona by Shumacher, et al. (1976). Separated from underlying Dm by conodont data and lithology. Basal unit (Dp1) is a slope-forming olive-green mud-shale 40 to 85 feet thick and grades into an upper unit (Dpu) of medium-bedded light yellow silty dolomite with white chert pods. Dp in Teapot Mountain quadrangle consists entirely of lower mud-shale unit.
- Dm Martin formation (300-400 feet). Consists of five units which were combined into four map units which in descending order are:
- Dmu Orange dolomite and siltstone unit (30-70 feet thick). Slope-forming thin- to medium-bedded fine-grained orange to orange-yellow silty dolomite interbedded with siltstone and shale. Scattered hematite concretions. Locally fossiliferous. Pachyphyllum and Hexagoraria corals have been collected from this unit (see Meader, 1976).
- Dmm Consists of two units which are in descending order:
- Sandy limestone unit (30-50 feet thick). Ledge-forming dark bluish-gray, thin- to medium-bedded sandy limestone. Contains calcareous silt and sand interlenses. Very fossiliferous. Atrypa brachiopods common to abundant. Other fossils are pachyphyllum corals, bryozoa, and abundant

crinoid stems and hash. A few crinoid calyxes have been found. Fossils are locally so crowded that the rock resembles coquina. Biostratigraphy of this unit and Dmu is summarized by Meader (1976). Upper part of unit commonly contains hematite concretions.

Aphanitic dolomite unit (200 feet thick \pm). Slope-forming light gray to light yellow aphanitic dolomite. Contains siltstone and sandstone interbeds in upper part.

- Dml Fetid dolomite unit (20-35 feet thick). Well-bedded, dark gray, laminated fetid dolomite. Commonly mineralized (the O'Carroll ore horizon of Eastlick, 1968, and others). Forms ledges.
- Dmb Beckers Butte sandstone member (see Teichert, 1965), approximately 40 feet thick. Friable, well-sorted, clean, well-bedded, medium- to coarse-grained sandstone. Weathers light brown to gray. Calcareous in its upper few feet. See Teichert (1965) for more information on Martin formation in central Arizona.
- €a Abrigo formation (0-450 feet thick). Divided into three members which grade into one another. €au and €am are not present north of the latitude of Hayden. €al is present in southern and central Dripping Spring Mountains but is absent in Teapot Mountain 7½ minute quadrangle (Fig. 3), see Krieger (1961, 1968c, 1968d). Units in descending order are:
- €au Upper brown sandy member (50-75 feet thick). Cliff-forming, brown, medium- to thick-bedded sandy dolomite or dolomitic sandstone. Crossbed laminae common. Approximately 20 feet above base contains a red oolitic hematite bed marked on map by a dashed line where observed which contains abundant shell fragments of phosphatic inarticulate brachiopods.
- €am Middle sandstone member (150-250 feet thick). White ledge-forming, medium-bedded, fine-grained quartzitic sandstone. Weathers to a distinctive ribbed topographic expression (ribs parallel bedding). Contains excellent ripple-mark surfaces. Scolithus (worm tubes?) is common throughout unit.

- €al Lower mudstone member (50-125 feet thick). Slope-forming olive-green, glauconitic mudstone and shale. Contains fossil trilobite and inarticulate brachiopod (*Billingsella?*) hash. Grades downward into €ba.
- €b Bolsa quartzite (0-300 feet thick, typically 50-100 feet thick). Mapped as two units. €bu is by far the most extensive. Bolsa is absent at Steamboat Mountain in Dripping Spring Mountains, Hayden 7½ minute quadrangle, where €rests on Precambrian Troy quartzite. See Krieger (1961, 1968) for further discussion. Units in descending order are:
- €bu Upper quartzite member (0-250 feet thick, typically 50-100 feet thick). Cliff-forming, fine-grained, medium-bedded, white, clean quartzite. Crossbedding laminae common. Generally rests on Troy quartzite but may rest on diabase. Basal pebble conglomerate containing clasts of Troy quartzite is present locally.
- €bl Lower arkosic member (0-150 feet thick). Present locally in thicker sections of €b. Dominately dark maroon to pinkish colored, poorly sorted, friable arkose and arkosic sandstone. Poorly sorted pebble conglomerates near base. €bl commonly rests on db and much of its reddish color may be from reddish clays derived from db. Unit closely resembles lithologies in the Troy quartzite and fills channels and irregularities on an erosional surface of moderate relief. Grades upward into €bu.

YOUNGER PRECAMBRIAN ROCKS*

A thick sequence of predominately clastic rocks which underlies the Cambrian Bolsa quartzite and overlies older Precambrian crystalline rocks is present throughout the mapped area. These rocks were originally considered Cambrian by Ransome (1903, 1919, 1923). These rocks underlie 1400 m. y. quartz monzonite and are intruded by 1150-1200 m. y. diabase sills which clearly place them in the Precambrian.

*See Figure 3 for northwest-southeast distribution and correlation of younger Precambrian rocks.

A well-exposed section of these rocks is present on Highway 177 in the central Teapot Mountain 7½ minute quadrangle. For a detailed discussion of younger Precambrian stratigraphy see Schride (1967). For interrelations between younger Precambrian and lower Paleozoic stratigraphies see Krieger (1961, 1968d) and Schride (1967).

db

Diabase. Dikes and sills abundant in Precambrian Apache group and Troy quartzite. Medium- to coarse-grained ophitic texture is defined by plagioclase (laboradorite composition) poikilitically encased in a pyroxene (augite) groundmass. Accessory minerals include biotite, amphibole, olivine, and magnetite-ilmenite. Diabase and gabbro pegmatites are present locally. Sills are often composite and invariably have chilled borders with enclosing sedimentary rocks in areas of poor outcrop. Diabase weathers into distinctive olive-green soils. Diabase is locally positionally overlain by Bolsa quartzite as at Ash Creek, Saddle Mountain 7½ minute quadrangle (contact here is also moderately sheared) and in U. S. Highways 60 and 70 roadcuts at Superior, Arizona. Typical thicknesses for diabase sills are 300-600 feet, but large sills may range to +1,200 feet. The accepted age for the diabase is 1150 m. y., based on several dating techniques (see Silver, 1960; Granger and Raup, 1959; Livingston and Damon, 1968; and Banks, et al., 1972). For more detail on the diabase see Schride (1967), Smith (1969, 1970), and Nehru and Prinz (1970).

tq

Troy quartzite (named by Ransome, 1919, 1923, for exposures at Troy Mountain, central Dripping Spring range). Generally 300-600 feet thick where present. Thicknesses are variable due to post-diabase pre-Bolsa erosion which produced a surface of moderate relief. Composed of two units which were difficult to separate in the mapping due to abrupt lateral and vertical variations. See Schride (1967) for more detail. The units in descending order are:

Upper quartzite member. Cliff- and ledge-forming, fine-grained, locally medium-grained, medium-bedded, white to reddish quartzite and feldspathic quartzite. When Ebu was inferred to overlie this unit, contact was placed

somewhat arbitrarily based where possible on cleanness and grain size. Becomes sandier and more feldspathic in its lower part. Equals upper quartzite member in Troy quartzite of Schride (1967).

Lower arkosic sandstone member (mostly 100-300 feet). Slope- and ledge-forming; red, maroon, white, poorly sorted arkosic and conglomeratic sandstone. Becomes more arkosic, poorly sorted, and conglomeratic near base. Arkosic sandstones have prominent lenticular cross bedding locally. Arkose member is well exposed northeast of Walnut Gap along Highway 177 in Teapot Mountain 7½ minute quadrangle. Probably equivalent to the Chedeski sandstone member of Schride (1967).

tqc

Basal conglomerate (0-30 feet thick). Coarse pebble and cobble conglomerate which superficially resembles Barnes conglomerate except for clasts of Mescal limestone and Dripping Spring quartzite and slightly more angular clasts. Pebble and cobble sized clasts are composed mainly of Apache group rocks and reworked quartzite clasts and red chert from the Barnes conglomerate. Matrix is reddish to maroon, poorly sorted arkose of similar composition to the clasts which it encloses. Shown by a conglomerate symbol where observed.

Apache Group

A series of three formational units which rest under Troy quartzite and on older Precambrian rocks is referred to the name Apache group. Named by Ransome (1903) for exposures in the Globe 30 minute quadrangle. Includes in descending order basalt, Mescal limestone, Dripping Spring quartzite, and Pioneer formation.

b

Basalt (0-300 feet, generally 75-150 feet thick). Flows of black to dark gray basalt. Commonly vesicular. Porphyritic varieties consist of plagioclase in a pyroxene groundmass of pyroxene and olivine largely altered to iddingsite and serpentine. Altered basalt has a greenish appearance and where coincident with diabase is difficult to distinguish.

- m Mescal limestone (0-350 feet, typically 150-250 feet thick). Two members mapped which in descending order are:
- m1a Upper algal member (0-150 feet, typically 100-150 feet thick). Equals algal member of Schride (1967). Ledge- and cliff-forming, thick-bedded, yellowish brown dolomite. Algal stromatolyte bioherms are common in the lower one-third of the unit. Member is not present in Tortilla Mountains or Dripping Spring Mountains south of Troy Mountain (Fig. 3). See Schride (1967) for further discussion.
- m1 Lower dolomite member (0-150 feet thick, typically 75-150 feet thick). Thin- to medium-bedded, white dolomite with abundant black chert bands and lenses locally. Rock weathers into closely spaced ribs where chert is present. Lower part of unit is commonly a sedimentary breccia which consists of angular chert and dolomite clasts in a matrix of brownish-gray, locally calcareous dolomite. Matrix of breccia becomes sandier in its lower part. See Schride (1967) for further discussion.
- ds Dripping Spring quartzite. Named by Ransome (1903, 1919) for exposures in the Dripping Spring Mountains. Divided by Schride (1967) and USGS mapping into three members (see also Granger and Raup, 1964). A four-member subdivision seemed more logical in the area of this mapping. In descending order the four units are:
- dsuq Upper arkosic quartzite member (50-100 feet thick). Light brown, reddish brown, and reddish green, fine-grained, medium-bedded arkosic quartzite interbedded with thin-bedded siltstone. Has a flaggy outcrop expression; forms cliffs and ledges. Joints are often stained with hematite and goethite and show Liesegang rings where the arkosic quartzite is intruded by diabase sills.
- dss Middle siltstone member (40-150 feet thick). Slope-forming, interbedded, thin-bedded siltstones and shales. Weathered surfaces are strong shale of reddish-brown. Shale is locally phyllitic and weathers into small slaty shingles and flakes which have a white micaceous sheen. Reddish-brown goethite stain is derived from syngenetic

pyrite (1-5% locally). Rare torbernite is derived from sparse syngenetic uraninite(?). Unit commonly intruded by diabase sills.

- dslq** Lower quartzite (40-80 feet thick). Light yellowish-brown to white, cliff-forming, thin- to thick-bedded, medium-grained, fairly clean quartzite. Lower portions more arkosic. Fractures commonly stained by goethite derived from overlying dss unit.
- dsb** Barnes conglomerate member (0-50 feet, generally about 30 feet thick). This unit is the most easily identified, persistent, and reliable marker unit in the Apache group section and perhaps the entire Precambrian, Paleozoic, and Mesozoic section. Consists of very well-rounded ellipsoidal pebbles and cobbles of gray, brown, and grayish-red quartzite with minor quartz and red jasper set in a matrix of medium-grained, poorly sorted arkosic quartzite. Forms ledges but is not as resistant as dslq.
- pf** Pioneer formation (0-300 feet thick, generally 150-200 feet thick). Slope-forming, dusky red-purple and brown arkose, and dusky purple siltstone and shale. Siltstone and shale are tuffaceous. Rocks of the Pioneer formation very commonly are speckled by distinctive white to light greenish-yellow spots which represent bleached areas around small (0.5 to 2 mm) pyrite cubes replaced by goethite. When spots are absent Pioneer may closely resemble dss.
- pfs** Scanlan conglomerate member (0-20 feet; usually 2-6 feet). Matrix and clast composition variable and depends for its character on the rock immediately underlying it. In schistose terrains, clasts are subrounded to angular pebbles of white quartz (locally abundant) and angular pebbles and granules of Pinal schist in a grayish-red to purple matrix of poorly sorted rock chips and arkose. In granitic terrains, clasts are rounded to angular pebbles of white quartz and local pebbles and cobbles of quartzite in a coarse arkosic matrix of granitic composition. This variety may resemble clast-poor variations of Barnes conglomerate. Commonly, few if any pebble clasts are present and unit consists entirely of a coarse-grained granitic arkose.

OLDER PRECAMBRIAN ROCKS*

or

Oracle quartz monzonite of Peterson (1938). Referred to in recent USGS mapping in Tortilla Mountains as Ruin granite for a rock of similar composition and age in Ruin Basin 10 miles northwest of Globe, Arizona (see Ransome, 1903). The name Oracle is preferred because outcrops in Tortilla Mountains extend more or less continuously to an identical-looking rock at Oracle, Arizona. The quartz monzonite in Ruin Basin is separated from that in the Tortilla Mountains by a 30-mile-wide belt of Pinal schist. Oracle refers to extensive exposures of batholithic extent in the Tortilla Mountains.

Petrographically the rock is a medium- to coarse-grained yellowish-gray to grayish-orange porphyritic (K-spar) biotite quartz monzonite. Biotite is commonly altered to chlorite. Accessory minerals are apatite, magnetite, and zircon with rare sphene. K-spar phenocrysts are commonly large (to 6 x 3 cm) and may be either orthoclase or microcline and commonly exhibit microperthitic intergrowths. Locally "or" contains numerous xenoliths of clots of Pinal schist. Biotite from the Oracle granite of Oracle, Arizona, gave a K-Ar age of 1420 m.y. (Damon, et al., 1962). Silver has an unpublished U-Pb zircon age of 1450 m.y. for this rock. Oracle quartz monzonite is locally cut by aplite and pegmatite dikes designated "ap" on maps. Also, the porphyritic phase commonly grades into a "hybrid" aplitic equigranular phase which was only mapped in a few areas (designated "hor" on the maps).

Oracle quartz monzonite is locally cut by a cataclastic east-west- to east-northwest-trending high-angle foliation (especially in Kelvin Riverside area). Schmidt (1971) reports that this foliation is cut by 1150 m.y. diabase sills in the northern Tortilla Mountains.

md₂

Madera quartz diorite. Named by Ransome (1903) for exposures near Mt. Madera in the northern Pinal Mountains. Ransome (1923) refers to at least two varieties in the Pinal Mountains. Several varieties are present north of Ray where some useful crosscutting relationships were established.

The rock symbolized as md₂ has the following characteristics: The predominate phase is a medium-grained biotite granodiorite with 4-20% biotite (generally 4-6% biotite) and is foliated locally. A more mafic phase has hornblende and is better termed a hornblende biotite quartz diorite. The hornblende in this rock forms typical elongate prisms. Locally the biotite granodiorite is foliated. In some areas biotite-poor md₂ closely resembles Granite Mountain porphyry (Tgm). In gullies west of the picnic ground 2 miles north of Ray mine the biotite granodiorite phase clearly cuts a more mafic "phase" (md₁).

md₁

Quartz diorite. Medium- to medium-coarse-grained biotite hornblende quartz diorite. Texturally this rock is distinct from md₂ in that hornblende (and possibly pyroxene) are distributed throughout rock as blocky or stubby equant crystal clusters in a lighter phase of plagioclase and minor quartz. The result is a splotchy "salt and pepper" or "shot gun" texture. The occurrence of hornblende in md₂ is as more typical elongate prisms which are not clustered. md₁ is the prominent md rock type in the central Teapot 7½ minute quadrangle, Telegraph Canyon of the Mineral Mountain 7½ minute quadrangle, and Cedar Mountain area of the Winkleman 7½ minute quadrangle.

Both types of md are commonly well foliated near their contacts with Pinal schist and grade into poorly foliated and unfoliated rock away from Pinal schist contacts suggesting a protoclastic deformational process during emplacement which is superimposed on an already regionally metamorphosed and deformed Pinal schist. Numerous attempts have been made to date Madera diorite. The age data are summarized in Table 2.

Fig. 4 Correlation of Older Precambrian Rocks
Ash Creek to Superior, Arizona

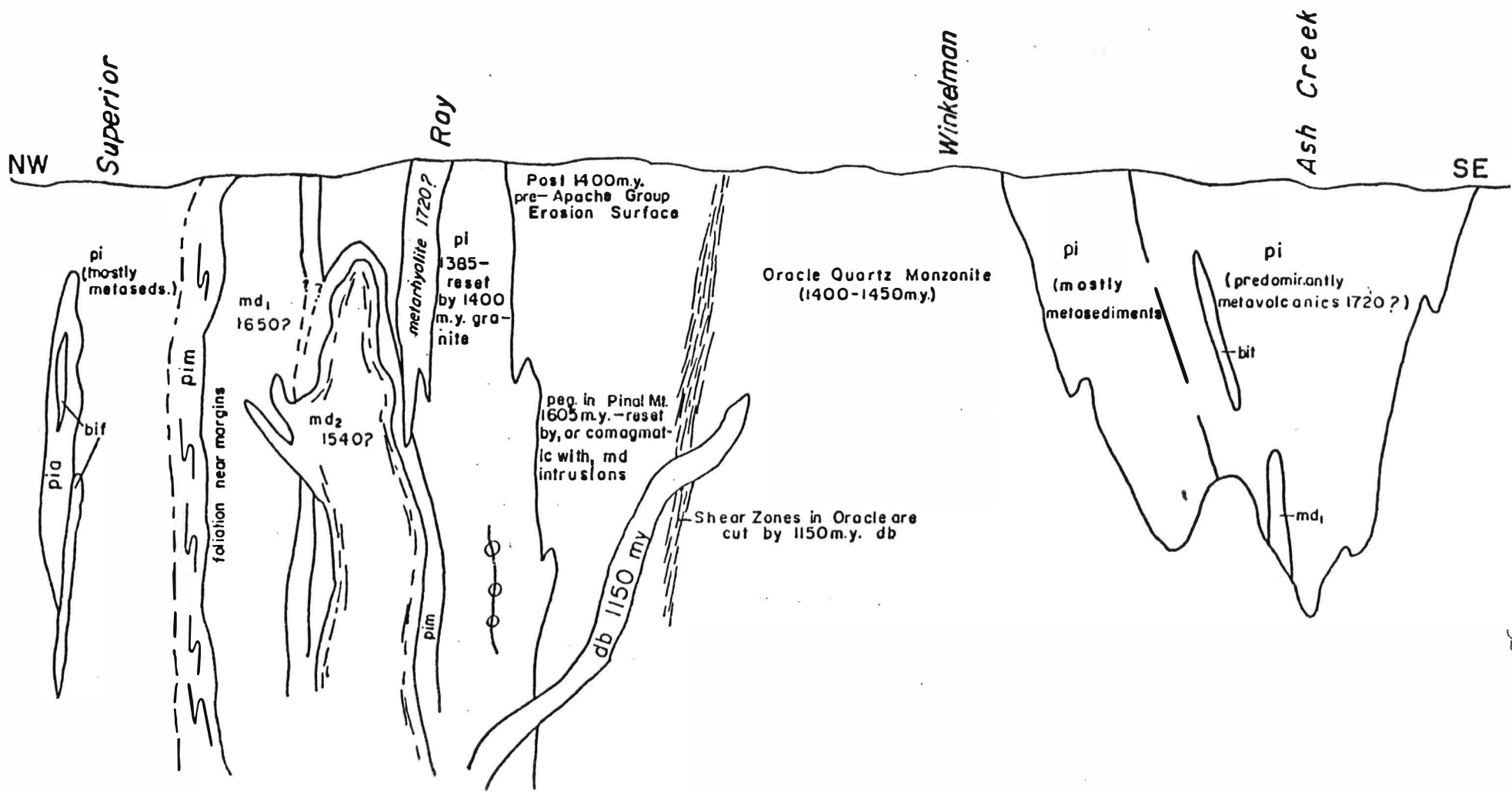


TABLE 2

AGE DATA FOR MADERA DIORITE

Comments	Method	Mineral	Date	Source
	K-Ar	biotite	1660	Damon, et al. (1962)
	K-Ar	hornblende	1630 \pm 60	Banks, et al. (1972)
foliated grano-diorite reset by intrusion of Tortilla quartz diorite	Rb-Sr	whole rock isochron	1775	Livingston and Damon (1968)
reset	K-Ar	biotite	68.6	Banks, et al. (1972)
reset	K-Ar	biotite	98	Banks, et al. (1972)
foliated Madera diorite	Rb-Sr	W.R. isochron A	1730 \pm 30	Livingston (1970)
	Rb-Sr	mineral isochron B	1580 \pm 60	Livingston (1970)
	Rb-Sr	mineral isochron C	1495 \pm 60	Livingston (1970)
	Rb-Sr	mineral isochron	1630	Livingston and Damon (1968)

Livingston (1969) interprets his 1970 data (presumably updated from Livingston and Damon (1968) as intrusion of a foliated phase of Madera at 1730 \pm 30 with possible intrusion of nonfoliated phases of Madera and metamorphism at 1540 m. y. If the U-Pb zircon dates of Silver (1964) on rhyolites in the Johnny Lyon Hills in the Pinal schist (approx. 1720 m. y.) are correct and if they correlate with metavolcanics at Ray and elsewhere, then the W.R. isochron is too old. Possibly the Madera was contaminated by radiogenic Sr from the Pinal schist during its emplacement. Given that there are at least two kinds of intrusions which have been mapped as Madera, the following scenario might best fit existing data: (1) depletion of Pinal schist (both volcanic and sediments) at about 1720 m. y., (2) regional metamorphism and deformation post-1720 but pre-1660, (3) emplacement of md₁ at about 1650 with accompanying contact metamorphism and deformation, (4) emplacement of md₂ (granodiorite and quartz diorite) at 1540 with

accompanying contact metamorphism and deformation, and (5) emplacement of 1400-1450 m. y. granitic batholiths with accompanying contact metamorphism and deformation. This writer would regard the regional 1720-1660 metamorphism and deformation to correlate with Mazatzal orogeny (Wilson, 1938; Silver, 1965). Post-Mazatzal events may reflect other as yet undefined orogenic episodes.

Pinal Schist

Named by Ransome (1903). Contains numerous lithologies which were hard to separate in mapping. The two principal types are metasedimentary and metavolcanics which generally occur in separate areas and are described below:

Metasediments:

In Telegraph Canyon area: Bluish-gray, fine- to medium-grained quartz muscovite schist and quartz muscovite chlorite schist with some feldspar. South of Telegraph Canyon the schist locally contains abundant porphyroblasts of prismatic chlorite pseudomorphosed after andalusite or sillimanite(?). Pods, veinlets, and veins of white quartz locally abundant. Rock weathers into small flakes and chips.

West of Telegraph Canyon schist is locally more phyllic and feldspathic and in places resembles metarhyolite.

In Ray area (north and west of Ray): Medium- to fine-grained reddish-brown, brown, and gray metagraywackes and arkoses (locally phyllitic). Rock is commonly spotted with porphyroblasts of chlorite and/or magnetite. Spotted appearance of schist near its contact with qmp is produced by the growth of andalusite.

Cedar Mountain (Winkleman quadrangle) and Ash Creek area: Dominantly metavolcanics. Dark to medium light gray, very fine-grained, dense metavolcanics of rhyolite to andasite composition. Lithologic units trend northeast. Separation was difficult and units were only partially mapped. Metavolcanics resemble massive flows, some with finely laminated flow banding, some may have been ash flow tuffs. A small patch of vesicular basalt was observed in the Ash Creek exposure. Cleavage is well developed in metarhyolite or dacite units at Ash Creek. Metarhyolite near Ray has a Rb-Sr age of 1500 ± 100 m. y. which Livingston (1969) interprets as

a metamorphic age. Livingston (1970) further suggests that the primary age of this rock is 1650 ± 100 m. y. Similar rhyolites intercalated in the Pinal schist is the Little Dragoon Mountains, Cochise County, Arizona, yield U-Pb zircon ages of 1720 m. y. Possibly the Rb-Sr age reflects metamorphism related to the emplacement of Madera diorite plutons.

pim Recrystallized and deformed Pinal schist. This rock occurs in proximity to stocks of md and Tqm. Rocks are locally highly deformed and crenulated near plutonic centers. Here, rock is generally a spotted, coarse muscovite schist which is more resistant to erosion than regular pi. Spots are produced by andalusite(?). A highly deformed rock in upper Walnut Canyon west of Teapot Mountain was also mapped as pim.

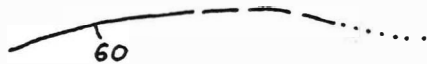
pia Amphibolite. Large east-west to north-northwest-striking lenses up to several hundred feet wide and 1 mile long within Pinal schist west of Telegraph Canyon. Rock is about 80% hornblende. Thought by Schmidt (1967) to have a basic volcanic protolithology.

STRUCTURE

Primary Structures

Planar Elements

Layering...



trace of contact showing dip where measured, dashed where uncertain, dotted where projected or concealed

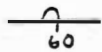
...in sedimentary rocks



strike and dip of bedding



strike of vertical bedding



strike and dip of overturned bedding



strike and dip of overturned overturned bedding ($>180^\circ$ of rotation)

...in metamorphic rocks



strike and dip of bedding plane foliation



strike and dip of vertical foliation



strike and dip of foliation in higher grade or severely deformed Pinal schist (pim)



strike of vertical foliation in "pim"

...in plutonic and volcanic rocks



strike and dip of flow foliation



strike of vertical flow foliation

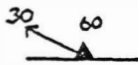
Linear Elements

...in sedimentary rocks



direction of material transport by water as determined from cross bedding, imbrication, or current ripple marks

...in metamorphic rocks



foliation showing trend and plunge of mineral lineation

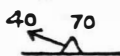


trend of horizontal mineral lineation

...in plutonic rocks



trend and plunge of mineral lineation aligned perpendicular to flow direction (a "b" lineation)



trend and plunge of mineral lineation contained within flow foliation. Direction of flow is at 90° to lineation



trend of horizontal flow lineation

Secondary Structures



bedding showing trend and plunge
of bedding plane slickensides

Faults

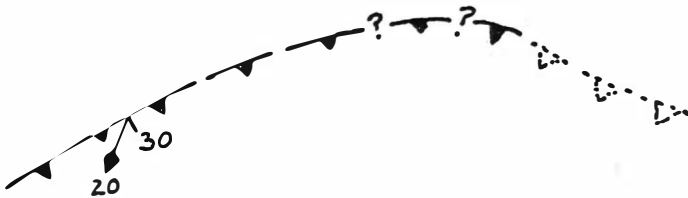
High angle faults:



trace of fault showing dip and trend
and plunge of slickensides where
measured, dashed where uncertain,
questioned where extremely uncertain,
dotted where projected or concealed.
Ball and bar on relatively downthrown
side; arrows show sense of lateral
separation

Low angle faults ($<45^\circ$)...

...on maps



trace of low angle fault showing dip
and trend and plunge of slickensides
where measured, dashed where
uncertain, questioned where extremely
uncertain, dotted where concealed

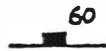
...on cross sections



low angle normal fault, dotted where
projected



low angle reverse fault, dotted where
projected



strike and dip of joint



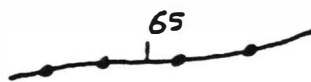
strike and dip of vertical joint



strike and dip of mineralized fracture



strike and dip of mineralized joint

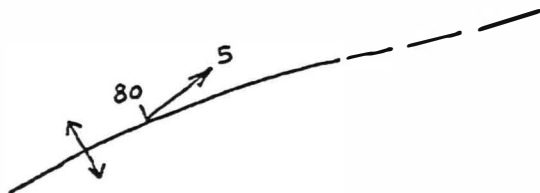


strike and dip of mineralized fault

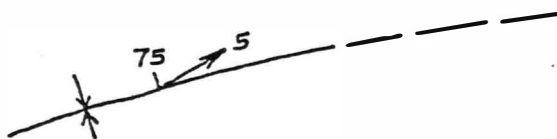
Folds



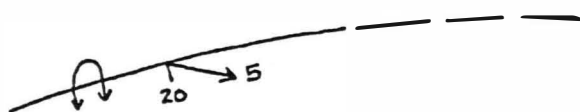
trace of flexure showing dip of axial plane and trend and plunge of axis; arrows indicate direction of limb dips, dashed where uncertain



trace of antiform showing dip of axial plane and trend and plunge of axis, dashed where uncertain. All folds in unmetamorphosed Phanerozoic rocks are anticlines with the exception of Telegraph Canyon fold which is a synclinal antiform



trace of synform showing dip of axial plane and trend and plunge of axis, dashed where uncertain. All folds in Phanerozoic rocks are synclines



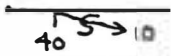
trace of shallowly inclined or recumbent fold showing dip of axial plane and trend and plunge of axis, dashed where uncertain



strike and dip of axial plane of minor antiform showing trend and plunge of axis



strike and dip of axial plane of minor synform showing trend and plunge of axis



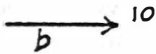
minor fold pair showing strike and dip of axial plane and trend and plunge of axis; S or Z asymmetry determined by viewing down plunge of axis



foliation showing trend and plunge of crenulations



mean trend and plunge of cascade folie melange



mean trend and plunge of boudin axes

STRUCTURAL GEOLOGY

Major structural features of the Ray-Superior map area are shown on Figure 1. Discussion of these features below is arranged chronologically according to orogenic events.

STRUCTURES OF THE SAN ANDREAS OROGENY

High-Angle Normal Faults

Concentrator Fault

The Concentrator fault is the principal structure of the San Andreas orogeny in the Ray-Superior region. It is a major high-angle normal fault with west side down extending southward into the vicinity of Copper Butte. The Concentrator fault dips steeply to the west with normal displacement that involves all stratigraphic units (except the Quaternary alluviums). This is in contrast to Creasey's interpretation (Creasey, 1983) which shows most recent movement on the Concentrator fault as pre-Apache Leap tuff. For example, in the S 1/2 of sec. 36, T 2 S, R 12 E, the Apache Leap Tuff is clearly in fault contact with Precambrian age Madera Diorite and Paleozoic formations on the east. The Concentrator fault cuts all units up to and including the youngest gravels (Big Dome age). The Concentrator fault thus, implicitly cuts the Copper Butte fault, although the intersection of these two faults is covered. However, the Concentrator fault appears to continue south into the hanging wall of the Copper Butte fault. The trace of the Concentrator fault appears to have a left lateral separation south of its intersection with the Copper Butte fault.

Major changes occur along the trace of the Concentrator fault where it crosses the projection of the Last Turn Hill shear zone (see below). Normal separation on the Concentrator fault is much greater north of the Last Turn Hill shear zone than it is south of the shear zone. North of the Last Turn Hill shear zone, normal stratigraphic fault on the Concentrator fault is at least 7000' where the fault transverses the western boundary of the Bowman Basin in the central part of sec. 36, T 2 S, R 13 E. South of the Last Turn Hill shear zone, normal separation along the Concentrator fault is only about 100 to 200 feet, as measured by offsets of Miocene volcanic strata. South of the shear zone, the Concentrator fault appears to be a simple, single strand fault break where it intersects Tertiary volcanic rocks. To the north, the Concentrator fault cuts Paleozoic rocks and relationships are more complex with many parallel fault slivers. These relationships suggest the Concentrator fault may be an old structure which was reactivated in late Tertiary time.

Older mapping by E.D. Wilson shows the Concentrator fault merging into and becoming the Copper Butte fault. In the center of sec. 12, T 3 S, R 12 E, the Copper Butte fault projects

towards exposures of the Concentrator fault in the NW 1/4 of sec. 12. However, the intersection of the faults is covered by Quaternary colluvium. During the mapping, another north-south trending fault not mapped by Wilson or Creasey, was found cutting Picketpost Mountain volcanics in the S 1/2 of sec. 12, and the central part of sec. 13, T 3 S, R 12 E. This fault is on direct projection with the Concentrator fault and is therefore inferred to be a southern extension of it. Because the Concentrator fault cuts all of the Miocene sedimentary and volcanic units, it is inferred to be younger than the Copper Butte fault. Slickenside data along the exposures of the Concentrator fault plunges steeply down-dip to the west or at an oblique angle down-dip to the southeast. North-south striking segments seem to feature dip-slip slickenside data whereas northeast-striking segments feature southwest plunging oblique slickensides. The roadcut exposure we will visit south of Superior is along a northeast-striking segment of the Concentrator fault where it juxtaposes mid-Miocene Big Dome equivalent(?) indurated conglomerates in the hanging wall against Precambrian Mescal Limestone of the Apache Group in the footwall. Excellent southwest-plunging slickensides are present in the plane of the Concentrator fault within the roadcut.

Livingston Fault

The Livingston fault is the westernmost strand of the Mineral Creek fault zone north of Ray. Galiuro-age movements along the Mineral Creek fault zone are discussed in a subsequent section. San Andreas-age normal movement took place along this zone principally along the Livingston fault. As established by surface exposures and drill hole data, the Livingston fault dips steeply eastward. In exposures north of Ray in the SE 1/4 of sec. 2, T 3 S, R 13 E, the structure on trend with the Livingston fault dips west and normally juxtaposes Apache Leap Tuff against Quaternary alluviums. Thus, at least some of the movement along the Livingston fault is of Quaternary age. Terrace alluviums (unit "Qs2") have been offset by this fault. West of Mineral Creek, the Qs2 unit is cut by the fault at the 2200 foot contour. East of Mineral Creek, a terrace alluvium identical to Qs2 is present at about the 2250 to 2300 foot contour. Thus, 50 to 100 feet of Quaternary offset along the Livingston fault is indicated.

Diabase Fault

The Diabase fault is a complex fault zone in the eastern part of the Pearl Handle Pit at the Ray Mine. At its northwest end, the Diabase fault may split where it merges with the Mineral Creek fault zone. To the southeast, the Diabase fault projects parallel to the Big Dome-Apache Group contact at the southwestern border of the Dripping Spring Mountain range. Cornwall and others (1971) infer that the Diabase fault is locally overlapped by the Big Dome Formation. However, exposures along the southeastern projection of the Diabase fault in the Kearney quadrangle are mapped by Cornwall and Krieger (1975) to directly juxtapose Big Dome Formation against Apache Group strata. Unpublished mapping by this author in the Hayden quadrangle farther to the southeast also demonstrates that Big Dome Formation is normally juxtaposed

against Paleozoic rocks west of the 79 Mine. In all of the above mentioned exposures, or its projections dip 50 to 85 degrees west and normally juxtapose mid-Miocene (17 to 14 Ma) Big Dome Formation against older Cretaceous to Precambrian rocks. Thus, it appears that the Diabase fault has experienced post-mid-Miocene normal movements in several areas.

In the Pearl Handle Pit at the Ray Mine, the Diabase fault truncates both the Paleocene age Granite Mountain porphyry and the Emperor fault. From section B-B', Cornwall and others (1971) estimate that the Diabase fault has 1200 feet of normal stratigraphic throw. At least some of this apparent normal displacement is probably of post-mid-Miocene age (see discussion above). The post-mid-Miocene age movements are on-strike with, and in part, coincide with post-mid-Miocene age movements on the Livingston fault segment of the Mineral Creek fault zone to the north.

Bishop Fault

The Bishop fault is a northwest striking, steeply west dipping (dips are 70 to 80 degrees to the southwest) fault in the western part of the Pearl Handle Pit at the Ray Mine. The Bishop fault cuts the Emperor fault and offsets it by a normal displacement of about 30'. The southeastern projection of the Bishop fault is concealed by Ray Mine dump materials. Nevertheless, the Bishop fault is one of the youngest structures at the Ray Mine and is permissively related to the San Andreas orogeny.

Folds

Northeast-Southwest Trending Folds

At the Ray Mine, Phillips and others (1974) describe northeast trending mid-Tertiary arching that parallels the alignment of the Granite Mountain Porphyry stocks. The folding broadly warps mid-Miocene Apache Leap Tuff and Big Dome Formations. In addition, the arching occurs at a location where no major dip-slip motion has occurred along fractures of San Andreas age. Offset increases on the Mineral Creek fault zone northwest of the fold and probably on the Diabase fault southeast of the area. Where the Diabase fault crosses the trace of the arch, some 1200 feet of normal throw is present. This movement however, may be related to Miocene normal faulting (see previous section).

Regional Significance

The Concentrator, Livingston, and Diabase faults are the principal structural expressions of the San Andreas orogeny in the Ray-Superior region. The pattern of the slickenside data discussed above for the Concentrator fault indicates that extension in the Ray area during San Andreas time was along an east-west azimuth. More northeasterly striking segments of the fault indicate that strike-slip components were also locally important and are consistent with a strike-slip trans-tensional

deformation style in areas affected by San Andreas transtension. As such, the Concentrator fault is an example of the Basin and Range stratotectonic assemblage of the San Andreas orogeny (see Keith and Wilt, 1985). No evidence was found during the mapping for San Andreas transpression in the Ray-Superior region. Thus, available evidence indicates that the Ray-Superior region deformed predominantly in transtension during the San Andreas orogeny.

STRUCTURES OF THE GALIURO OROGENY

Low-Angle Normal Faults

Copper Butte Fault

The Copper Butte fault west of Ray is a low-angle normal fault of major extent. It extends southward into the Grayback Mountain quadrangle, through the Kearney quadrangle, (the Ripsey fault of Schmidt, 1971) to the vicinity of Crozier Peak, Winkleman 15' quadrangle, (the Camp Grant fault of Krieger, 1974) and probably extends on to San Manuel. This fault is a member of a group of faults which extend along the west margin of the Tortilla hinge line and as a group is characterized by a period of low-angle normal displacement. One member of this group offsets the San Manuel-Kalamazoo orebody.

The low-angle normal displacement on the Copper Butte fault can be dated in the Ray map area. In the SW 1/4 of sec. 12, T 3 S, R 12 E, Apache Leap Tuff, dated at 20 m.y., lies in low-angle normal fault contact with Pinal Schist and Whitetail conglomerate. The low-angle fault is interpreted to be an imbricate slice of the Copper Butte fault. One mile farther northwest, the Copper Butte fault is overlapped unconformably by volcanics which postdate the Apache Leap Tuff and which yield age dates of 18 to 16 m.y. Thus, the period of low-angle normal faulting occurred between 20 and 18 m.y. It should be noted that this fault may have had an earlier period of reverse displacement, but the present juxtaposition of stratigraphic units indicate the latest normal movement occurred during the 20 to 18 m.y. period. Also, movement on the Copper Butte fault appears to be younger than movement on the Battle Axe fault because of truncation relationships in the SW 1/4 of sec. 12, T 3 S, R 12 E. Geologic relationships to the south do not substantiate, but are consistent with normal displacement along the entire system at about the same time as in the Copper Butte area. For example, in the vicinity of San Manuel, the San Manuel formation is commonly offset by normal displacement, and age dates of the San Manuel yield 24 m.y. Thus, much of the movement in the south is post-24 m.y. Also, the Big Dome formation (14-17 m.y.) is not generally known (with one exception of the White Canyon fault) to be involved in the low-angle faulting, although it occurs in close proximity to normally faulted San Manuel formation. Hence, normal faulting may be pre-17 m.y. in age.

One interesting feature of the Copper Butte fault is the

contrast in structural coherency of the Pinal schist in the hanging wall and footwall blocks. Pinal schist in the hanging wall of the fault is strongly deformed, broken, and shattered. Pinal schist in the footwall block appears to exhibit only the metamorphic structures dating from Precambrian time. This shattering is thought to be related to near-surface movement on the Copper Butte fault under low confining pressure.

White Canyon Fault

During the mapping, a fault not previously mapped by other workers was found in the White Canyon area, west of the Copper Butte fault. Exposures of this fault are best seen along White Canyon in sec. 14, T 3 S, R 12 E. The White Canyon fault probably continues northwesterly into sec. 3, T 3 S, R 12 E, and sec. 34, T 2 S, R 12 E, where it juxtaposes various units of the Picketpost Mountain volcanics against Apache Group and Paleozoic stratigraphy in the footwall. Dips along the White Canyon fault range from 35 to 60 degrees westerly. Slickenside data along the White Canyon fault is invariably dip-slip in nature.

Bowman Basin Fault System

Easterly-dipping Paleozoic and Apache Group strata northeast and south of Bowman Basin in sections 23, 24, 26, and 25 of T 2 S, R 12 E, and sections 29, 30, 31, and 32 of T 2 S, R 13 E, and sections 5, 6, and 7 of T 3 S, R 13 E, and sections 1 and 12 of T 3 S, R 12 E are affected by numerous low-angle normal faults that are herein collectively referred to as the Bowman Basin fault system. These faults generally dip to the southwest from 10 to 70 degrees. Some of the faults are spoon-shaped in plan view (especially those to the south and east of Bowman Basin). The Battle Axe fault in the N 1/2 of sec. 7, T 3 S, R 12 E, is a steeply dipping near-vertical fault which may represent the upturned southern edge of a major low-angle normal fault beneath Lime Point, sec. 6, T 3 S, R 13 E. Slickenside data along various faults of the Bowman Basin fault system consistently plunges to the southwest and averages about S 60 W.

The age of the Bowman Basin fault system is mid-Miocene, as evidenced by tilted Apache Leap Tuff in the upper plates of the faults, especially those north of Bowman basin mapped by Creasey (1983). North and south of Bowman Basin, faults of the Bowman Basin fault system are truncated by the high-angle, normal Concentrator fault.

Emperor Fault

The Emperor fault is a major low-angle fault in the lower portions of the Ray open pits. Exposures at the Ray Mine indicate that the last movement along the Emperor fault occurred after the porphyry copper-molybdenum mineralization and after intrusion of the Granite Mountain porphyry in mid-Paleocene time. If Granite Mountain porphyry in the lower plate of the Emperor fault correlates with Granite Mountain porphyry in the upper plate, then northeastward normal movement of about 1500' is indicated. This

movement would not be enough to offset the hydrothermal alteration zoning documented at Ray by Phillips and others (1984; article is reproduced in this guidebook). The Emperor fault also probably juxtaposed the Pinal Schist over the Apache Group prior to porphyry copper mineralization in the early phases of the Laramide orogeny (see below). The Emperor fault is also cut by the Bishop normal fault which probably developed during the San Andreas orogeny (see above). The low-angle normal fault movement on the Emperor fault is probably of Miocene age by analogy with known Miocene age low-angle normal faults discussed above.

Teapot Mountain Fault

The Teapot Mountain fault is an important structural feature in the Ray area. This high-angle normal fault extends northward from the Ray pit up Mineral Creek and essentially marks the northwestern boundary of the Dripping Springs range. Whitetail conglomerate in the hanging wall on the west is relatively downfaulted against Pinal schist on the east. Where exposed, the Teapot Mountain fault dips 50 to 65 degrees to the west. Drill holes by Kennecott west of the Teapot Mountain fault in the hanging wall as deep as 1700' did not intersect the Teapot Mountain fault. This established that the fault must dip at least 45 degrees to the west.

The Teapot Mountain fault can be traced from the NW 1/4 of sec. 10, T 3 S, R 13 E, north-northeasterly for about two miles. It disappears beneath Quaternary alluvial cover at the mouth of Devils Canyon. The fault may be truncated by a northwesterly striking fault in the NE 1/4 of sec. 34, T 2 S, R 13 E. It is possible however, that the Teapot Mountain fault may project northward beneath the Apache Leap dacite cover and would be present underneath Devils Canyon.

Deep drilling by ASARCO and Inspiration in the Devils Canyon area east of Superior indicates that a major north-trending fault, roughly on projection with the Teapot Mountain fault, is present in Apache Leap dacite subcrop beneath Devils Canyon. The deep drilling indicates a block of Pinal schist to the east, faulted against a block of Whitetail and Paleozoic rocks on the west. Drill holes collared in the east block penetrate +/- 1,000 feet of Apache Leap dacite, a few hundred feet of Whitetail, and then goes directly into Pinal schist or in some cases Schultze granite. Drill holes collared in the west block penetrate +/- 1,000 feet of Apache Leap dacite, up to 3,000 to 4,000 feet of Whitetail conglomerate, and finally penetrate Paleozoic rocks at 5,000 or 6,000 feet. These relationships are similar to those along the Teapot Mountain fault in the Ray area. Here, the block west of the fault contains a very thick section of Whitetail conglomerate, possibly up to 3,000 feet. Like subcrop beneath Devils Canyon to the north, the easterly block of the Teapot Mountain fault is locally overlain by Apache Leap Tuff with a very thin section of Whitetail conglomerate deposited on Apache Group basement in fault blocks east of the Teapot Mountain fault.

The above discussed relationships suggest that the Teapot

Mountain fault and its presumed extension to the north are part of a major post-Whitetail, pre-Apache Leap normal faulting episode. The Teapot Mountain fault is also a major structural boundary in the Ray area. Rocks west of the fault generally dip eastward; those east of the fault dip southerly or shallowly to the west. The major question encountered in the interpretation of the map data was whether the easterly dips in the Whitetail conglomerate in the hanging wall of the Teapot Mountain fault were caused by antithetic rotation of the Whitetail during normal movement on the fault or whether these easterly dips were caused by monoclinical folding of the Whitetail prior to normal movement on the Teapot Mountain fault. In any case, all of the above discussed kinematics pre-date the deposition of the Apache Leap Tuff at 20 Ma.

Two major alternatives could explain tectonics along the Teapot Mountain fault. Monoclinical folding of the Whitetail sediments is a possibility, because dips in this unit become progressively steeper to the west. This suggests a monoclinical bending of the Whitetail sediments towards a monoclinical axis on the west. This same pattern is present to the south in the Hackberry formation stratigraphy of the Kearny area. The normal movement on the Teapot Mountain fault would postdate monoclinical folding of the Whitetail but would predate deposition of the Apache Leap Tuff. This normal movement could be an early harbinger of the post-Apache Leap Tuff low-angle movements on the Copper Butte, White Canyon, and Bowman Basin fault systems. At the time of normal movement on the Teapot Mountain fault, antithetic normal movement took place on the Sleeping Beauty fault (see below).

An alternative view, which many would find equally attractive, is that the Teapot Mountain fault represents the breakaway zone for extensionally-produced growth fault-style half-graben basins. The thick Whitetail exposures west of the Teapot Mountain fault would represent graben fill. As movement along the fault continued, antithetic eastward tilting of the Whitetail section took place. The more shallow dips in eastern exposures could be explained by small-scale angular unconformities that developed in the sedimentary basins during growth faulting. In this view, the Teapot Mountain fault would ultimately flatten downward and at depth, would become a master fault into which the Copper Butte, White Canyon, and Bowman Basin fault systems are rooted. The Apache Leap Tuff would then have been deposited during an overall episode of growth faulting that occurred in syn- to post-Whitetail time (circa 28 Ma?) and ended in late Picketpost Mountain volcanic time (circa 15 Ma). This author's view is that normal faulting, similar to the above scenario, did take place on the Teapot Mountain fault, but it was superimposed on an earlier monoclinical folding of Whitetail formation. Thus, at least some of the eastward tilting is related to normal movement on the Teapot Mountain fault.

Sleeping Beauty Fault

West of Sleeping Beauty Mountain, a north-northeast striking, steeply east-dipping fault named the Sleeping Beauty

fault is present. At its northern end in the SW 1/4 of sec. 2, T 2 S, R 13 E, the fault is apparently truncated unconformably by the Apache Leap Tuff in a manner similar to the Teapot Mountain fault. From here, the Sleeping Beauty fault may be traced for 3 1/2 miles to the south where it apparently terminates near its intersection with the Last Turn Hill shear zone in the NW 1/4 of sec. 8, T 3 S, R 13 E in the Pinal Schist. For most of its length, the Sleeping Beauty fault dips 50 to 60 degrees east and normally juxtaposes lower stratigraphy of the Whitetail conglomerate against overturned, to steeply upright units of Paleozoic and Apache Group rocks. Slickensides along the fault in the NE 1/4 of sec. 5, T 3 S, R 13 E, strongly suggest an episode of normal slip along the Sleeping Beauty fault. The normal slip episode is post-Whitetail and pre-Apache Leap Tuff and would, therefore, be of the same age as normal slip on the Teapot Mountain fault. Evidence for a pre-Whitetail reverse movement on the Sleeping Beauty fault will be developed in a later section.

Reverse Faults

Mineral Creek Fault Zone

The Mineral Creek fault zone is a major fault zone found in the east part of the area mapped. The Mineral Creek fault zone strikes down Mineral Creek north of Ray and probably merges in a complex way with the diabase fault system at, and southeast of Ray. In general, the Mineral Creek fault system juxtaposes a relatively thin section of Whitetail conglomerate-Apache Leap Tuff-Big Dome Formation on the east, against Pinal schist on the west. In detail, the Mineral Creek fault zone is composed of several fault strands. The east-dipping, westernmost fault strand is named the Livingston fault, following the suggestion of Neil Gambell. The term School fault (more broadly used in previous literature) is reserved for that part of the Mineral Creek fault zone which is composed of reverse faults which dip 30 to 60 degrees west and crop out east of the presumed trace of the Livingston fault.

In cross section, the School fault is a low-angle reverse fault near the surface and is interpreted to steepen at depth. The Pinal schist block, west of the Livingston fault, is interpreted to have moved up along a steeply-dipping reverse fault into which the School and Livingston faults merge at depth. It is an open question as to whether the School fault is younger than the Livingston fault or vice-versa. Drill hole information, combined with the map data, suggests that the Apache Leap Tuff has been offset in a reverse manner by the School fault by some 1500 feet.

Sun Fault

The Sun fault is a N 60 E striking, northwest-dipping fault mapped by Fountain (1981) in the west pit at Ray. The Sun fault is on projection with a N 60 E striking, northwest-dipping unnamed fault that traverses the northern pit wall of the Pearl Handle Pit

to the east. This unnamed fault is shown on the map of Cornwall and Banks (1971); it is probably a northeastward extension of the Sun fault. The Sun fault, as defined here, extends northeastward to where it joins the Mineral Creek fault zone and Diabase fault system at a complicated triple junction in the SE 1/4 of the SW 1/4 of sec. 11, T 3 S, R 13 E.

The Sun fault system is permissibly a reverse fault of middle Tertiary age by the following circumstantial argument: South of the Sun fault, a major low-angle fault named the Emperor fault is present. A northeasterly inclined Apache Group section is present in the lower plate of the Emperor fault. Deep drilling (up to 2200') by Kennecott north of the Sun fault has failed to encounter a major flat-lying Emperor fault analog. Also, 1/4 mile southeast of Ray, there is a faulted sliver of Dripping Spring Quartzite in the hanging wall of the Sun fault. This sliver, in part, could represent a piece of lower plate Apache Group that has been reversely upthrown along the Sun fault. If so, the Emperor fault would also have been reversely upthrown by the Sun fault and would now be eroded off in the Precambrian block north of the Sun fault.

The relationship of the Sun fault to the Mineral Creek fault zone suggests that the above postulated reverse movement along the Sun fault would have occurred in mid-Miocene time in concert with reverse motion along the School fault element of the Mineral Creek fault zone. The main evidence for this synchronous timing is that reverse movement along the School fault rapidly dies out along the fault immediately southeast of its intersection with the Sun fault. If the above scenario is correct, then the Sun fault marks the southeastern boundary of a basement wedge of Pinal Schist and Madera Diorite that has moved upward and eastward over mid-Miocene rocks along the School and Sun faults.

Reverse Movement along Low-Angle Normal Faults

Evidence for antecedent reverse movement on the low-angle normal faults is found at two localities. Examination of small fold structures in the Pinal schist indicates possible early reverse movement on the Copper Butte fault. In the W 1/2 of sec. 18, T 3 S, R 12 E, numerous small-scale "S" and "Z" folds of very brittle character deform the Pinal Schist. These folds suggest that northeast shear of possible Late Cretaceous to mid-Tertiary age affected the upper plate of the Copper Butte fault. Whether this is related to reverse slip on the Copper Butte fault is not clear, however, the relationships are permissive.

The best evidence for antecedent reverse slip along the low-angle normal faults is provided by exposures along the White Canyon fault. In the NW 1/4 of sec. 24, T 3 S, R 12 E, just west of well CB-9, exposures along the White Canyon fault display reverse drag of reddish Whitetail lacustrine facies in the lower plate of the fault. However, rocks in the upper plate of the White Canyon fault at this locality are composed of a much younger gravel unit (unit "Tgo"). Therefore, cumulative juxtaposition along the White Canyon fault is normal in nature with the normal

movement postdating reverse movement. Because the reverse drag effects Whitetail conglomerate, the antecedent reverse movement along the White Canyon fault must be Oligocene to early Miocene in age.

Folds

Spine Syncline

In the south-central part of the mapped area, the Whitetail formation, the Apache Leap Tuff, and several units of the Picketpost Mountain volcanics are broadly warped by a synclinal feature originally referred to as the Spine syncline by Eldrid Wilson. The Spine syncline extends from the area of the "spine" in sections 29 and 32, T 3 S, R 13 E, northwestward for some six miles to sec. 2, T 3 S, R 12 E. At its southeastern end, the Spine syncline is a fairly sharp fold that plunges to the southeast where its trace is lost in exposures of the Pinal Schist and Oracle Granite in the SE 1/4 of sec. 29, T 3 S, R 13 E. Dips in each limb at this locality are as steep as 45 to 60 degrees. To the northwest, the Spine syncline is a much more open broad fold with dips in each limb ranging from 10 to 20 degrees.

The Spine syncline folds beds as young as the Big Dome Formation (14 - 17 Ma). Beds of the Upper Picketpost Mountain volcanics which overlap the Copper Butte fault in the SE 1/4 of sec. 2, T 3 S, R 12 E, are also folded by the Spine syncline. Therefore, available evidence suggests that the Spine syncline postdates movement along the low-angle normal faults.

School Fold

North and east of Ray, mid-Miocene Tuff beds that are possibly outliers of the Picketpost Mountain volcanic field (19 - 15 Ma), are folded into a broad to tight syncline. The syncline occurs immediately east of the School reverse fault (in the lower plate) and is thus named the School syncline. The syncline can be traced from the NW 1/4 of sec. 2, T 3 S, R 13 E, where it is truncated by the School fault, two miles southward into the NE 1/4 of sec. 14, T 3 S, R 13 E where it may also be truncated by the School fault. Throughout its length, the School syncline closely parallels the trace of the School reverse fault. The strong spatial correspondence of the School fold and reverse fault suggests that the two are kinematically related. Both structures cut units probably of the Picketpost Mountain volcanics. As such, the School fold and reverse fault are post-18 to 15 Ma and probably formed at the same time as the Spine syncline.

Texas Zone Structures

Last Turn Hill Shear Zone

General Description

An element of the Texas zone in the Ray area may be the Last Turn Hill shear zone which extends in a west-northwest direction

from the west pit portion of the Ray Mine (SW 1/4 of sec. 10 and NW 1/4 of sec. 15, T 3 S, R 13 E) 2 1/2 miles northwest to the San Luis Mine (SW 1/4 of sec. 7, T 3 S, R 13 E). The Last Turn Hill shear zone is about 1/2 mile wide and consists of numerous west-northwest to east-west striking near-vertical shears that cut the Pinal Schist. Farther to the northwest, in the Mineral Mountain quadrangle, several high-angle northwest near-vertical faults occur in the Pinal Schist and are along the projection of the Last Turn Hill shear zone. In between these exposures, an extensive area of middle Tertiary Picketpost Mountain volcanics is present. Picketpost Mountain volcanics are cut by numerous north-south trending normal faults. Several of the normal faults however, bend more northwesterly, or have northwest to east-west strikes where they cross the projection of the Last Turn Hill shear zone beneath the volcanic cover. Also, the Concentrator fault appears to bend from a north-south trace to a northwest trace where it intersects the projection of the Last Turn Hill shear zone.

The Last Turn Hill shear zone appears to be a major crustal break and may be part of a regional west-northwest striking flaw in the Texas Zone. Generally, the rocks north of the projection of the shear zone comprise a terrane of Paleozoic sedimentary rocks strongly deformed by thrusting (see subsequent sections). The rocks south of this zone are crystalline basement rocks. Thus, a net vertical offset is inferred along this fault zone. However, the Last Turn Hill shear zone appears to have had both vertical and left-lateral displacement along its trace. The evidence for left-lateral displacement is the apparent offset of north-south fault structures and dragfolds adjacent to the major shears.

A problem exists in extending the Last Turn Hill shear zone southeastward into the Dripping Springs range. A possible solution to this problem is that the Last Turn Hill shear zone merges with the Diabase fault via the North End faults, bends to the southeast, and forms the southeast boundary fault to the Dripping Springs range. A lesser element may cross over the Dripping Springs range in the vicinity of the Ray silver mines and extend on to the southeast to the vicinity of the Christmas mine where it may become part of the Joker fault and the Christmas fault. The crustal flaw may further extend down to the Christmas area. Southeast of Christmas, several west-northwest structures cut Williamson Canyon volcanics and merge with the Red Rooster fault, which in this area, is the main structural boundary of the northern Galiuro Mountains.

Galiuro-age Movement

Evidence for left slip movement of Galiuro orogeny age exists along the Last Turn Hill shear zone south of Teapot Mountains in sections 8 and 9, T 3 S, R 13 E. Here, the Pinal Schist is juxtaposed against the Whitetail conglomerate by a west-northwest to northwest striking fault that dips 55 to 70 degrees northeast. Bedding attitudes in the conglomerate facies of the Whitetail Formation strike northwest approximately parallel to the trace of

the above mentioned fault. Farther to the north however, the bedding attitudes of the Whitetail Formation change to a north-northeast strike. The overall strike pattern of the Whitetail formation is consistent with left-lateral drag along the above mentioned fault. This drag would have occurred after deposition of the Whitetail formation, and prior to the deposition of the Apache Leap Tuff (about 28 to 20 Ma). Possibly, left slip on this element of the Last Turn Hill shear zone accompanied monoclinical flexing of the Whitetail formation prior to extrusion of the Apache Leap Tuff at 20 Ma.

Regional Significance

The Ray-Superior region contains excellent examples of Galiuro orogeny structural developments. Evidence for both regional northeast-southwest compression and northeast-southwest extension (in some cases on the same structure) is present and demonstrates complexity of interpreting dynamic tectonic developments of the Galiuro orogeny. This author's bias is that the regional dynamics of Galiuro orogeny were driven by weak, northeast-southwest compression (see Keith and Wilt, 1985). This is in obvious contrast to the overwhelming conclusion in the recent literature which interprets mid-Tertiary tectonic developments as products of regional northeast-southwest extension of the crust. Undoubtedly, the low-angle normal faults that are widespread throughout the Ray-Superior region can be interpreted as evidence for regional mid-Tertiary extension. In contrast, the folds and reverse faults, which are unequivocally of mid-Miocene age, can be interpreted in the context of regional compression. The main point is that compelling evidence for both compression and extension is present in the Ray-Superior region and that any interpretation of Cenozoic tectonic development must include all of the above described structures.

STRUCTURES OF THE LATE LARAMIDE

West- to Southwest-Directed Reverse Faults

Sleeping Beauty Fault

East of the Teapot and Sleeping Beauty Mountains, Laramide reverse movement may have taken place along the Sleeping Beauty fault in late Laramide time (60 - 43 Ma; see previous section for location and description of Galiuro age movement on Sleeping Beauty fault). As previously discussed, for most of its length, the Sleeping Beauty fault normally juxtaposes Whitetail formation on the east against overturned or steeply upright Paleozoic and Apache Group strata. At its southern end however, the Sleeping Beauty fault appears to reversely juxtapose Pinal Schist against Pinal Schist that is just beneath the Pioneer Formation of the Apache Group in the S 1/2 of sec. 5, T 3 S, R 13 E. Also, brittle fold data in faulted Pinal Schist along the southern segment of the Sleeping Beauty fault in the NW 1/4 of sec. 8, T 3 S, R 13 E, suggest components of reverse and strike-slip in the fault. Reverse movement on the Sleeping Beauty fault is also

consistent with the geology of the block east of the Sleeping Beauty fault. East and south of the Sleeping Beauty fault, the Whitetail formation depositionally rests on Pinal Schist in the NE 1/4 of sec. 8, and SE 1/4 of sec. 9, T 3 S, R 13 E West of the fault however, thin Whitetail formation rests on upper Paleozoic strata in SW 1/4 of sec. 21, T 2 S, R 13 E.

The relationships are consistent with reverse slip on the Sleeping Beauty fault in pre-Whitetail time (pre 28 Ma) with the uplifted block moving south and/or westerly. This movement would postdate east-directed thrusting on the Walnut Canyon thrust and Telegraph Canyon fold because the Sleeping Beauty fault appears to truncate the Walnut Canyon thrust as well as steeply upright to inverted Apache Group and Paleozoic strata of the displaced portion of the Walnut Canyon thrust-related Telegraph Canyon fold. The inferred southwest-directed reverse faulting is consistent with late Laramide southwest-directed thrusting of synkinematic peraluminous Wilderness assemblage plutons that postdate porphyry copper mineralization elsewhere in SE Arizona (see Keith and Wilt, 1985; Keith and others, 1980).

Southwest-Directed Folds

Belmont Mine Fold

South and east of Superior, a NNW-SSE trending large overturned fold in the Horquilla Formation was mapped by Peterson (1969) near the Belmont Mine. The fold is of interest because the sense of overturning of the middle limb indicates the fold formed in response to southwest-directed shear. Bending of Horquilla strata by the fold predates deposition of the Whitetail formation, which angularly truncates tilted Horquilla strata to the east.

The Belmont Mine fold occurs not far west of the projected trace of the Sleeping Beauty fault beneath the Apache Leap Tuff cover. Conceivably, it could have formed at the same time as inferred late Laramide west-southwest directed reverse movement occurred on the Sleeping Beauty Fault.

STRUCTURES OF THE MID-LARAMIDE OROGENY

Intrusions and Mineralization

Dike Swarms

Immediately south of the Ray porphyry copper deposit, a major east-northeast to east-west striking dike swarm is present. The dike swarm consists mainly of rhyodacite porphyry dike swarms of the Ray plutonic suite. One of the dikes has yielded a K-Ar age of 62 Ma (Banks and others, 1972). East of Mineral Creek, the dike swarm traverses through the northern Dripping Spring Mountains. The swarm terminates at the southeasterly projection of the Last Turn Hill shear zone.

The dike swarm(s) probably intruded east-west to east-

northeast striking tension gashes. Relationships of the dike swarms to west-northwest striking structural elements such as the Last Turn Hill shear zone, suggest the dike swarms were emplaced synchronously with left slip on the west-northwest striking structural elements (see below). Regionally, dike swarms similar to those south of Ray are widespread and may be traced for up to 60 miles along strike. In many areas, the dike swarms bend into parallel with, or terminate at west-northwest striking structural elements. Numerous radiometric dates (for example, see section on Laramide intrusive rocks in this guidebook) establish that the dike swarms were emplaced throughout southeastern Arizona between 70 and 60 Ma and that the entire region was undergoing weak NNW-SSE extension in mid-Laramide time. Mid-Laramide NNW-SSE extension stands in strong contrast with the contractional tectonics that both predate and postdate mid-Laramide structures during the early and late Laramide, respectively.

Porphyry Break

The Granite Mountain porphyry intrusions, at and west of the Ray porphyry copper deposit, are diffused along a N 70 E striking fracture zone referred to as the Porphyry Break (Metz and Rose, 1966). The zone is 3000 to 4000 feet wide and can be traced from the northeast part of the Ray orebody for about two miles to the main Granite Mountain porphyry stock west of Granite Mountain in the southeastern part of the Teapot Mountain quadrangle. The eastern terminus of the Porphyry Break roughly coincides with the southeast projection of the Last Turn Hill shear zone. In detail, the east-northeast striking Porphyry Break exerts a major physical control fracture related to mineralization of the Ray Mine.

The porphyry break can be interpreted in a similar way to the dike and vein swarm data. That is, the Porphyry Break appears to be a N 70 E striking zone of tensional features that were opening in NNW-SSE extension during intrusion of the Granite Mountain porphyry stocks and emplacement of the sulfide system at Ray circa 60 - 62 Ma. The overall regional control on the Porphyry Break could have been deep-seated left slip on west-northwest striking basement flaws along the southeast projection of the Last Turn Hill shear zone beneath the northwest portion of the Dripping Spring Mountains.

Ray Porphyry Copper Deposit

The Ray porphyry copper deposit is the principal economic geologic feature in the Ray-Superior region. It is well described in references included with this guidebook. Of interest here is the setting of the Ray zone sulfide system in its regional tectonic context. Work by Phillips and others (1974) has established that the hypogene zoning patterns have not been significantly offset by any of the structures that traverse the Ray Mine vicinity. These structures include the Mineral Creek fault zone, Diabase fault, Emperor fault, and Sun fault. Phillips and others (1974) state that "the presence of essentially the same kind of alteration and mineralization on opposite sides of all of the major faults that cut the orebody, limits the post-mineral displacement to no more

than a few hundred feet" (page 1249).

The above constraint has strong implications for the thrust juxtaposition along the Emperor fault which requires at least 3000 feet of slip to place Pinal Schist over easterly inclined Apache Group (Phillips and others, 1974). Because post-mineral slip on all structures that traverse the Ray orebody is no more than a few hundred feet, much of the thrust juxtaposition along the Emperor fault must be pre-mineral.

High-Angle Strike-Slip Faults

Last Turn Hill Shear Zone

Left-slip faulting can be inferred to have taken place along the Last Turn Hill shear zone (for location, see previous section) in middle Laramide time. Evidence for strike-slip motion along the Last Turn Hill shear zone is inferred from moderate- to steeply-plunging "S" and "Z" folds in a west-northwest, steeply north dipping strand of the Last Turn Hill shear zone along Highway 177 in the W 1/2 of sec. 8, T 3 S, R 13 E.

Left-slip along the Last Turn Hill shear zone can also be inferred from the relationship between an east-northeast striking quartz vein swarm that intersects the shear zone in the SW 1/4 of sec. 8 and the NE 1/4 of sec. 17, T 3 S, R 13 E. Here, an east-northeast striking, steeply south dipping quartz vein swarm intersects the Last Turn Hill shear zone. Several of the veins bend in, to parallel the shear zone where they intersect it. If the quartz veins are interpreted as gash veins, then left-slip along the Last Turn Hill shear zone can be inferred during the emplacement of the quartz veins.

Left-slip along the Last Turn Hill shear zone is probably of mid-Paleocene age if the quartz veins are Paleocene. The quartz veins cut the northeast portion of the Paleocene age Granite Mountain porphyry stock and locally contain copper mineralization. As such, the quartz veins are probably also Paleocene in age, by analogy with the dated copper mineralization at Ray, two miles to the east.

STRUCTURES OF THE EARLY LARAMIDE OROGENY

Low-Angle Thrust Faults

Walnut Canyon Thrust

The Walnut Canyon thrust, originally mapped by Eldrid Wilson, is one of the major structural features of the Ray-Superior region. The Walnut Canyon thrust is named for exposures in upper Walnut Canyon in the N 1/2 of sec. 5, T 3 S, R 13 E and the S 1/2 of sec. 32, T 2 S, R 13 E.

In general, the Walnut Canyon thrust juxtaposes a semi-

regional sheet of Pinal Schist over younger Apache Group and Paleozoic strata north of the Last Turn Hill shear zone. The Pinal Schist sheet underlies an area of at least 17 square miles. In its western exposures, the Walnut Canyon thrust juxtaposes Pinal Schist over now doubly inverted Apache Group strata in Telegraph Canyon. To the east, the Walnut Canyon thrust juxtaposes Pinal Schist over Mississippian and Pennsylvanian strata in the upper Wood Canyon and upper White Canyon areas. The Pinal Schist-bearing upper plate of the Walnut Canyon thrust is probably present in the area between Telegraph Canyon on the west and Wood Canyon on the east which is largely covered by Picketpost Mountain volcanics. The main evidence for the presence of the plate is the presence of abundant Pinal Schist lapilli in tuff units of the Picketpost Mountain volcanics that presumably overlie the Pinal Schist in the upper plate of the Walnut Canyon thrust lower plate between Telegraph Canyon and Wood Canyon.

Farther to the east, in upper Walnut Canyon, the Walnut Canyon thrust juxtaposes Pinal Schist over Pennsylvanian Horquilla Formation and a fault slice of Troy Quartzite. to the north, in the S 1/2 of sec. 32, T2 S, R 13 E, the Walnut Canyon thrust places overturned, younger Precambrian Apache Group strata, diabase, and Troy Quartzite over easterly dipping Pennsylvanian Horquilla Formation. Still farther north, in the E 1/2 of sec. 29, T 2 S, R 13 E, the thrust juxtaposes doubly inverted (!!) Cambrian and Devonian Lower Paleozoic units against easterly dipping Pennsylvanian Horquilla Formation.

The doubly inverted section in sec. 29 occurs six miles east of the doubly inverted section in the Telegraph Canyon area. In the eastern exposures, the doubly inverted section occurs in the upper plate of the Walnut Canyon thrust, whereas in the Telegraph Canyon area, the doubly inverted section occurs in the lower plate. The doubly inverted sections are inferred to represent the rotated, middle overturned limb of the Telegraph Canyon fold (see below). As such, easterly transport of the detached overturned middle limb of the Walnut Canyon fold is estimated to be about six miles. Slickenside data along or just beneath the Walnut Canyon thrust generally plunges easterly and is consistent with the inferred eastward transport.

In all of its exposures, the Walnut Canyon thrust dips easterly as do Paleozoic and Apache Group strata in the lower plate. The easterly dip is probably not the original dip of the Walnut Canyon thrust. The easterly dip was probably induced by eastward monoclinial tilting and/or easterly antithetic tilting during the low-angle normal fault events that affected the Ray-Superior region during the Galiuro orogeny in mid-Tertiary time. In accord with the thrust model outlined above, the original dip of the Walnut Canyon thrust was probably shallowly to the west or southwest.

In the Ray-Superior region, the Walnut Canyon thrust postdates deposition of Paleozoic strata and predates the porphyry copper deposit at Ray, if the Walnut Canyon thrust is related to

the Emperor thrust (see below). By regional analogy with similar east- and northeast-directed thrust faults elsewhere in southeastern Arizona, the Walnut Canyon thrust is probably an early Laramide Tombstone assemblage structural phenomenon (see Keith and Wilt, 1985). If so, the age of the Walnut Canyon thrust would be about 80 to 70 Ma.

Emperor Thrust Fault

In the bottom of the Pearl Handle and West Pits at the Ray Mine, a major domal-shaped low-angle fault named the Emperor thrust fault by Metz and Rose (1966), juxtaposes Pinal Schist over an easterly inclined section of lower Apache Group and diabase sills. Work by Phillips and others (1974) showed that alteration patterns related to the Ray porphyry copper-molybdenum system (62 to 60 Ma) were not offset by the Emperor thrust. Thus, Phillips and others (1974) inferred that Pinal Schist juxtaposition along the Emperor thrust occurred prior to deposition of the Ray porphyry copper system. The juxtaposition probably also occurred prior to intrusion of the Granite Mountain porphyry (62 Ma); especially if the Granite Mountain porphyry in the upper and lower plates of the Emperor thrust in the Pearl Handle Pit are offset equivalents. Thus, if the above described scenario is correct, the Emperor thrust at Ray predates emplacement of Ray plutonic suite and its related porphyry copper-molybdenum system. Because the juxtaposition on the Emperor fault closely resembles those on the Walnut Canyon thrust are possibly part of the same thrust system. Farther to the south, in the Tortilla Mountains, Krieger (1974) has documented similar, now easterly tilted thrusts that also may be southerly extensions of the Walnut Canyon-Emperor thrust system. Significantly, these tilted thrusts are also intruded by rhyodacite porphyry intrusions similar to the Ray plutonic suite.

Folds

Telegraph Canyon Fold

One of the most spectacular structural phenomena in the Ray-Superior region is the Telegraph Canyon fold. The Telegraph Canyon is named for its exposures in Telegraph Canyon in the SW 1/4 of sec. 29 and the W 1/2 of sec. 32, T 2 S, R 12 E. As presently exposed, the Telegraph Canyon fold is an antiformal syncline. The easterly limb of the fold consists of an overturned, overturned (!!) section of Apache Group sediments.

The Telegraph Canyon antiformal syncline is interpreted to have developed as follows: During the early Laramide orogeny, east-west to northeast compression produced a major overturned fold of the Apache Group and Paleozoic section. Continued compression caused the middle, overturned limb to break. A portion of the overturned middle limb, and the anticlinal hinge of the Telegraph Canyon fold was carried about six miles eastward along the Walnut Canyon thrust. In Miocene time, the

Walnut Canyon thrust, together with the Telegraph Canyon overturned syncline, were passively rotated (top-to-the-east) by antithetic rotation on westerly dipping low-angle normal faults and monoclinical folding in the Teapot Mountain area. The result, in the Telegraph Canyon area was that the Telegraph Canyon overturned syncline was rotated another 60 to 90 degrees easterly resulting in the synclinal antiformal configuration. Thus, in the Telegraph Canyon area, originally horizontal beds of the Apache Group have been rotated (top-to-the-east) up to 255 degrees.

Drag Folds on the Walnut Canyon Thrust

In easterly exposures of the Walnut Canyon thrust, two flexures are present in Paleozoic and Apache Group strata in the upper plate immediately above the Walnut Canyon thrust. In the E 1/2 of sec. 29, T 2 S, R 13 E, an anticlinal synform (upside-down anticline) is present. The eastern limb is simply overturned. The western limb, between the synform axis and the Walnut Canyon thrust is doubly inverted. Beds in this limb have experienced as much as 220 degrees of top-to-the-east rotation. The synform closely parallels the Walnut Canyon thrust for one mile; at its southern end, it appears to be truncated by the thrust. The parallelism of the two structures suggests that the synform is a drag fold along the thrust where the overturned middle limb of the Telegraph Canyon fold has been further dragged by easterly motion related to the thrust. Easterly rotation of the thrust and the overturned middle limb of the Telegraph Canyon fold in mid-Miocene time further enhanced the upside-down aspect of the geology.

To the south, in the S 1/2 of sec. 32, T 3 S, R 13 E, another drag fold, similar to the previously discussed drag fold, is present. Here, steeply dipping, right-side-up Apache Group strata are folded into an overturned configuration immediately east of the Walnut Canyon thrust. These strata are inferred to be in the right-side-up limb of the displaced Telegraph Canyon fold and are dragged into overturned dips by eastward movement along the Walnut Canyon thrust.

SUMMARY OF LARAMIDE, GALIURO, AND SAN ANDREAS OROGENIES IN THE RAY-SUPERIOR REGION

From all of the above text, the following summary of Laramide, Galiuro, and San Andreas tectonics in the Ray-Superior region can be constructed.

- 1) Early Laramide (80 to 70 Ma); East-west to northeast compression; formation of the Telegraph Canyon fold, Walnut Canyon thrust, Emperor thrust, and drag folds along the Walnut Canyon thrust.
- 2) Middle Laramide (70 to 60 Ma); East-northeast weak compression and northwest-southeast extension; emplacement of the Ray plutonic suite (Tortilla quartz diorite, rhyodacite porphyry

dike swarms, Granite Mountain porphyry, and Teapot Mountain porphyry), emplacement of the Ray porphyry copper-molybdenum system, left-slip on the Last Turn Hill shear zone, and emplacement of quartz vein swarm in sec. 17, T 3 S, R 13 E.

- 3) Late Laramide (60 to 43 Ma); Northeast-southwest compression; Reverse slip along the Sleeping Beauty Fault, and formation of the west- to southwest-vergent fold in the Pennsylvanian Horquilla Formation southeast of Superior, Arizona.
- 4) Mid-Galiuro (28 to circa 22 Ma); Northeast-southwest compression; Deposition of Whitetail formation units and subsequent north-south monoclinical folding in the Teapot Mountain area (Whitetail formation is deposited in an initial depocenter immediately east of the monoclinical fold analogous to the Hackberry formation in the Tortilla Mountains to the south). Left-slip on Last Turn Hill shear zone and left drag of Whitetail stratigraphy north of Last Turn Hill shear zone.
- 5) Mid-Galiuro (circa 22 to 20 Ma); Continued east-west compression; Normal west-down movement on the Teapot Mountain fault, and antithetic normal east-down movement on the Sleeping Beauty fault; possible continued deposition of upper Whitetail units, possible reverse movement on proto-White Canyon and Copper Butte faults.
- 6) Late Galiuro (20 to 17 Ma); Continued east-west compression; Eruption of Apache Leap Tuff (20 - 19 Ma), and lower part of Picketpost Mountain volcanics and Big Dome Formation (19 - 16 Ma).
- 7) Late Galiuro (16 to 15.5 Ma); Continued east-west to northeast-southwest compression; Emplacement of low-angle normal faults (White Canyon, Copper Butte, and Bowman Basin faults systems), normal movement on the Emperor fault.
- 8) Late Galiuro (15.5 to 15 Ma); Continued east-west to northeast-southwest compression; eruption of upper Picketpost Mountain volcanics.
- 9) Late Galiuro (15 to 13 Ma); Continued east-west compression; formation of Spine syncline, School reverse fault and fold.
- 10) Early San Andreas (13 to 10? Ma); East-west transtension; eruption of basalt unit in northwestern Bowman Basin.
- 11) Main San Andreas (12? to 8? Ma); Continued east-west transtension Major dip-slip motion on north-south segments of the Concentrator fault, left oblique slip on northeast segments of the Concentrator fault, dip slip on the Bishop, Livingston, and Diabase faults.
- 12) Late San Andreas (10? to 2 Ma); Continued east-west transtension; Deposition of clastic sedimentation in closed, graben- like basins in the Superior and Winkleman areas.

- 13) Late San Andreas (2 to .6 Ma); Continued east-west transtension; Integration of modern drainage systems and formation of erosional terraces.
- 14) Latest San Andreas (.6 to 0 Ma); Continued east-west transtension; normal offset on Livingston fault, and offset of Quaternary terraces, continued downcutting in now completely integrated Gila River drainage system (Mineral Creek and Walnut Creek drainages).

REFERENCES

- Banks, N. G., Cornwall, H. R., Silberman, M. L., Creasey, S. C., and Marvin, R. F., 1972, Chronology of intrusion and ore deposition at Ray, Arizona, Part I, K-Ar ages: *Econ. Geol.*, v. 67, p. 864-878.
- Banks, N. G., and Stuckless, J. S., 1973, Chronology of intrusion and ore deposition at Ray, Arizona - Part II, Fission-track ages: *Econ. Geol.*, v. 68, p. 657-664.
- Barrett, L. F., 1972, Igneous intrusions and associated mineralization in the Saddle Mountain mining district, Pinal County, Arizona: M.S. thesis, University of Utah, 90 p.
- Clayton, L. B., 1975, Chemical classification of the Williamson Canyon volcanics, Pinal County, Arizona: Unpub. KEI-GRLD Rept., 3 p.
- Berry, K., 1975: M.S. thesis, University of Arizona.
- Creasey, S. C., Peterson, D. L., and Gambell, N. A., 1975, Preliminary geologic map of the Teapot Mountain quadrangle: U.S. Geol. Survey Open-file Rept. 75-314, scale 1:24,000.
- Creasey, S. C., and Kistler, R. W., 1962, Age of some copper-bearing porphyries and other igneous rocks in southeastern Arizona: U.S. Geol. Survey Prof. Paper 450-D, Art. 120, p. 1-5.
- Cornwall, H. R., Banks, N. G., and Phillips, C. H., 1971, Geologic map of the Sonora quadrangle, Pinal and Gila Counties, Arizona: U.S. Geol. Survey Map GQ-1021, scale 1:24,000.
- Cornwall, H. R., and Krieger, M. H., 1975a, Geologic map of the Kearny quadrangle, Pinal County, Arizona: U.S. Geol. Survey Map GQ-1188, scale 1:24,000.
- Cornwall, H. R., and Krieger, M. H., 1975b, Geologic map of the Grayback quadrangle, Pinal County, Arizona: U.S. Geol. Survey Map GQ-1206, scale 1:24,000.
- Damon, P. E., 1971, The relationship between late Cenozoic volcanism and tectonism and orogenic-epeiorogenic periodicity, *in* Turkekian, K. K., ed., Conference on "The late Cenozoic glacial age": New York, John Wiley and Sons, p. 15-35.

- Damon, P. E., and Bikerman, M., 1964, Potassium-argon dating of post-Laramide plutonic and volcanic rocks within the Basin and Range province of southeastern Arizona and adjacent areas: Arizona Geol. Soc. Dig., v. 7, p. 63-78.
- Damon, P. E., Mauger, R. L., and Bikerman, M., 1964, K-Ar dating of Laramide plutonic and volcanic rocks within the Basin and Range province of Arizona and Sonora, in Cretaceous-Tertiary boundary including volcanic activity: India, 22nd Internat. Geol. Cong. Rept., pt. 3, proc. sec. 3, p. 45-55.
- Damon, P. E., and Mauger, R. L., 1966, Epeiorogeny-orogeny viewed from the Basin and Range province: Am. Inst. Mining Metall. Engineers Trans., v. 235, no. 1, p. 99-112.
- Damon, P. E., and others, 1970, Correlation and chronology of ore deposits and volcanic rocks: U.S. Atomic Energy Comm. Ann. Prog. Rept., no. C00-689-130.
- Granger H. C., and Raup, R. B., 1964, Stratigraphy of the Dripping Spring quartzite, southeastern Arizona: U.S. Geol. Survey Bull. 1168, 119 p.
- Granger H. C., and Raup, R. B., 1969, Geology of the uranium deposits in the Dripping Spring quartzite, Gila County, Arizona: U.S. Geol. Survey Prof. Paper 595, 108 p.
- Heindl, L. A., 1963, Cenozoic geology in the Mammoth area, Pinal County, Arizona: U.S. Geol. Survey Bull. 1141-E, 41 p.
- Huddle, J. W., and Dobrovolsky, E., 1952, Devonian and Mississippian rocks in central Arizona: U.S. Geol. Survey Prof. Paper 233-D, 112 p.
- Johnson, M. G., and Todd, V. R., 1973, A summary of radiometric age determinations of igneous rocks from southeastern Arizona: Isochron/West, no. 8, p. 1-20.
- Johnson, N. M. Opdyke, N. D., and Lindsay, E. H., 1975, Magnetic polarity stratigraphy of Pliocene-Pleistocene terrestrial deposits and vertebrate faunas, San Pedro Valley, Arizona: Geol. Soc. America Bull., v. 86, no. 1, p. 5-12.
- Krieger, M. H., 1961, Troy quartzite (younger Precambrian) and Bolsa and Abrigo formations (Cambrian), northern Galiuro Mountains, southeastern Arizona: U.S. Geol. Survey Prof. Paper 424-C, p. 160-164.

- Krieger, M. H., 1968a, Geologic map of the Holy Joe Peak quadrangle, Pinal County, Arizona: U.S. Geol. Survey Map GQ-669, scale 1:24,000.
- _____ 1968b, Geologic map of the Brandenburg Mountain quadrangle, Pinal County, Arizona: U.S. Geol. Survey Map GQ-668, scale 1:24,000.
- _____ 1968c, Geologic map of the Saddle Mountain quadrangle, Pinal County, Arizona: U.S. Geol. Survey Map GQ-671, scale 1:24,000.
- _____ 1968d, Stratigraphic relations of the Troy quartzite (younger Precambrian) and the Cambrian formations in southeastern Arizona: Ariz. Geol. Soc., Southern Arizona Guidebook III, p. 22-32.
- _____ 1974a, Geologic map of the Putnam Wash quadrangle, Pinal County, Arizona: U.S. Geol. Survey Map GQ-1109, scale 1:24,000.
- _____ 1974b, Geologic map of the Winkleman quadrangle, Pinal and Gila Counties, Arizona: U.S. Geol. Survey Map GQ-1106, scale 1:24,000.
- _____ 1974c, Geologic map of the Crozier Peak quadrangle, Pinal County, Arizona: U.S. Geol. Survey Map GQ-1107, scale 1:24,000.
- Krieger, M. H., Cornwall, H. R., and Banks, N. G., 1973, The Big Dome formation and revised Tertiary stratigraphy in the Ray-San Manuel area, Arizona, in Changes in stratigraphic nomenclature by the U.S.G.S. 1972: U.S. Geol. Survey Bull. 1394A, p. A54-A62.
- Lindgren, W., 1905, The copper deposits of Clifton-Morenci, Arizona: U.S. Geol. Survey Prof. Paper 43, 375 p.
- Livingston, D. E., 1970, Geochronology of the older Precambrian rocks in Gila County, Arizona: Ph.D. thesis, University of Arizona, 224 p.
- Livingston, D. E., and Damon, P. E., 1968, The ages of stratified Precambrian rock sequences in central Arizona and northern Sonora, in Geochronology of Precambrian stratified rocks - International Conference, Edmonton, Alberta, 1967 Papers: Canadian Jour. Earth Sci., v. 5, no. 3, pt. 2, p. 763-772.

- McDowell, F. W., 1971, K-Ar ages of igneous rocks from the western United States: *Isochron/West*, no. 2, p. 2.
- Meador, 1976: M.S. thesis, University of Arizona.
- Metz, R. A., and Rose, A. W., 1968, Geology of the Ray copper deposit, Ray, Arizona, *in* *Geology of the porphyry copper deposits*: Tucson, University Arizona Press, p. 177-188.
- Nehru, C. E., and Prinz, M., 1970, Petrology of the Sierra Ancha sill complex, Arizona: *Geol. Soc. America Bull.*, v. 81, no. 6, p. 1733-1766.
- Pashley, F. E., 1966, Structure and stratigraphy of the central, northern, and eastern parts of the Tucson Basin, Arizona: Ph.D. thesis, University of Arizona, 273 p.
- Peterson, D. W., 1968, Zoned ash-flow sheet in the region around Superior, Arizona: *Arizona Geol. Soc., Southern Arizona Guidebook III*, p. 215-222.
- _____ 1969, Geologic map of the Superior quadrangle, Pinal County, Arizona: U.S. Geol. Survey Map GQ-818, scale 1:24,000.
- Peterson, N. P., 1938, Geology and ore deposits of the Mammoth mining camp, Pinal County, Arizona: *University of Arizona-Arizona Bur. Mines Bull.* 144, 63 p.
- Phillips, C. H., 1976, Geology and exotic copper mineralization in the vicinity of Copper Butte, Pinal County, Arizona: *New Mexico Geol. Soc. Spec. Pub.* 6, p. 174-179.
- Ransome, F. L., 1903, Geology of the Globe copper district, Arizona: *U. S. Geol. Survey Prof. Paper* 12, 168 p.
- _____ 1904, The geology and ore deposits of the Bisbee quadrangle, Arizona: *U.S. Geol. Survey Prof. Paper* 21, 168 p.
- _____ 1919, The copper deposits of Ray and Miami, Arizona: *U.S. Geol. Survey Prof. Paper* 115, 192 p.
- _____ 1923, Description of the Ray quadrangle: *U.S. Geol. Survey Folio* 217, 24 p.

- Reid, A. M., 1969, Biostratigraphy of Naco (Pennsylvanian) in south-central Arizona: Ph. D. thesis, University of Arizona, 308 p.
- Ross, C. A., 1973, Pennsylvanian and early Permian depositional history, southeastern Arizona: Am. Assoc. Petroleum Geologists Bull., v. 57, no. 5, p. 887-912.
- Scarborough, R. B., 1975: M.S. thesis, University of Arizona.
- Schmidt, E. A., 1967, Geology of the Mineral Mountain quadrangle, Pinal County, Arizona: M.S. thesis, University of Arizona, 111 p.
- _____ 1971, A structural investigation of the northern Tortilla Mountains, Pinal County, Arizona: Ph. D. thesis, University of Arizona, 248 p.
- Schumacher, S., Witter, D. P., Meader, S. J., and Keith S. B., 1976, Late Devonian tectonism in southeastern Arizona: Arizona Geol. Soc. Digest, v. X, p. 59-70.
- Silver, L. T., 1960, Age determinations on Precambrian diabase differentiates in the Sierra Ancha, Gila County, Arizona (abs.): Geol. Soc. America Bull., v. 71, no. 12, p. 1973-1974.
- _____ 1964, The use of cogenetic uranium-lead isotope systems in zircons in geochronology: Geophys. Abs., no 211, item 9.
- _____ 1965, Mazatzal orogeny and tectonic episodicity (abs.): Geol. Soc. America Spec. Paper 82, p. 185-186.
- Simmons, F. S., 1964, Geology of the Klondyke quadrangle, Graham and Pinal Counties, Arizona: U.S. Geol. Survey Prof. Paper 461, 173 p.
- Smith, D., 1969, Mineralogy and petrology of an olivine diabase sill complex and associated unusually potassic granophyres, Sierra Ancha, central Arizona: Ph. D. thesis, California Inst. Technology, 314 p.
- _____ 1970, Mineralogy and petrology of the diabasic rocks in a differentiated olivine diabase sill complex, Sierra Ancha, Arizona: Contr. Mineral. and Petrology, v. 27, no. 2, p. 95-113.
- Teichert, C., 1965, Devonian rocks and paleogeography of central Arizona: U.S. Geol. Survey Prof. Paper 464, 181 p.
- Willden, R., 1964, Geology of the Christmas quadrangle, Gila and Pinal Counties, Arizona: U. S. Geol. Survey Bull. 1161-E, 64 p.

APPENDIX I

Historical Notes and Discussion

HISTORICAL NOTES

The following materials are letters containing discussions between Fred Zoerner and S.B. Keith about some of the regional geologic problems. The discussions are of interest because they are "time capsules" of some of the Kennecott thinking about Ray and its regional geologic context. As there were then, many problems in the Ray regional geology remain unsolved today. The interested reader should compare these discussions with current comments in this field guide (especially the comments regarding the age and tectonics of the Whitetail basin and nature of the Teapot fault).

28 April, 1976

I have read Stan Keith's contribution to the quarterly and would like to make some comments. Some new data also has come in since your visit.

The Ray mineral district is not on a basement cored uplift. It appears to be at or just east of the front.

Although Stan has backed down^{on} a Tertiary age for the "Red Hills granodiorite" his conclusions about mineralization are far fetched. The granodiorite crops out in the chlorite propylitic zone and doesn't affect the alteration pattern. A more leucocratic rock (about 9% chlorite-after biotite?) occurs in the same area farther west. These bodies are well outside the strong LP response and have not been encountered in drilling. While giving his presentation he mentioned a Teapot Mountain Porphyry dike, but it is really a rhyolacite dike, very dissimilar to Teapot.

The "megabreccia block" is distinctly discordant to the strike of bedding in the Whitetail. The long dimension of the block is 30-40° off from my data and 40-70° off from Creasey's data. In contrast the Kearny Megabreccia is a maximum of 10-20° off and usually subparallel to the strike of bedding in the San Manuel. The outcrops in Devil's Canyon may not be of the same block for they lie off trend.

There appears to be problems with the Teapot Fault. The Whitetail basin pinches out on the Dripping Spring Range and the Apache Leap Tuff appears to have draped over the range. If the depositional basin is downdropped relative to its source area, why does it exist to elevations equal to that of the top of the Dripping Springs Range? Using Keith's interpretation, the range should have been buried under the Whitetail. The Teapot Fault is still enigmatic.

Is regional compression really present? Can the crust transmit compressional stress over the distance required by the subduction model? I believe the answer arrived at by many who have studied the problem is no. Is the compression here a local manifestation of vertical uplift due to massive intrusion of the crust by melts from subduction zones? Stan uses "thrusts" for evidence of compression. What pushed them? If they were pushed why are the rocks in the plate not strongly folded? I think body forces of gravity tectonics explains the pattern better.

The Red Hills as a strongly uplifted basement block is questionable. I have seen a block that ripped up through cover, but it also had a rhyolite plug in it.


Mining in a key area northeast of the Pearl Handle has exposed the School Fault as Apache Leap Tuff over rhyodacite tuff. Slickensides show a southwestward movement direction. Mining has not progressed far enough to expose the east dipping reverse fault.

As I pointed out in the meeting, the Rustler does not turn south like I show, but follows its strike as shown at the surface. It is covered by Tertiary rocks and the School Fault. However a NNE-trending normal fault dipping west does exist where I projected the Rustler.

Neil found an outcrop by Little Box Dam that shows Big Dome over rhyodacite tuff. It's location confirms Stan's hypothesis that the School Fault is east of Mineral Creek. The outcrop is in a recently eroded gully.

We are building a good data base, but the tectonic environment of Ray is still poorly understood. Hopefully we can get together when I move to Salt Lake in a few weeks.

Sincerely,



Frederick P. Zoerner

FPZ/jr

18 May, 1976

I have read Fred Zoerner's comments regarding my quarterly report and presentation at Ray and would like to comment on his comments. The response is in approximate order to the points raised by Zoerner.

1. The structural position of Ray. The Red Hills block is not a basement-cored uplift in the classic sense. Rather it is a structurally elevated narrow basement prism or slice which I interpret to have been "emplaced" to its present level by several events of compressive deformation. The mechanism of emplacement is interpreted to be along high-angle reverse faults of the Mineral Creek fault zone which flatten upward. The western boundary of the Red Hills block is marked by the Teapot Mountain fault which appears to be a high-angle normal fault with west side down. The cumulative normal movement on the Teapot Mountain fault has left the Red Hills block relatively high. The south end of the Red Hills block is marked by the North End fault system. The exact nature of this fault is presently equivocal because Pinal schist logged in holes north of the fault may be Pioneer formation of the Apache group. My current thinking on the North End fault zone is that the Red Hills block is up relative to the Ray orebody in the Pearl Handle pit south of the North End fault. This is consistent with the new pit mapping north of the Pearl Handle pit by Steve Hoelscher. However, the argument has been made by the Ray people that the Pinal schist/Apache group juxtaposition with Pinal schist relatively up to the north is illusory because the Pinal schist is allocthonous resting in the upper plate of the Emperor fault. Reinterpretation of existing drilling and new drilling would be needed to substantiate either model. For now, I prefer the interpretation that the Pinal schist north of the North End fault zone in the Red Hills block is autocthonous and that the Emperor fault-- if it exists north of the North End fault zone-- has been faulted up and subsequently removed by erosion.

2. Red Hills mineralization and "Red Hills granodiorite." Subsequent mapping has established that Red Hills granodiorite is very likely Madera diorite, for a rock petrographically identical to the Red Hills was found in

the Dripping Spring Mountains to be depositionally overlain by younger Precambrian Apache group rocks. Nevertheless, the Madera diorite does intrude an older gabbroic or noritic rock within the Red Hills block which has also been called Madera diorite. A rock petrographically identical to this rock outcrops extensively in the Mineral Mountain and Teapot Mountain $7\frac{1}{2}$ minute quadrangles and is referred to as the Madera diorite in mapping by Creasey, et al. (1975) and Schmidt (1966). The rock is referred to in my mapping tentatively as the Telegraph Canyon norite for exposures in the Telegraph Canyon area of the Mineral Mountain quadrangle. Petrography is required to reliably establish a rock name.

As both of these rocks are older than 1.67 b. y., they obviously cannot determine any alteration pattern which is of necessity superimposed on such rocks. I thought I gave this impression at the Ray talks. I still argue that the dike in dispute is identical to rocks at the type Teapot Mountain porphyry locality on the southeast slopes of Teapot Mountain. It is interesting that Zoerner in his 1975 Red Hills mapping labeled this as Teapot Mountain porphyry (Ttm) although the more recent editions of this map show the dike as rhyodacite porphyry (Tkr). In any case mineralized fractures clearly cut this rock.

3. The "megabreccia block." For my money the megabreccia landslide origin is still the best bet. The compiled strike and dip data plus my own data do not show that great a discordance. Some discordance should be expected as the encasing Whitetail is a fanglomerate. Strikes and dips in fanglomerates on a local scale can vary considerably. An impressive argument for a landslide origin is the internal fabric of the megabreccia. Regardless of origin, the blocks are descriptively a classic megabreccia, i. e., a monolithic internally brecciated rock. The "crackle breccia" texture implies that movement occurred throughout the entire block and was not restricted to specific fracture sites as one observes in faulted blocks. Although obviously less coherent, landslides feature a fabric where every clast within the landslide mass has moved relative to its neighbors. I have never observed crackle breccias within even the most highly faulted rocks, and the Dripping Spring Mountains are one of the most highly faulted mountain ranges I know of. Despite the high density of faults in the Dripping Springs, the rock within each fault block is unbrecciated. In contrast, clasts within obvious landslide masses in the Dripping Spring Mountains and Dripping Spring Valley are internally shattered even if they maintain their stratigraphic integrity.

4. The Teapot Mountain fault and Whitetail basin of deposition. Fred's Whitetail basin argument is hard to understand. The Whitetail basin was developed prior to 32 m. y. Deposition of the Apache Leap tuff at 20 m. y. does not have anything to do with Whitetail depocenters. East or southeast of the Teapot Mountain fault the Whitetail thicknesses range from several hundred feet to zero. The geology clearly indicates that the

Whitetail thins to the east. In contrast, west or northwest of the Teapot Mountain fault Whitetail is in probable excess of 5,000 feet. Such facts clearly suggest that the Teapot Mountain fault separated a potential source high from a basinal low to the west. Drilling in the Apache Leap tuff plateau to the north suggests analogous relations (see Ray notes).

Subsequent tectonics (post-32 and pre-20 m.y.) raised the Whitetail basin relative to the Red Hills block via tilting. By 20 m.y. erosion had beveled the area flat such that Apache Leap was extruded over a relatively flat surface that included Whitetail rocks west of the Teapot fault and pre-Whitetail rocks east of the Teapot fault. The resulting flat-lying sheet of dacite was then tilted by broad-folding which was locally "enhanced" by reverse faulting along preexisting fractures (e.g., the Mineral Creek fault zone). The result was northeast-dipping Apache Leap tuff on Teapot Mountain, a synclinal low in Mineral Creek, southwest-dipping Apache Leap tuff east of Mineral Creek fault zone, and a possible anticlinal crest over the northern Dripping Spring Mountains at Government Mountain. The timing of this folding is post-16 m.y. as Big Dome age rocks are also folded. Post-Apache Leap tuff displacement on the Teapot fault is minor (if there is any at all) for Apache Leap tuff can reasonably be projected from Teapot Mountain to Mineral Creek without any displacement. The last major amount of normal displacement on the Teapot Mountain fault appears then to be post-Whitetail (32 m.y.) but pre-Apache Leap tuff (20 m.y.).

5. Compression or vertical uplift. The question of regional compression versus vertical uplift is an academic Pandora's box. I maintain that the regional folding and reverse faulting, which is geometrically real, is best explained by compression. What is more important, however, is that for places like Ray we understand and reach agreement about the geometry of the geology that we are working with in time and space. The dynamic causes of such a geometry is at the practical level of secondary importance. I am convinced that the detailed mapping by Kennecott north of Ray has shown just how poorly we do understand the tectonic setting of complex places like Ray. The party line in southeast Arizona is that there are two principal periods of post-75 m.y. deformation: Laramide (75-50 m.y.) and Basin and Range (40-0 m.y.). The mapping in the Ray area alone has established that there are not two but six periods of major deformation!

- 75-50 m.y. - north-northwest folding and low-angle reverse faulting
- 50-32 m.y. - north-south fault-bounded basins (normal faulting)
- 32-20 m.y. - reverse faulting and tilting (folding?)

- 20-18 m. y. - low-angle normal faulting
- 16-12(?) m. y. broad northwest-trending folding and reverse faulting (wrench faulting)
- 12(?) - 0 m. y. north- to northwest-trending basin and range normal faulting.

There are five periods of postmineral deformation to move and jostle orebodies. This structural complexity may account for some of the exploration frustration at places like Copper Butte and Pioneer-Alabama. In my mind, further mapping of this kind can only be beneficial for it will of necessity give us more sophisticated exploration constraints in existing orebodies as well as wildcat prospects. Information gained by mapping is comparatively cheap compared to drilling or geophysics.

Sincerely yours,

Stanley B. Keith

SBK:gp

MISCELLANEOUS RAMBLING DISCUSSIONS (circa 1976)

Normal movement probably occurred along bounding faults between the compressive episodes, but the overall effect is elevation of the central Pinal schist block relative to the adjacent blocks. The faults bounding this crystalline block are thought to be steeply dipping at depth. Near surface under low confining pressure they attain low dip angles as the material expands laterally. The most recent compression of upper Tertiary age predates the movement on the Concentrator fault and the Basin and Range extensional event. This upper Tertiary compression appears to fold Galiuro volcanic rocks, dated at 20 m.y., and the Big Dome formation, dated at 14 to 17 m.y. Formation of the Spine syncline in the Copper Butte area is post-20 or 18 m.y. True Basin and Range structure is dated as post-14 m.y. Thus, the late compressional event appears to have been active approximately 16 to 17 m.y. ago. The folding in that area appears to record effects of a regional compressional late Tertiary event older than displacement on the Concentrator fault, the Diabase fault, and the Livingston fault of the Mineral Creek fault zone. Some of the movement appears to be very recent; displacements occur in some of the most recent Pleistocene terrace gravels north of Ray.

Megabreccias

A large block of shattered Paleozoic rocks enclosed in Whitetail conglomerate occurs in the hanging wall of the Teapot Mountain fault. Origin of this block is controversial. F. Zoerner contends that this is a fragment of basement, probably faulted into place. The block contacts do not parallel attitudes of the enclosing Whitetail sediments, and the block appears to be oblique to bedding. S. Keith contends, as Creasey that the overall trend of the Paleozoic block is subparallel to the strike of the Whitetail sediments. Secondly, the block is internally shattered and brecciated similar to the Kearny megabreccia. Thirdly, the stratigraphic section within the shattered blocks is telescoped north, presumably by internal bedding plane faults which have faulted out less competent units and retained more resistant units. This is thought to have been the result of "landsliding" under low confining pressure. Fourthly, nearby diabase and Apache group sediments do exist as a megabreccia deposited upon Whitetail conglomerate in Devils Canyon, one-quarter mile upstream from the confluence with Mineral Creek(?).

Keith interprets the Paleozoic block as a megabreccia or a slide block, the source of which is the relatively high crystalline block between the Teapot Mountains and Mineral Creek faults. Clastics and megabreccia blocks slid off into the developing Whitetail basin to the west. This event is thought to be pre-32 m.y., which is the youngest age obtained in the Whitetail conglomerate. Actual age of the deposition may extend back into Eocene time. The Whitetail formation then is thought to

be deposited in a fault trough, and the argument can be developed that this fault trough formed in response to rifting or Basin and Range-style structure which is post-Laramide and pre- to mid-Tertiary in age. The southward extension of the Teapot Mountain fault is not well defined. It can be traced to about 1,000 feet north of the North End fault in the vicinity of Red Hills. Somehow, the Whitetail basin must truncate or be truncated by the Last Turn Hill zone. In any event, the Whitetail section markedly thins to the south toward the Last Turn Hill zone and to the east of the Teapot Mountain fault.

Tertiary Stratigraphy

Stratigraphy of the upper post-Whitetail Tertiary gravels used in this study is as follows: The oldest unit is the San Manuel formation, a sequence of tilted gravels dated at 24 to 18 m.y. This is overlain unconformably by generally gently inclined or horizontal gravels of the Big Dome formation dated at 14 to 17 m.y. These are overlain unconformably by the Quiburis formation dated at 5 m.y., and unconformably above this are small patches of terrace gravels which appear to be about .01 to .6 m.y. in age. The Big Dome formation is largely gravels in the vicinity of Kearney. In the vicinity of Ray, significant amounts of rhyolite Tuff interfinger with the gravels. In the Copper Butte area, age-equivalent rhyolite Tuffs and flows exceed in volume the Big Dome-equivalent gravels.

Summary

In summary, the area north of Ray is a block of ground which has alternatively been under compression in Laramide time, then a release of compression and perhaps active rifting. Further compression in mid-Tertiary time, release, and then a late Tertiary compression with final release during development of Basin and Range structure. It is suggested that the Dripping Springs range acted as a buttress during these various compressional events, and the response of the Dripping Springs range to this deformation has been to strongly shatter and fault the rocks exposed.

Dips in the Whitetail conglomerate were established during rotational tectonism associated with a compressional event between 24 and 20 m.y. The Whitetail formation was rotated at the same time the San Manuel formation was rotated. In the Ray area, this rotation predated the 20 m.y. Apache Leap Tuff. Keith believes that the field evidence supports the idea that much of this rotation was in response to compressive stresses as it is closely associated in time and space with the reverse movement of thrusting on faults. Slickenside directions indicate that the compressive tectonic transport has been in a northeast-southwest direction, and the subsequent tensional tectonic transport has been in the very same direction, only the sense of movement has been reversed. Normal faults do not seem to have produced any associated significant rotation of the blocks. Most of the steep dips in the map area have been produced by folding. This is shown to be the case in the Telegraph Canyon area.

Exploration Significance

Possible exploration significance results are as follows:

1. The Red Hills sulfide system is probably autochthonous. Evidence for a low-angle fault underlying the sulfide system is not present.

2. Possible deep mineralization may be present west of the surface trace of the Teapot Mountain fault, but this mineralization would have to be tested by very deep drill holes. Keith suggests that DDH 1007 did not intersect the Teapot Mountain fault. It is possible that after passing through a thick section of Whitetail conglomerate, this drill hole intersected Apache group megabreccia and finally Precambrian Pinal schist in the hanging wall of the Teapot Mountain fault.

3. Further mapping has established that the granodiorite or quartz diorite in the Red Hills area probably is a phase of the Madera diorite. Similar granodiorite is exposed in the Dripping Springs range overlain unconformably by Apache group sediments. The Laramide age suggestion of Keith (1976) is thus invalid.

4. The most attractive areas for exploration in the Red Hills area are the south and southeast of the present drilling between the Red Hills area and the Ray pit.

5. Neil Gambell maintains that the sulfide system at Red Hills and that of the Ray deposit are separate systems. This argument is based mainly on independent patterns of alteration and mineralization. The Red Hills system is younger than Teapot Mountain porphyry, as mineralization in the Red Hills area cuts that igneous rock type.

6. Geologic mapping by Keith has provided some evidence explaining the source of the aeromagnetic anomaly in the White Canyon area. The anomaly is centered in the area of Paleozoic rocks which have been extensively intruded by basaltic sills. Similar basaltic rocks intrude Paleozoic sediments in the Galiuro Mountains, and these sills are thought to be related to the Williamson Canyon volcanic sequence.

7. Amount of movement on the Copper Butte fault has not been established definitely. However, Keith regards displacement up to about 1 mile as possible, with the hanging wall having moved westerly. Movement of the upper plate of this fault from Ray is very unlikely.

8. The Concentrator fault is well exposed in road cuts northwest of Ray. Slickensides exposed in these cuts show that latest movement on the Concentrator fault is not entirely dip slip. The slickensides rake off to the southeast. This implies that the Magma vein, which is offset by the Concentrator fault, is not displaced purely by dip-slip movement but may have been displaced also to the south.

9. Scattered mineralization along east-west fractures cutting Paleozoic sediments in the Teapot Mountain quadrangle is regarded as possible Magma-type vein mineralization but has no economic value. The mineralization is simply too sparse to be of any interest.

In summary, the best mineralization exposed in the Ray mapping area is that in the Red Hills area. Possible deep exploration potential exist in the footwall of the Teapot Mountain fault concealed by postmineral Whitetail conglomerate in the hanging wall. The fault block of Pinal schist containing the Red Hills mineralized area is a block of very large postmineral-positive structural relief. Mineralization exposed probably represents the deep expression of a porphyry system. Pre- or postmineral rotation of the mineralized block is problematic.

Keith's mapping at Ray has failed to generate any new exploration targets in the Ray area. In the Copper Butte area, the exotic mineralization at Copper Butte appears to be offset by a strand of the Concentrator fault. Additional reserves of low-grade oxide copper mineralization may be encountered by drilling across the Concentrator fault from the Copper Butte deposit. The source of the exotic copper mineralization at Copper Butte remains a mystery, probably the copper was derived from the same source as the red schist facies of the Whitetail formation. Keith's mapping north of Copper Butte failed to disclose any outcrops of red schist in place in the Pinal schist units mapped.

ADDENDUM TO STAN KEITH'S RAY REPORT

Bowman Basin Fault System (Plates II, VIII, and IX)

Preparation of structure cross section (Plates VII and IX) for the Ray map area provides new information on the Bowman Basin fault system.

The Bowman Basin fault system is a series of low-angle, spoon-shaped, imbricate gravity glide faults lying north of the Battle Axe fault zone. The Bowman Basin fault itself is considered to be the low-angle fault which runs up along Highway 177 to just west of Walnut Gap, then bends and continues to the west south of the feature known as Bowman Basin (see index map which accompanies Stan Keith's report).

The west end of the Bowman Basin fault appears to be truncated against the Concentrator fault. In the S 1/2 of sec. 36, the fault dips about 20 to 30 degrees to the west; slickensides in the fault plane trend S 70 W and plunge about 15 to 30 degrees indicating that low-angle normal movement was from east-northeast to west-southwest. This low-angle normal movement appears to have been cut by high-angle normal movement related to the last movement on the Concentrator fault.

Another group of low-angle faults lies north of Bowman Basin. These structures are mapped by Creasey and can be viewed from Bowman Gap looking north. Large landslide-like blocks of Paleozoic rocks apparently have shifted westward from Apache Leap in this area. The low-angle normal faults in the Bowman Basin area may be part of the same system of low-angle gravity glide features found farther north toward Superior. All of these low-angle faults may be soled or floored into one large low-angle fault which Keith terms the Bowman Basin fault.

Age relationships of these low-angle faults to the Concentrator fault suggest that the basin formed to the west in the vicinity of Florence sometime before movement on the Concentrator fault. The low-angle faults represent caving off of large blocks from the plateau-like area of Apache Leap, and, under the influence of gravity, these blocks moved westward into the basin. This structure is thought to be analogous to large similar structures along the margin of the Colorado Plateau (e.g., near the Grandwash cliffs, northwest Arizona).

Bowman Basin is a low area in which erosion has removed hanging wall rocks and exposed relatively less-deformed rocks in the footwall of the Bowman Basin fault. Rocks of the upper plate are strongly deformed, cut by normal faults, and show rotation of blocks. Slickensides are abundant on small normal faults, and they consistently trend N 60 E. This structural pattern is consistent from Walnut Gap up to the town of Superior. This entire region seems to be characterized by low-angle gravity glide faults which have moved from the Apache Leap plateau westward toward Florence Basin.

Structural relationships between the Bowman Basin fault and the Concentrator fault as outlined above, creates some geometrical problems in interpretation. The Bowman Basin fault is not found west of the trace of the Concentrator fault, yet if the normal movement on the Concentrator fault is younger than the Bowman Basin fault, the latter should lie at depth, west of the Concentrator fault.

Tortilla-Northern Galiuro Mountains Cross Section C-C' (Plate XII)

The Romero Wash fault is interpreted as a folded thrust. Structure beneath the San Pedro River Valley is thought to be broad, open folds in the "foreland" of the monoclinial belt. Thicknesses of mid-Tertiary volcanic rocks and sedimentary rocks shown on the cross section should be considered to be probable minimum thicknesses. A significant feature of the mid-Tertiary geology is the requirement that the west margin of the Galiuro Mountains be bounded by a major west-dipping normal fault is interpreted as near vertical and could flatten at depth. The west side of the San Pedro River Valley is not bounded by a comparable Basin and Range fault.

Crozier Peak Structure Cross Section A-A' (Plate IV)

The Smith Wash fault near Crozier Peak is interpreted as a

low-angle reverse fault which steepens at depth. The cumulative reverse motion on this fault is contrary to the displacement shown on Medora Kreiger's map. A late period of normal movement has dropped the San Manuel formation back to the west, but this displacement is relatively minor compared to the earlier reverse movement. Earlier interpretation of last year of the Smith Wash fault by Keith show that the fault dip flattens with depth. The dip is now thought to steepen with depth to conform with the concept of compressive origin of the monoclinial uplift.

Tortilla-Northern Galiuro Mountains Cross Section B-B' (Plate XI)

The structural interpretation along this section is similar to that along section C-C' (Plate XII), specifically with the folded Romero Wash fault's gently warped and folded sediments beneath the San Pedro River Valley and reverse movement on the Smith Wash fault. The Camp Grant fault, a low-angle normal fault, is located at the west edge of this section. Very reliable offsets along the Camp Grant fault indicate about 1.5 miles of normal dip-slip movement.

Ray Structural Study Cross Section B-B' (Plate IX)

This section contains several dog legs in order that the section passes essentially normal to the structural grain and also so that the section can maximize use of surface information from diamond drill holes in the Ray mine area. Beneath Teapot Mountain, the Whitetail formation is thought to rest unconformably, but nearly parallel to underlying beds of Precambrian Pioneer formation. The Pioneer formation has moved laterally and produced a megabreccia on the east which grades into relatively undeformed Pioneer formation directly beneath Teapot Mountain. Movement of the plane of dip along the contact between these formation is from west to east.

The Ray structural cross sections (Plates VIII and IX) and structural development of the Ray area may best be described in age sequence. The structural cross section are an attempt to present an interpretation which is consistent with field observations with paleogeographic constraints.

The oldest major flat thrust structure in the Ray area is thought to be the Walnut Canyon thrust which is shown on the west edge of the cross sections. It is thought to be caused by a compressive event, and it is associated with extreme crustal shortening. The Telegraph Canyon fold, a large recumbent fold of nappe-like dimensions, has been chopped off by the Walnut Canyon fault, and part of this recumbent fold has been thrust eastward to the vicinity of Walnut Canyon. The overturned beds east of the highway represent the middle limb of this recumbent fold; the roots of this fold are in the Telegraph Canyon area. The crustal shortening implied by the inferred movement on the Walnut Canyon fault is about 8 or 9 miles. If the folded beds are restored to a horizontal position, then the inferred shortening is about 10 to 12 miles. This large-scale thrusting is one of the earliest events recorded in the structure of the Ray area, and pieces of

the Walnut Canyon fault are preserved across the structural cross section.

Monoclinical uplifts of the type found farther to the south, if present in the Ray area, postdate the Walnut Canyon thrust. The recumbent fold and associated thrust is thought to have formed under shallow cover, probably related to an uplift to the east. The tectonic slip line is from west to east or from southwest to northeast. The age of the Walnut Canyon fault is not well bracketed. One piece of relevant data is found in upper Arnett and upper Walnut Canyon where a mineralized fault cuts and offsets the Walnut Canyon fault. That offset can be interpreted several ways. The most simple explanation is that the high-angle fault offsets the Walnut Canyon fault and was later mineralized. This mineralization is similar to mineralization in the Superior area which is associated with the Laramide Schultze granite. This would date the fault as older than Laramide mineralization. Another interpretation is that there has been postmineral reactivation on the mineralized fault and that second period of movement offset the Walnut Canyon fault. In this case, the Walnut Canyon fault could be postmineral or post-Laramide.

Correlation of Low-Angle Faults

Upon completion of the structural cross sections, it became apparent that the Walnut Canyon fault, the Copper Butte fault, and the Emperor fault may all be part of the same coherent thrust sheet. If this hypothesis is correct, then a reliable date on the thrusting may be obtained in the Ray area where the patterns of mineralization at Ray are superimposed upon the Emperor thrust fault and the mineralization at Ray is thought to have been emplaced into a thrust faulted terrane. This means that the Granite Mountain porphyry, the porphyries at Ray, and mineralization has intruded the Emperor fault, and by implication, the Copper Butte fault. Thus, the major low-angle displacement would be pre-62 m.y. Warping and folding of Laramide to mid-Tertiary age has deformed the Emperor and Copper Butte faults. In addition, low-angle normal movement along the Copper Butte and Emperor faults has occurred and is probably middle to late Tertiary in age. This late normal movement on the Copper Butte fault may be about 1 mile.

The low-angle thrust fault system of which the Walnut Canyon, Copper Butte, and Emperor faults are related cannot be traced much farther north than the Ray map area. There is no evidence, for example, that low-angle thrusting is present in the area of Superior. To the south of Ray, however, one may correlate the flat faults at Ray with the Romero Wash fault in the vicinity of Crozier Peak. Here, the Romero Wash fault has been emplaced and then later folded by the monoclinical event and intruded by an 80.6 m.y. sill. If this correlation is correct, then the low-angle thrusting could be of regional extent, extending at least from the Ray vicinity down into Crozier Peak, Winkleman, Saddle Mountain and probably farther south where the Romero Wash fault is concealed by alluvium, and could be early Laramide (i.e., late Cretaceous) in age. Thus, a large area could be involved in this premineral thrust event.

APPENDIX II

"The Ray Orebody"

by

Donald S. Fountain

THE RAY OREBODY

BY

Donald S. Fountain
Division Geologist
Ray Mines Division
Kennecott Minerals Company

Presented to

The Arizona Geological Society
Field Trip No. 2
March 17, 1981

TABLE OF CONTENTS

	<u>Page</u>
Tour Route Map	1
Description of Stops	2
Introduction	4
Lithologies	4
Diagram of Ore Related Rock Units	5
Stratigraphic Section, Ray Area	7
Geologic Map	8
Geologic Map Explanation	9
Geology-Ore Distribution Sections.....	10
Ore Type Distribution	14
Ore Distribution Map	15
Zoning	16
Structure.....	17
Generalized Cross Section.....	21
Summary	23
References	25

STOP 1

Stop One is located on Section A-A' near A' on the 2490 level.

To the north is Ray's central silicate mining area. The stop with regard to the hypogene zoning is located on the east edge of the ore shell.

The diabase to the east is pyrite halo, sulfides are 3 volume percent, the chalcopyrite to pyrite ratio is 1:10. Biotite alteration is moderate with relict db texture still present. Supergene alteration is dominated by jarosite and clay alteration.

Looking west along A-A':

The area immediately below is our South Silicate mining area.

The road running along the Pearl Handle Pit edge is the old dike road, (2000 elevation). Paralleling this road is the basin bounding Diabase Fault.

The Diabase Fault bisects the hypogene system and establishes a boundary between the silicate and sulfide ore being mined.

Looking into the Pearl Handle Pit keep in mind the mining operation has developed a window through the upper plate of the Emperor Fault. This window exposes the Apache Group rocks, including the diabase, which have been down dropped on the west side along the Diabase Fault.

The mining area just north of the Pearl Handle is primarily stripping in the leached cap. The color change from red brown to black green in the middle of the bench is the Apache Group, rock contained in a horst block bounded by the Diabase and North End Faults.

STOP 1 (cont'd)

In the distance you can see the West Pit, which is located in the enriched pyrite halo. The bulk of the secondary sulfide ore produced at Ray has come from this area, through the underground block cave operations prior to 1955, and open pit operations since. Development of the chalcocite blanket was influenced by the east dipping West End Fault, (the slope failure along the west end is easily recognizable), the south dipping North End and the north dipping Sun Fault. The apparent extension of the pyrite halo is due, in part, to rotation of west ore shell on the Diabase Fault.

STOP 2

The second stop is in the Cairo area of the Pearl Handle Pit. The 1700 mining level is currently providing the bulk of our sulfide ore. Along the southern end of the level is an exposure of the Diabase Fault with upper plate Pinal Schist (west side) against diabase. Moving to the north along the bench, change in rock types demonstrates the effect rock type can have on the minerals formed.

STOP 3

The third stop is on the 1660 level in the Pearl Handle Pit. Exposures of the Emperor Fault overlying diabase and Apache Group rocks demonstrate some of the difficulty in recognizing structures from drilling. Granite Mountain Porphyry, which was the mineralizer at Ray, can also be viewed at this stop.

THE RAY OREBODY

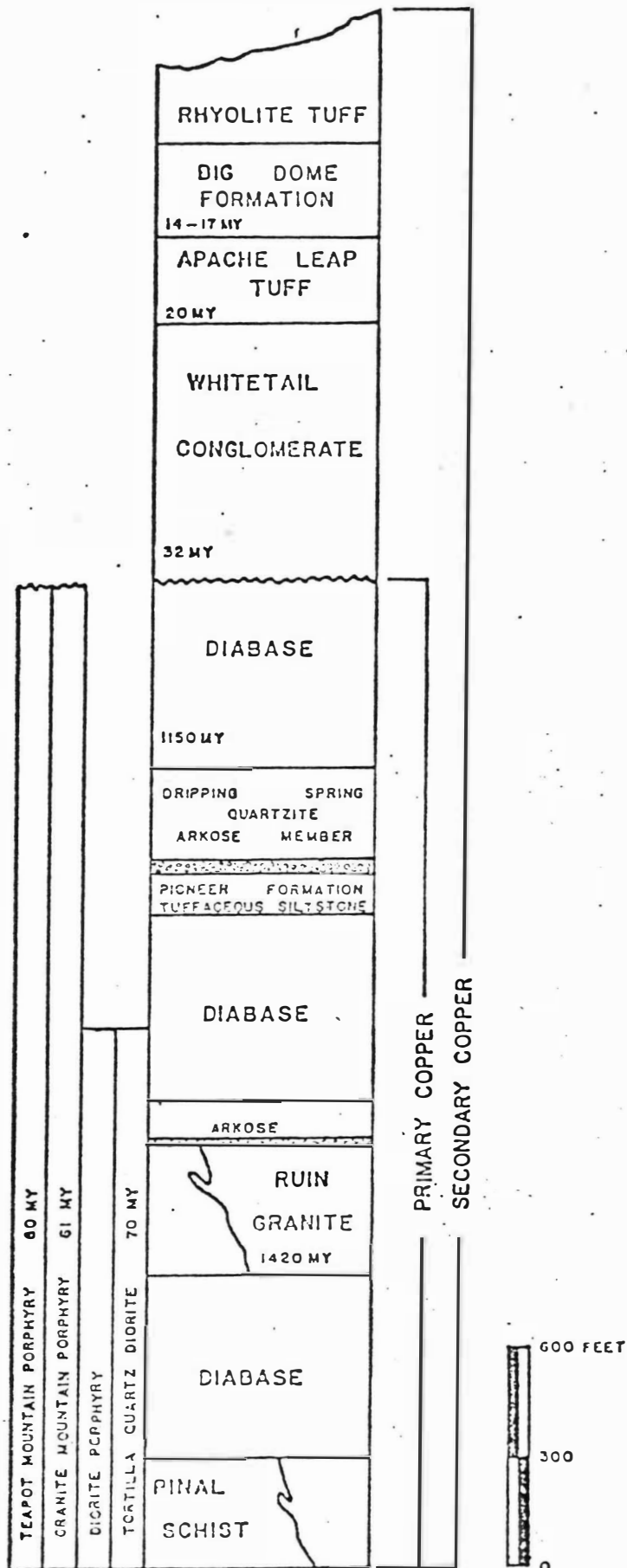
INTRODUCTION

The Ray Mine is owned and operated by Kennecott Minerals Company and is located in eastern Pinal County, Arizona, seventy miles southeast of Phoenix. The deposit has been a major copper source since 1911, producing an estimated 3 million tons of copper. The bulk of the production has been derived from sulfide ores. Mining was accomplished by underground methods until 1955 when full conversion to open pit methods was achieved.

Currently we are mining approximately 26,000 tons of sulfide ore and 14,000 tons of silicate ore on a seven-day-per-week basis. The sulfide ore is crushed to minus 10 inches at the mine and shipped by rail some 18 miles to the concentrator and smelter at Hayden. The silicate ore is processed entirely at the mine using a percolation/agitation leaching system with the final product being electrowon cathode copper.

LITHOLOGIES

The diagram on page 5 shows the lithologic units which are important in the Ray deposit. The oldest rock is the Pinal Schist which is composed of quartz-sericite and quartz-chlorite-epidote metasediments, as well as some metavolcanic units. A metarhyolite unit in the schist has been dated at 1660 m.y. (Livingston and Damon, 1968).



LITHOLOGIES (cont'd)

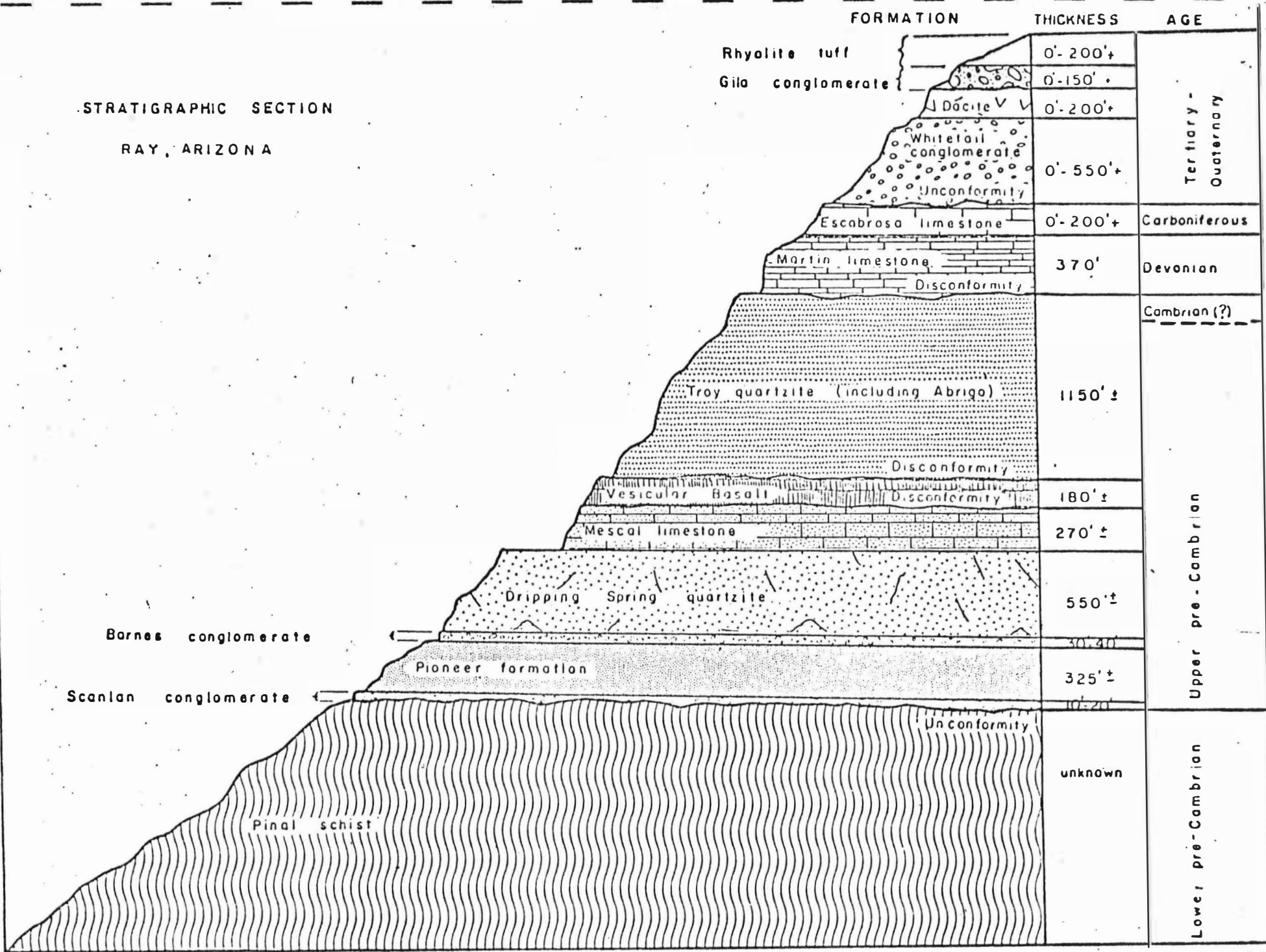
The Ruin or Oracle Granite, which is compositionally a quartz monzonite, intrudes the schist and has been dated in the Winkelman area at 1420 m.y. (Livingston and Damon, 1968). Following a long period of erosion, the younger Precambrian quartzose sediments of the Apache Group were deposited.

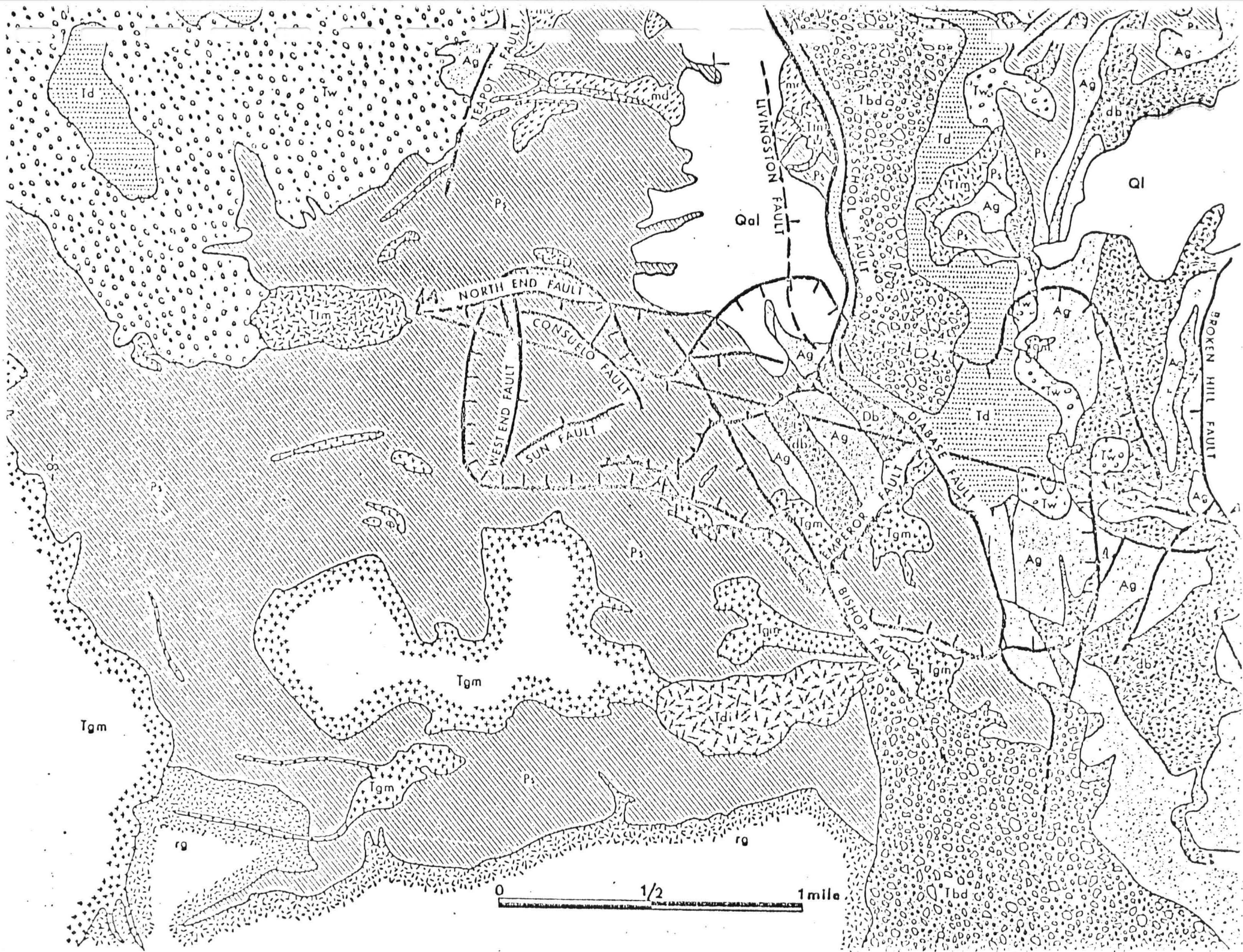
The Pioneer Formation is approximately 230 feet thick and consists of interbedded arkose and tuffaceous siltstones with a basal conglomerate (Scanlan Conglomerate member). Above the Pioneer Formation, there is typically 40 feet of basal Dripping Spring (Barnes Conglomerate). Above this we have approximately 250 feet of the lower arkose-quartzite member of the Dripping Spring. Although the upper Dripping Spring, the Mescal Limestone and the Troy Quartzite are present east of the mine, they are not important from the standpoint of copper mineralization. The entire stratigraphic section for the Ray area is shown on page 7.

Extensive diabase intrusions, mostly as sills, occurred 1150 m.y. ago (Livingston and Damon, 1968). The preore mineralogy of the diabase is variable; however, the bulk of it appears to have been a hornblende-pyroxene labradorite diabase with minor quartz, biotite, orthoclase, magnetite and apatite. At Ray, this diabase is an important host rock. In the mine area there are two sills which average about 500 feet in thickness. The sills prefer certain stratigraphic horizons which are:

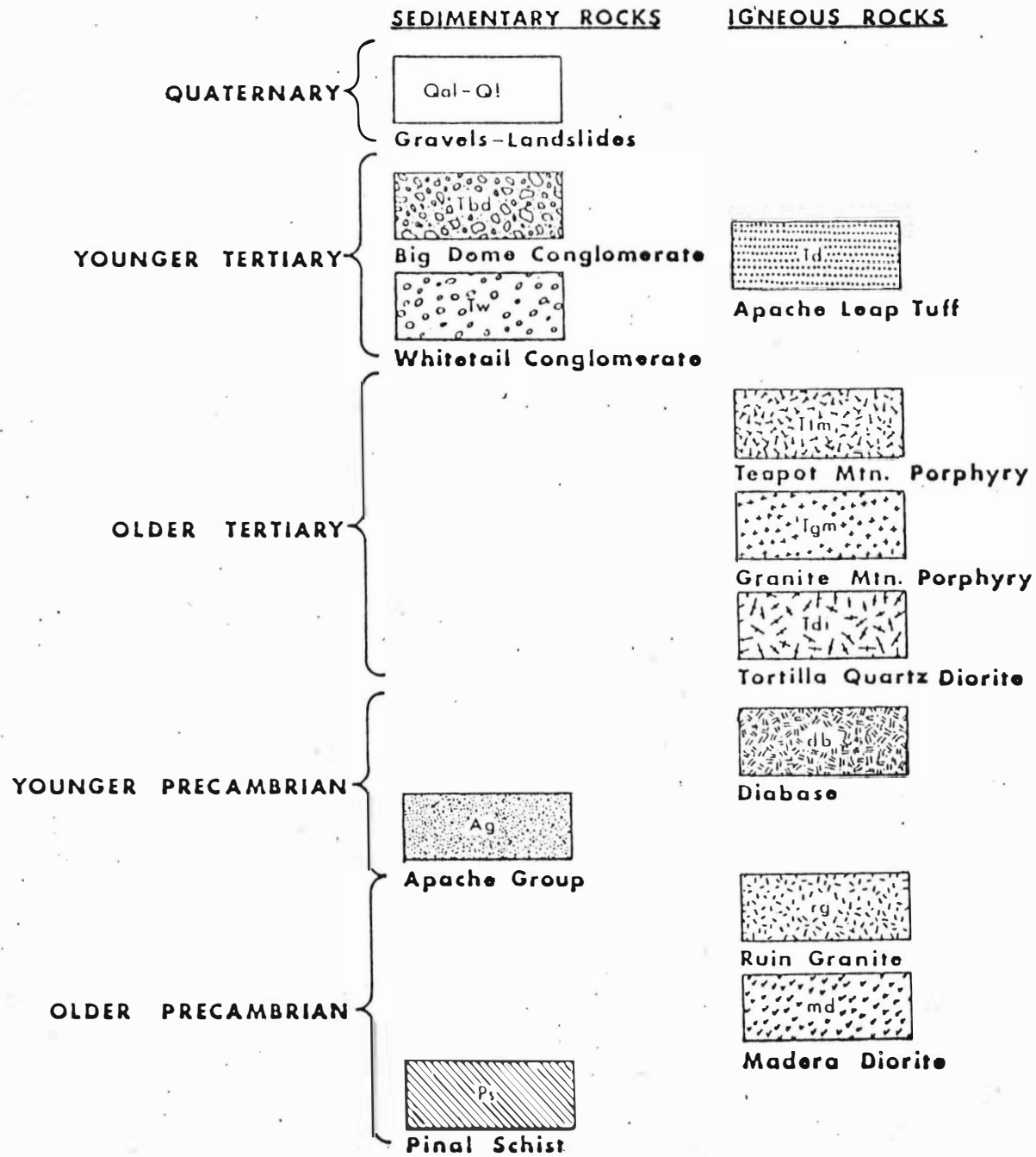
STRATIGRAPHIC SECTION

RAY, ARIZONA





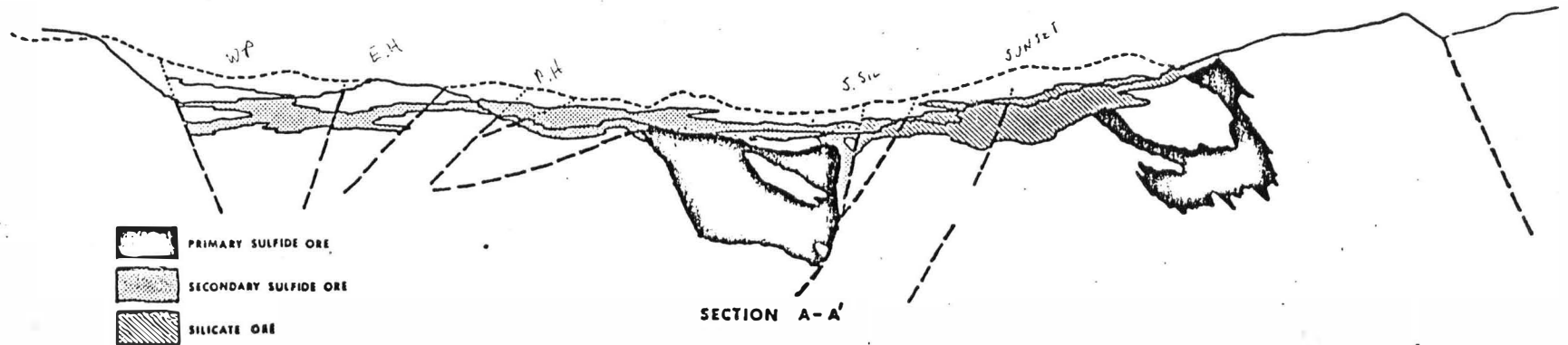
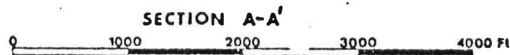
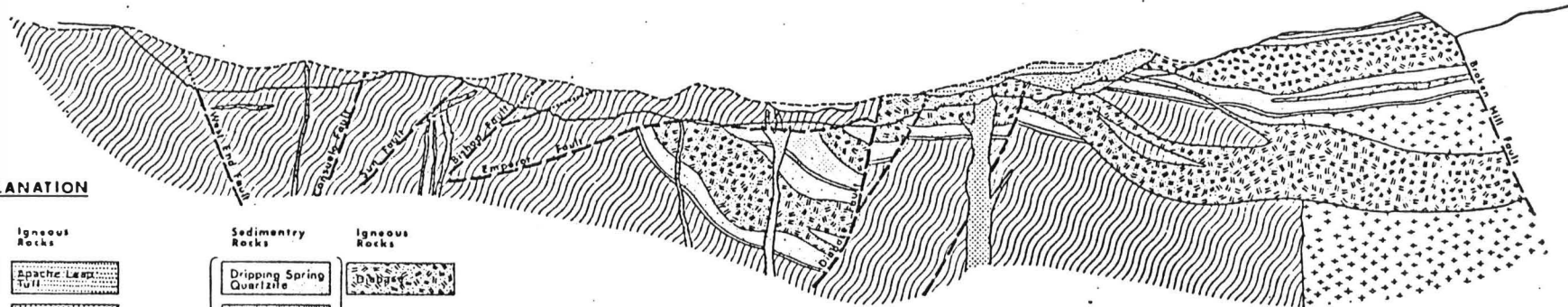
EXPLANATION



EXPLANATION

Sedimentary Rocks		Igneous Rocks	
Whitetail Conglomerate	Apache Leap Tuff	Dripping Spring Quartzite	Apache Group
	Quartzite-Mica Porphyry	Barnes Conglomerate	
		Pioneer Formation	
		Scanlan Conglomerate	
			Older Precambrian
			Pinal Schist
			Granite

-10-



SECTION A-A'

LITHOLOGIES (cont'd)

(1) the Pinal Schist-Ruin Granite about 300 feet below the Apache Group, (2) the middle of the Pioneer Formation, and (3) between the lower arkose and upper siltstone members of the Dripping Spring Quartzite. Going north through the mine, the sill in the Pioneer migrates downward into the schist and granite. Likewise, the upper sill in the Dripping Spring Quartzite migrates downward into the Pioneer Formation. Economic hypogene copper mineralization is not found in Precambrian rocks above the upper diabase sill in the Dripping Spring Quartzite.

The Tortilla Quartz Diorite (Sonora Diorite) dated at approximately 70 m. y. (Banks and others, 1973) is largely restricted to the south and west sides of the deposit. Depending upon its location within the sulfide system, the quartz diorite can contain ore grade (at least 0.4% copper) hypogene copper mineralization.

The Granite Mountain Porphyry has been dated at 60 m. y. (see Banks and others, 1972-1973, Livingston and others, 1968, and McDowell, 1971) and has been long considered to be the causative intrusive at Ray. The rock is in reality a porphyritic granodiorite composed of oligoclase, quartz, biotite-magnetite, and orthoclase phenocrysts with an orthoclase matrix (Cornwall and others, 1971). At the present surface, the main mass of Granite Mountain Porphyry is west of Ray in the Granite Mountain area where it is at least two miles in diameter and appears to have intruded near a northwest trending Pinal Schist/Ruin Granite contact.

LITHOLOGIES (cont'd)

In the mine, there are several small masses of Granite Mountain Porphyry which are aligned in a N70°E direction along a zone of weakness referred to as the "Porphyry break" (Metz and Rose, 1966). Diamond drilling indicates that some of these masses may coalesce at depth to form a stock central to the hypogene ore mineralization.

The Teapot Mountain Porphyry is slightly younger than the Granite Mountain Porphyry and intrudes as stocks and dikes along a northeast trend north of Ray. The Teapot is characterized by large euhedral orthoclase and quartz phenocrysts. The Calumet Breccia Pipe may be associated with one of the Teapot Mountain stocks. The upper portion of the pipe contains secondary copper mineralization and supergene effects have largely masked relationships between mineralization and fragmentation. Recent drilling shows two periods of hypogene mineralization. The first period is associated with the main stage of mineralization at Ray and is characterized by pyrite-chalcopyrite-quartz veins which are terminated at fragment boundaries. The second period fills the breccia interstices, cuts the fragments and is characteristically galena-sphalerite-dolomite and/or rhodochrosite.

In summary, the major Laramide intrusive masses in the Ray district are all mineralized, all intrude along a northeast trend and they vary compositionally (south to north) from quartz diorite, to granodiorite, to quartz monzonite.

LITHOLOGIES (cont'd)

The tertiary began with the deposition of the Whitetail Conglomerate 32-plus million years ago (Cornwall and others, 1971). The Whitetail at Ray is divided into two facies. One is reddish brown and is composed primarily of schist fragments. The other is light brown and contains abundant Paleozoic Limestone and Apache Group/diabase fragments, with minor schist. Both Whitetail facies exhibit poor sorting and bedding.

The Apache Leap Tuff (Superior Dacite) sheet was deposited 20 million years ago (Creasey and Kistler, 1962). The Apache Leap Tuff is about 230 feet thick and is a rhyodacite (Cornwall and others, 1971), with a light pink to white basal unit overlain by a red to black welded vitrophyre which grades upward into a light reddish brown tuff. Supergene solutions have rendered the vitrophyre unit unrecognizable over the deposit.

The Big Dome Formation was named for the exposure south of the mine (Krieger and others, 1974). A biotite tuff within the Big Dome has been dated discordantly at 14 and 17 m.y. (Cornwall and others, 1971). In the deposit area, the Big Dome can be subdivided into a schist-porphry facies and a coarser grained, gray mixed limestone-Apache Group facies.

The youngest rock unit at Ray is a water lain rhyolite tuff. This light pink to brown tuff appears to interfinger with the Big Dome

LITHOLOGIES (cont'd)

in places and may resemble it in age. Approximately three miles west of Ray, in the Copper Butte area, age-equivalent rhyolite tuffs and flows exceed in volume the Big Dome-equivalent gravels.

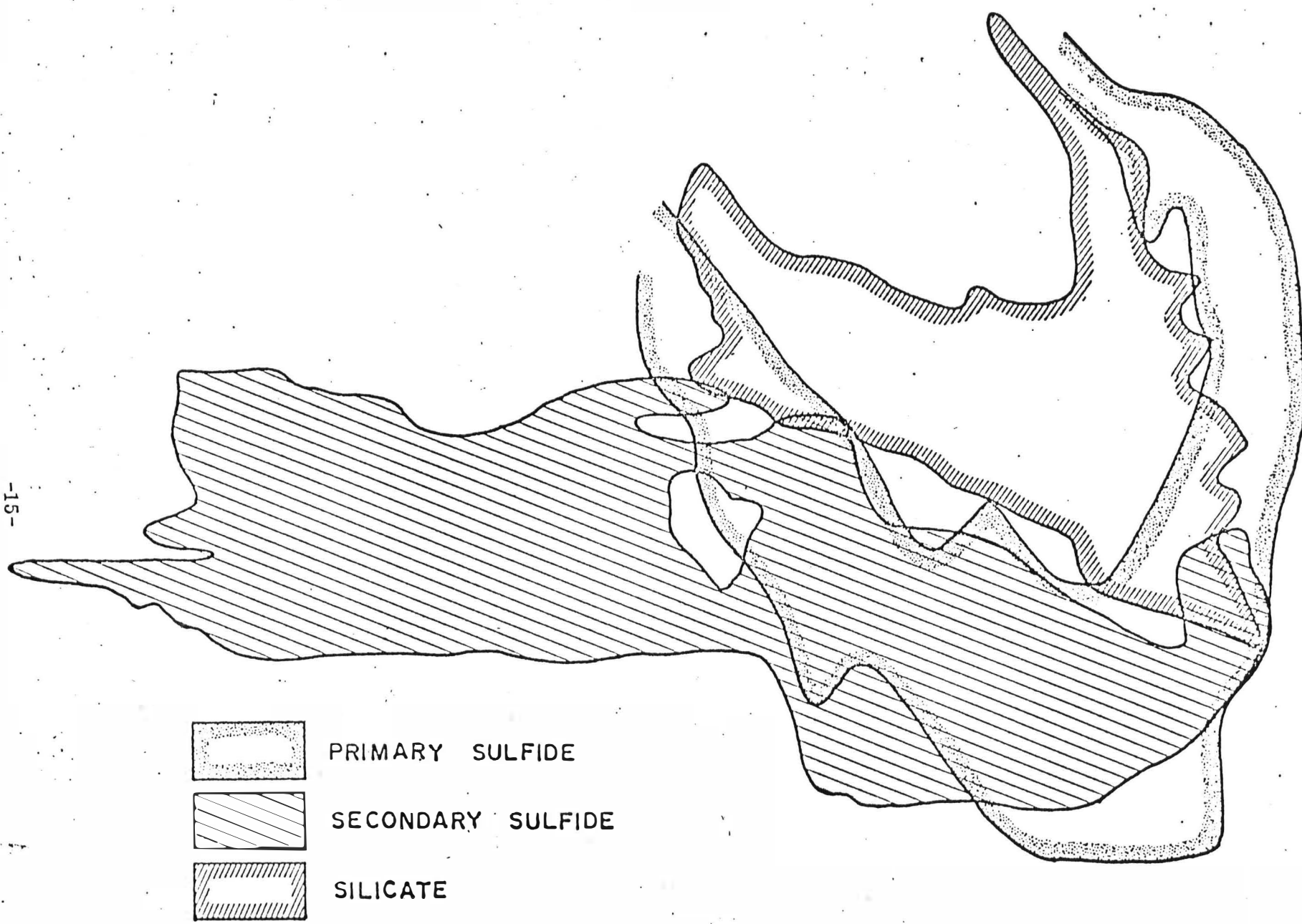
Secondary copper mineralization can be found in any of the lithologies shown on page 5 with the exception of the Ruin Granite.

The geologic map on page 8 gives a general feeling for the distribution of the major rock units. The western part of the mine is predominately Pinal Schist, while the eastern portion is mixed diabase and undifferentiated Apache Group. Note the masses of Granite Mountain Porphyry and the onlap of the postmineral volcanics and sediments.

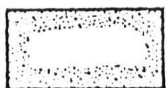
ORE TYPE DISTRIBUTION

Page 15 illustrates the distribution of the various ore types at Ray. Of interest is the location of the secondary chalcocite zone to the west of and above the hypogene ore zone. Most of the chalcocite occurs in the Pinal Schist which is the dominant rock type in the western portion of the mine. The location of the chalcocite orebody is affected by structure. The hypogene orebody is horseshoe shaped with the open end being the result of the combined effects of postmineral faulting, intrusion and erosion. Note that the Diabase Fault bisects the hypogene ore zone.

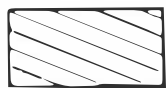
The silicate orebody was developed in the low total sulfide-high



-15-



PRIMARY SULFIDE



SECONDARY SULFIDE



SILICATE

ORE TYPE DISTRIBUTION (cont'd)

chalcopyrite core zone and is essentially restricted to the area east of the Diabase Fault. The combination of low available sulfur and the composition of the diabase were probably responsible for the formation of copper silicates in this area.

Several small zones of native-oxide copper mineralization occur in the orebody and are largely fault controlled. The largest area of this type of mineralization occurs in the north central portion of the mine where the North End, Emperor, Diabase, Livingston and School Faults converge.

ZONING

The deposit exhibits a typical hypogene sulfide zoning pattern with an outer high sulfide-low copper pyrite halo, an ore zone of moderate sulfide content characterized by approximately equal amounts of chalcopyrite and pyrite, and an inner low sulfide-high copper zone which is chalcopyrite in the diabase and, in places, pyritic in the quartzose rocks.

The bulk of the ore grade (at least 0.40% copper) mineralization occurs in the semi-reactive, mafic, Precambrian diabase host rock. Molybdenite mineralization favored the quartzose lithologies.

In the Precambrian rocks and the Granite Mountain Porphyry, the hypogene alteration zones from the inside out are (a) biotite-K-feldspar, (2) quartz-sericite and (3) epidote-chlorite. In the diabase, biotite-clay

ZONING (cont'd)

alteration predominates in both the core and ore zones. Chlorite and epidote increase outward into the pyrite halo. There is no extensive development of hypogene sericite or K-feldspar in the diabase. In all rock types, the frequency of quartz veins decreases outward from the center of the deposit.

STRUCTURE

The Ray Mine area has a complex tectonic history. High angle normal and reverse faults have been active at various intervals over a long period of time. Some structures that developed prior to the formation of the orebody have been intermittently active up to recent times. The area has alternately been under compression in Laramide time, then a release of compression and perhaps active rifting. Further compression in mid-Tertiary time, release, and then a late Tertiary compression with final release during development of basin and range structures.

The most obvious fault systems at the Ray Mine are the Diabase and Emperor Faults. Several other significant faults are documented in the mine area, including the Bishop, North End, Sun, West End, Consuelo, School and Livingston Faults. In the silicate orebody there is at least one additional unnamed fault with several hundred feet of displacement.

The Diabase Fault is a moderately to steeply westerly dipping normal fault, characterized by several tens of feet of gougy, broken and

STRUCTURE (cont'd)

brecciated rock and up to a few feet of strong gouge. In the Pearl Handle Pit, the hanging wall of the Diabase Fault contains the downthrown diabase/Apache Group sequence, which is overlain by schist in the upper plate of the Emperor Fault.

In the northern corner of the Pearl Handle Pit the normal displacement of the Diabase Fault is about 800 feet, west side down. Southeastward in the mine the displacement increases to more than 2,000 feet. The Diabase Fault terminates the Emperor Fault to the east. East of the Diabase Fault, the Emperor Fault was uplifted and eroded away.

The Diabase Fault bisects the hypogene ore shell, dropping the ore to the west (See sections, page 10). The fault also tends to form a boundary separating the secondary copper mineralization; chalcocite to the west and copper silicates to the east. The chalcocite, and to some degree the copper silicates, tend to penetrate the primary sulfide zone to greater depths along this fault. Native copper and some cuprite mineralization also tend to be localized along the Diabase Fault.

There have probably been several episodes of movement along the Diabase Fault during and following Tertiary time. Drag folding in some areas indicates both reverse and normal movement; the most recent being normal. Slickensides on native copper sheets within the fault zone indicate fairly recent movement. Fault zones to the north of the mine, which may be an extension of one strand of the Diabase

STRUCTURE (cont'd)

Fault, displace pleistocene terrace gravels.

The Emperor Fault is commonly characterized by several feet of dense, dark gouge and up to tens of feet of gougy, broken and brecciated rock. On the whole, the fault dips about 10 to 30 degrees southeasterly in the Pearl Handle Pit and northerly in the West Pit.

The upper plate, consisting mainly of schist with some porphyry and minor diabase, overlies schist, some porphyry and the diabase/ Apache Group sequence in the mine area.

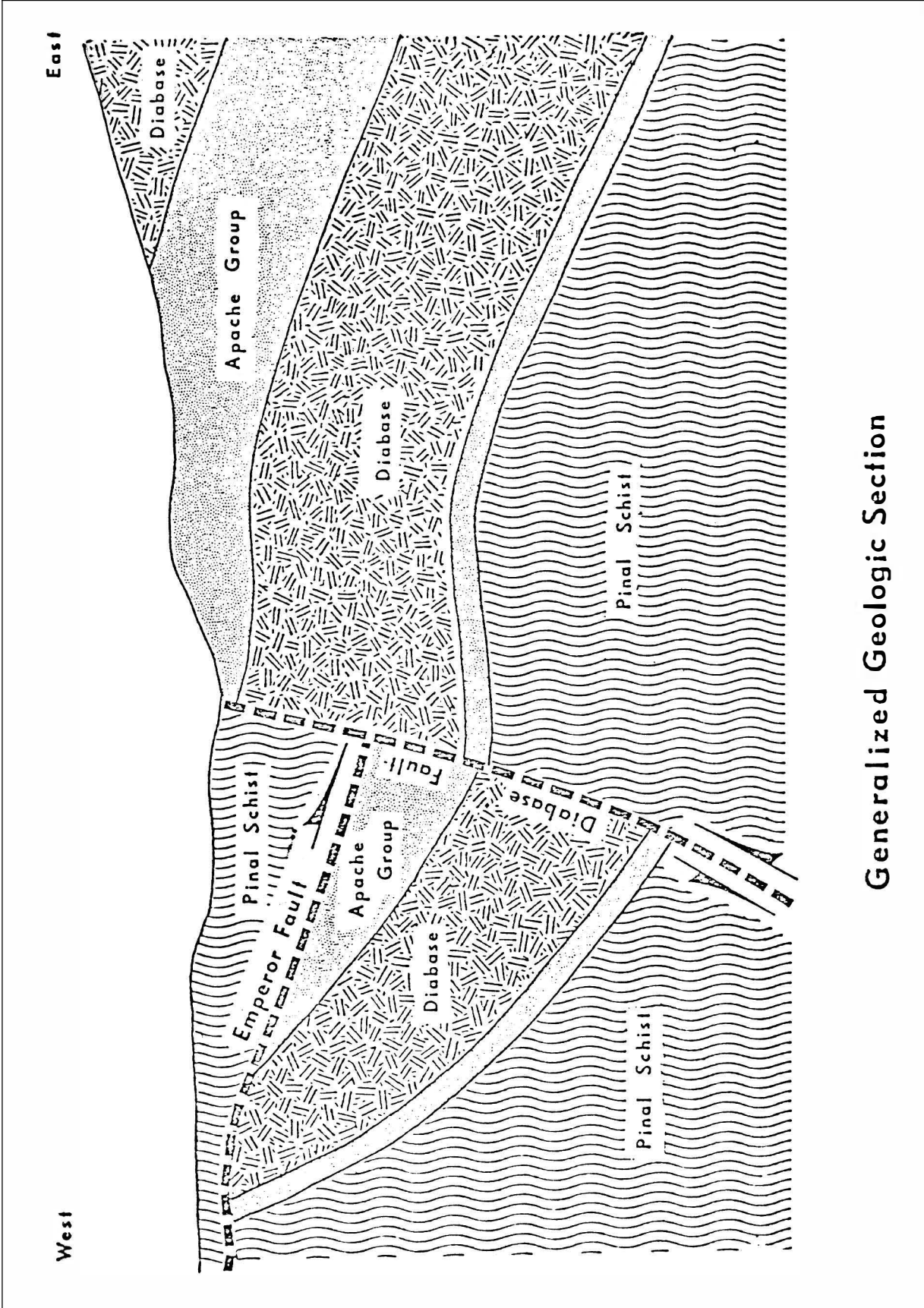
It is now believed the Emperor Fault is a gravity slide rather than a thrust fault. For a number of years it was an open question whether the small masses of Granite Mountain Porphyry in the mine area were offset by the low angle Emperor Fault. Drilling indicated the porphyry intruded up through the lower plate as dikes and small apophyses, mushrooming out above the fault. In some cases, the mushrooming suggested the likelihood of Granite Mountain Porphyry offset along the Emperor Fault. A few years ago mining exposed an area where porphyry occurred in both the upper and lower plates. The fault was observed to cut across the porphyry; however, due to the close spatial relationship between the porphyry masses in the lower plate and those in the upper plate, the post porphyry movement is believed to be minimal.

The intrusion of the main Granite Mountain Porphyry stock

STRUCTURE (cont'd)

southwest of the mine probably uplifted that area, causing a gravity slide that moved to the northeast over the Ray Mine area with a shallow northeasterly dip. Sometime later several porphyry masses intruded the Ray Mine area, moving upward through and mushrooming out above the Emperor Fault. It was this late intrusive event that provided the hydrothermal solutions that formed the bulk of the rock alteration and mineralization for the Ray Orebody. Further uplift on the Granite Mountain to the west and the downfaulting along the Diabase Fault to the east steepened the dip on the Emperor Fault causing additional minor movement. This mechanism would set the age of the main movement along the Emperor Fault at 60 to 61 million years ago. The generalized section on page 21 illustrates the present relationship of the Diabase and Emperor Faults.

North of the mine and extending up the Mineral Creek valley is a complex fault zone composed of several fault strands and may, in part, be an off-shoot of the Diabase Fault. The east dipping westernmost fault strand is named the Livingston Fault; the term School Fault is reserved for that part of the Mineral Creek Fault zone which is composed of reverse faults that dip 30-60 degrees west and crop out east of the trace of the Livingston Fault. The School Fault is a low-angle reverse fault near the surface and is interpreted to steepen at depth. The Pinal Schist block on the west has moved up. The geometry



Generalized Geologic Section

STRUCTURE (cont'd)

of this fault is inferred from analogy to other basement uplifts of Laramide age. In the case of the Ray area, however, much of the Laramide style deformation is probably of Miocene age. It is an open question as to whether the School Fault is younger than the Livingston Fault or vice-versa.

The West End Fault, located on the west slope of the West Pit, strikes north-south with a steep easterly dip. This fault has economic significance since it essentially terminates the western extension of the chalcocite mineralization in the West Pit area.

The North End Fault forms a sharp boundary between rock alteration types in the Schist along the north side of the West Pit area. Quartz-sericite alteration to the south abruptly changes to a chlorite-epidote assemblage north of the fault. The North End Fault may be a westerly extension of one strand of the Diabase Fault.

At least four major fault systems, the Diabase, Emperor, North End and School-Livingston Faults, converge in the area of the northeast slopes of the Pearl Handle Pit creating an extremely complex structural zone. Large blocks of rock have been rotated and moved out of sequence. Attempts to make detailed drill hole correlations in this area have been very difficult.

SUMMARY

The Ray orebody was developed in older and younger Precambrian rocks. Stratigraphically, the highest unit of the Apache Group affected by the hypogene ore solutions appears to be the arkose member of the Dripping Spring Quartzite. The deposit is thought to be genetically related to the 60 to 61 million year old Granite Mountain Porphyry. Secondary copper mineralization is found in the Precambrian rocks (excluding the Ruin Granite), the Laramide intrusives, and the Tertiary conglomerate and volcanic units.

Supergene chalcocite mineralization formed above and lateral to the hypogene copper orebody, largely in the pyrite halo. The bulk of the silicate/oxide orebody formed in a low total sulfide-high chalcopyrite environment.

The bulk of the ore grade (at least 0.40%) copper mineralization occurs in the semi-reactive, mafic, Precambrian diabase host rock. Molybdenite mineralization favored the quartzose lithologies.

The Ray orebody is located in a very complex structural area. Several major structures have played an important role in the emplacement and subsequent displacement and secondary enrichment of the orebody. The high angle Diabase and the low angle Emperor Faults are the most important and obvious structures in the mine area. The Diabase Fault down dropped the western portion of the primary ore

SUMMARY (cont'd)

zone and terminates the eastward extension of the Emperor Fault. The Emperor Fault tends to define the lower limits of the chalcocite enrichment blanket in the Pearl Handle Pit area. The convergence of several major fault systems in the northeast Pearl Handle Pit area has created a very complex zone. Oxide type mineralization extends to greater depths within this area; either as the result of greater groundwater flow circulating through this zone or the down dropping of blocks containing copper minerals that were oxidized at higher elevations.

REFERENCES

1. Banks, N. G., Cornwall, H. R., Silberman, M. L., Creasey, S. C., and Marvin, R. F., 1972, Chronology of intrusion and ore deposition at Ray, Arizona --Part I, K-Ar ages: *Econ. Geology*, v. 67, p. 864-878.
2. Banks, N. G., and Stuckless, J. S., 1973, Chronology of intrusion and ore deposition at Ray, Arizona--Part II, Fission-track ages: *Econ. Geology*, v. 68, p. 657-664.
3. Cornwall, R. R., Banks, N. G., and Phillips, C. H., 1971, Geologic map of the Sonora quadrangle Pinal and Gila Counties, Arizona: U.S. Geol. Survey Quad Map GQ-1021.
4. Creasey, S. C., and Kistler, R. W., 1962, Age of some copper-bearing porphyries and other igneous rocks in southeastern Arizona, in *Geol. Sur. Research 1962: U.S. Geol. Survey Prof. Paper 450-D*, p. D1-D5.
5. Krieger, M. H., Cornwall, H. R., and Banks, N. G., 1974, Big Dome Formation and revised Tertiary stratigraphy in the Ray-San Manuel area, Arizona, in U.S. Geol. Survey Bulletin 1394-A, Changes in stratigraphic nomenclature by the U.S. Geological Survey, 1972 by Cohee, G. V., and Wright, W. B., p. A54-A62.
6. Livingston, D. E., Damon, P. E., 1968, The ages of stratified Precambrian rock sequences in central Arizona and northern Sonora: *Canadian Journal of Earth Sciences*, Vol. 5, p. 763-772.
7. Livingston, D. E., Mauger, R. L., and Damon, P. E., 1968, Geochronology of the emplacement, enrichment, and preservation of Arizona porphyry copper deposits: *Econ. Geology*, v. 63, p. 30-36.
8. McDowell, F. W., 1971, K-Ar ages of igneous rocks from the western United States: *Isochron/West*, No. 2, p. 1-17.
9. Metz, R. A., and Rose, A. W., 1966. Geology of the Ray copper deposit, Ray, Arizona, in Titley, S. R., and Hicks, C. L., eds., *Geology of the porphyry copper deposits, southwestern North America*: Tucson, University of Arizona Press, p. 177-188.
10. Phillips, C. H., Gambell, N. A., and Fountain, D. S., 1974, Hydrothermal alteration, mineralization, and zoning in the Ray Deposit: *Econ. Geology*, v. 69, p. 1237-1250.

APPENDIX III

"Hydrothermal Alteration, Mineralization, and Zoning
in the Ray Deposit"

by

C. H. Phillips et al
Economic Geology 1974

Hydrothermal Alteration, Mineralization, and Zoning in the Ray Deposit

C. H. PHILLIPS, N. A. GAMBELL, AND D. S. FOUNTAIN

Abstract

Hypogene alteration and sulfide mineralization were studied in the diabase, Granite Mountain Porphyry, and quartzose Precambrian rocks at Ray. The bulk of the ore (+ 0.4% Cu) occurs in the mafic reactive Precambrian diabase sills. In plan view, the ore zone is horseshoe-shaped and presently does not appear to be associated with a large central mass of Granite Mountain Porphyry. The ore zone is surrounded by a zone of higher sulfides, most of which is pyrite. The center of the deposit is characterized by a low sulfide-high chalcopyrite assemblage.

Most of the copper occurs as chalcopyrite with minor bornite. Molybdenite appears to favor the Granite Mountain Porphyry and quartzose Precambrian rocks.

Hypogene alteration zoning patterns in the Ray deposit are affected by the host rock composition. In the diabase, a biotite-clay zone grades into a chlorite-epidote zone. Sericite and K-feldspar are rare alteration products. Secondary magnetite is common in the high copper zone. In the quartzose Precambrian rocks a zone of K-feldspar-biotite alteration occurs in the low sulfide core and in the high copper zone. A sericite zone overlaps the K-feldspar and biotite zone in the high copper zone and decreases outward to the propylitic zone.

Introduction

THE Ray copper deposit is situated in Pinal County, Arizona, about 70 miles due north of Tucson. The current production from Ray is 35,000 tons per day made up of roughly equal amounts of three ore types: chalcocite, chalcopyrite, and copper silicates. By far the greater part of past production has been from secondary chalcocite ores. It is only in the last decade that the primary sulfide mineralization has become an important ore type.

Despite the existence in 1968 of detailed surface and subsurface studies of the stratigraphy and structure and preliminary data on the alteration and geochemistry (Metz and Rose, 1966) in the vicinity of the Ray orebody, several pressing geologic questions concerning the Ray deposit remained unsolved. Among them were (1) the peculiar shape of the orebody, which had been developed by drilling during the mid-60s, (2) the apparent lack of the symmetric zoning found at some other porphyry copper deposits, (3) the direction and amount of displacement on major faults through the orebody and, perhaps more important, the time of their movement, pre- or postmineral, and (4) the exploration-related question: where would the ultimate vertical and horizontal limits of ore mineralization be found? The limit of the ore-grade copper was the most urgent of these questions due to necessary engineering and property decisions.

A review of the pre-1968 geologic work on the Ray deposit indicated that additional detailed work

on alteration and sulfide zoning would be the best means of further defining the Ray geology. It was assumed that some kind of regular zoning must exist, even if atypical. After indications of a pyrite halo were located, the copper distribution in various rock types was roughed out. Once this was done, it became obvious that the Ray deposit was concentrically zoned, and the general sulfide relationship discussed below was evident. The preliminary study of copper and sulfide distribution was so successful that by the end of 1969 it was decided to complete the study in detail and to include work on the alteration zoning. At that time the project was divided into a study of the three parts: quartzose Precambrian rocks, diabase, and porphyry.

Vertical sections through the sulfide system which have maximum drill hole density and rock type continuity were selected for the detailed study. The purpose here was to obtain the maximum amount of interpretable data in the minimum time. Within the rock types, the drill samples were composited into approximate 50-foot samples; heavy minerals were physically separated, and the total weight percent sulfide and magnetite as well as the chalcopyrite:pyrite ratios were determined. The method used for sulfide and magnetite determinations was a physical separation which tended to give low values for both total sulfides and chalcopyrite:pyrite ratios. Generally these numbers calculate to within 20 percent of the copper assays, and curves plotted from different data sets consistently have the same shape. Some of the data presented here in graphic form

Symbol	Intensity	Explanation	Approximate Percent of Rock
1		Single or questionable occurrence	
2	Trace	Minute portion of rock but found by checking several samples with care	Much less than 1%
3	Weak	Minute portion of rock but common	—1%
4	Moderate	Very common, easily found in any sample	Less than 5%
5	Strong	Obvious, a major constituent	5% or more
6	Intense	All available parts gone to this mineral (pyrox-biotite)	Generally more than 20%
7	Total	Rock consists mainly of this	More than 50%

FIG. 1. Alteration-mineralization notation method at Ray. The advantages of this system over percentage estimates are that it is more rapid, provides three distinct categories of less than or near 1 percent, and does not imply the precision of a percentage.

have been adjusted to approximate agreement with the copper assays.

In the quartzose Precambrian rocks, assay averages for MoS_2 were also contoured, but these data were so incomplete that only a very general pattern was evident.

The scope of the study was limited to outlining the vertical and horizontal distribution of those alteration minerals which could be readily identified with a hand lens or petrographic microscope with a minimum of X-ray or microprobe assistance. Because of the time involved, no attempt was made to count or estimate percentages of specific minerals; the frequency of occurrence was noted by utilizing the same system used in core logging at Ray as outlined in Figure 1. It is important to stress that the

conclusions derived in this paper are the result of a detailed study of a small portion of a large, complex porphyry copper orebody. Optimistically, the data are a good approximation of the truth and will be of interest to those engaged in mining geology or related fields.

District Geology

Because the geology and ore deposits of the district have been discussed in detail by Ransome (1919), Metz and Rose (1966), and by Cornwall et al. (1971), only a brief resumé of the Ray geologic setting follows.

The Ray sulfide system is developed in a variety of Precambrian rocks and in Laramide intrusives (Fig. 2). The oldest of the Precambrian rocks is the Pinal Schist. This is a sequence of metamorphosed shale, siltstone, sandstone, and conglomerate with flows or plutons of a rhyolitic(?) porphyry. Rarely, some biotite-rich zones which appear to have been a porphyry of dioritic composition are encountered.

The Precambrian Ruin Granite, a coarsely crystalline quartz monzonite, intrudes the schist but post-dates the metamorphism. Although the Ruin does not crop out in the mine area, it is consistently encountered in the subcrop along the eastern side of the sulfide system.

Overlying the Pinal Schist and Ruin Granite are the Pioneer Formation and Dripping Spring Quartzite of the upper Precambrian Apache Group. These are quartzitic clastic rocks ranging from tuffaceous mudstone to arkosic conglomerate. They are not differentiated in Figure 2.

The youngest Precambrian rock, diabase, occurs as dikes and sills in all the older rocks. The diabase is the most receptive rock to copper mineralization at Ray. The sills in the Pioneer Formation, the Pinal Schist, and the Ruin Granite are the most important hosts of mineralization. Some of the diabase in the Dripping Spring Quartzite contains ore-grade mineralization, but most of this sill is restricted by erosion and geologic structure to the pyrite halo.

A series of Laramide intermediate to acidic dikes and stocks intrude all the older rocks. These in-

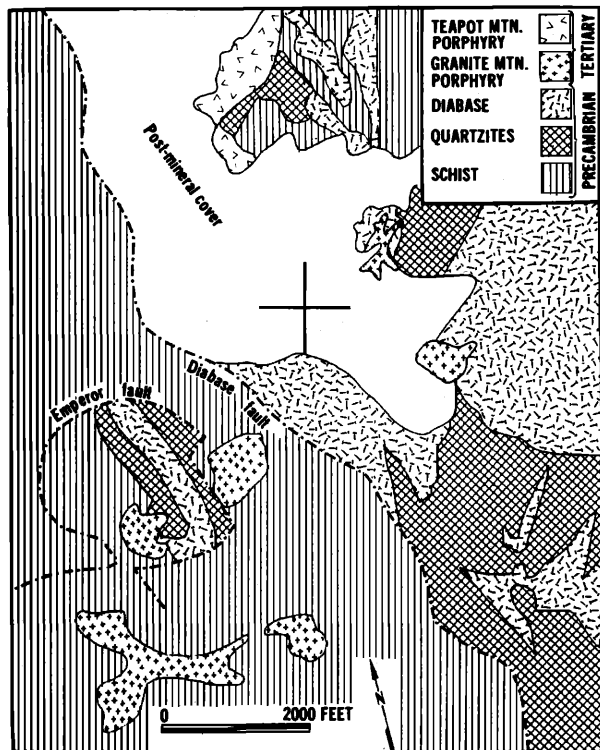


FIG. 2. Generalized geologic map of the Ray copper deposit. The cross on the figure is a reference point enabling the reader to correlate Figures 2, 3, 4, and 6A.

trusives are discussed in detail by Cornwall et al. (1971). The Ray sulfide system affects most of the Laramide intrusions including the Tortilla Quartz Diorite (Sonora Diorite of Ransome), the Teapot Mountain Porphyry quartz monzonite, the Granite Mountain Porphyry, and many of the dikes.

The sulfides were introduced after crystallization of the Granite Mountain Porphyry, and this rock is assumed to be genetically related to the ore deposit. The unaltered rock is granodiorite and commonly porphyritic; locally, however, it grades into subporphyritic and equigranular textures. The two breccia pipes in the mine area appear to be associated with the Teapot Mountain Porphyry. The age of the mineralization is not unequivocally established, but we believe, on the basis of limited crosscutting relationships, that the breccia pipes and the Teapot Mountain Porphyry are younger than much, but not all, of the mineralization.

Stratified Oligocene, Miocene, and later volcanic and clastic rocks overlie parts of the sulfide body. These postmineral rocks tend to thin and/or pinch out over the Ray deposit, indicating arching along the northeasterly trend of the Granite Mountain Porphyry intrusions.

The relation of geologic structure to placement of the sulfide system is obscure. Cornwall et al. (1971) showed that the entire region is complexly faulted. The results of the authors' work indicates that premineral fault and fracture zones have no major effect on the shape of the sulfide or alteration zones beyond very local and minor disruption of the pattern. The foliation of the schist, which parallels the trend of the porphyry stocks as well as the mid-Tertiary arching, may represent some sort of deep structure that controlled the location of the porphyry stocks, but this is a problematical relationship. At least one igneous contact does modify the zoning. This is the north-trending contact between Precambrian granite and schist on the eastern side of the deposit (in the subcrop).

Two large faults cross the orebody, the Diabase-Ray-School Fault (hereafter referred to as the Diabase Fault) and the Emperor Fault. The Diabase Fault dips to the west and trends northerly across the orebody and at the surface separates older rocks on the west from younger rocks on the east resulting in apparent reverse movement. The Emperor Fault has shallow north or easterly dips and is considered to be a thrust. It is cut by the Diabase Fault and is known only on the west or hanging wall side of the Diabase Fault. The thrust places older schist above younger quartzites and diabase so that at depth there are younger rocks in the hanging wall than in the footwall of the Diabase Fault (Fig. 6b), the opposite of the surface indications. Therefore,

movement on the Diabase Fault can be either reverse or normal. The direction and total displacement on either fault has never been determined satisfactorily. The displacement on the Diabase Fault exceeds 1,500 feet, while the minimum movement on the Emperor Fault is about 3,000 feet with some very late movement indicated on both faults. Obviously, large postmineral displacement of the sulfide system (and orebody) had to be considered as a possibility on both of these faults until evidence to the contrary such as that presented here was developed.

The hypogene sulfide minerals identified in or near the Ray deposit are pyrite, chalcopyrite, molybdenite, galena, and sphalerite. Occasionally, small amounts of tennantite, tetrahedrite, and bornite have been seen.

Hypogene Copper, Sulfide and Alteration Zoning

Systematic changes of sulfide content and copper grade related to rock type changes in the Ray orebody have long been recognized (Metz and Rose, 1966; Metz and Caviness, 1968). Consequently, the

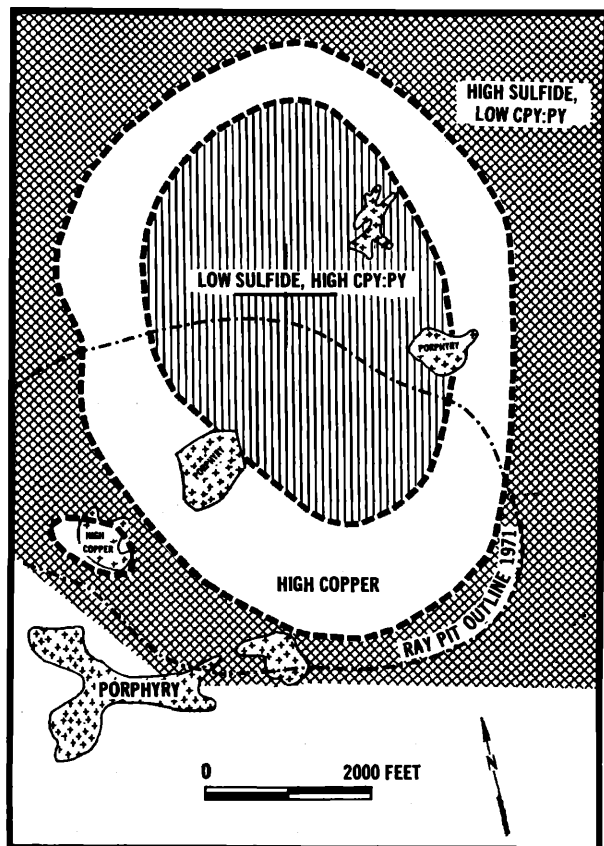


FIG. 3. Generalized zoning of hypogene sulfides in the Ray deposit. The porphyry shown is the Granite Mountain Porphyry.

zoning study was separated into specific rock units: (1) quartzose Precambrian rocks, (2) diabase, and (3) Laramide porphyry.

The zoning of sulfides and the surface location of the Granite Mountain Porphyry stocks are shown in Figure 3. The central part of the sulfide system is characterized by a low content of total sulfide and a high ratio of chalcopyrite to pyrite. Despite the high percentage of copper sulfide in the total sulfide, the total copper in the rock mass is relatively low; consequently, this zone is referred to as the "low-grade core". The high copper zone or "doughnut" surrounding the low-grade core is much more copper-rich than the core, even though the ratio of chalcopyrite to pyrite is lower. This is due to the increase in the total sulfide content. The increase in total sulfide continues regularly with distance from the center of the system and is accompanied by a decreasing relative amount of chalcopyrite, finally resulting in a high-sulfide, low-copper pyrite halo around the high copper zone.

Note that the center of the zonal pattern does not coincide with any of the porphyry stocks but that the one stock to the southwest (within the Emperor thrust plate) very definitely affects the pattern.

Quartzose Precambrian Rocks

Copper distribution

The average copper content intersected in drilling of the quartzose Precambrian rocks is shown in Figure 4. The contours are in increments of 0.1 percent copper and demonstrate the circular nature of the high copper zone. The open area to the northwest is caused by a combination of sparse drilling data through postmineral cover and a large stock of late or postmineral Teapot Mountain Porphyry (Fig. 2). The southwestern bulge is interpreted to be caused by the stock of Granite Mountain Porphyry located there (Fig. 3). The low-grade core averages from 0.2 percent copper to less than 0.1 percent while the high copper zone locally averages as high as 0.5 percent. The pyrite halo generally lies beyond the outer 0.2 percent contour.

Sulfide and magnetite distribution

Additional details of the zoning are illustrated in the graphs of Figure 5. Except for the data at 600 and 2,100 feet of Figure 5, all data are from drill holes along the line A-A' in Figure 4. Total sulfide content, percent chalcopyrite in the sulfide portion of the rock, and the abundance of magnetite are plotted along this line. The low-grade core lies on the left side and the pyrite halo on the right. The total sulfide content increases with distance from the center of the sulfide system to the outer part of

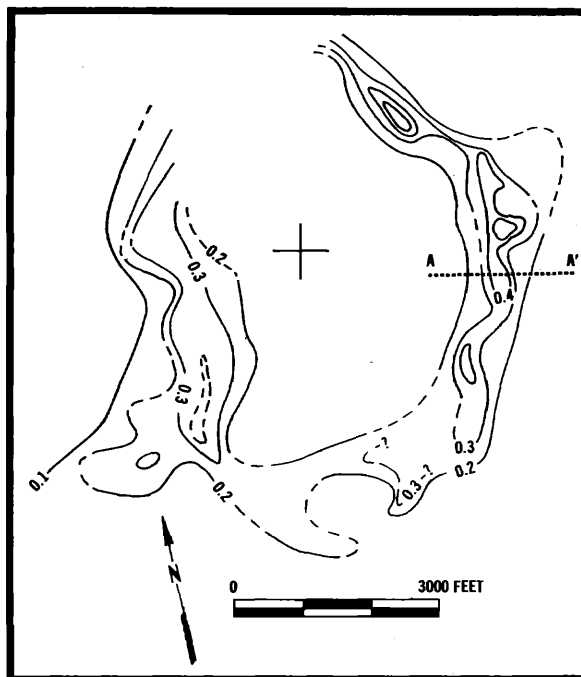


FIG. 4. Contoured copper distribution in the quartzose Precambrian rocks at Ray. Contour interval is 0.1 percent copper.

the high copper zone or inner pyrite halo. As shown by this particular set of data, there is usually a break in the total sulfide curve at the boundary between the low copper core and the high copper doughnut. The maximum total sulfide in the schist typically falls between 3 and 5 weight percent; the minimum would fall far to the left of the samples plotted in the graph and would be less than 1 percent. The slope of the chalcopyrite curve also changes in the high copper zone with a decrease from more than 40 percent chalcopyrite in the core to 2 percent or less in the pyrite halo.

The magnetite content in the schist is usually low with the maximum concentration falling near the exterior limit of the high copper zone or in the pyrite halo as in Figure 5.

The major (granite-schist) contact noted in Figure 5 is the only known premineral structure which has an appreciable effect on the sulfide system. Chalcopyrite increases relative to pyrite, and the percent total sulfide tends to level out or decrease at the contact. These changes occur in both rocks and extend laterally as much as 300 feet on either side of the contact.

Alteration zoning

In the quartzose Precambrian rocks, the common hypogene alteration products including vein materials are quartz, K-feldspar, biotite, sericite, epi-

dote, calcite, anhydrite, chlorite, and rutile. With exception of chlorite and rutile, these are listed in sequence from oldest to youngest.

Some alteration minerals are restricted entirely or largely to veins, as are quartz, K-feldspar, epidote, calcite, and anhydrite. Biotite, sericite, chlorite, and especially rutile, are uncommon in veins. For discussion, the veins can be categorized by their mineralogy and by their relative age as determined from crosscutting relationships. It must be noted that the categories or types of veins are defined somewhat arbitrarily because the vein types tend to be gradational and the crosscutting relationships cannot all be seen at any specific location. Also, evidence contrary to the usual crosscutting sequence is frequently found.

The sequence of vein formation in the quartzose Precambrian rocks is:

1. Quartz, K-feldspar, with calcite and chalcopryrite, and with or without pyrite or molybdenite. These veins have no biotite in the vein or as wall alteration. No crosscutting by the next oldest veins has been found; nonetheless, the lack of biotite here combined with a strong trend throughout the deposit to follow biotite with sericite seems adequate to establish a pre-biotite vein type.

2. This vein type is the same mineralogically as the preceding except that biotite occurs in the vein or adjacent wall rock. For reference these veins are called K-feldspar-biotite veins. Biotite in the vein will usually be coarse and lie against the vein wall. In the wall rock the biotite occurs as microscopic crystals or minute felted masses scattered throughout the rock for some distance from the vein, forming a broad, weak alteration envelope. In hand samples the envelope is evident as an almost imperceptible brownish color change paralleling the vein. Calcite usually lies along the vein center in very irregularly shaped crystals or groups of crystals. Minute veinlets of calcite may cut through other vein minerals but never were observed to be cut in turn. Locally, these K-feldspar-biotite veins show a gradational change to the next youngest vein type whereby part of the K-feldspar is altered to sericite. Biotite in the envelope close to the vein is also altered to sericite.

3. Quartz-sulfide veins with occasional calcite and prominent sericite envelopes. There seems to be a continuous series of these veins containing from roughly equal amounts of chalcopryrite and pyrite to those containing pyrite as the only sulfide. As a rule, the younger veins in the series have lower ratios of chalcopryrite to pyrite and more strongly developed sericite envelopes. As the pyrite halo is approached from the high copper side, chalcopryrite

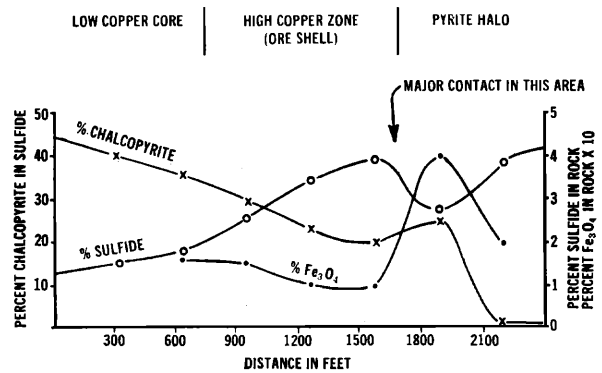


FIG. 5. Graphical distribution of magnetite and total sulfide and abundance of chalcopryrite in the total sulfide along line A-A', Figure 4. The five points on the left are composite averages in schist, the two points on the right are averages in Ruin Granite.

diminishes in frequency of occurrence while epidote becomes more common. Whether the lack of chalcopryrite in the pyrite halo is largely due to an abundance of the latest veins in this zone or to lateral zoning in contemporaneous veins is an unanswered question.

4. Pyrite veins frequently cut the quartz-sulfide veins and are relatively rare in the center of the deposit, tending to occur in the high copper zone or pyrite halo.

5. Molybdenite veins. These are generally thin fracture fillings cutting most copper-bearing veins, but cut by quartz-pyrite veins. Very small amounts of molybdenite may accompany any of vein types 1 through 3.

6. Anhydrite. There are uncommon occurrences of veins with purple anhydrite and quartz which cut all other veins in the vicinity, but it is not certain that the anhydrite veins are later than the quartz-sulfide veins. Rarely these veins contain pyrite but the anhydrite always seems to be later than the pyrite.

7. Vuggy veins with quartz, calcite, and sulfides. Such veins have vugs lined with small euhedral crystals of quartz, chalcopryrite, molybdenite, pyrite, and calcite.

8. Gray quartz veins. These quartz veins are barren of any sulfide mineralization and have no recognized wall-rock alteration.

Quartz forms the major part of most veins with the exception of monomineralic veins of sulfide. It apparently spans the entire time of mineralization. Widespread silicification as a fine-grained wall rock replacement is unknown at Ray; quartz was introduced only as a vein mineral. In thin section it is a mosaic of anhedral crystals with the exception of the very late, vuggy veins.

K-feldspar and biotite are roughly coextensive in the sulfide body and both have their maximum development in the core of the deposit, diminishing outward to very infrequent occurrence in the propylitic zone. K-feldspar usually forms a discontinuous selvage along the vein wall with grain sizes or even the larger masses being too small for reliable hand sample identification. Most of it is transparent with the maximum coloration being a translucent, creamy white. Though the earliest K-feldspar may be older than the formation of biotite, there is strong evidence from both individual veins and from the vein type age relationships pointing to a progression from K-feldspar-biotite to sericite. The younger sericite replaced vein K-feldspar, hypogene and rock biotite, and feldspars, obliterating much of the earlier alteration. The sericite ranges from scattered flakes hardly more than wisps along plagioclase cleavages through massive replacement by felted mats of minute crystals or by clumps of large crystals visible to the unaided eye. Like K-feldspar and biotite, sericite alteration covered the entire sulfide system but reached its greatest intensity from the outer part of the high copper zone through the inner portion of the high sulfide zone.

Epidote occurs as trace amounts in K-feldspar-bearing veins and more frequently in much later quartz-sulfide veins. In the quartz-pyrite veins, epidote is only sporadically found at the inner edge of the high sulfide zone, but as the propylitic zone is approached it becomes the dominant alteration product. It forms as a thin discontinuous coating along vein walls or less commonly as replacements in the wall rock. Outward in the sulfide system, the epidote spots and patches give way to an almost continuous selvage along the vein which finally comes to constitute the major part of the vein. Epidote seems to increase with the outward lessening of sericite and vein quartz.

Within the quartzose Precambrian rocks, chlorite can be found throughout the sulfide system, but in such small amounts that it is impossible to define any zoning. It may occur as an isolated, microscopic clot in wall rock or veins, as coarse leafy masses in veins, or rarely as innumerable megascopic patches in the wall rock. Generally, chlorite is a very small part of the vein or of the wall-rock alteration. Often, when it occurs with or near biotite, it surrounds or invades the biotite, obviously as a replacement, however, biotite does not seem to be a prerequisite for chlorite formation.

Rutile is a definite alteration product near veins of the quartz-K-feldspar-biotite variety with a frequency of zero to perhaps three very small crystals or crystal groups per thin section. It is commonly

found along these veins but never as anything more than trace amounts.

The distinction among vein, vein envelope, and wall-rock alteration is sometimes a difficult one because the obvious change from vein to vein envelope or to wall rock in the hand sample is frequently less definite in thin section. The vein filling and the wall-rock alteration products are often intermingled along the vein boundary; wall-rock alteration becomes progressively weaker with distance from the vein and may exhibit gradational zoning outward from the vein, that is, the envelope has a decreasing intensity of alteration and a transitional change of mineralogy away from the vein. Because of the overlap and repetition in the crosscutting sequence and to the apparent gradual change of alteration products within veins, it seems likely that the differences between the various vein types and their wall-rock alteration are indicative of continuous progressive alteration and mineralization rather than stages of mineralization caused by pulses or abrupt changes in the mineralizing fluids. The crosscutting more accurately represents periods of recurrent fracturing during continuous fluid flow and alteration than it does discrete stages of mineralization. Periodic fracture formation also affects the intensity of alteration measured by the amount of wall rock altered to a given mineral because this intensity must be governed, at least in part, by the fracture density during the period of time the given mineral is forming. If fracture density is high, the alteration envelopes overlap and the entire rock is altered; generally, if the fracture density is low, the alteration will be weak. If the fracture density has a zonal pattern, it will control the zonal distribution of alteration intensity and to some degree the zonation of alteration mineralogy. For example, in the siliceous Precambrian rocks, the development of a zone of strong sericite alteration along the inner edge of the pyrite halo could be controlled by the pattern of late fracturing rather than by laterally varying pressure-temperature-chemical conditions. In fact, much of the alteration zoning normally mapped could be largely controlled by the development of sequential fracture patterns.

Diabase

Because of the limited drilling beyond the 0.1 percent copper cutoff, the preore mineralogy of the diabase in the Ray area is uncertain. Wide variation in the mineralogy of the diabase is reported in central Arizona (Short et al., 1943; Peterson, 1962; Shride, 1967). The lower diabase sill at Ray contained significant quantities of hornblende (Table 1) and is almost certainly similar to Short's "normal diabase" at Superior.

TABLE 1. Preore Composition of the Diabase in the Ray Area (after Rose, 1960, unpublished private report)

Plagioclase, An ₄₅₋₅₅	40-70%
Hornblende or pyroxene	25-50%
Quartz	5%
Biotite	(?) 5%
Orthoclase	0-5%
Magnetite	3%
Apatite	1%

The following description of alteration and mineralization in the diabase is derived primarily from work on the lower sill on the eastern side of the Ray orebody. This sill extends from the core of the sulfide system eastward into the pyritic halo and is the most extensive diabase sill within the zone of hypogene mineralization. In the low sulfide, high chalcopyrite core, much of the lower sill has been oxidized and now forms a large part of the Ray silicate copper orebody.

Sulfide mineralogy

The bulk of the sulfide mineralization in the diabase is controlled by stockwork fracturing. The sulfides are concentrated in both the veins and the adjacent alteration envelopes, decreasing outward into the wall rock to occasional disseminated grains.

Chalcopyrite and pyrite are the major hypogene sulfide minerals in the diabase. Bornite is present in minor quantities and is always found as incipient

to partial replacements of chalcopyrite. Bornite in the diabase, schist, and porphyry is generally restricted to that portion of the sulfide system in which the abundance of chalcopyrite exceeds that of pyrite. Molybdenite in the diabase occurs most frequently along the outer edges of quartz-chalcopyrite-pyrite veins and is less abundant than in the more siliceous rocks. Limited assay data indicate that the highest concentration of molybdenite in the diabase occurs inside the +0.40% copper ore zone.

Sphalerite with minor galena is present in veins with chalcopyrite, pyrite, quartz, and calcite. These veins are late and occur in the zone of highest copper concentration and outward through the high pyrite zone.

Tennantite is found in veins with quartz, calcite, chalcopyrite, and pyrite. The veins are usually pinkish in color and have a banded texture.

Copper, sulfide, and magnetite distribution

The horizontal distribution of copper in the lower sill has been contoured from drill hole data (Fig. 6A). The figure was generated by averaging copper assays from over 100 diamond drill holes that penetrated the sill. The copper distribution exhibits a horseshoe shape with the shoe opening to the north. The north-south elongation of the horseshoe is perpendicular to the northeasterly trend of the porphyry intrusions. If, however, a plot of total sulfides including those in the pyrite halo is considered,

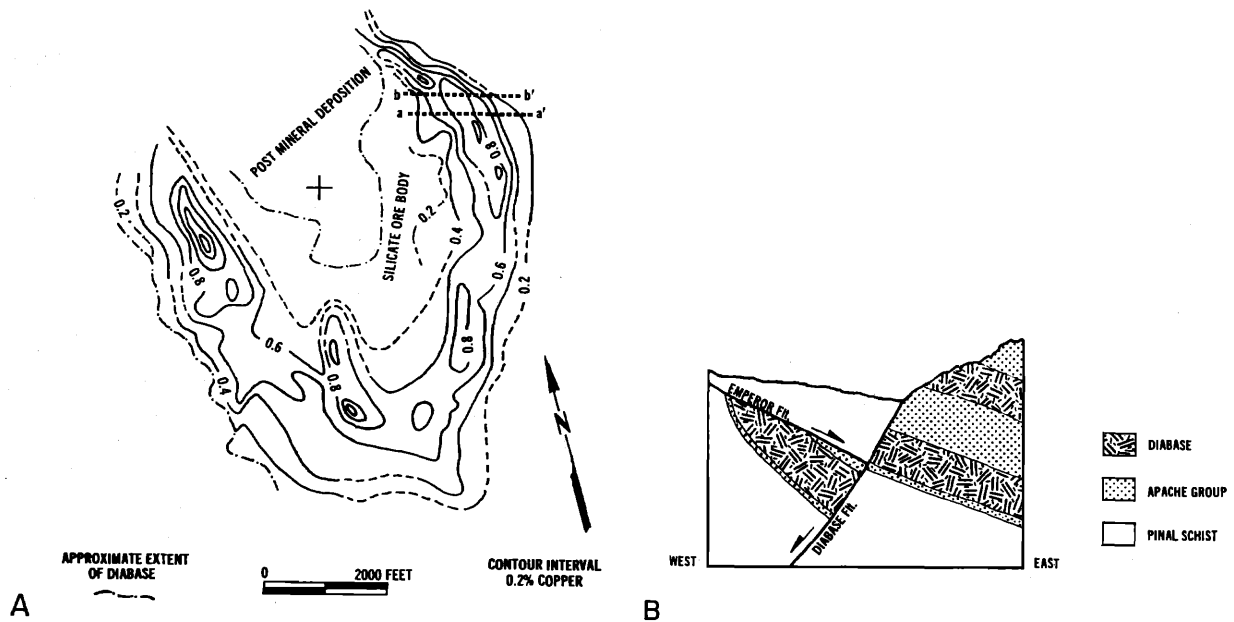


FIG. 6A. Plan view of the hypogene copper distribution in the lower diabase sill at Ray, Arizona. The contours indicate the average grade for the entire thickness of the lower sill at a given point without reference and elevation.

FIG. 6B. Generalized cross section (not to scale) illustrating the extent of the lower diabase sill beneath the Emperor Fault.

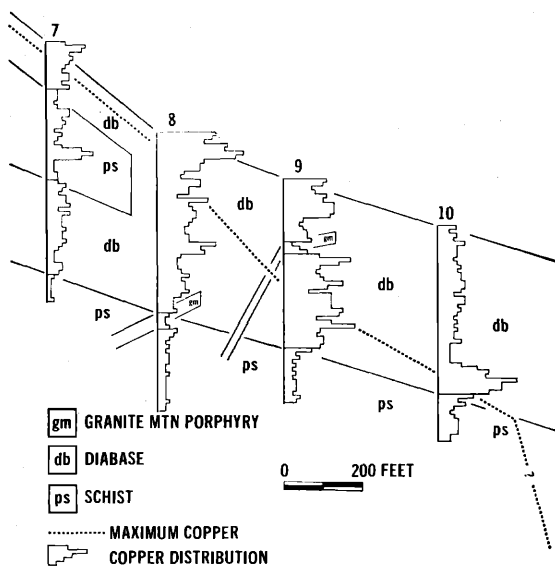
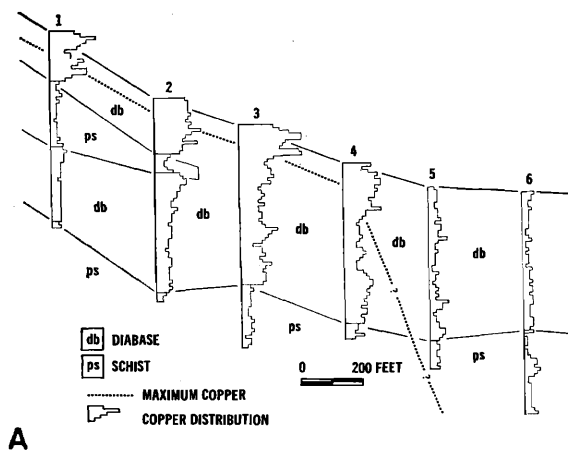


FIG. 7A. Hypogene copper distribution in drill holes along section a-a' (Fig. 6A). Note the high copper concentration at the top of the sill.

FIG. 7B. Hypogene copper distribution in drill holes along section b-b' (Fig. 6A). Note the high copper concentration in the lower part of the sill in holes 9 and 10.

an elongation approximately parallel to the intrusions is observed. The north-south elongation of the copper values in the diabase is probably the result of the premineral distribution of the diabase because the diabase is terminated against the Emperor Fault on the western side of the orebody (Fig. 6B). The open end of the horseshoe is the result of the effects of postmineral faulting, intrusion of a Teapot Mountain Porphyry stock, and erosion which, combined, have eliminated the diabase in this area.

Two vertical sections, a-a' and b-b' (Fig. 6A), in an area of fairly complete drilling were selected for

a detailed study of the copper distribution within the sill. The copper distribution in diamond drill holes along these two sections is illustrated in Figures 7A and 7B. Here the lower diabase sill has intruded the Pinal Schist, splitting into two branches on the west side of the section. In section a-a' (Fig. 7A), the maximum copper grade follows the top of the sill in holes 1 through 4 and plunges abruptly between holes 4 and 5. In contrast, section b-b' (Fig. 7B) clearly shows no such rapid plunge of the maximum copper grade; instead, the maximum concentration of copper appears to deepen regularly with respect to the top of the sill as the mineralization is followed from hole 8 through holes 9 and 10. The downward plunge (east of hole 10) of the highest copper values below the diabase is an interpretation based on data from other drill holes in the near vicinity.

Figure 8 contains four graphs illustrating the zoning of copper, total sulfide, chalcopyrite, and magnetite along section a-a'. The dotted line in each graph is the average across the total thickness of the lower diabase sill.

In holes 1 and 2 (Fig. 8A) where the sill branches around a large included lens of schist, the average copper content for the top branch is shown by line a, for the bottom branch by line b, and for the schist by line c. The maximum average copper content for the entire thickness of the diabase sill is in hole 3 with rapidly decreasing average copper content on either side. Note the break in the curve at hole 5, marking the change from the high copper doughnut to the pyrite zone.

The histogram in the upper righthand corner of Figure 8A shows the frequency distribution of copper assay values in the diabase along section a-a'. The positive skewness in the distribution is the result of an overabundance of lower copper values. This is to be expected in a zoned porphyry copper deposit where there is low-grade copper both in the low total sulfide-high chalcopyrite zone and in the high total sulfide-low chalcopyrite zone.

Along section a-a', total sulfide, total magnetite, and the percent chalcopyrite in the sulfides were determined on pulp composites for each of the holes with the exception of hole 2. Samples from this hole were not available. In Figures 8B, 8C, and 8D, points a and b represent the upper and lower branches of the diabase, and point c is the schist.

The total sulfide by weight content along a-a' is shown in Figure 8B. An average of the sulfide data for the diabase in hole 1 shows that there is little difference between it and the schist. The sulfide content gradually increases from hole 1 to 4, then dramatically increases between 4 and 5. This change in gradient represents the inner edge of the

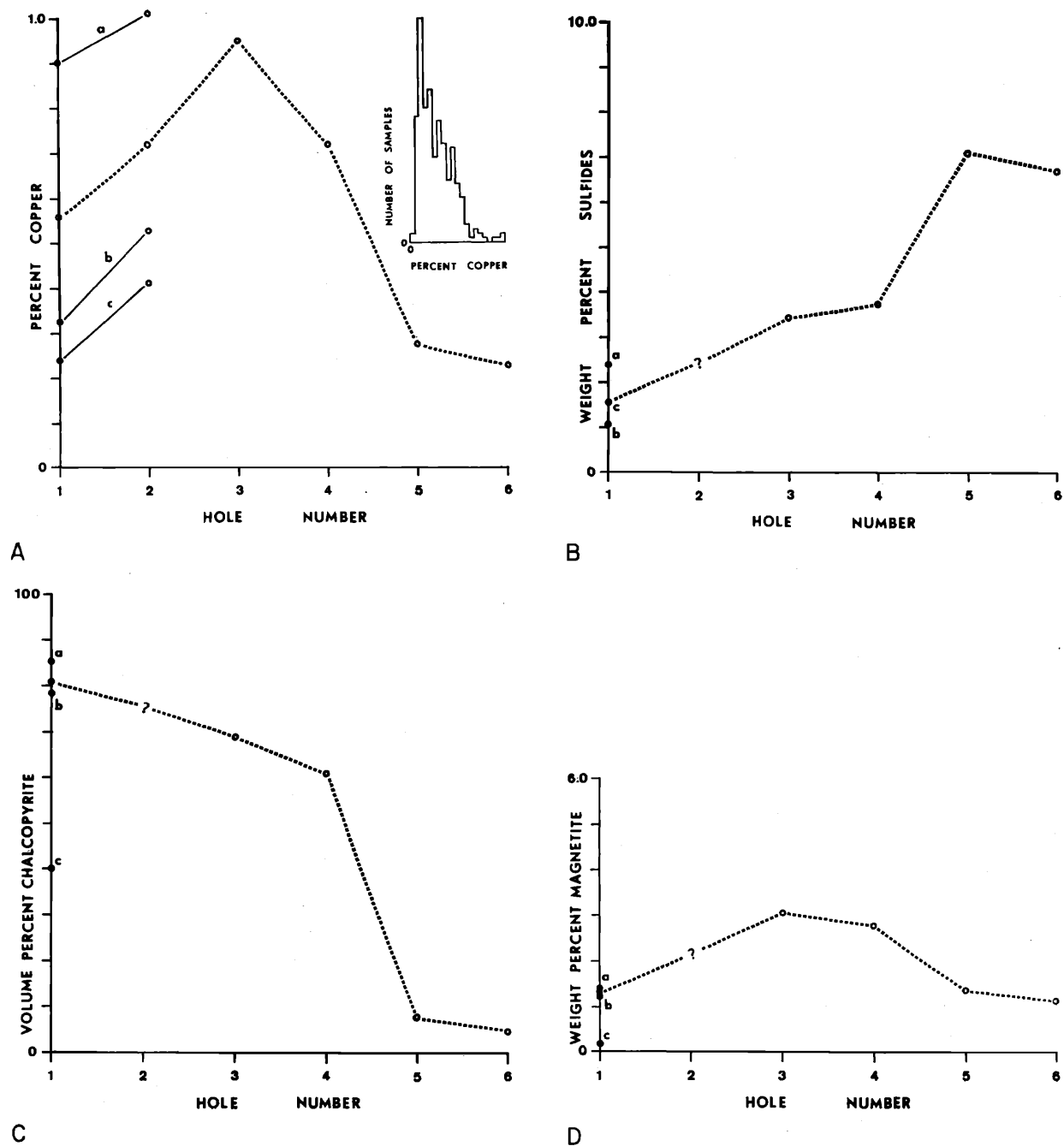


FIG. 8A. Total copper distribution along section a-a'. Lines a and b represent upper and lower diabase, while c is a schist lens. Classes in histogram are in units of 0.10 percent copper.

FIG. 8B. Weight percent sulfides in the rock along section a-a'. Points a and b are diabase, while point c is a schist lens and the average of a and b. Dashed line connects data points for the diabase.

FIG. 8C. Volume percent chalcopyrite in the sulfides. Point a and b are diabase and point c is schist. Note the drop in chalcopyrite in the schist.

FIG. 8D. Weight percent magnetite in the rock. Points a and b are diabase and point c is schist. Compare this curve to Figure 8A.

pyrite halo. In hole 6 the sulfides begin to drop off as the strong sulfide mineralization weakens outward in the pyrite halo.

The affinity of the diabase for copper is illustrated in Figure 8C, where the proportion of chalcopyrite in the sulfides along section a-a' is plotted.

The schist in hole 1 shows a drastic difference in chalcopyrite content relative to the diabase in the same hole. The ratio of chalcopyrite to pyrite in the diabase is about 83/17, whereas in the schist it is 40/60. Referring to Figures 8A and 8B, the sulfide content of the schist is approximately equal to that of the diabase, while the copper grade in the schist is lower than the diabase. From the standpoint of total copper and the ratio of chalcopyrite to pyrite, the schist in hole 1 is equivalent to the diabase between holes 4 and 5. Figure 8D illustrates what the authors believe could be one of the more important aspects of this study: At Ray the diabase contains both disseminated and vein secondary magnetite in addition to primary magnetite. The shape of the magnetite curve resembles the copper curve (Fig. 8A). Observations made on drill core also show that vein magnetite frequently accompanies the better chalcopyrite mineralization.

Alteration zoning

Biotite is one of the most common alteration products in the diabase. It occurs as a fine-grained mesh in vein envelopes and as thin rims surrounding disseminated magnetite and sulfide grains in the wall rock. Megascopically, biotite envelopes are easily distinguished from the less altered wall rock. The width of the vein envelopes is directly related to the size and frequency of occurrence of the quartz-sulfide veins. In a well-mineralized area with strong stockwork veining, the wall rock may be totally altered for tens of feet. Coarse-grained (2.5 mm) secondary biotite is encountered in some quartz-sulfide veins and is most common in the low sulfide-high chalcopyrite core of the deposit.

Two distinct color varieties of secondary biotite are present: brown and olive-green. The dark brown biotite exhibits a slight tendency to form closer to the vein than the olive-green. A small number of observations have shown that the olive-green variety becomes more abundant outward from the high copper zone. The difference in color may be due to variation of the titanium content (Heinrich, 1965) of the biotite. Additional work is needed on the color varieties of secondary biotite and their distribution in the sulfide system.

Within the vein envelopes most of the secondary biotite is an alteration product of pyroxene and hornblende. The biotitization in vein envelopes is accompanied by alteration of the plagioclase to an orange-brown clay. Secondary biotite may be present along the twin planes in the plagioclase.

Secondary biotite in vein envelopes has a widespread lateral distribution in the lower diabase sill. It is present in the low sulfide-high chalcopyrite core outward through the high copper zone and into

the high sulfide-high pyrite zone. It is most intense in the high copper zone, where strong biotite alteration correlates with high copper values.

Secondary magnetite is found in the wall rock and vein envelopes as disseminated anhedral blebs and subhedral, needle-like crystals. Both forms commonly are enclosed by an inner envelope of sphene and an outer envelope of biotite or chlorite. Secondary magnetite also occurs in veins with quartz and sulfides. In some veins chalcopyrite occurs as islands in magnetite and appears early; however, chalcopyrite and pyrite veins appear to cut most magnetite veins. In the high sulfide-high pyrite zone some quartz-sulfide veins are cut by quartz-magnetite veins that in turn are cut by pyrite veins.

Secondary sphene and rutile are present in the altered diabase, and they exhibit a zonal relationship with rutile closer to the veins than sphene. Light gray to white sphene envelopes some anhedral magnetite grains in the wall rock. In most cases the sphene is itself enveloped in secondary biotite or chlorite and may show some alteration to calcite. Bright orange, crystalline aggregates of alteration rutile are usually restricted to the vein envelopes associated with strong biotite alteration. The predominant sulfide in the vein and the envelope may be either pyrite or chalcopyrite.

Both early and late barren quartz veins are present in the diabase. Mineralized quartz veins are abundant in the low sulfide-high chalcopyrite core outward through the high copper zone. In the pyrite halo vein quartz decreases markedly. Fine anhedral quartz is present in many vein envelopes with biotite and clay.

The chief alteration product of the plagioclase in the diabase is a light orange-brown clay mineral. This alteration is most intense in vein envelopes and accompanies strong biotite alteration of the mafic minerals. Kaolinite, identified by X-ray analysis, was observed as a constituent of a few quartz-sulfide veins. The varieties of clay minerals present in the vein envelopes were not identifiable with the petrographic microscope.

Secondary K-feldspar is a rare alteration product in the Ray diabase. Only occasional K-feldspar has been noted as pink blebs and wisps in veins, and these occurrences show no apparent zonal relationships within the sulfide system.

Like K-feldspar, hypogene sericite in the diabase is not abundant within the limits of this study. In the high sulfide-high pyrite zone, sericite and clay minerals are present as partial replacements of plagioclase in the vein envelopes. Biotite, after the mafic minerals, is also present in these envelopes. Late-stage sphalerite-galena veins frequently have sericitic envelopes. Where these veins cut earlier quartz-

sulfide veins with biotite envelopes, the biotite is altered to sericite.

A light green variety of chlorite is common in veins, vein envelopes, and the wall rock. Like biotite, chlorite may envelop disseminated sulfide and magnetite grains in the wall rock. There is usually some remnant biotite in or adjacent to the chlorite, and it is fairly certain that most of the chlorite was generated later than the secondary biotite. Primary hornblende is partially to completely altered to chlorite-biotite. Chlorite in vein envelopes seems to be related to the introduction of late calcite in the vein. Such veins frequently exhibit an inner chlorite and an outer biotite envelope. Coarse-grained, leafy chlorite was noted as the chief constituent of some pyrite veins in the pyrite halo. Minor quantities of chlorite are encountered in many veins throughout the sulfide system. The frequency of chlorite occurrence in the diabase increases outward from the center of the sulfide system.

Though occasional grains and radiating crystalline clusters of epidote occur in quartz-sulfide veins throughout the high copper zone, epidote is most abundant in the pyrite halo where it occurs in pyrite veins and more extensively in the vein envelope as an alteration product of plagioclase. Secondary biotite and chlorite are also present. Granular epidote rimming and veining a clay product in a plagioclase site suggests that the epidote is a late alteration.

Milky-white calcite in quartz-sulfide veins commonly occurs near the center of veins as a filling with microveinlets cutting the sulfide grains. In some cases calcite floods the vein envelopes and replaces earlier formed clay minerals. Although it appears to be largely a late mineral, calcite is most abundant in veins in the high copper zone and shows a tendency to decrease, both inward and outward, from this zone. It is theorized that calcite crystallization or deposition may have been favorably influenced by the calcic nature of the plagioclase (labradorite) in the unaltered diabase.

Anhydrite was not noted in the thin sections studied; therefore, the following discussion will be based entirely on megascopic observations. Coarsely crystalline, light purple anhydrite is present as a major constituent of some quartz-sulfide veins. The principal sulfide may be either pyrite or chalcopyrite. Minor quantities of coarse-grained chlorite or vein biotite with rarer K-feldspar may also be present. The abundance of purple anhydrite increases with depth. For some unknown reason the greatest concentration of purple anhydrite is restricted to the high copper zone on the southwestern side of the orebody west of the Diabase Fault.

Minor quantities of orange to white crystalline chabazite occur in some quartz-sulfide veins in the ore zone and outward through the pyrite halo. Chabazite appears to be a late vein filling.

A major problem that needs additional work deals with when and how some alteration features in the diabase took place, i.e., late deuteric and Precambrian or hydrothermal and Laramide. An example is uralitization. Much of the pyroxene in the diabase shows partial to complete alteration to fine-grained amphibole. The authors believe that at least part of the uralitization in the diabase is the result of hydrothermal alteration. This is compatible with the tendency to form hydrous silicate alteration products, and to date, petrographic studies indicate decreasing uralitization and increasing pyroxene with increasing distance outward from the orebody.

Granite Mountain Porphyry

The porphyry, as exposed in outcrops and in drill core, does not form a single stocklike mass centrally located within the sulfide system but occurs as several irregularly shaped stocks or chonolithic masses and as smaller dikes and sills. On a district scale, the distribution of the intrusives is controlled by a poorly defined zone known as the porphyry break (Metz and Rose, 1966), which is some 3,000 to 4,000 feet wide and trends N. 70°E. away from the main stock on Granite Mountain. The porphyry masses, dikes, and sills now exposed on the surface and by drilling were emplaced and solidified in advance of the invasion of ore-bearing hydrothermal solutions.

Drilling to depths in excess of 3,000 feet has not encountered a large single stock that would explain the position of the Ray orebody by providing a central igneous source. Drilling does indicate that the outcropping Granite Mountain stocks, shown in Figure 2, are roughly connected with extensive, small chonolithic intrusions at depth in the center of the sulfide system. There is some indication that the larger porphyry masses may have acted as individual centers for mineralization and alteration. An example is the small, isolated area of high copper zone mineralization around the intrusive on the southwest side of the high copper doughnut (Fig. 3). The small size and irregular shape of the intrusives make it difficult to define zoning patterns or trends within the porphyries themselves.

Copper distribution

The porphyry was a poorer host for copper mineralization than the diabase. Only 17 percent of the rock within the final limits of the open pit is comprised of Granite Mountain porphyry with an average, and rather uniform, copper grade of 0.21

percent copper. Only 6 percent of the porphyry contains more than 0.4 percent copper.

Alteration zoning

Most of the alteration within the porphyry is restricted to veins or veinlets and their margins. Pervasive alteration is rare, occurring only where veins are strongly developed and closely spaced with merging or overlapping alteration envelopes. The predominant alteration mineral assemblage is K-feldspar, quartz, biotite, and sericite. Clays and chlorite are less common alteration products. Calcite and anhydrite are occasionally present.

Two main types of veins were observed in the porphyry. Biotite-K-feldspar veining, common throughout the rock, appears to have been followed by a phase of less frequently encountered quartz-sericite alteration. Although most of the samples studied were drill core from the primary sulfide zone, it is possible that some alteration minerals such as clays, sericite, and perhaps quartz, may, in part, be supergene.

Secondary K-feldspar is a common alteration mineral throughout most of the porphyry. It is most abundant as envelopes on early quartz veins and a replacement of plagioclase and, rarely, biotite. Secondary K-feldspar is distinguished by its association with quartz veins and its grain size, which is normally larger than matrix orthoclase and smaller than primary phenocrysts.

Most of the biotite in the porphyry occurs as fresh books that are a primary constituent of the rock. Typical secondary biotite, though not abundant, is best developed as envelopes on quartz-K-feldspar veins and as discrete crystals in veins. Some of the primary biotite is rimmed or completely replaced by chlorite. In or along the quartz-sericite veins, biotite is replaced by sericite. Sulfides also commonly replace biotite.

Sericite occurs throughout the porphyry as a weak to moderate replacement of feldspars, particularly along twinning planes of plagioclase. It is moderately to strongly developed as selvages on quartz veins, where it may replace all minerals except quartz. Strong pyrite mineralization is associated with this type of veining. Quartz-sericite alteration appears to be later, superimposed upon or crosscutting the biotite-orthoclase alteration. Where strongly developed, this later alteration nearly obscures evidence of the earlier biotite-K-feldspar phase.

In areas where veining is not strongly developed or closely spaced, fresh books of primary biotite and plagioclase remain essentially unaltered.

Replacement quartz and vein quartz is ubiquitous and is associated with all phases of hydrothermal

activity. Quartz replaces biotite and feldspars. Most early quartz veins have orthoclase selvages with or without secondary biotite. These veins contain pyrite and chalcopyrite, and in some areas calcite and/or anhydrite occur as late cavity filling or replacement minerals. Later quartz veins up to an inch or more wide have strongly developed sericite envelopes and frequently show strong pyrite mineralization with little or no chalcopyrite. Crosscutting both of these vein systems are clear quartz veins with very narrow, if any, alteration envelopes; these may also contain small amounts of molybdenite and chalcopyrite.

Though the limited extent of porphyry bodies within the sulfide system precludes the demonstration of systematic sulfide or silicate zoning in the porphyry, the limited data available suggest that in the porphyry stocks which overlap the core and high copper zone (Fig. 3), sulfides are more abundant in the high copper zone. The small stock which lies to the southwest of the high copper doughnut (Fig. 3), is associated with an isolated repetition of features characteristic of the high copper zone. This stock has the highest total sulfide content of any of the Granite Mountain stocks and contains slightly below the average of chalcopyrite in the sulfide. It is more pyritic than porphyry inside the high copper doughnut but not as pyritic as the adjacent schist. The frequency of occurrence of molybdenite is also much higher near the center of this porphyry than in the surrounding pyritic rocks. Recent field work indicates similar reductions in the total sulfide content accompanied by increased copper and sometimes molybdenum associated with other porphyry stocks that lie beyond the limits of Figure 3. This field work shows the gross extent of sulfide mineralization to be on the order of seven square miles and roughly coextensive with the area intruded by the Granite Mountain Porphyry.

Summary and Conclusions

Ray is atypical in the family of porphyry coppers in that the porphyry is present, not as a central mass, but as several stocks, each of which is mineralized and which cumulatively form a very small part of the total rock mass in the sulfide system, and that most of the hypogene ore is restricted to a much older ferro-magnesian host rock, diabase. The latter feature is nearly unique.

In plan view, the zonal distribution of the hypogene alteration and mineralization is concentric and symmetric, and in a gross sense is similar to other porphyry copper deposits (Lowell and Guilbert, 1970; James, 1971). The total sulfide content is low in the center of the system and increases outward for a distance of about 3,000 feet to a maxi-

imum of from 3 to 8 weight percent sulfide, and then decreases, approaching zero, 6,000 to 8,000 feet from the center. The ratio of chalcopyrite to pyrite follows a reverse pattern with the highest chalcopyrite ratio in the center, decreasing outward. Changes in the gradients of total sulfide and chalcopyrite ratios define three zones:

1. A low sulfide-high chalcopyrite core that rarely contains ore-grade copper (0.4 percent),
2. A zone of changing total sulfide gradient in which the total sulfide content increases rapidly and the ratio of chalcopyrite to pyrite decreases, and
3. The pyrite halo where the total sulfide content reaches a maximum and is largely pyrite, and total copper is low.

While this pattern is present in all rock types, the actual quantity of sulfide and the ratio of chalcopyrite to pyrite are controlled by the host rock chemistry. The diabase sills contain both more sulfide, particularly outside the low sulfide core, and a higher ratio of chalcopyrite to pyrite than the siliceous rocks. Iron-rich units of the Precambrian schist tend to show the same affinity for sulfides and copper that the diabase sills do. The iron-rich rocks are much better hosts for copper mineralization at Ray than are the siliceous rocks, presumably because the iron-rich rocks are chemically more reactive.

The zoning of hypogene alteration products is markedly affected by rock type. In the siliceous Precambrian rocks, an older biotite-K-feldspar alteration extends throughout the area of the sulfide system. This alteration was most intense in the low-grade core and weakened with distance from the center. Superimposed on the biotite-K-feldspar alteration is a later period of sericite alteration that obliterated much of the earlier alteration (this later period need not be a discrete event but simply a stage of a continuing process). The sericite extends throughout the sulfide system but reaches maximum intensity near the interface of the high copper zone and the pyrite halo. Overlapping and extending beyond the sericite is an irregular propylitic zone in which epidote is the principal alteration product. In all rock types the frequency and abundance of quartz veins decrease outward from the center of the sulfide system.

The alteration in the diabase departs from that of the typical porphyry copper in the absence of a major zone of sericitic alteration. The characteristic alteration of the diabase is abundant biotite with clay. In the pyrite halo, biotite becomes less abundant, epidote and chlorite become more common, and sericite is seen rarely.

The diabase has a distinct propensity to alter to biotite rather than to K-feldspar or sericite, both of which are uncommon in the diabase. In many instances biotitized diabase is only inches away from sericitized schist or quartzite, strongly suggesting biotite must have formed in diabase from the same solutions that produced sericite in the silicic rocks.

Although the gross zoning pattern seems to be superimposed on some of the porphyry stocks, there are indications that certain—possibly all—of the stocks did act as separate centers of hydrothermal activity. The large concentric zoning pattern, which includes the Ray orebody, could be the result of the coalescence of the hydrothermal flow associated with the several stocks within the pattern. The alternative—a single center of mineralization in the small, irregular intrusions in the core of the sulfide system—still necessitates some additional source for areas to the west, beyond the map coverage (Fig. 2), that have mineralization suggestive of the low-grade core or the high copper zone.

Practical results of the study have been a clearer picture of the geometry of the Ray sulfide system as well as strong indications of where future prospecting should be concentrated. The presence of essentially the same kind of alteration and mineralization on opposite sides of all the major faults that cut the orebody, limits the postmineral displacement to no more than a few hundred feet.

Perhaps one of the most significant conclusions reached is an indication that magnetite in the diabase is concentrated in the vicinity of the high copper zone or inner pyrite halo. This magnetite concentration might affect the interpretation of magnetic data in southern Arizona.

Previous publications (Metz and Rose, 1966; Metz and Caviness, 1968) on the Ray deposit state that the maximum copper concentration occurs at the top of the diabase sills and that the topmost sill would contain a higher percentage of copper than the next underlying sill. Although this is true for specific locations, new drill data does not support the concept as a general rule. Shallow pyritic sills have been found to be underlain by ore-bearing sills, and in some cases the maximum copper content is found at the bottom of sills. The actual distribution depends on the zoning pattern.

The integration of new data, with the observed lateral expansion of the sulfide system with depth, indicates that the Ray orebody lies in the upper part of the system. Very probably the flat-lying, reactive diabase sills accentuated the upward constriction of the high copper zone.

Other interesting features, still under study, of the Ray deposit are the widespread occurrence of calcite, the zoning relationship of sphene and rutile,

and the possible uralitization of pyroxene. These features may be unique and related to the diabase.

Acknowledgments

As at most large ore deposits, the geologic work has been carried on by many able men. We wish particularly to acknowledge the work of Robert Metz as well as numerous geologists from Bear Creek Mining Company and Kennecott Exploration Services, especially Allen James, supervising geologist (retired) of Kennecott Operating Properties; John Wilson, director of Kennecott Exploration Services; and Denis Norton, formerly chief of Geochemical Research and Laboratory Division of Kennecott Exploration Services. Henry Cornwall and Norman Banks of the U. S. Geological Survey have contributed to our work at Ray through many discussion sessions.

GEOLOGY DEPARTMENT
RAY MINES DIVISION
KENNECOTT COPPER CORPORATION
HAYDEN, ARIZONA 85235
October 30, 1973; May 31, 1974

REFERENCES

- Cornwall, H. R., Banks, N. G., and Phillips, C. H., 1971, Geologic map of the Sonora Quadrangle, Pinal and Gila Counties, Arizona: U. S. Geol. Survey Map G. Q. 1021.
- Heinrich, W. E., 1965, Microscopic identification of minerals: New York, McGraw Hill Book Company, 414 p.
- James, A. H., 1971, Hypothetical diagrams of several porphyry copper deposits: *ECON. GEOL.*, v. 66 p. 43-47.
- Lowell, J. D., and Guilbert, J. M., 1970, Lateral and vertical alteration-mineralization zoning in porphyry ore deposits: *ECON. GEOL.*, v. 65, pp. 343-408.
- Metz, R. A., and Caviness, C. R., 1968, Recent developments in the geology of the Ray area in southern Arizona: *Arizona Geol. Soc. Guidebook III*, p. 137-146.
- Metz, R. A., and Rose, A. W., 1966, Geology of the Ray copper deposits, Ray, Arizona, in Titley, S. R., and Hicks, C. L., eds., *Geology of the porphyry copper deposits, southwestern North America*: Tucson, University of Arizona Press, p. 177-188.
- Peterson, N. P., 1962, Geology and ore deposits of the Globe-Miami district, Arizona: U. S. Geol. Survey Prof. Paper 342, 151 p.
- Ransome, F. L., 1919, The copper deposits of Ray and Miami, Arizona: U. S. Geol. Survey Prof. Paper 115, 192 p.
- Short, M. N., Galbraith, F. W., Harshman, E. N., Kuhn, T. H., and Wilson, E. D., 1943, Geology and ore deposits of the Superior mining area, Arizona: *Arizona Bur. Mines Bull.* 151, 159 p.
- Shride, A. F., 1967, Younger Precambrian geology in southern Arizona: U. S. Geol. Survey Prof. Paper 566, 89 p.

Appendix IV

Late Cretaceous and Cenozoic Orogenesis
of Arizona and Adjacent Regions:
A Stratotectonic Approach

by

S.B. Keith and J.C.Wilt

LATE CRETACEOUS AND CENOZOIC OROGENESIS OF ARIZONA AND ADJACENT REGIONS: A STRATO-TECTONIC APPROACH

Stanley B. Keith
MagmaChem Exploration Inc.
10827 S. 51st St.
Phoenix, AZ 85044

Jan C. Wilt
Consulting Geologist
3035 S. Shiela Ave.
Tucson, AZ 85746

ABSTRACT

Strato-tectonic analysis of Late Cretaceous - Cenozoic stratigraphy, structure, and resources of Arizona and adjacent regions reveals the presence of three major diachronous orogenic events: 1) Laramide orogeny of late Cretaceous to late Eocene; 2) Galiuro orogeny (new) of late Eocene to mid-Miocene, which was formerly called the mid-Tertiary orogeny; and 3) San Andreas orogeny (new) of late Miocene to present, which includes Basin-Range nomenclature.

Laramide orogeny in the Basin and Range Province consists of five major, eastward-younging, sequential assemblages that include, from oldest to youngest: 1) metaluminous, quartz alkalic, hydrous magmatism; Cu-Au porphyry deposits; and E-W to WNW-trending, wedge uplifts and folds (Hillsboro assemblage); 2) metaluminous, alkali-calcic, hydrous magmatism; Pb-Zn-Ag vein and replacement deposits; and NE-directed folds and thrusts (Tombstone assemblage); 3) metaluminous, calc-alkalic, hydrous magmatism; large zoned porphyry Cu-Mo systems; and E-W to NE-striking dikes and distributed left shear on WNW-striking faults (Morenci assemblage); 4) peraluminous, subalkaline, hydrous plutonism; regional-scale, SW-directed thrust faults and related mylonitic deformation (Wilderness assemblage); and 5) greenschist-grade, mostly sodic, metagraywacke beneath crustal-scale, SW-directed, thrusts (Orocopia assemblage).

Galiuro orogeny consists of three major, westward-younging, sequential assemblages that include, from oldest to youngest: 1) low-energy sedimentation in reverse(?) - faulted basins (Mineta assemblage); 2) extensive, metaluminous, calc-alkalic and alkali-calcic, hydrous ignimbritic magmatism; Au-Ag-W and Pb-Zn-Ag veins and replacements; local, coarse clastic sedimentation with megabreccia units; and crustal-scale, NW-SE-trending, broad folds, and NW-striking

reverse(?) faults (Galiuro assemblage); and 3) metaluminous, alkalic, hydrous magmatism; Au-Ag veins and minor Cu replacements; coarse clastic sedimentation; major low-angle normal (detachment) faults, minor reverse faults, and continued crustal-scale warping (Whipple assemblage).

San Andreas orogeny consists of two orogenic assemblages: 1) NE-SW to E-W trending folds (Transverse assemblage); and 2) metaluminous, alkaline, anhydrous, iron-rich, magmatism; N-S trending horsts and grabens; internally drained, lacustrine basins with fringing coarse clastics; and industrial mineral deposits (Basin and Range assemblage).

INTRODUCTION

In spite of a general agreement on a tripartite division of late Cretaceous-Cenozoic orogenesis in Arizona and adjacent regions, there is considerable disagreement on the tectonic style and dynamics of each orogenic event. Several recent developments provide new constraints for structural and dynamic interpretations of the various orogenic events. Perhaps the most significant development is the discovery of the Cordilleran two-mica granites (Miller and Bradfish, 1980; Keith and others, 1980). Several thousand line miles of deep seismic sections were shot in 1979 to 1981 during the southern Arizona oil play. The seismic data showed conclusively that southern Arizona is pervasively underlain by numerous low-angle seismic reflectors down to depths of 15 km (Keith, 1980; Reif and Robinson, 1981). Drilling results north of Tucson provided persuasive evidence that the top of one array of strong reflectors was a major low-angle fault (Reif and Robinson, 1981).

Results of recent mapping in western Arizona and adjacent southeastern California (Haxel and Dillon, 1978; Reynolds and others, 1980; Frost and

Martin, 1982; Haxel and others, 1984) have documented the regional extent of several events of low-angle thrusting that range in age from late Jurassic to early Tertiary. In addition, recent mapping and geochronological studies have shown the low-angle normal faults of middle Miocene age are distributed through a broad region (Davis, 1980; Shakelford, 1980; Frost and Martin, 1982). Since 1980, several hundred chemical analyses and several hundred new radiometric dates (Shafiqullah and others, 1980; Frost and Martin, 1982) provide a powerful new data base for regional stratigraphic correlation of igneous units. As a result of these new breakthroughs and the abundance of quantitative data, concepts of late Cretaceous and Tertiary orogenesis must be adjusted to fit the new data.

Approach and Methodology

The resynthesis of late Cretaceous - Cenozoic orogenesis presented in this paper is based on a detailed strato-tectonic approach. A strato-tectonic correlation chart consisting of 100 strato-tectonic columns from limited geographic areas was prepared with the columns projected to a ENE-WSW line, approximately perpendicular to the North American plate margin. Data used included stratigraphy and structural data from detailed quadrangle mapping, geochronological data, igneous rock chemical composition, and metal contents of associated mineral deposits. The igneous rocks were categorized according to a new chemical classification of igneous rocks based on magma series chemistry and metal contents of associated mineral deposits currently being developed by Keith.

After compilation of the large, strato-tectonic, correlation chart, the data were organized in a manner similar to that used by Coney (1972) into strato-tectonic assemblages that contained unique arrays of lithologies, structures, mineral resources, isotopes, and magma chemistry. These assemblages are named for particular type areas and are shown on a summary strato-tectonic chart (Fig. 1) and are also presented in a series of assemblage maps (Fig. 2-7). Where rock and resource features differed, but were associated with the same structural features, the strato-tectonic assemblages were subdivided into facies. On a larger scale, similar strato-tectonic assemblages were grouped into broader orogenic phases that reflect different stages of orogenic development. All of the above strato-tectonic facies, assemblages, and phases of a given orogeny are generally diachronous (Fig. 1).

Results

Analysis of the strato-tectonic correlation chart revealed three major orogenies in the late Cretaceous and Cenozoic that can be subdivided into orogenic phases and strato-tectonic assemblages (Table 1). The orogenies are: 1) Laramide orogeny (85-43 Ma); 2) Galiuro orogeny (37-13 Ma); and 3) San Andreas orogeny (13-0 Ma). Where necessary, the strato-tectonic assemblages of the orogenies were subdivided into different facies. More detailed characteristics of the various assemblages and their facies are shown in Tables 2-4 and are discussed below in order of decreasing age.

OROGENY	OROGENIC PHASE	ASSEMBLAGES	MAGMATISM	TECTONICS	MINERAL RESOURCES	EPOCH	TIME
SAN ANDREAS	Basin & Range	Basin & Range	basaltic volcanism	grabens	salt, cinders, sand gypsum, zeolites	PLIOCENE	0-13
	Transverse	Transverse	none or rare	en echelon folds trending NE-SW	petroleum, gas	PLIOCENE	0-13
GALIURO	Culminant Galiuro	Whipple	local qtz. alkalic volcanics	gravity slide detachments	Cu-Au-Ag in detach. flts; Au vns	mid-MIOCENE up OLIGOCENE	28-13
	Medial Galiuro	Galiuro	alkali-calcic volc. & dikes	NW-trend folds NW dikes	Pb-Zn-Ag vns Au vns	MIOCENE	38-18
	Initial Galiuro	Mineta	rare volcanics coarse clastics	local basins little data	U, Cu clastics	up OLIGOCENE low MIOCENE	38-28
LARAMIDE	Culminant Laramide	Echo Park Green River Rim Wilderness Orocopia	peraluminous calcic & calc-alk.	SW-dir. thrusts	Au vns & dissem. W, base metals	EOCENE	56-43
	Medial Laramide	Morenci	calc-alkalic dikes & stocks	NE dikes & veins	porphyry copper	EOCENE PALEOCENE	75-50
	Initial Laramide	Denver Tombstone Laramie Hillsboro	alkali-calcic volc. & stocks alkalic stocks & volcanics	NE dir. folds & thrusts NE-shorelines E-W wedge uplifts	Pb-Zn-Ag coal Cu-Au	CRETACEOUS PALEOCENE CRETACEOUS	80-60 85-65
SEVIER			alkalic stocks	S or E dir. thrusts	Au-Cu	CRETACEOUS	105-85

Table 1. General framework of Cretaceous and Cenozoic orogenesis in Arizona.

OROGENESIS, ARIZONA AND ADJACENT REGIONS

OROGENIC PHASE	ASSEMBLAGE	SEDIMENTATION	MAGMATISM	STRUCTURAL FEATURES	MINERAL RESOURCES	AGE (Ma)
Culminant LARAMIDE	Echo Park	arkosic alluv. fans	generally absent	NW-trending sharp asymm. downfolds en echelon	uranium	56-43
	Green River	alluv. plains, mudflats & lacustrine facies	none	large NW to N-S trending asymmetrical thrust uplifts	oil shale, potash uranium?, oil, gas	56-43
	Rim	fluvial gravels	none	shallow NE-dip paleoslope (Eocene erosion surfaces)	none	56-43
	Wilderness	none	calc-alkalic and calcic, hydrous peraluminous 2-mica granitoids	shallow-dipping mylonite zones low-angle SW-dir. thrusts large amount of transport	Au disseminations & veins W veins, minor Ag-Pb-Zn	80-43 AZ 80-38 ? AZ 50-43 NM
	Orocopia	none	none greenschist meta. of metagraywackes	large regional thrusts Chocolate-Vincent thrust vy. large amt shortening	quartz pod. w/ local anomalous Au	60-43 AZ
Medial LARAMIDE	Morenci	none	calc-alkalic, epizonal plutonism & volcanism hydrous, metaluminous	NE to ENE striking dikes distributed left shear through Texas Zone	porphyry Cu-Mo; Cu-Zn skarns; Cu-Ag vns; fringing Zn-Pb-Ag	75-50 AZ 59-50 NM
Initial LARAMIDE	Denver	cse. clastics in asym. basins E of E-facing basement uplifts	local nepheline alkalic magmatism	N-trend, E-facing monoclinial uplifts		74-72 UT 68-64 AZ 70-65 CO
	Tombstone	continental clastics large exotic blocks interbd volcani-clast.	alkali-calcic, hydrous plutonism & pyroclast. volcanism, metalumin.	NW strike, NE-dir. folds & thrusts with 1-10 km shortening	Pb-Zn-Ag veins & replacement deposits	80-70 AZ 70-64 NM
	Laramie	regress. marine-nonmar. ss, sh, ls, bentonite	none vy few volc. clasts	N60W trend shorelines broad N60W folds	coal abundant oil, uranium	85-72 AZ 85-65 NM
	Hillsboro	coarse contin. clastics congl. & alluv. fans	alkalic hydrous volc. & small stocks metaluminous	E-W wedge uplifts & basins WNW-ESE strik., high-angle reverse faults on uplifts	epigenetic Cu-Au porphyries	85-65

Table 2. Summary of assemblages of the Laramide orogeny in Arizona.

This paper presents a summary description of the various orogenies and their component assemblages. Detailed documentation and dynamic and plate tectonic interpretation of the different assemblages, and comparison with previous work will be presented later. For example, detailed documentation, dynamic analysis, and plate tectonic significance of the Laramide strato-tectonic assemblages will be presented in Keith and Wilt (1986).

LARAMIDE OROGENY

In any given area the Laramide orogeny can generally be subdivided into three broad phases that sequentially overprint earlier phases in a systematic manner (Table 2). On a regional basis the orogenic phases are diachronous in that all phases of the Laramide orogeny become generally younger in a west to east direction (Fig. 1). Only the culminant phase (Paleocene-Eocene) of Laramide orogeny is summarized in detail in this paper. However, for completeness, the earlier Laramide phases are briefly summarized below.

Initial Laramide Orogeny

The initial Laramide orogeny is subdivided into two strato-tectonic assemblages in both the Colorado Plateau and Basin and Range provinces. In the Basin and Range Province, initial Laramide orogeny

consists of the Hillsboro assemblage, followed by the Tombstone assemblage. In the Colorado Plateau Province, initial Laramide orogeny consists of the Laramie assemblage, post-dated by the Denver assemblage.

With respect to time, Laramie and Hillsboro assemblages are equivalent. The Laramie assemblage of the Colorado Plateau and Rocky Mountain provinces consists of fine-grained sediments from marine and coastal nonmarine (coal-bearing) facies of the regressive, Late Cretaceous, epicontinental sea. Strandline facies contain detritus with volcanic components and exhibit facies relationships with straight, N60W-trending shorelines that are parallel to broad folds with coal accumulations in the synclines. The Hillsboro assemblage (Keith, 1984) of the Basin and Range Province consists of coarse continental clastics and minor volcanic components that were deposited in west-northwest-trending basins adjacent to west-northwest-trending, commonly double-sided, wedge uplifts. The magmatic component of the Hillsboro assemblage consists of quartz-bearing, alkalic, metaluminous volcanics and epizonal stocks that are associated with copper-gold mineral deposits.

With respect to time, the Denver and Tombstone assemblages are equivalent. The Denver assemblage was named for the 'Denver basin type' of Chapin and Cather (1981) and occurs mainly in Colorado and New

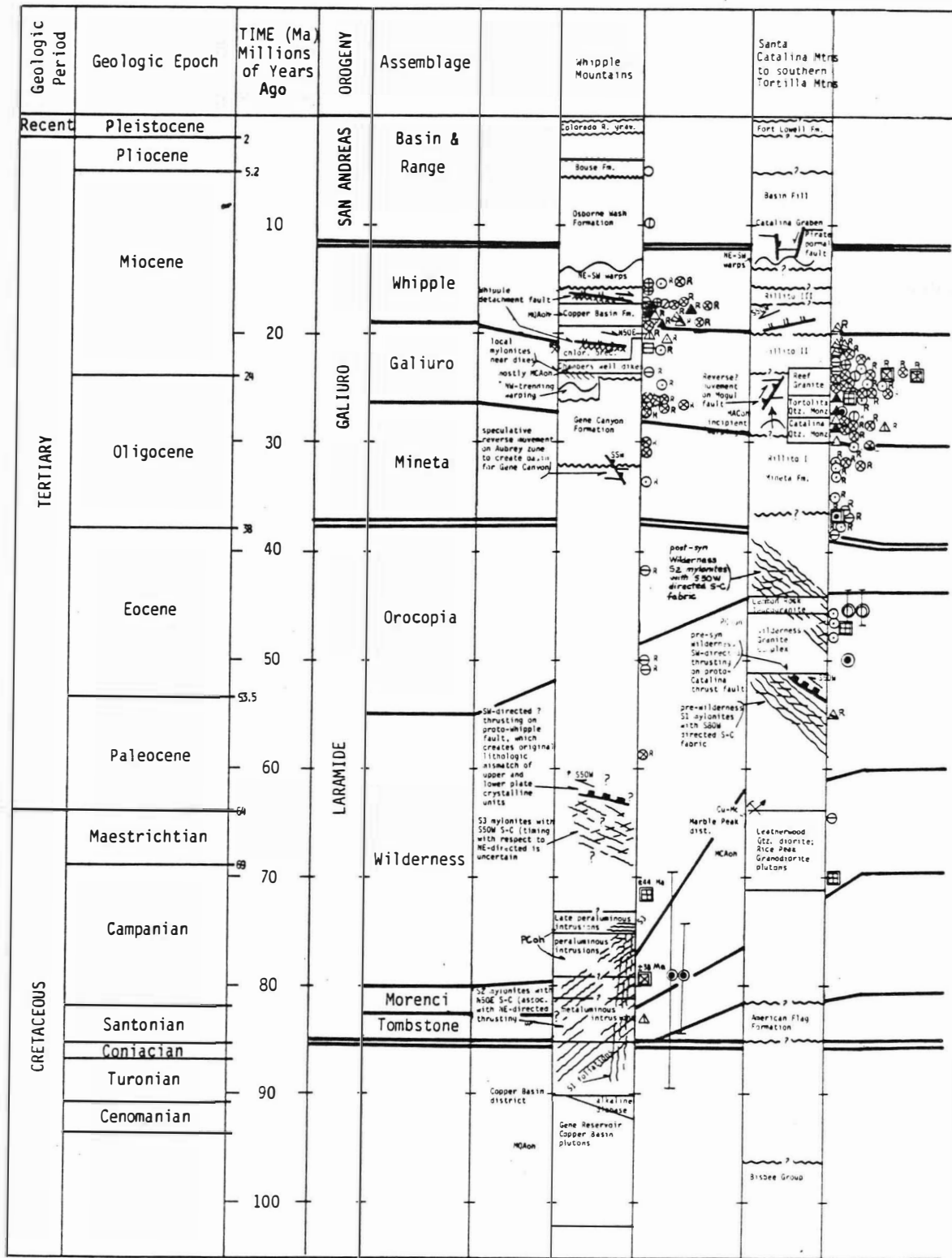
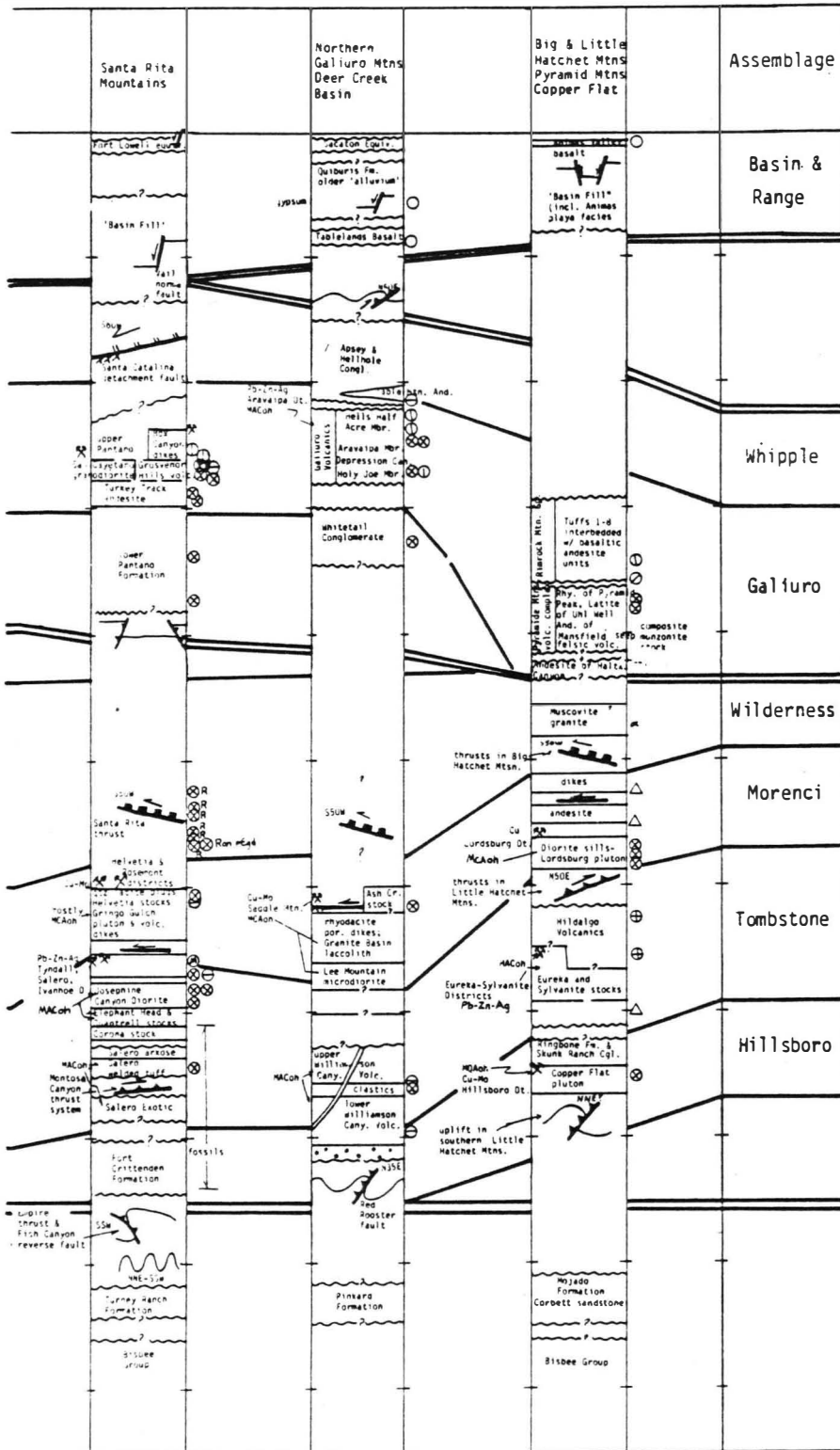
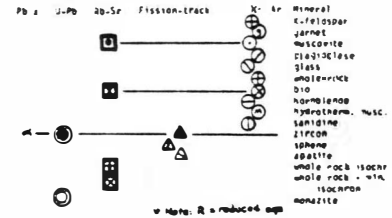


Figure 1. Summary strato-tectonic correlation diagram for late

OROGENESIS, ARIZONA AND ADJACENT REGIONS



EXPLANATION FOR AGE DATES*



EXPLANATION FOR MAGMA SERIES CHEMISTRY**

Symbol Magma Series
 P-Cu Peraluminous calc-alkalic oxidized hydrous series
 PC-Ah Peraluminous calc-alkalic hydrous series
 M-Cu Metaluminous calc-alkalic oxidized hydrous iron-poor series
 MA-Cu Metaluminous calc-alkalic oxidized hydrous iron-poor series
 MA-Ah Metaluminous alkali-calcic oxidized hydrous iron-poor series
 H-Ah Metaluminous quartz-alkalic oxidized hydrous iron-poor

*Magma series chemistry is determined from chemical data in the literature classified according to a new serial chemical classification of igneous rocks being developed by S. B. Kerr.

- grabens formed by normal faults
- folds
- overturned fold & reverse fault
- low-angle normal (detachment) fault
- direction of transport
- uplift
- high-angle reverse fault
- reverse-fault s bounded graben
- mylonitization with S-C fabric
- SW-directed thrust fault
- strike-slip fault
- reverse fault

Cretaceous-Cenozoic orogenesis in Arizona and vicinity.

Mexico. There, it consists of coarse arkoses and conglomerates deposited in asymmetrical synclinal downwarps that are generally east of east-facing basement uplifts that were formed during Maestrichtian to Paleocene time. In Arizona the Tombstone assemblage of Keith (1984) is late Cretaceous (85-69 Ma) and consists of alkali-calcic, metaluminous igneous rocks, with minor volcaniclastic sedimentary rocks, lead-zinc-silver mineralization, and northeast-directed folding and thrust faulting.

Medial Laramide Orogeny

Medial Laramide orogeny in the Basin and Range Province of Arizona only consists of the Morenci assemblage of Keith (1984). Here, the Morenci assemblage is late Cretaceous to early Paleocene in age (75-50 Ma) and consists of calc-alkalic, metaluminous, epizonal plutons and associated large, zoned, porphyry copper-molybdenum systems. Sedimentation is conspicuously absent. The principal structures of the Morenci assemblage are the regional, dike swarms that strike east-west to northeast. The dikes generally occur between west-northwest-striking structural elements of the pre-existing Texas Zone which underwent regional, left shear during medial Laramide orogeny.

Culminant Laramide Orogeny

Green River Assemblage

The Green River Assemblage is largely synonymous with, and is named after the 'Green River-type basins' of Chapin and Cather (1981); these basins exist in a northwest-trending belt through northwest New Mexico, western Colorado, northern Utah, and central Wyoming. In Arizona, the southwestern outcrops of the Baca Formation represent the southwesternmost extension of the Baca Basin, which is mainly developed to the northeast in west-central New Mexico (Chapin and Cather (1981).

Echo Park Assemblage

The Echo Park assemblage is largely synonymous with and is named after the 'Echo Park-type basins' of Chapin and Cather (1981); these basins exist in a north-south belt through central New Mexico and central Colorado. In Arizona, a possible candidate for an Echo Park assemblage is the pre-25 Ma Chuska Sandstone which occurs in a northwest-trending syncline that post-dates the east-facing Defiance monocline of the Denver assemblage.

Rim Assemblage

The name Rim assemblage was given by Keith (1984) to the gravels along the Mogollon Rim in southern Coconino County and southern Navajo and Apache counties. The assemblage was named for the 'Rim gravels' of Peirce and others (1979) and earlier workers. Because of the good exposures, accessibility, and documentation in the literature, the Mogollon Rim south of Show Low is designated as a type area for the Rim assemblage.

Lithologically, the Rim assemblage consists of fluvial gravels with very well-rounded clasts which can be as large as boulders. Structurally, the Rim gravels overlie a regional, very gently inclined, northeasterly dipping paleoslope, the 'Eocene erosion surface' of Epis and Chapin (1975). In the Mogollon slope region the unconformity below the 'Rim gravels' truncates successively older rocks to the south (Peirce and others, 1979).

The Rim assemblage is probably of middle to late Eocene age (52 to 43 Ma). The 'Rim gravels' at Round Top Mountain contain andesite and latite boulder clasts of Laramide volcanics that yield K-Ar dates as young as 54 Ma and are overlain by a rhyolite ignimbrite dated at 28 Ma (Peirce and others, 1979). Near Eager, gravel deposits that are probably correlative with Rim gravels have yielded middle Eocene vertebrate teeth (Young and Hartman, 1984). Similarly, the Frasier Well gravels, a probable Rim gravel equivalent in the western Mogollon Rim, have also yielded a middle Eocene age on a gastropod fauna (Young, 1982). Thus, rocks that cap the Mogollon Rim segment of the Colorado Plateau are most likely middle Eocene in age. The 'Rim gravels' rest on the Paleocene-Eocene unconformity and overlie an unconformity of late Eocene-early Oligocene age that is associated with the Oligocene drainage reversal (Peirce and others, 1979).

Wilderness Assemblage

The name Wilderness assemblage was given by Keith (1984) to peraluminous igneous rocks of Paleocene-Eocene age and related mylonitic and recrystallized metamorphic rocks that occur throughout the Basin and Range Province of Arizona and nearby areas. The name Wilderness was chosen for well-exposed, well-documented, peraluminous plutonic rocks of middle Eocene age in the Wilderness of Rocks area of the main range of the Santa Catalina Mountains near Tucson (Keith and others, 1980). This area is designated as the type area of the Wilderness assemblage.

Rocks of the Wilderness Assemblage

There are no sedimentary or volcanic rocks in the Wilderness Assemblage. A prominent 'magma gap' in southeastern Arizona during the Eocene from 55 to 38 Ma had long been recognized by numerous workers (Damon and Mauger, 1966; Snyder and others, 1976; Coney and Reynolds, 1977; Keith, 1978). However, this gap has been filled in recent years with a newly recognized kind of magmatism, the muscovite- and garnet-bearing, peraluminous granites (Keith and others, 1980; Miller and Bradfish, 1980; Wright and Haxel, 1982). Although the 'magma gap' of older work is now largely occupied by the peraluminous granitoids, there is a gap in volcanism in the surface stratigraphy so term 'volcanic gap' could be substituted for 'magma gap'.

In Arizona the peraluminous granitoids assigned by Keith (1984) to the Wilderness assemblage are now recognized to be the most widespread and most voluminous product of Laramide magmatism (Fig. 2).

OROGENESIS, ARIZONA AND ADJACENT REGIONS

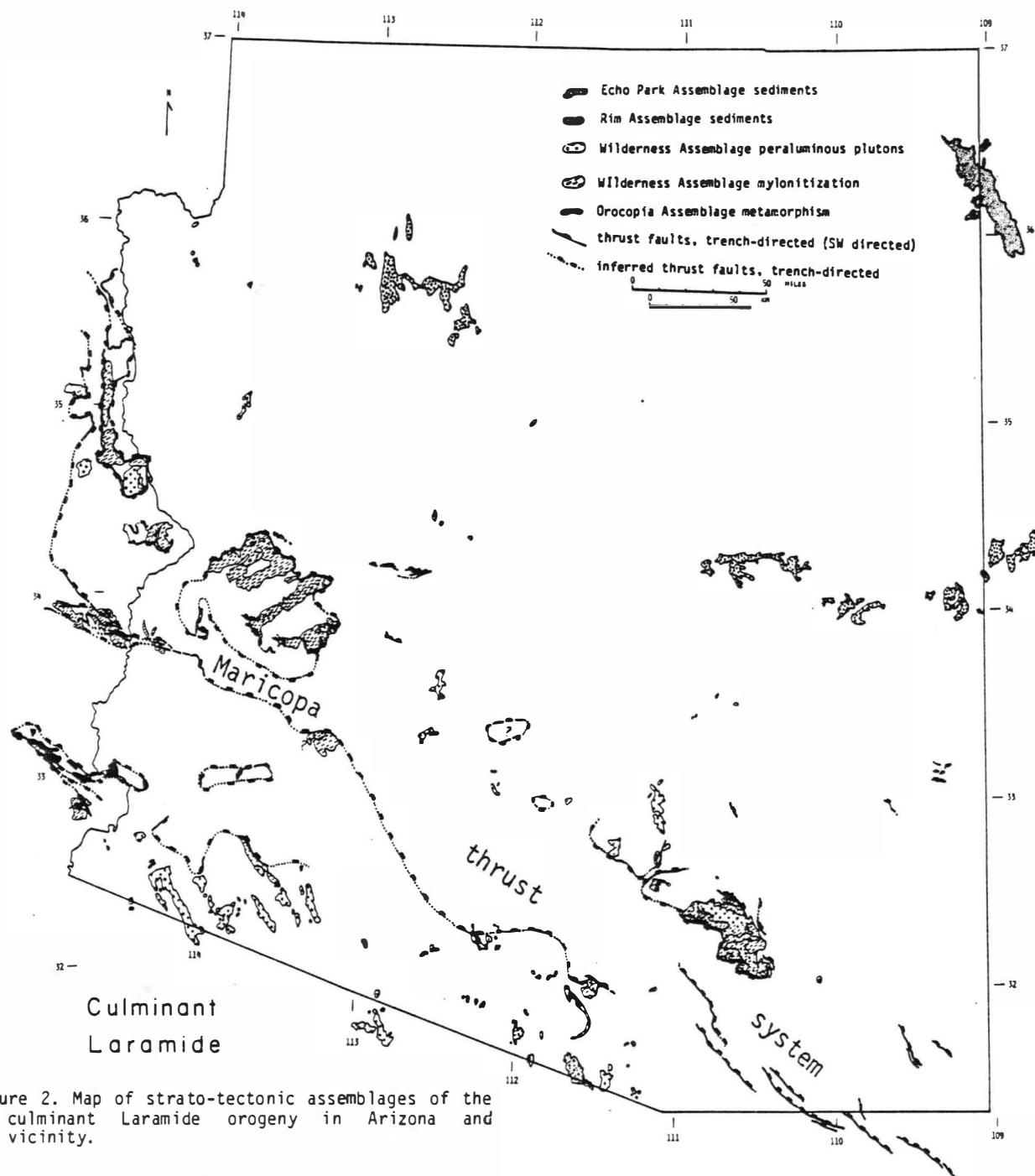


Figure 2. Map of strato-tectonic assemblages of the culminant Laramide orogeny in Arizona and vicinity.

Wilderness assemblage plutons generally occur as sills with low-volume, late phases occurring as dikes that are discordant to the earlier sills. Magmatism of the Wilderness assemblage consists of peraluminous, muscovite- and garnet-bearing granitoids that commonly contain well-developed

alasko-pegmatite complexes in their upper portions. The lower portions of the complexes contain biotite as the principal mica mineral while the upper parts are dominated by muscovite and garnet. In strong contrast to other Cretaceous and Cenozoic magmatism, Wilderness assemblage plutons do not contain mafic

minerals such as olivine, pyroxene or hornblende. Chemically, they are peraluminous, calc-alkalic, iron-poor to weakly iron-rich, hydrous, and oxidized with strontium initial ratios ranging from 0.7085 to 0.725, which is distinctly higher than other Cenozoic magmatism.

Petrologic evidence strongly suggests that the two-mica granites crystallized within the crust, probably at depths equal to or greater than 10 km. Firstly, the lack of surface volcanism suggests that the Wilderness assemblage plutons did not intrude close enough to the ground surface to produce volcanism; magmatism at depths of less than 5 km commonly produces volcanism. Secondly, fluid inclusion data from mineral deposits or from pegmatites and leucogranite phases associated with Wilderness plutons indicate high CO₂ densities (greater than 0.70) requiring a considerable pressure correction for depths to at least 4.5 km (as in the OK pluton of Theodore and others, 1982). A third depth indicator is the widespread distribution of phenocrystic, magmatic muscovite of celadonic composition which indicates depths of greater than 10 km (Anderson and Rowley, 1981). Fourthly, recent geobarometry on garnet, feldspar, and mica in peraluminous plutons in Arizona indicates deep crystallization depths; for example depths of 10 km or more (Wilderness granite in Santa Catalina Mountains; L. Anderson, pers. commun., 1985). Fifth, because Wilderness assemblage plutons have numerous and abundant pegmatites, the water content was probably high. Burnham and Jahns (1962) estimate that water contents for pegmatitic granites are between 8 and 12 weight percent H₂O; they constructed water depth curves that indicate pH₂O of 10 weight percent in a pegmatite would equilibrate with the overlying lithostatic load at about 13 km. A sixth depth indicator is the presence of metamorphic minerals such as kyanite and staurolite in the metamorphic aureoles of several of the Wilderness assemblage plutons, as in the Catalina, Harquahala, and Cargo Muchacho mountains. Minimum depths for staurolite stability at amphibolite grade temperatures are about 8 km. At amphibolite grade temperatures (450°C) the kyanite stability requires approximate minimum depths of 12 km (Holdaway, 1971).

Structural Features of the Wilderness Assemblage

Structures of the Wilderness assemblage consist of mylonitic zones, southwest-directed thrust faults of regional extent, and synkinematic peraluminous sills. The widespread, regionally developed, shallowly dipping, mylonitic zones exhibit a general southwest-directed shear. 'S' surfaces of the mylonites invariably contain a mineral lineation that trends N50-70E to S50-70W. These shear zones are commonly associated with low-angle, southwest-directed thrust faults and synkinematic, peraluminous plutons (Keith, 1982). Regional seismic data (Keith, 1980; Reif and Robinson, 1981) strongly suggest that many of the seismic reflectors can be correlated with surface outcrops of the mylonites. Many of the mylonitic zones are shallowly dipping and northeasterly inclined towards and beneath

Precambrian crystalline rocks along the southwestern boundary of the Colorado Plateau (Otton, 1981).

In Arizona a major northwest-trending zone of southwest-directed thrust faults of the Wilderness assemblage may be present and is herein named the Maricopa thrust system (Fig. 2). Within the Maricopa thrust system are numerous southwest-directed thrusts and southward-overturned folds, many of which are nappe dimension. The western portion of the Maricopa thrust system is well-displayed in California in the Big and Little Maria mountains. Outcropping thrust faults mapped by Haxel and others (1984) that probably comprise parts of the Maricopa thrust system include the Window Mountain Well thrust in the Sierra Blanca Mountains and possible thrust north of the Sil Nakya Hills that would be responsible for southwest-overturning strata there. The zone continues southeast of Tucson and is marked by major, southwest-directed thrusting in the Huachuca Mountains (Fig. 2) and continues into northeast Sonora, Mexico, to Sierra Cabullona.

Northeast of the Maricopa thrust system, a northwest-trending belt of highly tectonized (commonly mylonitic), plutonized, and metamorphosed crystalline rocks are exposed as windows beneath an unmetamorphosed, unmylonitized, upper plate composed mainly of Precambrian crystalline rocks. The plutonized and tectonized crystalline terranes are generally separated from their 'cover' by profound low-angle fault zones that circumscribe the crystalline rocks and produce a 'pseudo-cored' aspect. The term 'pseudo-core' is applied because recent drill hole results summarized by Reif and Robinson (1981) suggest that the plutonized and tectonized basement exists regionally beneath unmetamorphosed cover. Portions of the profound low-angle faults that surround the underlying crystalline 'pseudo-cores' have experienced low-angle, normal separation during the mid-Tertiary, as widely recognized (Davis, 1983; Davis and others, 1980). However, compelling evidence discussed below shows that regional, low-angle, thrust faults juxtaposed nonmylonitic crystalline basement over mylonitic crystalline basement prior to middle Tertiary (Drewes, 1981; Keith, 1982; Haxel and Grubensky, 1984).

An example of a window into the crystalline basement of the lower plate is in the Rincon Mountains where ductile, southwest-directed, flexural-flow, fold deformation of Paleozoic rocks on the east side of the range (Lingrey, 1982) is cut by the Barney Ranch pluton (at least 37 Ma) that was assigned by Keith and others (1980) to the Wilderness suite of plutons. This fold deformation occurs in the lower plate of a regional, low-angle fault that juxtaposes nonmylonitic Precambrian crystalline rocks (1400 Ma or older) over deformed Paleozoic and Cretaceous sections on both sides of the mountain range (Drewes, 1974, 1977; Keith, 1983). Similar, large scale, older over younger, low-angle, fault juxtapositions occur in the Tortolita Mountains (Keith, 1983) and in the Rawhide and Buckskin Mountains of west central Arizona (Shackelford; 1980).

OROGENESIS, ARIZONA AND ADJACENT REGIONS

Timing of Thrusting. Excellent relationships in the Santa Catalina and Rincon Mountain crystalline complexes indicate southwest- to west-southwest-directed tectonite fabrics and southwest-directed thrusting are synchronous with peraluminous magmatism, although the plutons tend to be late kinematic. Near Mount Lemmon in the Santa Catalina Mountains both the 70 Ma Leatherwood quartz diorite and the early, shallowly-dipping phases of the 45-50 Ma leucogranite phase of the Wilderness granite have been deformed by west-southwest-directed S-C mylonitic fabrics. These fabrics are intruded by steeply dipping, later dikes of the leucogranite showing that the mylonitic fabric developed slightly before and during emplacement of the Wilderness suite of middle Eocene age. Other areas showing strong evidence of synchronicity of thrusting, mylonitization, and peraluminous plutonism include the Eastern Peninsular Ranges (Simpson, 1984), the Big Maria Mountains (Hamilton, 1982; Martin and others, 1982), the central Harquahala Mountains (Reynolds and others, 1980), and the Gunnery Range and Papago Indian Reservations (Haxel and others, 1984).

Regional Magnitude of Thrusting. Both geometric reconstructions and petrology of peraluminous magmatism provide strong evidence for the regional magnitude of southwest-directed thrusting. Where southwest-directed thrusting is present, very large amounts of horizontal transport are suggested by the difficulty of matching upper plate lithologies with lower plate lithologies on a regional basis. For example, in the Rincon Mountains east of Tucson, nonmylonitic, generally 1625 Ma, granodioritic, Precambrian rocks in the upper plate of the Catalina fault and their probable analogs in the eastern Rincon Mountains and Johnny Lyon Hills cannot be matched with mylonitic, generally 1400 Ma, granitic, Precambrian rocks in the lower plate anywhere in the mountain range. Importantly, the nonmylonitic Precambrian rocks of the upper plate are commonly juxtaposed over deformed Paleozoic rocks in the lower plate beneath portions of the Catalina fault and its analogs in an older over younger, thrust sense. To remove the nonmylonitic upper plate from the generally mylonitic or deformed lower plate along a line parallel to the lineation requires cumulative transport of at least 35 km, which is the exposed outcrop width of lower plate rocks parallel to lineation.

In the Rawhide, Buckskin, and Northern Plomosa Mountains extensive lithologic mismatches occur between predominantly mylonitic lower plates (generally without 1400 Ma granitic protolith) and nonmylonitic upper plates (with widespread, 1400 Ma granitic, Precambrian protolith). As in the Rincon Mountain example, younger rocks may exist in the lower plate beneath the Precambrian upper plate. In the Buckskin Mountains and Rawhide Mountains Shackelford (1980) has mapped a 'middle plate' of tectonized Paleozoic and Mesozoic rocks above the Rawhide-Buckskin detachment fault. In an area in the northern Rawhide Mountains, Shackelford shows that these Paleozoic rocks are structurally overlain by Precambrian crystalline rocks. The Precambrian

crystalline rocks in that upper plate are, in turn, unconformably overlain by mid-Tertiary volcanic and clastic rocks. Thus, Paleozoic and Mesozoic strata are erosionally missing above the Precambrian in the upper plate, although they are present, though tectonized, above the Precambrian in the middle plate. If the Precambrian-bearing upper plate existed as a regional sheet from the Rawhide to the Plomosa Mountains, then a minimum overlap of 35 km is implied along a line parallel to the widespread N50E-S50W lineation in the lower plate. Similar extensive lithologic mismatches exist between upper and lower plates in the Whipple, Chemehuevi, Sacramento, Dead, and Newberry Mountains of southeastern California and southernmost Nevada.

Ultimate amounts of transport could have been much greater than the minimum of 10 to 35 km deduced directly from the overlap of nonmatching lithologies. Overall transport may have been related to regional, southwest-directed transport on the Maricopa thrust system. The upper plates of the Maricopa thrust system throughout west-central Arizona mainly consist of nonmylonitic, Precambrian, crystalline rocks unconformably overlain by mid-Tertiary clastics and volcanics. This terrane is typical of the 'Mogollon Highlands' of Cooley and Davidson (1963) where Paleozoic and Mesozoic strata south of the Colorado Plateau were stripped away by erosion during the Mesozoic through early Tertiary. The 'plate' of Tertiary deposited on nonmylonitic Precambrian, which is predominantly 1400 Ma granite, is the structurally highest plate in the Riverside, Whipple, Rawhide, Buckskin, Harquahala, Big Horn, Harquar, and Plomosa Mountains. The lower plates in this region consist of tectonically imbricated, Precambrian, Paleozoic, and Mesozoic protoliths. The occurrence of Mesozoic protoliths in the mylonitic lower plate beneath well-documented nonmylonitic Precambrian rocks in the upper plate thus indicates a regional, older over younger, thrust-relationship. Seismic data indicate that the surface of lithologic mismatch may project beneath the Colorado Plateau in a geometry consistent with regional, southwest-directed thrusting.

If the Maricopa thrust is taken as the leading edge of the above mentioned, regional, thrust 'plate', then present lithologic overlap between the 'plate' bearing the Mogollon Highlands terrane and the lower plates containing Paleozoic and Mesozoic protoliths would be at least 90 km projected to and along the line of the lower plate lineation, which is N50E-S50W. This would be the amount of transport required to remove the overlap. Ninety km is the distance between the Riverside Mountains in southeastern California (the southwesternmost exposures in the upper plate where middle Tertiary unconformably overlies Precambrian) and the northern Rawhide Mountains in western Arizona (the northernmost exposures where metamorphosed Paleozoic sections occur in the lower plate).

Regionally, intrusion of shallow level, metaluminous plutons of the Morenci assemblage by deep level, peraluminous plutons of the Wilderness assemblage suggests regional thrusting occurred

after the Morenci assemblage intrusions in any given area. For example, in the Santa Catalina Mountains, Leatherwood suite plutons of the Morenci assemblage are associated with shallow level (less than 3 km), porphyry copper-skarn mineralization of early Paleocene age (Keith and others, 1980). They are intruded in the Eocene by the Wilderness granite, which probably crystallized at depths of 10 km or more (see discussion of Wilderness assemblage rocks). Thus, at least 7 km of crust was added to the Santa Catalina area after Morenci assemblage intrusion and prior to Wilderness assemblage intrusion. The only logical way to accomplish this is to thicken the crust by regional thrusting on a proto-Catalina fault during culminant Laramide orogeny in early Eocene time.

Six to eight km thicknesses of thrust plates above Wilderness assemblage plutons is consistent with field relationships in several areas that indicate upper plate thicknesses of 3 to 12 km. Examples include 5 to 8 km thickness for the upper plate of the Baboquivari thrust system on the Papago Reservation (Haxel and others, 1984); a 6 km thickness of upper plate in the Johnny Lyon Hills 40 km east of Tucson; a 3 km thickness of the rotated Precambrian plate above the imbricated Paleozoic section in the northern Rawhide Mountains (Davis and others, 1980); and as much as 12 km of tilted crystalline Precambrian rocks in the Mohave Mountains (Howard and others, 1982). In the Arizona State A-1 well (Reif and Robinson, 1981) the upper plate is at least 2.3 km thick and consists of 1400 Ma granite.

Amounts of southwest-directed thrusting may also be estimated from the petrologic data. For example, using a petrologically estimated thickness of thrust plate above a given Wilderness assemblage pluton of about 8 km and a regional dip from seismic data of the Maricopa thrust system beneath the Colorado Plateau of about 30° , then about 150 km of thrust overlap is required using the sine function. This figure roughly agrees with lithological overlap evidence presented earlier.

Age of Wilderness Assemblage

In common with metaluminous magmatism of the earlier Laramide, peraluminous granitoids of the Wilderness assemblage are generally older in the west and younger in the east. In the Old Woman Mountains of southeastern California, Miller and Bradfish (1980) report an approximately 80 Ma Rb-Sr isochron for the Sweetwater Wash pluton. To the east U-Pb data from the Pan Tak pluton in the Coyote Mountains is about 58 Ma (Wright and Haxel, 1982). About 60 km further to the east in the Santa Catalina Mountains, the Wilderness granite is 44-50 Ma (Keith and others, 1980). Peraluminous plutonism, mylonitization, and southwest-directed thrusting occur in southeast California between 85 and 75-70 Ma, between 70 to 60 Ma in western Arizona, and between 60 to 44 Ma in southeastern Arizona.

On a regional scale, the peraluminous plutons occupy the youngest part of the west to east

magmatic sweep on the time-distance curve of Coney and Reynolds (1977). In any given time slice, the peraluminous plutons occupied a diffuse plutonic belt west of the older metaluminous magmatism and moved eastward with the metaluminous magmatism in a coordinated, paired fashion (Keith and Reynolds, 1981). Thus, Wilderness assemblage magmatism in any given area represents the culmination of Laramide orogeny.

Reduced Isotopic Ages. Wilderness assemblage plutonism, deformation, and metamorphism is accompanied by widespread resetting of relatively nonresistant K-Ar and fission-track, isotopic systems. The reduced isotopic ages are about the same age as or slightly younger than the emplacement of the peraluminous granites in the general vicinity. As with the peraluminous plutons of the Wilderness assemblage and the magmatism of Laramide strato-tectonic assemblages in general, Wilderness assemblage reduced ages become younger eastward. For example, in the Transverse Ranges of southeast California, Miller and Morton (1980) have obtained numerous reduced K-Ar dates that range from 85 to 72 Ma. To the east in the Big Maria Mountains K-Ar cooling ages on Precambrian through Mesozoic metasedimentary rocks range from 72-50 Ma (Martin and others, 1982). In western Arizona numerous reduced K-Ar ages cluster between 60-44 Ma (Shafiqullah and others, 1980). In each area, the reduced K-Ar and fission track dates coincide with emplacement ages of peraluminous plutons of the Wilderness Assemblage.

Orocopia Assemblage

The name Orocopia assemblage was given by Keith (1984) to Laramide recrystallization phenomena in older schistose rocks that possibly were Jurassic or Cretaceous metagraywackes and that now occur in the lower plate of the regional Chocolate Mountain thrust system of southeastern California and southwestern Arizona. Laramide recrystallization is indicated by numerous reduced K-Ar ages that record termination of a metamorphic event that was possibly associated with the final emplacement of schistose rocks, such as the Orocopia, Rand, and Pelona schists summarized by Haxel and Dillon (1978). The term Orocopia assemblage was chosen for recrystallization phenomena in the Orocopia Schist beneath the Chocolate Mountain thrust within the Orocopia Mountains in southeastern California.

Rocks of Orocopia Assemblage

There are no sedimentary, volcanic, or plutonic rocks in the Orocopia assemblage. Rather, Orocopia assemblage 'rocks' consist of metamorphism and recrystallization phenomena in rocks that predate Orocopia assemblage tectonism. Orocopia assemblage metamorphism consists of greenschist-grade metamorphism of metagraywackes that had previously been metamorphosed to blueschist grade (Ehlig, 1968; Graham and England, 1976). The original blueschist-grade metamorphism could have occurred in an accretionary melange wedge developed above the subduction zone from late Jurassic through

OROGENESIS, ARIZONA AND ADJACENT REGIONS

mid-Cretaceous time. The greenschist metamorphism of the Orocochia assemblage would then be related to emplacement via underthrusting beneath the North American plate. The original metamorphism of the schists is no older than 163 Ma, which is the date of a pre-metamorphic, pyroxene-hornblende diorite dike that intrudes metagraywackes of the lower plate (Mukasa and others, 1984) and may pre-date final emplacement subsequent to 85 Ma. Numerous reduced K-Ar ages between 47 to 60 Ma reflect cooling and termination of metamorphism of the Orocochia Schist perhaps during the last phases of emplacement. For example, the Pelona Schist beneath the Vincent thrust in the San Gabriel Mountains was metamorphosed during the Paleocene (Ehlig, 1968). The concentration of K-Ar and Rb-Sr isotopic ages from the Pelona Schist and Vincent thrust in the interval between 50 to 60 Ma suggested to Haxel and Dillon (1978) that the metamorphism occurred in Paleocene time.

Structural Features of Orocochia Assemblage

Structures herein assigned to the Orocochia assemblage consist of the regional thrust faults of the Chocolate-Vincent-Rand thrust system, which is regionally present throughout southeastern California and southwestern Arizona (Haxel and Dillon, 1978; Crowell, 1981). Principal thrusts are the Rand thrust in the Rand Mountains of northeastern Kern County, the Vincent thrust in the San Gabriel Mountains of northern Los Angeles County, and the Chocolate Mountain thrust in Riverside and Imperial counties of southeastern California and southern Yuma County in southwestern Arizona.

These structures are very large, very shallowly inclined, northeast-dipping, possibly southwest-directed, regional thrust faults. The foliation fabric within schists of the lower plate below the thrusts generally have northeast-southwest-trending lineation. The upper plate of the Orocochia-Vincent thrust system is commonly affected by thrust-related mylonitic fabric that cuts retrograded granulites, amphibolite-grade paragneiss and orthogneiss of Precambrian through possibly mid-Cretaceous age. The thrust-related mylonites in the upper plate commonly contain a northeast-southwest-trending lineation parallel to lineation in the lower plate schistose rocks. Tectonic transport directions for the upper plate mylonites yield contradictory results, with some suggesting northeast and some indicating southwest transport.

Magnitude of Thrusting. Lateral transport along Orocochia assemblage thrust faults probably was at least 150 km and may have been as much as 625 km or more. The metagraywackes, minor metapelites, cherts, and mafic metavolcanic rocks in the lower plates of Orocochia assemblage thrust faults have no lithologic analogs anywhere in the North American upper plate. In southeastern California and southern Arizona, an overlap of North American upper plate rocks over lower plate metagraywackes of the Orocochia Schist and correlatives can be inferred to

be at least 150 km projected parallel to a N50E-S50W line, which is the average trend of lineation in the lower plate schistose rocks.

Evidence for continent-scale underthrusting of Franciscan-like materials beneath North America was reported by Helmstaedt and Doig (1975). They obtained samples of blueschist eclogite from inclusions in the nepheline alkalic diatremes of mid-Tertiary age at Garnet Ridge and Moses Rock in the Four Corners Region of Arizona and Utah. The affinity between the eclogite inclusions and the Franciscan-like rocks was affirmed by lawsonite cores within amphibole phenocrysts and jadeite cores within pyroxene phenocrysts from the eclogite inclusions. Helmstaedt and Doig (1975) suggested that the only way to get a high-pressure, low-temperature assemblage beneath a continental area such as the Colorado Plateau was to invoke massive continent-scale underthrusting of Franciscan-like materials beneath North America. If it is assumed that the eclogite inclusions are indeed underthrust Franciscan, then the amount of implied lithologic overlap would be at least 625 km.

Missing Crust. A remarkable structural feature of the Orocochia assemblage thrusting is that deep level schistose terranes or metagraywacke packages have been commonly juxtaposed under supercrustal assemblages of the North American plate. Deeper North American crust, such as the granulite layer which would be expected in a normal crustal profile, is commonly missing. There are places, such as in the San Gabriel and Orocochia Mountains, where the granulite lower crust is locally preserved in the upper plate, but for the most part the granulite crust is missing in the upper plate. In effect, the North American crust throughout much of the western Mojave desert region is a rootless, crystalline plate that is resting allochthonously on a probable schistose basement. Some of the deep crustal COCORP seismic lines recently shot across the western Mojave block show numerous reflecting horizons at depth beneath the western Mojave that could in part represent the schistose basement. Based on the seismic data, the base of the present crust in the western Mojave region occurs no deeper than 20 to 25 km, which is about half of the expected thickness for normal continental crust. Thus, the possibility exists that regional-scale tectonic erosion of the North American plate occurred during Orocochia assemblage metamorphism and thrusting.

Age of Orocochia Assemblage

Relative age relationships and geochronologic calibration along the various thrust faults suggest Orocochia assemblage thrusting occurred after 85 Ma and terminated about 60 Ma. In the San Gabriel Mountains hornblende-biotite quartz diorite in the upper plate that is in fault contact with the Vincent thrust yields K-Ar dates on hornblende of 67 Ma (Miller and Morton, 1980). One of the plutons in the San Gabriel Mountains has yielded a U-Pb date on zircon of 80 +/- 10 Ma (Carter and Silver, 1971). Thus, available evidence in the San Gabriel

Mountains indicates emplacement of the Vincent thrust after 80 Ma.

In the Randsburg area, Silver and others (1984) report a U-Pb date of ≈ 86.5 Ma on zircon from a granite in the upper plate that is cut by the Rand thrust zone. This date strongly suggests that emplacement of the schist beneath the Rand thrust is younger than 85 Ma. In the southeasternmost Chocolate Mountains, minimum ages for rock juxtapositions along the Chocolate Mountains thrust are Paleocene based on K-Ar data on the Marcus Wash Granite, which cross-cuts the thrust (Haxel and Dillon, 1978).

In any given area, Orocochia assemblage tectonism appears to post-date Wilderness assemblage tectonism. In several areas of southern California, Wilderness assemblage, peraluminous alaskites are truncated by the Chocolate-Vincent thrust system of the Orocochia Assemblage.

Termination of Laramide Orogeny

The termination of Laramide orogeny on the Colorado Plateau is represented by a widespread unconformity known as the 'Eocene erosion surface' (Epis and Chapin, 1975). In the San Juan Basin in northwestern New Mexico rocks of the San Jose Formation below the Eocene erosion surface are Wasatchian (early Eocene or as young as 50 Ma) (Baltz, 1967). Along the Mogollon Rim segment of the Colorado Plateau in Arizona, 'Rim gravels', which contain clasts yielding early Eocene dates, could be middle Eocene in age and rest beneath the late Eocene-early Oligocene unconformity as they are locally overlain by late Oligocene-Miocene volcanics (28 Ma K-Ar date by Peirce and others, 1979). This regional unconformity of late Eocene to early Oligocene age described by Peirce and others (1979) separates the Laramide and Galiuro orogenies on the Colorado Plateau.

In supercrustal stratigraphic sections of southern Arizona, the Laramide-Galiuro boundary is contained in an unconformity between medial Galiuro orogeny volcanics and sediments and medial Laramide, Morenci assemblage, igneous rocks. In southern Arizona, the unconformity represents a gap of about 20-40 million years (Damon and Mauger, 1966). Thus, conventional use of unconformities yields poor control for the Laramide-Galiuro boundary.

Analysis of the strato-tectonic correlation chart (Fig. 1), however, reveals that little or no time separates Galiuro from Laramide orogeny, because active Laramide deformation, metamorphism, and plutonism was occurring at mid- to sub-crustal levels throughout Eocene time (Wilderness and Orocochia assemblages). In any given area, Orocochia assemblage tectonism post-dates Wilderness assemblage plutonism and is thus the youngest Laramide event, where its presence can be established (southwestern Arizona and southeastern California). In southeast Arizona, however, Wilderness assemblage is the youngest proven Laramide event, although Orocochia assemblage may

exist at depth. From the strato-tectonic chart, the termination of Laramide orogeny in southeastern Arizona and southwestern New Mexico is placed at about 43 Ma and in western Arizona and southeastern California at about 38 Ma.

GALIURO OROGENY

The Galiuro orogeny was originally named by Keith (1977) to differentiate two fundamentally different and independent orogenic events of the middle and late Tertiary: "The style of the Galiuro orogeny (35-15 m.y.) is characterized by: 1) Broad NW-trending elongate uplifts with intervening syntectonic basins containing continental clastic deposits; 2) Broad NW-trending, low-plunging folds; 3) NW-trending dike swarms; 4) Denudational faulting and megabreccia landslides directed away from uplifts; 5) Widespread calc-alkaline magmatism peaking 24-27 m.y. ago; 6) Emplacement of metamorphic core complexes accompanied by SW-NE-trending lineation" (Keith, 1977).

In Arizona these orogenic phenomena have previously been referred to the mid-Tertiary orogeny (Eberly and Stanley, 1978; Shafiqullah and others, 1980). The term 'mid-Tertiary orogeny' is a time term that does not precisely reflect the diachronous nature of orogenic phenomena. In the northwestern United States, Tertiary orogenic phenomena very similar to Galiuro orogeny in Arizona are Eocene or early Tertiary in age; in Baja California similar phenomena are 15 to 5 Ma or middle to late Tertiary in age. Similarly in New Mexico, Galiuro orogenic phenomena are 37 to 22 Ma or early to middle Tertiary in age.

Classically, orogenic nomenclature typically has evolved from some reference region that contained rocks and structures that are considered representative of the orogeny. Thus, geographic terminology, such as 'Sevier' and 'Laramide', is preferable to time terminology, in order to conform with terminology for other orogenies and to emphasize physically locatable phenomena. In southeastern Arizona, rocks, structures, and mineral deposits that are excellent examples of Galiuro orogeny phenomena are well exposed in the Galiuro Mountains and surrounding mountain ranges. Thus, the Galiuro Mountains and vicinity (especially exposures in the Santa Catalina and Tortilla mountains) is designated as the type area for the Galiuro orogeny.

The beginning of Galiuro orogeny in the Basin and Range Province of southern Arizona may be placed at the unconformity below the base of Galiuro assemblage volcanics or underlying Mineta continental clastics. In any given area, the Galiuro orogeny can generally be subdivided into three broad phases that sequentially overprint previous phases in a systematic manner. Galiuro orogeny is divided into initial, medial, and culminant phases that may consist of one or more strato-tectonic assemblages that exhibit lateral or vertical facies relationships with one another (Table 3). On a regional basis, Galiuro orogenic

OROGENESIS, ARIZONA AND ADJACENT REGIONS

OROGENIC PHASE	ASSEMBLAGE	SEDIMENTATION	MAGMATISM	STRUCTURAL FEATURES	MINERAL RESOURCES	AGE (Ma)
Culminant GALIURO	Whipple	coarse & fine clastics megabreccia blocks	alkalic hydrous volcanics & local epizonal stocks (metaluminous)	low-angle normal detachment faults SSE-NNW-trending folds NW-SE striking thrusts & reverse faults	Cu-Au-Ag in vns, replacement lenses & in detach. faults epithermal Au-Ag vns hotspring Mn & U	18-11 ? CA 34-13 AZ 28-18 ? NM
Medial GALIURO	Galiuro Datil Facies South Mountain Facies	local clastics interfinger with volcanics clastics interfinger with volcanics	alkali-calcic hydrous ignimbritic volcanics & epizonal plutons (metaluminous) calc-alkalic hydrous volcanics and epizonal plutons (metaluminous)	broad NW trend folds NW and NE-trending dikes broad NW trend folds NW trend dikes minor NE trend dikes	Pb-Zn-Ag +/- F vns & replacements epithermal Ag hotspring Mn Au +/- Cu-W veins & disseminated deposits	38-18 NM 28-18 AZ 22-18 CA 30-22 AZ 31-14 CA
Initial GALIURO	Mineta	coarse & fine clastics & evaporites in lacustrine environ.	rare volcanics mostly within 'volcanic gap'	local broad basins poss. WNW trend. reverse faults	uranium clay exotic copper	38-28

Table 3. Summary of assemblages of the Galiuro orogeny in Arizona.

phases are diachronous and, in a general way, become younger from east to west (Fig. 1).

Initial Galiuro Orogeny

Mineta Assemblage

Rocks deposited during the initial Galiuro orogeny are sporadically scattered throughout the Basin and Range Province of Arizona (Fig. 3) and are herein named the Mineta assemblage. The name Mineta is taken from the Mineta Formation of Chew (1952) and Clay (1970) along Mineta Ridge in the eastern Redington Pass area about 40 km northeast of Tucson, which is designated as the type area for Mineta assemblage. Other reference areas include the Teran Basin sequence of the southeastern Galiuro Mountains (Scarborough and Wilt, 1979) and the Gene Canyon Formation of the southeastern Whipple Mountains (Davis and others, 1980) where the Gene Canyon Formation is exposed. Mineta Assemblage is conceptually similar to the lower Unit I of Eberly and Stanley (1978) and the pre-ignimbrite sediments of Wilt and Scarborough (1981).

Rocks of the Mineta Assemblage

Mineta Assemblage rocks are predominantly continental sedimentary rocks that consist primarily of fine-grained lacustrine sediments and secondarily of coarse-grained, typically reddish, conglomerates in alluvial fan deposits; they typically range from 650 to 3400 m thick. Thinner accumulations are typically relatively thin, basal conglomerates that either conformably or unconformably underlie the volcanic-dominated medial Galiuro assemblages. Volcanics are only rarely present in Mineta assemblage rocks and consist of thin volcanic flows, such as Turkey Track andesite, or thin ash flow tuffs. Fine-grained facies of the Mineta assemblage commonly contain carbonates and gypsum in laterally widespread, lacustrine facies. Away from basin centers, braidplain deposits are common with fanglomerate facies locally occurring near basin edges.

Mineta assemblage sedimentary rocks contain fine-grained, low energy, lacustrine facies that occupied what may have been laterally continuous basins of considerable geographic extent. For example, some fine-grained strata that may have been deposited in a basin that pre-dated the present Rincon Mountains include: the claystone member of the Pantano Formation south of the Rincons, the fine-grained facies of Rillito I of Pashley (1966) northwest of the Rincons, fine-grained Mineta Formation, and gypsiferous mudstones of the Teran Basin sequence northeast of the Rincons. All of these formations contain a Turkey Track andesite dated at 27-28 Ma (Damon and Mauger, 1966; Shafiqullah and others, 1978; Scarborough and Wilt, 1979). Thus, it appears that the area now occupied by the Rincon Mountains was a broad depocenter for Mineta assemblage rocks in Oligocene time.

In southeasternmost California and west-central Arizona, lacustrine limestone and evaporite-bearing mudstones are important parts of the Gene Canyon Formation and lower Artillery Formation. The overall sedimentology of these rocks suggested to Davis and others (1980) that Gene Canyon Formation mantled a low topography that was developed on Proterozoic crystalline rocks. Tuffs interbedded with lacustrine deposits in the Gene Canyon Formation in the southern Whipple Mountains are as young as 24 Ma on the basis of radiometric dating (Davis and others, 1982). As in the exposures around the Rincon Mountains, the Gene Canyon basin pre-dated elevation of the Whipple Mountains.

Where stratigraphic relationships are well documented, initial sedimentation in Mineta assemblage basins is predominantly conglomeratic reflecting an initial interval of rapid sedimentation. The upper portions of these Mineta assemblage formations commonly consist of large amounts of lacustrine sediments such as carbonates and gypsiferous mudstones. In basins with a long history of sedimentation, the lacustrine units may be overlain by younger fanglomerate units that

commonly contain megabreccia clasts and that probably reflect subsequent Galiuro orogenic events.

Structural Features of Mineta Assemblage

Structural data for Mineta assemblage is difficult to document; but, where structures are present or can be reasonably inferred from sedimentologic evidence, Mineta assemblage strata may have accumulated in a series of basins that are elongate in an east-west to west-northwest direction. These basins are bordered by steep, E-W to WNW-trending, elongate uplifts that were possibly bounded by reverse faults. A good example of Mineta assemblage structural features is the Babocomari Basin between the northern Huachuca Mountains and the southern Mustang Mountains. Here, a thick sequence of older deformed gravels is probably equivalent to the Mineta assemblage part of the Pantano Formation (Vice, 1974). The northern boundary of the Babocomari basin is marked by a east-west to WNW-trending fault zone along and just north of the Babocomari River in the area of the Babocomari Ranch. Hayes and Raup (1968) show this fault as a steep to intermediate, north-dipping reverse fault that juxtaposes Paleozoic of the southern Mustang Mountains over the older gravels of the Mineta assemblage. Volcanic rocks intercalated within these conglomerates yield a date of 38.9 Ma (Marvin and others, 1973) from south of the Babocomari River and dates of 27.2, 26.1, and 24.3 Ma from a thin volcanic unit intercalated in the gravels along the Babocomari River near the Babocomari Ranch (Vice, 1974; Shafiqullah and others, 1978). The southern boundary of the basin is marked by the Kino Springs fault zone, which is a near vertical fault that cuts the Mineta assemblage sediments for about 12 km (8 miles) along strike.

Another Mineta assemblage basin is the lower part of the Pantano Formation between the Rincon and Santa Rita Mountains (Finnell, 1970; Brennan, 1962) where outcrops of the lower fanglomerate member of the Pantano are restricted to an east-west trending zone that is partly bounded by WNW- to E-W striking, nearly vertical faults on the south (Scarborough and Wilt, 1979). However, on the eastern side of the outcrops, the claystone member seems to positionally overlap the eastern projection of the structural boundary. The basin probably filled up rapidly with fanglomerates derived from the east and southeast (from clast data in Brennan, 1962, and paleocurrent data reported by Cooley and Davidson, 1963). By the time the middle Pantano was deposited, the claystone member overlapped the previous southern boundary of the basin. Other areas (Fig. 3) that possibly contained west-northwest-trending basins of Mineta assemblage sediments include the Comobabi Mountains, the northern Quijotoa Mountains, the Whipple Mountains (Davis and others, 1980), and the southern part of the Teapot Mountain quadrangle, where there are thick sequences of White Tail Conglomerate south of a west-northwest-trending fault zone.

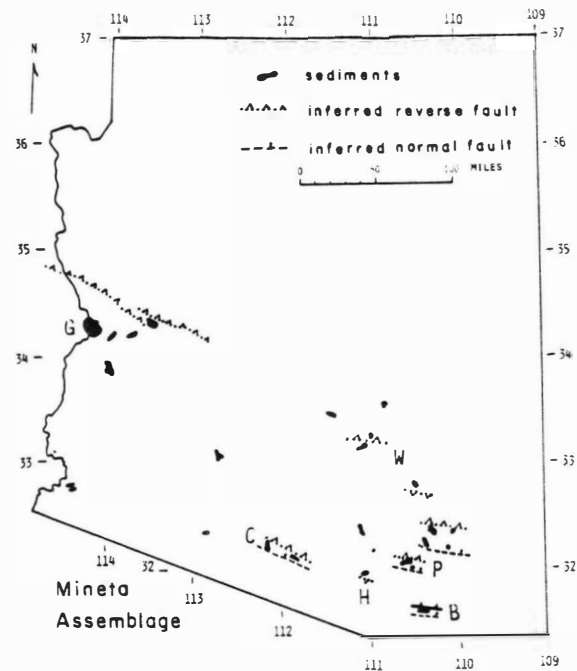


Figure 3. Map of Mineta assemblage of the initial Galiuro orogeny. Locations are Babocomari Basin (B), Pantano Fm. (P), Helmet Fanglom. (H), Whitetail Congl. (W), Gene Canyon Fm. (G), and Comobabi area (C).

Although data is limited, Mineta assemblage basins may have developed with a southwest-facing asymmetry, as the best documented basins of the Mineta assemblage occur south of E-W to N60W-striking structures. The southern boundaries of Mineta assemblage basins appear to be steep, near vertical faults that may also represent recurrent movement on elements of the Texas Zone; they are positionally overlapped by lacustrine facies of Mineta assemblage, which suggests that the southern parts of the basin were not active throughout deposition of Mineta assemblage. The faults along the northern sides of the basins probably were active throughout Mineta assemblage deposition because, where mutual contacts occur, the faults cut the entire Mineta assemblage and are not positionally overlapped by Mineta assemblage strata.

Age of Mineta Assemblage

Because volcanic units are rare within strata of Mineta assemblage, age dates are not abundant. In southeastern Arizona, volcanics within clastic units of Mineta assemblage in the Babocomari basin have yielded four radiometric dates that range between 38.9 Ma and 24.3 (Marvin and others, 1973; Vice, 1974; Shafiqullah and others, 1978). In the Pantano Formation southeast of Tucson, four K-Ar determinations on three samples range from 36.7 to

OROGENESIS. ARIZONA AND ADJACENT REGIONS

28 Ma (Damon and Mauger, 1966; Marvin and others, 1973; Shafiqullah and others, 1978). In the northern Tucson Mountains thin Mineta assemblage conglomerates occur beneath the Rillito Andesite, which has been dated at 38.5 Ma (K-Ar on biotite; Damon and Bikerman, 1964). A plagioclase K-Ar date of 31.4 Ma and 27.9 Ma (Damon and Bikerman, 1964) has been obtained from Turkey Track andesite porphyry in the Helmet Conglomerate, a possible Mineta assemblage unit in the east central Sierrita Mountains south of Tucson. In the northern Galiuro Mountains 50 km north-northeast of Tucson, White Tail Conglomerate that is unconformably overlain by 28 Ma Galiuro Volcanics has yielded a date of 32 Ma (Krieger and others, 1979). Thus, in southeastern Arizona, numerous K-Ar dates on clastic formations assigned to the Mineta assemblage range in age from 39 to 28 Ma.

Mineta assemblage rocks appear to be younger in western Arizona and southeasternmost California. Four K-Ar dates on volcanics intercalated into the Gene Canyon Formation in the southeastern Whipple Mountains range in age from 31.8 to 25.7 Ma (Davis and others, 1982). Gene Canyon Formation or Artillery Formation strata in the Northern Plomosa Mountains have yielded a K-Ar age date of 25 Ma on biotite from a thin rhyolitic tuff unit (Eberly and Stanley, 1978). The lower Artillery Formation is unconformably overlain by the basalt member, which is probably 16-21 Ma based on two K-Ar whole rock dates on basalts from the basalt member (Shackelford, 1980; Eberly and Stanley, 1978). Thus the lower Artillery Formation is pre-21 Ma. In a similar fashion, redbeds at Adair Park in the southern Laguna Mountains north of Yuma are unconformably overlain by Kinter Formation clastics which contain a 23 Ma ash (Olmsted and others, 1973). Thus, dates within Mineta assemblage rocks range from 31 to 24 Ma in western Arizona and are younger than in eastern Arizona, where they range from 39 to 28 Ma.

Medial Galiuro Orogeny

Galiuro Assemblage

The name Galiuro assemblage is given to products of the medial Galiuro orogeny that post-date the Mineta assemblage, where they are both present, and that otherwise unconformably overlie Morenci assemblage of the Laramide orogeny or older rocks. Rocks, structures, and mineral deposits of the Galiuro assemblage are especially well developed in the Galiuro Mountains and surrounding mountain ranges. Thus the Galiuro Mountains and vicinity are designated as the type area for the Galiuro assemblage. Rocks of the Galiuro assemblage are especially well exposed in the Mogollon-Datil volcanic field of southwestern New Mexico and this area is designated as a reference area for volcanic rocks of the Galiuro assemblage.

The term Galiuro assemblage is broadly equivalent to the mid-Tertiary 'ignimbrite flareup' of Coney (1976), to the middle Unit I of Eberly and Stanley (1978), and to the ignimbrite package of

Wilt and Scarborough (1981). In addition, Eberly and Stanley (1978) designated this unit (the ignimbrite-dominated middle Unit I) as the mid-Tertiary orogeny in their Figure 2. As used in this paper, Galiuro assemblage is also broadly equivalent to the 'mid-Tertiary orogeny' of Shafiqullah and others (1980) and of Damon and others (1984). Where in contact with Mineta assemblage rocks, Galiuro assemblage rocks are generally concordant to and locally conformable with the underlying Mineta strata. In general, Galiuro assemblage rocks are separated by angular unconformities from the overlying Whipple assemblage, where the assemblages are in mutual contact. Locally, basin-fill and basaltic volcanics of the Basin and Range assemblage of the San Andreas orogeny may unconformably overlie Galiuro assemblage rocks.

Rocks of the Galiuro Assemblage

Sedimentary Rocks. Sedimentary rocks of the Galiuro assemblage are generally subordinate in volume to Galiuro igneous rocks, but locally sedimentary sequences can be very thick (locally greater than 1.5 to 3.3 km). Where present, Galiuro assemblage sedimentary rocks consist of conglomeratic material, debris flows, and megabreccia units near uplifts and of braidplain sediments away from the uplifts. Because sedimentary rocks of the Galiuro assemblage commonly interfinger with volcanic facies, the sediments have a strong volcanoclastic component. In thick sedimentary sections where both Mineta and Galiuro assemblages are present without Galiuro volcanic rocks as a separating datum, the upper conglomerates which commonly contain megabreccia units are assigned to the Galiuro assemblage. For example, in the Pantano basin southeast of Tucson, the fine-grained, gypsiferous claystone member of the Pantano Formation is assigned to the Mineta assemblage; the overlying fanlomerate member, designated by Drewes (1977) as the upper Pantano, is assigned to the Galiuro assemblage.

Within the Hackberry Formation of Schmidt (1971) in the Ray and Hayden area is a spectacular horizon of megabreccia slide blocks described by Schmidt (1971) and Krieger (1977); some of these blocks are up to 3 km long and 1/2 km thick and consist of Paleozoic and Precambrian sediments that are highly crackled but maintain their internal stratigraphy. Krieger (1977) suggested that the megabreccia units were emplaced at high velocities into the depositional basin on top of an air cushion that kept deformation of the underlying soft sediments to a minimum. The Hackberry Formation interfingers locally with the Andesite of Depression Canyon, which is dated at about 25 Ma (Creasey and Krieger, 1978). Paleocurrent data and paleoclast data indicate that the source of much of the Hackberry sediments was from the Tortilla Mountains to the west. Thus, while the Tortilla Mountains was rising rapidly to the west, the Galiuro Volcanics were being deposited in a trough to the east. Other similar relationships are well-documented in the Cloudburst Formation in the southern Tortilla

Mountains (Weibel, 1981) and the basalt member of the Artillery Formation in western Arizona (Shackelford, 1980; Otton, 1982).

Igneous Rocks. The widespread magmatism expressed both as plutons and large volumes of locally thick, ignimbritic volcanics is the best known feature of the Galiuro assemblage (Fig. 4). Volcanics commonly occur in large volcanic fields which generally have andesitic basal units that interfinger upward into more silicic units, which commonly are regional ash flow sheets. Many of the ash flow sheets are associated with extensive caldera development, such as the Bursum caldera in the western part of the Mogollon-Datil field. Thicknesses of the volcanic piles vary from several hundred meters to several thousand meters. For example, the section of Galiuro Volcanics in the southern Galiuro Mountains is at least 3 km thick and thins to about 0.5 km in the northern Galiuros. Local accumulations of volcanoclastic sediments generally constitute less than 10 percent of the section, although some of the sedimentary sections that interfinger with volcanic piles may be as much as 3.5 km thick. Plutons of the Galiuro assemblage range from hypabyssal dike swarms to large, composite batholiths and range from intermediate to silicic compositions. An example of plutonism of the Galiuro assemblage is the Catalina Suite within the central part of the Tortolita-Catalina crystalline complex (Keith and others, 1980).

Chemically and metallogenically, magmatism of the Galiuro assemblage can be divided into two distinct facies that are herein named the South Mountain facies and the Datil facies. Geographically, South Mountain facies magmatism generally occurs west of a N30W trending line through Tempe, Arizona, whereas the Datil facies predominates northeast of the line. Datil facies volcanism locally occurs in significant amounts west of the N30W line within the region predominated by South Mountain facies.

South Mountain Facies. The South Mountain facies is named for the South Mountain Granodiorite and related microdiorite dikes and gold mineralization in the South Mountains south of Phoenix. Because the South Mountain igneous complex has been well described and dated by Reynolds (1982) and Reynolds and Rehrig (1980), the South Mountains are designated as the type area of the South Mountain facies. In western Arizona and southeastern California, magmatism of the South Mountain facies is expressed by hypabyssal dikes, small stocks, and extensive calc-alkalic volcanism. Because this magmatism is well documented in the Chocolate Mountains of Imperial County in southeastern California (Crowe and others, 1979), this area is designated as a reference area for South Mountain facies magmatism.

Magma series chemistry of South Mountain facies magmatism displays metaluminous aluminum contents, calc-alkalic alkalinity, and is hydrous, oxidized, and generally iron-poor. Strontium isotopic initial

ratios range between 0.705 and 0.709 indicating that a small crustal component is present.

Datil Facies. The Datil facies is named for the extensive and thick volcanic sequences in the Mogollon-Datil volcanic field of western New Mexico. Because of the long history of documentation and abundant geochronological and geochemical data for the Mogollon-Datil volcanic field, this region is designated as the type area for the Datil facies. The Mogollon-Datil volcanic field is a composite of numerous interfingering volcanic centers and caldera complexes (Bornhorst, 1982). Almost the entire field is characterized by alkali-calcic magma chemistry.

Another reference area for Datil facies of the Galiuro assemblage is the Galiuro Mountains of southeastern Arizona where there is also abundant documentation (Creasey and Krieger, 1978; Creasey and others, 1981). This extensive volcanic field is present throughout the 75 km length of the mountain range, is dated at 28 to 22 Ma, and is of alkali-calcic alkalinity. Similar geochronologic and geochemical control now exist for extensive volcanic piles in the Superstition Mountains northeast of Phoenix (Stuckless and Sheridan, 1973), in the central Plomosa Mountains in west-central Arizona (Shafiqullah and others, 1980), and in the Turtle Mountains of southeastern California (R. Hazelett, pers. commun., 1985). Plutons of the Datil facies are widespread and locally constitute small to moderate-sized batholiths. The Catalina suite batholith has especially good geochronologic, map, and geochemical control (Keith and others, 1980) and is designated as a reference area for Datil facies plutonism.

Magma series chemistry of Datil facies magmatism displays metaluminous aluminum contents, alkali-calcic alkalinity, and is hydrous, oxidized, and generally iron-poor. Strontium isotopic initial ratios range between .705 and .710 and generally are between 0.7069 and 0.7096 indicating that a small crustal component is present.

Structural Features of the Galiuro Assemblage

Large-scale Folds. The most significant structural feature of the Galiuro orogeny is a set of regionally extensive, long wavelength, large amplitude, open, broadly folded, northwest-striking, warps or anticlines and synclines (Fig. 4). Culminations of the Galiuro assemblage anticlinal arches coincide with areas of widespread, reduced, K-Ar and fission-track, isotopic dates. Galiuro assemblage fold phenomena represent broader, crustal-scale warping that precedes the more obvious and more resolved, more northerly trending, en echelon folds of the Whipple Assemblage. Thus, the folds shown on Figure 4 are not defined by attitude data taken from lower plate, mylonitic foliation within the crystalline cores of lower plate windows through arched, Wilderness assemblage thrusts (metamorphic core complexes of recent literature). Rather, the folds are inferred from more regional data, such as distribution and thickness of Galiuro

OROGENESIS, ARIZONA AND ADJACENT REGIONS

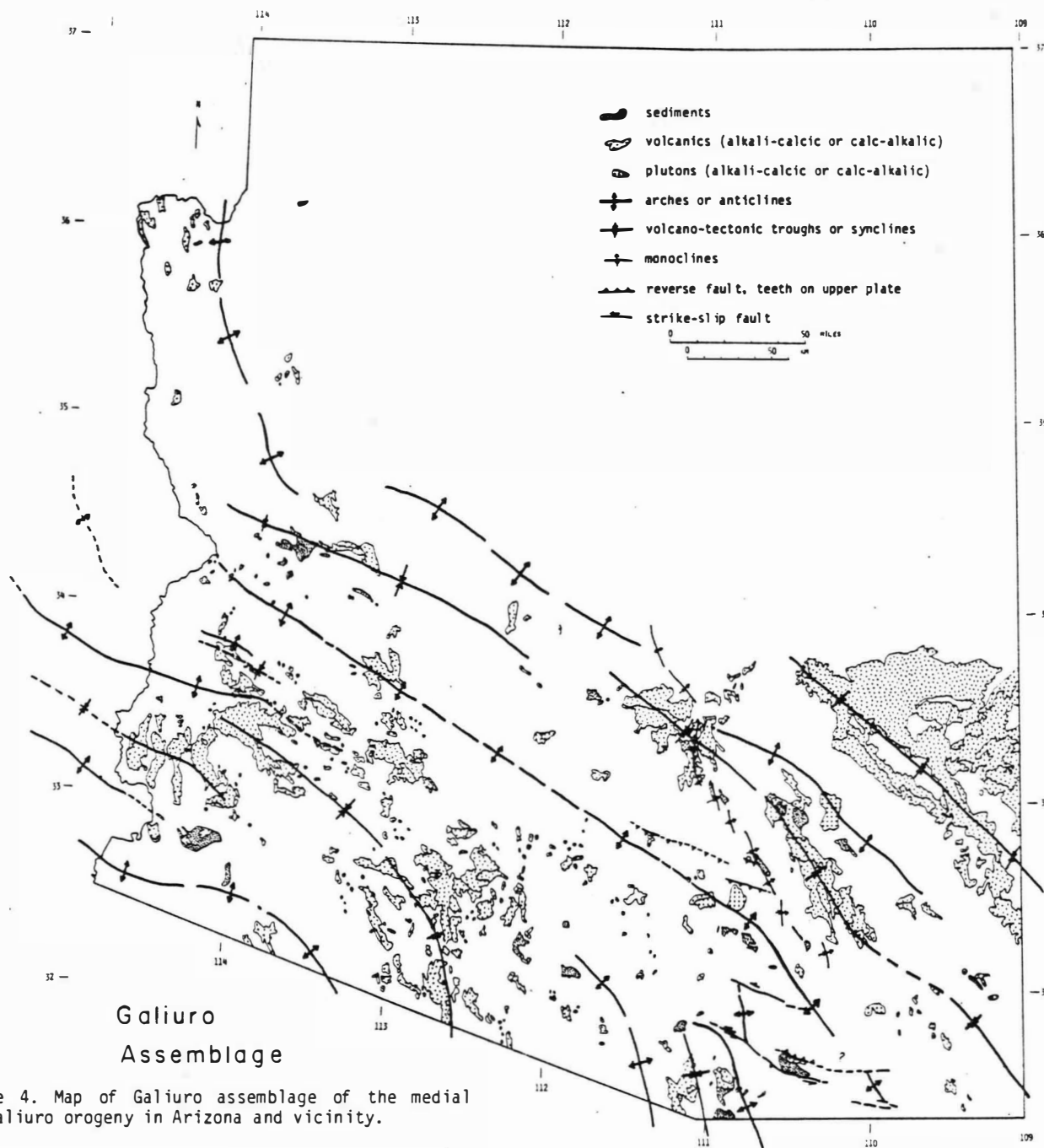


Figure 4. Map of Galiuro assemblage of the medial Galiuro orogeny in Arizona and vicinity.

assemblage volcanics and sediments; distribution and transport directions inferred from areas underlain by Whipple assemblage detachment faults (Fig. 5); distribution of reduced, mid-Tertiary, age dates; and presence of regional warp-like deformation of low-angle reflectors on regional seismic sections shot for the recent petroleum play (Keith, 1980).

Amplitudes of Galiuro assemblage warps are very large. From seismic data that was shot for the Arizona oil and gas play of 1979-1980, the amplitude or structural relief of some of the warps is as much as 6 km (20,000 feet) (Reif and Robinson, 1981). One unpublished seismic line that was shot in the Tucson region was from the southwestern Rincon Mountains

across the Tucson Basin. The seismic section showed a dramatic zone of strongly continuous seismic reflectors that correlated well with surface outcrops of the Catalina fault. To the southwest the zone of strongly continuous, seismic reflectors dipped southwest and flattened at a depth of about 2 seismic seconds. This corresponds with a depth of about 6 km (20,000 feet) below sea level beneath Tucson. As the Catalina fault can reasonably be projected over the top of Mica Mountain to the northeast at an elevation of about 3 km (10,000 feet) above sea level, an amplitude of about 9 km (30,000 feet) is possible for anticlinal warping of the Catalina fault.

Another independent way of assessing the structural relief developed on Galiuro assemblage warps is petrologic in nature. Because of the extensive presence of volcanic components, it is clear that magmatism of the South Mountain facies is shallow level (typically within 3 km) compared to the deeper level of peraluminous plutons of the culminant Laramide orogeny. In the crystalline core of the northwestern Santa Catalina Mountains, alkali-calcic plutons locally contain miarolitic cavities which indicate shallow depth levels of probably less than 2 km. These shallow plutons intrude plutons of the Wilderness assemblage that were emplaced at deep levels of 8-10 km or more. Thus, at least 6 km of uplift and erosional removal occurred in the crystalline core of the Santa Catalinas between 44 and 24 Ma.

An even greater amount of structural relief can be inferred from reduced age dates obtained from older rocks in the crystalline cores of the anticline-like uplifts. In the Santa Catalina Mountains, K-Ar ages for hornblende or large muscovite grains from older rocks are either not reset or are only partially reset (Keith and others, 1980), indicating that temperatures in the lower plate prior to 30 Ma were not greater than 400° C. However, K-Ar determinations on biotite and fission track determinations on zircon and sphene consistently yield reduced ages between 28 and 24 Ma, suggesting cooling below 200° C. If the reduced ages are related to uplift refrigeration of K-Ar clocks, then between Eocene (44 Ma) and mid-Oligocene (24 Ma) the complexes cooled from 400° to 200° C., which represents uplift of 8 km assuming a normal crustal geotherm of 25° C/km. By 18 Ma fission track ages on apatite are reset suggesting that another 4 km of uplift had occurred between 22 and 18 Ma for a cumulative total of 12 km. Most, if not all, of the structural relief associated with the arches was probably generated after 28 Ma, because lacustrine strata of the Mineta assemblage once occupied basins that extended across the now uplifted arches. This uplift totaled about 8 km of uplift from 28 Ma to 24 Ma, with an additional 4 km of uplift between 22 and 18 Ma. With these kinds of uplift rates, it is not surprising that Galiuro assemblage sediments contain widespread megabreccia blocks of all sizes.

The fold warps are also characterized by long wavelengths. The distance between anticlinal crest

and synclinal, volcano-tectonic troughs (one-half wavelength) is about 30 to 40 km as indicated by seismic data. Between the anticlinal crests are large synclinal troughs that represent major sags or synclinal basins in which substantial amounts of Galiuro assemblage volcanics and sediments accumulated.

One of the best examples of such a synclinal trough is the Galiuro Mountains where at least 4 km of Galiuro assemblage volcanics and sediments have accumulated in a trough between the Pinaleno and Santa Catalina mountains. The distance between the crests of the anticlines is about 80 km and the thickest parts of the Galiuro Volcanics occur in the trough along an axis approximately midway between the crests. Attitudes of bedding, foliation, and low angle joints in the Pinaleno Mountains show that the Pinaleno Mountains also occupy a broad, anticlinal arch (Thorman, 1980; Rehrig and Reynolds, 1980). Similarly, attitude data for volcanics in the Galiuro Mountains show that the Galiuro Volcanics (Creasey and others, 1981) are broadly warped into a broad synclinorium containing several smaller scale anticlines and synclines. The northwest-trending trough or depression may have continued to the southeast into the central Chiricahua Mountains where a thick volcanic section of the Rhyolite Canyon Formation is present.

Similar volcano-tectonic troughs are inferred to exist from the Ajo Range and Batamote Hills and Crater Mountains in the Ajo region to the Castle Dome Mountains in Yuma County, through the Chocolate Mountains of southeastern California, and from the Garlock fault southeast through Barstow to the Bristol and Bullion Mountains in southeastern California. Significantly, the amount of volcanic and sedimentary material deposited in the volcano-tectonic troughs is approximately the same as the amount of material erosionally removed from uplifts centered on the anticlinal axes shown on Figure 4.

An obvious kinematic interpretation of the fold phenomena is that they reflect crustal shortening. From inspection of Figures 4 and 5, the approximate axis of shortening relative to the Galiuro assemblage folds is along a N30E to N40E line. The amount of crustal shortening related to the warping may be calculated from the amplitude and wavelength data. For example, if amplitudes of 10 km and half wavelengths of 40 km are assumed for a typical fold, the shortening is 3 percent.

Smaller-Scale Monoclines and Folds. The best examples of north- to northwest-trending monoclinial structures of the Galiuro assemblage are the segmented monoclines along the Tortilla Mountains. Because the monocline system occurs for most of its strike length along the west side of and parallel to the San Pedro Valley, in this paper it is called the San Pedro monocline system. It extends from the Superior area for some 160 km to the eastern Rincon Mountains at its southeast end. The San Pedro monocline system is composed of a series of north-northwest-trending monoclines which locally

OROGENESIS, ARIZONA AND ADJACENT REGIONS

display an en echelon pattern. The monocline system itself is defined by moderately to steeply dipping, to slightly overturned, east-dipping, middle limbs.

Reverse Faults. Intra-Galiuro assemblage reverse faulting is difficult to document, but where present, may be large scale. A probable example of a reverse fault of the Galiuro assemblage is the Black Canyon Ranch fault in the Black Hills segment of the southern Tortilla Mountains about 3 km southwest of San Manuel mapped by Weibel (1981). The Black Canyon fault is a WNW-striking fault that dips 35° to 75° South; it juxtaposes, with reverse separation, Precambrian granite (1400 Ma) and San Manuel granodiorite (Laramide) over a thick sequence of fanglomerate within the Cloudburst Formation. The amount of reverse slip could have been at least 2 km, which is the thickness of the Cloudburst Formation on the north side of the fault. More speculatively, at least 2 to 4 km of reverse separation with a northeast sense of vergence is indicated along the south-dipping Mogul fault in the northern Santa Catalina Mountains and the North Star fault in the Picacho Mountains. Here, analysis of the Phillips drilling results north of the North Star fault zone (Reif and Robinson, 1981) indicates possible Wilderness assemblage thrust plates may be offset during Galiuro assemblage uplift of the Santa Catalina Mountains south of the Mogul fault.

Dike Swarms. The numerous prominent dike swarms of both South Mountain and Datil facies of Galiuro assemblage commonly trend northwest (Rehrig and Heidrick, 1976). However, nearly as many dike swarms of Galiuro Assemblage strike northeast. Some of the northwest-striking dike swarms include the Aravaipa dike swarms in the western Santa Teresa Mountains (Simons, 1964), the central Dragoon Mountains dike swarm (Gilluly, 1956), the South Mountain dike swarm (Reynolds, 1982), the Harquahala dike swarms, the Castle Dome dike swarms, and the Chambers Well dike swarm in the Whipple Mountains (Davis and others, 1982). Some of the northeast- to east-striking dike swarms of Galiuro Assemblage are the Stockton Pass dike swarm (Thorman, 1980), the Eagle Pass dike swarm, the Apache Pass dike swarm, and the central Santa Rita and Box Canyon dike swarms (Drewes, 1972), and the Sacramento Mountains dike swarm in southeast California (Spencer and Turner, 1982).

Mylonitic shear zones. Although most (75-85 percent) of the mylonite development in the lower plates of the crystalline complexes probably developed during earlier Laramide and Sevier orogenies, mylonitic shear zones of middle Tertiary age were developed at least locally in several areas. Known areas of mid-Tertiary mylonitization include the deformed Tortolita Quartz Monzonite of the Catalina suite (Keith and others, 1980), the deformed South Mountain plutonic complex at South Mountain (Reynolds, 1982; and Reynolds and Rehrig, 1980), and a similar mylonitic pluton in the southeastern part of the Picacho Mountains 45 km northwest of Tucson (W. Rehrig and S. Keith, unpub. data). The present attitudes of the above-described shear zones, in combination with S-C fabric data,

indicates that the shear zones have low-angle normal shear.

Age of Galiuro Assemblage

Age of Magmatism. Age patterns for Galiuro assemblage are well constrained because of abundant radiometric dates on the widespread igneous components. In general, the age patterns of Galiuro assemblage rocks are the mirror image to that of Laramide assemblages; that is, Galiuro Assemblage rocks become younger to the west (Coney and Reynolds, 1977; Wilt and Scarborough, 1981). This westward younging applies to both South Mountain and Datil facies magmatism and also to reduced dates by K-Ar, fission track, and Rb-Sr mineral isochron methods on older crystalline rocks now exposed in the central, uplifted cores of Galiuro and Whipple assemblage warps.

The ages of calc-alkalic magmatism of South Mountain facies of the Galiuro assemblage are oldest in eastern Arizona (30 to 28 Ma) and younger to the west from south-central Arizona (29 to 22 Ma) to western Arizona (28 to 24 Ma) to the southern Colorado River region (29 to 21 Ma) to southeastern California (23 to 19 Ma). In the eastern Chiricahua Mountains of eastern Arizona there are dates on two samples of the metaluminous, calc-alkalic Faraway Ranch Formation yield dates between 29.6 and 28.0 Ma (Shafiqullah and others, 1978). To the west in the southern Santa Rita Mountains, the Grosvenor Hills volcanics, is a fairly widespread volcanic pile with calc-alkalic chemistry. Four K-Ar dates from three samples of Grosvenor Hills volcanics and a related subvolcanic laccolith range from 27 to 29 Ma (Drewes, 1972). To the northwest at the type locality of the South Mountain Facies at South Mountain south of Phoenix, the South Mountain intrusive complex is calc-alkalic (Keith and Reynolds, unpub. geochemical data) and is well dated between 26 and 22 Ma by K-Ar, Rb-Sr, and U-Pb techniques (Reynolds, 1982). To the west in the Harquahala Mountains 100 km west of Phoenix widespread, calc-alkalic, microdiorite dike swarms of the South Mountain Facies are dated at 28 to 25 Ma (Shafiqullah and others, 1980). To the south in the southeast Chocolate Mountains, the main volumes of volcanism are calc-alkalic and erupted between 30 and 22 Ma based on numerous K-Ar dates (Crowe and others, 1979). Farther to the west volcanism in the Diligencia Formation of the northeastern Orocofia Mountains is calc-alkalic and has yielded three K-Ar dates which range from 23.0 to 19.1 Ma (Spittler and Arthur, 1982).

The Datil facies of the Galiuro assemblage exhibits a broader geographic distribution than the South Mountain facies and thus exhibits a more obvious pattern of younging to the west. In southwest New Mexico the magmatism is mainly 38 to 24 Ma and becomes younger westward from southeasternmost Arizona (28 to 22 Ma) to south-central Arizona (28 to 22 Ma) to the Phoenix region (24 to 16 Ma) to west-central Arizona (22 to 18 Ma) and to southeastern California (22 to 18 Ma).

In the Mogollon-Datil volcanic field, alkali-calcic volcanics (Bornhorst, 1982) erupted in several volcanic cycles that range in age from 38 to 20 Ma (Elston and others, 1973). In the Peloncillo and Animas Mountains of southwesternmost New Mexico, an extensive field of caldera-related, alkali-calcic magmatism ranges from 37 to 24 Ma (Deal and others, 1978). In southeastern Arizona alkali-calcic magmatism, such as the Stronghold Granite of the central Dragoon Mountains yield K-Ar dates of 27 to 23 Ma (Damon and Birkman, 1964; Marvin and others, 1973) and volcanics in the southern Pinaleno Mountains yielded five fission track dates that range from 26.8 to 22.8 (Thorman, 1980). To the northwest Galiuro Volcanics of the alkali-calcic Datil facies yield numerous K-Ar dates that range from 28 to 22 Ma (Creasey and Krieger, 1978; Scarborough and Wilt, 1979).

In the Catalina and Tortolita Mountains northwest of Tucson, the Catalina suite of plutons is well-dated by K-Ar, fission track, U-Pb, and Rb-Sr geochronology at 27 to 24 Ma (Creasey and others, 1976; Keith and others, 1980). To the west in the Tucson Mountains age data show that the mid-Cenozoic volcanics in the eastern Tucson Mountains are 28 to 23 Ma (Damon and Birkman, 1964; Shafiqullah and others, 1978). Near Phoenix numerous K-Ar ages and geochemical data show that the majority of the Superstition Volcanics (below the Mesquite Flat breccia unit) have alkali-calcic alkalinity and are mostly 24 to 16 Ma (Stuckless and Sheridan, 1971). Northwest of Phoenix the Castle Creek volcanics are mainly alkali-calcic and are probably 22 to 18 Ma (C. Kortemier, pers. commun., 1985). Volcanism in the central Plomosa Mountains is shown by geochemical data (Gene Davis, pers. commun., 1985) to be alkali-calcic and has age dates of 20 to 18 (Shafiqullah and others, 1980). In southeastern California a large volcanic pile in the Turtle Mountains 40 km west of Parker, Arizona, has yielded numerous K-Ar dates between 22 and 18 Ma and is entirely alkali-calcic (Hazelett, pers. commun., 1985).

In any area where both facies are present, the South Mountain facies precedes the Datil facies. For example in the Phoenix region, the calc-alkalic South Mountain Granodiorite pluton and its associated microdiorite dikes and gold mineralization are 26 to 22 Ma in age (Reynolds, 1982). To the northeast in the Superstition Mountains, alkali-calcic Superstition Volcanics of the Datil facies are radiometrically younger and yield dates between 24 and 15 Ma (Stuckless and Sheridan, 1971). In the Chocolate Mountains of southeastern California, Crowe and others (1979) have documented an extensive volcanic pile. The lower part of the volcanic section (Unit A and Unit B) is chemically calc-alkalic and is assigned to the South Mountain facies. It is overlain by a younger sequence of more mafic lava flows (Unit C), which are alkali-calcic and are associated with manganese-silver deposits and are assigned to the Datil facies. Units A and B are calc-alkalic and yield numerous K-Ar dates that range from 35 to 24 Ma, whereas Unit C is commonly alkali-calcic and

yields K-Ar dates that range from about 26 to 22 Ma (Crowe and others, 1979).

Age of Structural Development. Galiuro assemblage warping and magmatism appear to be virtually coincident. Uplift of the lower plate gneisses was not underway during deposition of Mineta assemblage rocks because lacustrine facies of Mineta assemblage occupied basins across the sites of later Galiuro assemblage uplifts in the axes of the anticlinal warps. Thus, warping was not active in southeast Arizona prior to 28 Ma or in west-central Arizona and southeastern California prior to 25 Ma. However, by middle or late Galiuro assemblage, the gneisses had been uplifted and at least locally exposed to erosion because clasts of lower plate mylonitic rocks from the crystalline cores of the uplifts are locally present in the Galiuro assemblage sediments. For example, in the Whipple Mountains, mylonitic clasts are locally present in the conglomerates in upper portions of the Gene Canyon Formation. One of these mylonite clasts yielded an age of 83 Ma by the fission track method on sphene (Davis and others, 1982). Thus, in early Gene Canyon time (32-28 Ma) the area of the Whipple Mountains was occupied by lacustrine sediments, but by late Gene Canyon time (26 to 22 Ma) the basin had been disrupted by anticlinal uplift of the lower plate crystalline rocks, which began to supply mylonitic clasts to the Gene Canyon Formation.

Similarly, in the Santa Catalina mountains near Tucson, the Rillito II unit of Pashley (1966) contains mylonitic clasts that are derived from the mylonitic Wilderness complex in the crystalline core of the lower plate. A rhyolitic clast from Rillito II yielded a 22 Ma K-Ar date (H. W. Peirce and M. Shafiqullah, pers. commun., 1982) suggesting that the Rillito II is younger than 22 Ma. However, it contains clasts of Eocene aged Wilderness suite plutonic rocks which have yielded a reduced age of 26 Ma by the K-Ar method on muscovite. The area of the Santa Catalina-Rincon Mountains was also a site of lacustrine sedimentation during Mineta assemblage and before 28 Ma. By 26 Ma, the complex had been uplifted about 6 to 8 km and cooled from 400° to 200° C to refrigerate the K-Ar clock; after 22 Ma, the area was supplying clasts to basins adjacent to the uplift.

Volcanics intercalated with sedimentary units that contain mylonitic clasts are the same age as the reduced dates or cooling ages on the mylonitic rocks in the lower plate. For example in the Whipple Mountains, K-Ar dates from the Gene Canyon Formation are 31-25 Ma, and cooling ages on mylonitic clasts range from 26 to 16 Ma (Davis and others, 1982). In the Catalina Mountains fission track and cooling ages on mylonites are 28 to 18 Ma, and Rillito II strata that contain the mylonite clasts are post-22 Ma and probably are 22 to 18 Ma. In the Artillery Mountains, the basalt member of the Artillery Formation, which contains large megabreccia units of mylonitic rocks, yields dates from 21 to 16 Ma (Shackelford, 1980), and overlaps reduced ages on mylonites in the lower plate in the

OROGENESIS, ARIZONA AND ADJACENT REGIONS

nearby Harcuvar and Buckskin Mountains and more distant Whipple Mountains (26 to 16 Ma) (Reynolds and Rehrig, 1980; Davis and others, 1982). Thus, if the mylonites were predominantly formed during the middle Tertiary, as is widely advocated in the literature (Rehrig and Reynolds, 1980; Davis, 1980), then the mylonites would have had to be uplifted instantaneously from their deep formation depth in order to supply clasts for the syntectonic sedimentation associated with the uplift. It is more reasonable to support an older age (late Cretaceous to early Tertiary) for the formation of most of the mylonitic rocks in the lower plate throughout this region (Fig. 1).

Culminant Galiuro Orogeny

Whipple Assemblage

Because of the excellent exposures in the Whipple Mountains of southeastern California and the extensive work done there (Davis and others, 1980; Frost, 1981; Frost and Martin, 1982), the rocks, structures, and mineral deposits of the culminating Galiuro orogeny are named the Whipple assemblage and the Whipple Mountains are designated the type area for the Whipple assemblage.

Rocks of the Whipple assemblage are broadly similar to upper Unit I of Eberly and Stanley (1978) or to the post-ignimbrite sedimentary package of Wilt and Scarborough (1981). Whipple assemblage covers the interval of the 'Transition Phase or Stage' as used by Shafiqullah and others (1980) and Damon and others (1984). Whipple assemblage strata are commonly separated from older Galiuro assemblage and younger strata of the San Andreas orogeny by angular unconformities.

Rocks of the Whipple Assemblage

Sedimentary Rocks. Sedimentary rocks of the Whipple Assemblage consist of coarse clastic rocks and finer grained lacustrine facies (Fig. 5). In general, though, the frequency of megabreccia units, debris flows, and coarse clastic sedimentation appears to be less than that in the preceding Galiuro assemblage. Facies changes in Whipple assemblage sediments appear to be much more rapid and the size of basins seems to be smaller on an overall basis. In areas of known detachment faulting much of the sedimentation accumulated in small, half-graben basins between antithetically rotated blocks in the upper plate and were up to 15 km long and 2-3 km wide. Whipple assemblage sedimentation also appears to have a higher percentage of lacustrine facies than the Galiuro assemblage. Mylonitic clasts are widespread and much more common in Whipple assemblage strata than they are in Galiuro assemblage strata. Thicknesses of Whipple assemblage typically range from 200 m to 1500 m and are generally thinner than those of the underlying Galiuro assemblage.

A sedimentological feature of conglomeratic units of the Whipple assemblage is the tuffoni

weathering which leaves conspicuous water pockets or pock marks on more resistant exposures. Good examples of this tuffoni weathering are the tilted red conglomerate sections in the upper plate of the Plomosa fault in the northern Plomosa Mountains, the Camelback Formation on Camelback Mountain in north Phoenix, the Big Dome Formation south of Ray in Pinal County, the Apsey and Hall Hole Conglomerates in the Galiuro Mountains (Simons, 1964), and the Gila Conglomerate near the Gila Cliff Dwellings in southwestern New Mexico.

One of the best examples of Whipple assemblage sedimentation is the Copper Basin Formation in the Whipple Mountains. Here, the Copper Basin Formation angularly overlies the Gene Canyon Formation and consists of red sandstones, conglomerates, and siltstones with interbedded trachyandesites and trachitic volcanics (Teel and Frost, 1982). Primary sedimentary features such as mudcracks, ripple marks, and cross-bedding are abundant within the formation and suggest a fluvial or fan conglomerate deposition environment for much of the unit.

Other examples of Whipple assemblage strata occur in the Plomosa, Rawhide, and Buckskin Mountains. Here, the Whipple assemblage includes the Chapin Wash Formation, which is a manganiferous, fine-grained siltstone and mudstone facies of probable lacustrine origin, and the unconformably overlying Cobweb basalt. A characteristic feature of the Chapin Wash and Copper Basin formations is the pervasive brick red color.

Farther to the southeast Whipple assemblage strata include the Big Dome Formation, the San Manuel Formation of Heindl (1962), the Rillito II beds of Pashley (1966), which are predominantly reddish conglomerates with about 5-10 percent gneiss clasts, and the Rillito III beds, which are tilted, lighter gray colored sediments containing about 70-80 percent gneiss clasts.

Igneous Rocks. In general, igneous rocks of the Whipple assemblage are not as widespread as sedimentary rocks; however, they can locally reach considerable thicknesses (greater than 2000 m). Volcanic rocks are more common, but small to moderate size stocks of Whipple assemblage are locally present. Volcanism and epizonal plutons of Whipple assemblage affinity are especially well developed and have been well documented (Ransome, 1923; Thorson, 1971) in the Oatman district of the southern Black Mountains of northwestern Arizona. Thus, this area is designated as a reference area for Whipple Assemblage magmatism. Another reference area is the Socorro region of south central New Mexico, where extensive geochemical data and map control exist for the La Jara Peak Andesite and its intercalated ash flow tuffs (Osburn and Chapin, 1983).

Mineralogically, Whipple assemblage magmatism commonly lacks quartz but does not contain nepheline, so that rock types such as latite, trachyandesite, or shoshonite are common volcanic

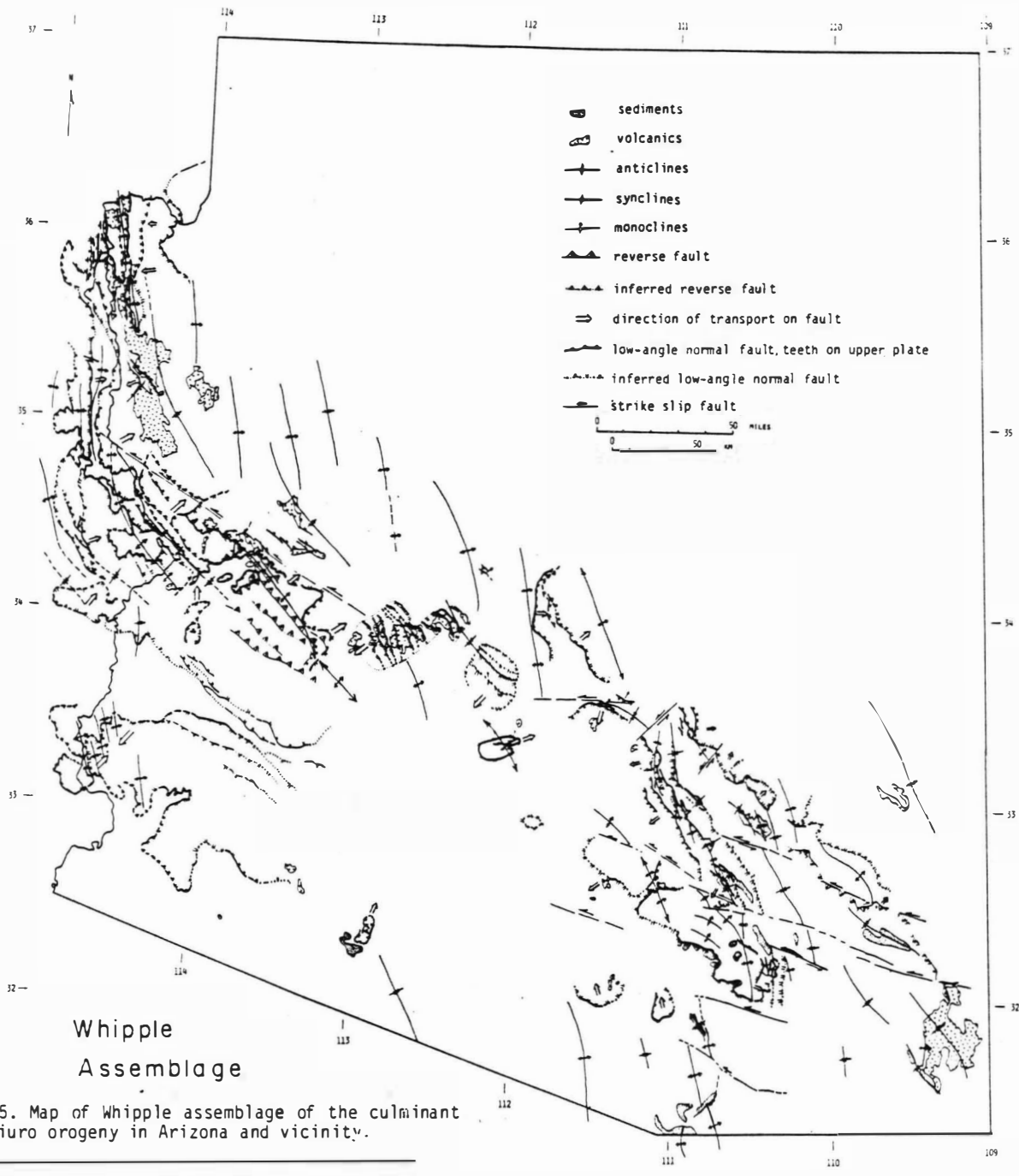


Figure 5. Map of Whipple assemblage of the culminant Galiuro orogeny in Arizona and vicinity.

phases and monzonite or quartz syenite are common intrusive phases. Biotite is the principal mafic accessory followed by hornblende and locally important augite, especially in augite monzonite stocks, such as those in the White Oaks and the Rio stock of Lincoln County, New Mexico, and the Times Porphyry and Moss Porphyry monzonitic stocks northwest of Oatman, Arizona (Thorson, 1971).

Magma series chemistry of Whipple assemblage magmatism displays metaluminous aluminum contents, alkali-calcic to mostly quartz alkalic alkalinity, and is hydrous, oxidized, and generally iron-poor. The strontium initial ratios range between 0.705 and 0.710 indicating that a small crustal component is present.

OROGENESIS, ARIZONA AND ADJACENT REGIONS

Ultra-potassic chemistry (where K_2O/Na_2O ratios exceed 3:1) is another feature of Whipple assemblage volcanism. Within these areas, ultra-potassic chemistry seems to be restricted to areas of high K_2O , quartz-alkalic volcanism (especially trachytic and high K-rhyolite phases). For example, Shafiqullah and others (1976) and Rehrig and others (1980) have reported ultrapotassic chemistry from trachytes at Picacho Peak 45 km northwest of Tucson and from rhyolites in the Vulture Mountains 45 km northwest of Phoenix. Ultra-potassic trachytes are found in the Copper Basin Formation of the western Whipple Mountains (L. Anderson, unpub. data) and ultra-potassic rocks are widespread in the Socorro area (Osburn and Chapin, 1983). Ultra-potassic chemical data has not been reported from older Galiuro assemblages.

Structural Features of Whipple Assemblage

Detachment Faults. The most well-studied structural elements of the Galiuro orogeny are the spectacular detachment faults. In previous literature the terms denudational fault (Armstrong, 1972), dislocation fault or dislocation surface (Rehrig and Reynolds, 1980), or decollement (Coney, 1980; Davis, 1980) have been synonymously employed when referring to these structures. The terms 'detachment fault' or 'low-angle normal fault' have been used in more recent literature (Frost and Martin, 1982; Davis, 1983) and are continued here.

Low-angle normal faults or detachment faults of the Whipple assemblage have been well described in the Whipple, Rawhide, Buckskin, and Harquahala region and in the Santa Catalina, Rincon, and Tortolita region. In both locations low-angle normal faults appear to have reutilized pre-existing, low-angle, thrust zones (Drewes, 1981). Haxel and Grubensky (1984) have recorded similar reutilizations for detachment-related faulting in the Comobabi Mountains on the Papago Indian Reservation and in the Kofa Mountains of Yuma County.

Many of the detachment fault zones occur in areas that are underlain by mylonitic rocks of the lower plate, and some observers have interpreted the spatial association as causative (Davis, 1983; Reynolds, 1982; Rehrig, 1982). However, areas affected by low-angle detachment faulting are commonly not geographically restricted to areas of mylonitic rocks in the lower plate (Davis and others, 1980). This is documented in the central Whipple Mountains where nonmylonitic gneisses and plutonic rocks underlie the detachment fault at Savahia Peak (Gross and Hillemeier, 1982). Detachment faulting in the Trigo Mountains occurs above nonmylonitic crystalline rocks (Garner and others, 1982), as it does in the Baker Peaks area of Yuma County (Pridmore and Craig, 1982). Similarly, detachment faulting in the Owshead Mountains in southern Death Valley places antithetically tilted, middle Tertiary rocks of the upper plate against nonmylonitic, probably mid-Cretaceous, granitoids (Davis and Fleck, 1977). In some of these areas, such as the Owshead Mountains and most of the Trigo

Mountains, there is no evidence of any former thrusting. Thus, tectonics responsible for mylonitic phenomena and detachment phenomena are not mutually coincident, and are, therefore, probably not causally related.

The structural style of detachment fault zones consists of a basal chloritic breccia zone, a microbreccia zone, and a microbreccia ledge with a planar surface, above which are unmetamorphosed and nonmylonitic rocks of the upper plate. The crystalline rocks of the upper plate commonly are positionally overlain by Mineta, Galiuro, and Whipple assemblage volcanics and sediments. These strata are tilted from a few degrees to near vertical but generally dip between 30 and 60 degrees. Areas characterized by the same dip directions are geographically distinct, so that it is possible to define domains of dip direction (Stewart, 1980; Rehrig and Heidrick, 1976) that inferentially overlie a single, common, basal detachment zone. In some places the dip domains can be inferred to represent antithetic tilting of middle Tertiary strata in the upper plate as a response to detachment faulting at depth. Not all of the tilt directions or dip domains can be interpreted as a result of detachment faulting; for example the tilted Galiuro Volcanics within the synclinorium of the southern Galiuro Mountains. In most places the tilt domains outline areas on the same flank of regional warps of Galiuro assemblage and dip away from the volcano-tectonic troughs. Areas of thick Galiuro sedimentation coincide geographically with axes that separate regions of inward dips on tilt domain maps.

On a subregional scale, tilt directions of the larger-scale blocks appear to be fairly consistent, but in detail, the geometries can be considerably more complex. A good example of the complexity has been documented by Gross and Hillemeier (1982) for small-scale, detachment-related structures in the western Whipple Mountains and the Buckskin Mountains. The overall movement as indicated within a given domain of tilted blocks may be counterbalanced by small scale, less noticeable, antithetic faults. Gross and Hillemeier (1982) demonstrate that simple, upper plate, synthetic, normal-fault models that are widely used in the literature cannot be structurally balanced, and leave gaping voids that somehow must be accounted for by more complex, keystone-like, fault relationships. Also, the obvious antithetic tilting of upper plate blocks may be, to some extent, counterbalanced by more subtle, synthetic tilting. Figure 10 in Gross and Hillemeier (1982) is especially spectacular.

Direction of Transport on Detachment Faults. In general, the strike of the tilted mid-Tertiary strata is perpendicular to the direction of tectonic transport on the underlying 'basal' detachment fault. Slickensides on the detachment surfaces are generally parallel to the dip direction of the overlying, tilted strata of mid-Tertiary age. Although the direction of dip of the tilted strata is commonly parallel to that of the lineation in the

mylonitic rocks of the lower plate, it is not always parallel. For example, lineation in the southern forerange of the Santa Catalina Mountains trends east-northeast to east-west, whereas the inferred transport direction during Whipple assemblage movement on the Catalina fault is thought to be S50W (Davis, 1983), a difference of about 30°. An even more discordant relationship is apparent in Redington Pass between the Santa Catalina and Rincon mountains where lineation in the lower plate of the Catalina fault analog trends N20-50W and is clearly discordant to the inferred, southwest-directed, normal transport along the Catalina fault system in mid-Tertiary time (Davis, 1983). As the lineation in the lower plate mylonites is not rigorously parallel to the tectonic transport of the overlying plate, a causal kinematic relationship between the lineation in the lower plate and the transport of the upper plate is not likely.

The strikes of the tilted blocks in the upper plate commonly strike between N20W and N50W. This implies that tectonic transport during detachment faulting is more or less parallel to a northeast-southwest direction. This has commonly been interpreted as an axis of regional, crustal extension (Davis, 1983; Frost and Martin, 1982). However, exceptions to the northeast or southwest transport are fairly frequent and include north transport on the Plomosa detachment fault in the Plomosa Mountains, implied north-northeast transport of Locomotive fanglomerate strata in the Ajo area, north to northwest transport on the Ajo Road fault (Gardulski, 1980), northwest transport on Helmet fanglomerate strata in the Sierrita Mountains, and west-northwest transport of the Helvetia klippe in the northern Santa Rita Mountains. These exceptions suggest that the transport direction above the low-angle normal faults may be a function of the geometry of the underlying, northwest-trending warps rather than a phenomena of regional crustal extension. In this model the detachment faults are smaller scale, near surface, denudational reactions to whatever process created the warps. For example, the previously mentioned anomalous directions could be transports directed down the noses of the folds; whereas the more common northwest-southeast transport directions could be directed down the more statistically prevalent flanks of the folds.

Magnitude of Transport on Detachment Faults.

The best constrained data for the amount of tectonic transport that can be ascribed to the detachment fault process is derived from offsets along synthetic normal faults in the upper plate. Offsets across upper plate synthetic faults in the Whipple Mountains are fairly well known and range from 0.3 to 1.5 km across the major synthetic faults (Gross and Hillemeier, 1982). In the Tortilla Mountains displacements along the Superstition-Tortilla detachment system range from 1 to 2.5 km (Lowell, 1968). If the reconstruction of Cooper (1960) of the San Xavier fault in the Pima mining district, and the beheaded porphyry copper deposit at Twin Buttes was moved to Mission-Pima, then the tectonic transport with respect to a basal detachment fault may have been about 10 km to the north-northwest

along the San Xavier detachment fault. In the northern Santa Rita Mountains, displacement of the Helvetia skarn in the Helvetia klippe relative to a presumed correlative skarn associated with the Broadwater plug north of Gunsight Knob is about 2 to 2.5 km to the west-northwest. In summary, known displacements across upper plate detachment fault structures are typically 1 to 3 km of normal slip. Thus, where displacements are firmly known, no large displacements on any single fault feature have been proven to exist.

Large amounts of displacement have been speculated to exist based on the regional dimensions of the detachment structures themselves or from tenuous matches of lithologies between the upper and lower plates. For example, Davis and others (1982) have speculated that northwest-trending dike swarms in the Mohave Mountains are offsets of a single dike swarm 22 km to the northeast of the Chambers Well dike swarm in the Whipple Mountains. However, they may simply be two different dike swarms of similar chemical composition, rather than the same dike swarm, as the wall rock geology differs in each case.

Other kinematic models of detachment faulting require little net slip on the basal detachment fault. For example, much of the antithetic tilting and accompanying synthetic faulting in the upper plate could be accompanied by antithetic faulting and synthetic tilting that would compensate for the offset on the more obvious synthetic faults (Gross and Hillemeier, 1982). At Savahia Peak in the Whipple Mountains, no more than 6 km of northeastward slip on the Whipple detachment fault would be required to produce the observed upper plate offsets (Gross and Hillemeier, 1982). In their model and ours, the upper plate is more or less, directionally distended, in situ, above the basal detachment structure in domino-like fashion.

Northwest-trending Folds and Arches. The broad, northwest-trending folds of the Galiuro assemblage continued to develop during Whipple assemblage time. However, newer, smaller-scale, more northerly trending folds were also developed at this time (Fig. 5). For example, the Whipple detachment fault which reutilized older Laramide thrust faults could have initiated between 22 and 18 Ma as a response to a broad, Galiuro assemblage, north-northwest-trending warp with its axis in the western Turtle Mountains. The principle detachment activity on the Whipple detachment fault would have occurred between 18 and 15 Ma (Davis and others, 1982). Between 15 and 13 Ma the smaller-scale warps, such as the Whipple-Chemehuevi anticline, developed on the shallow, northeast-dipping flank of the Turtle Mountains warp and deformed the Whipple low-angle fault complex. Similar north-northwest-trending anticlinal axes are present in Galiuro assemblage plutons and volcanics in the Santa Catalina and Tortolita Mountains.

The Spine syncline documented by Wilson (1962) southwest of Ray is a fairly sharp, northwest-trending syncline that deforms the 20 Ma

OROGENESIS, ARIZONA AND ADJACENT REGIONS

Apache Leap Tuff and 18-15 Ma rhyolitic volcanics. Immediately north-northeast of Ray, a similar north-trending syncline deforms 18 to 15 Ma volcanics and Whipple assemblage conglomerates east of the School reverse fault zone (Cornwall and others, 1971; Keith, 1983b). Broader folds deform the Mesquite Flat Breccia, a Whipple assemblage quartz alkalic latitic volcanic rock, in the central Superstition Mountains (Scarborough, 1981). Also, the Apsey Conglomerate is folded by a west-northwest- to northwest-trending syncline in the Apsey Creek area of the northwestern Galiuro Mountains (Keith, 1983b). To the southeast in the Klondyke area of the northeast Galiuro Mountains, the Hell Hole Conglomerate (Simons, 1964) is more strongly folded around north-northwest-trending anticlinal and synclinal fold axes. In the Orocopia Mountains of southeastern California, the Diligencia Formation (23 to 19 Ma and assigned here to the Galiuro Assemblage) has been folded by three major folds that trend N70W (Spittler and Arthur, 1982).

Northwest-trending Reverse Faults. Folds of Whipple Assemblage are commonly associated with reverse faults. Where in mutual contact, the reverse faults cut the detachment faults. In western Arizona a broad northwest-trending zone of reverse faults extends from the Dead Mountains in California on the northwest for some 120 km to the Harquahala Mountains on the southeast. Reverse faults in this western belt generally trend northwest and exhibit southwest-directed tectonic transport of the upper plate hanging wall. The best example of these reverse faults is the Lincoln Ranch fault pictured in Wilson (1962) in the south-central Rawhide and Buckskin Mountains. Exposures of the Lincoln Ranch fault in the Rawhide Mountains were mapped in more detail by Shackelford (1980). At least 600 m of structural throw are present where lower plate metasedimentary and mylonitic gneisses in the hanging wall are juxtaposed over Lincoln Ranch rebecks of the Whipple assemblage, in the footwall. The Lincoln Ranch fault clearly offsets the Rawhide-Buckskin detachment fault. To the northeast in the Alamo Dam area another southwest-directed, northwest-striking reverse fault offsets the Rawhide-Buckskin fault system with at least 90 m of reverse separation.

In central to southeastern Arizona another zone of diffuse reverse faulting directly cuts sedimentary rocks of the Whipple assemblage with movements of hanging wall to the northeast. On the west side of Camelback Mountain in the Phoenix region, megabreccia units and coarse arkosic units in the Camelback Formation are cut by a reverse fault dipping 30 degrees west that has about 60 m of reverse slip. In the Superstition Mountains a west-northwest-trending zone of folds and northeast-directed reverse faults cuts the youngest units of the Superstition volcanics dated at about 16-15 Ma (Scarborough, 1981; Stuckless and Sheridan, 1971). Near Ray, the School reverse fault zone cuts the 20 Ma Apache Leap Tuff and the overlying Big Dome Conglomerate and rhyolitic tuff (probably 18-15 Ma) and indicates up to 600 m of reverse slip (Cornwall and others, 1971; Keith, 1983b). Farther

to the southeast in the Galiuro Mountains Krieger (1968) mapped a number of WNW-striking, southwest-dipping reverse faults that cut the Holy Joe Peak member (26 Ma, Creasey and Krieger, 1978) of the Galiuro Volcanics.

An example of northeast-directed reverse faults in southern Arizona includes the Apache Pass fault in the northern Chiricahua Mountains shown by Sabins (1957) to deform middle Tertiary volcanics. Other examples of possible Whipple assemblage reverse faults are present in California. In the Orocopia Mountains, more tightly folded upper units of the Diligencia Formation are locally broken into northeast-directed reverse faults (Spittler and Arthur, 1982). In the Barstow region of the central Mojave, the middle Miocene Barstow Formation north of Barstow is cut by a major, northeast-dipping, southwest-directed, reverse fault that juxtaposes 18 Ma Pickhandle volcanics (Miller and Morton, 1980) over younger lacustrine units of the Barstow Formation, which is locally spectacularly folded.

Dike Swarms. Dike swarms that are cogenetic with quartz alkalic magmatism of the Whipple assemblage are locally present, but are not as extensive as the dike swarms of the Galiuro assemblage. Where present, the dike swarms generally strike northwest. In the western Whipple Mountains, late quartz alkalic dikes that strike north-northwest cut the calc-alkalic, Galiuro assemblage dikes of the Chambers Well dike swarm (Davis and others, 1982; L. Anderson, pers. commun., 1985). In the Vulture Mountains of west-central Arizona, an extensive swarm of latitic and high-K rhyolitic dikes of quartz alkalic chemistry strike northwest and have yielded several K-Ar whole rock dates that range from 18 to 16 Ma (Rehrig and others, 1980). Some of these Whipple assemblage dikes are cut by low-angle normal faults, whereas other dikes appear to intrude the low-angle detachment faults.

Age of Whipple Assemblage

Age of Volcanism. Age dates on volcanics in the Whipple assemblage range from 28 to 13 Ma or from late Oligocene to mid-Miocene. As with the earlier assemblages of the Galiuro orogeny, the rocks are older to the east and younger to the west. To the east in New Mexico Whipple assemblage rocks such as the La Jara Peak Andesite and interfingering Hell's Mesa tuffs in the Socorro region are about 27 to 24 Ma (Osburn and Chapin, 1982). In eastern Arizona in the central Chiricahua Mountains, the Rhyolite Canyon Formation and associated underlying monzonite stock are probably part of the Whipple assemblage and have been dated at about 25 to 23 Ma. Whipple assemblage alkaline volcanics at Picacho Peak and the Samaniego Hills are 22 to 15 Ma (Shafiqullah and others, 1976; Eastwood, 1970). Still farther west in the classic area of the Whipple Mountains of southeast California and in the Rawhide Mountains of western Arizona, quartz alkalic volcanics within the Copper Basin Formation and Chapin Wash Formation have yielded numerous age dates between 18 and 15 Ma (Martin and others, 1982). In northwestern Arizona

in the northern Black Range and El Dorado Mountains of southern Nevada, radiometric dates on the Patsy Mine Volcanics range from about 18 to 14 Ma (Anderson and others, 1972). Thus, from southwestern New Mexico to western Arizona and southeasternmost California, there appears to be a clear younging of Whipple assemblage volcanism that ranges from 27 to 23 Ma in New Mexico and from 18 to 15 Ma in the Colorado River region between Arizona and California.

Age of Faulting. Many of the detachment faults can be stratigraphically bracketed within the Whipple assemblage volcanism and sedimentation. Detachment faulting of the Whipple assemblage is slightly younger from southeast (18 to 15 Ma in central Arizona) to northwest (14 to 11 Ma in northwestern Arizona).

In the Whipple Mountains of southeastern California, Davis and others (1980; 1982) and Teel and Frost (1982) have shown that the Copper Basin Formation, which has yielded 6 K-Ar dates between 18.7 and 17.1 Ma, is a syntectonic deposit with respect to the detachment movement on the Whipple fault. A minimum age for the detachment fault is provided by numerous dates on the Osborn Wash Formation, which ranges in age from about 9 to 15.9 Ma (Davis and others, 1982); the Osborn Wash Formation is virtually flat lying and angularly truncates the Copper Basin Formation. Thus, detachment faulting in the Whipple Mountains occurred mainly between 18.7 and 15.9 Ma.

In the El Dorado and northern Black Mountains of southern Nevada and northwestern Arizona, detachment-related tectonics mainly occurred between 14 and 11 Ma. A pre-detachment volcanic unit named the Patsy Mine Volcanics has yielded several K-Ar dates between about 18 and 14 Ma. The Patsy Mine Volcanics is rotated and is angularly overlain by the Davis Mountain Volcanics which rest above the Bridge Spring Tuff datum. The Davis Mountain Volcanics have yielded several K-Ar dates between 13 and 11 Ma (Anderson and others, 1972) and are cut in many places by low-angle normal faults that are probably detachment related. The Davis Mountain Volcanics, which are commonly steeply tilted, are in turn overlain by nearly flat lying Muddy Creek Formation which has yielded K-Ar dates as old as 11 Ma (Anderson and others, 1972).

Detachment-related tectonics in west-central Arizona occurred approximately between 18 and 16 Ma. In the Vulture Mountains, steeply tilted, rhyolitic volcanics are cut by detachment-related, low-angle normal faults and have yielded K-Ar dates between 16 and 17 Ma (Rehrig and others, 1980). The low-angle normal faults are, in places, intruded by ultra-potassic, rhyolite porphyry dikes that are undeformed. One of these dikes has yielded a K-Ar age on biotite of 18 Ma. Further confirmation of the 18 to 15 Ma age of faulting is provided by K-Ar whole rock dates of 13.5 Ma on essentially untilted, post-detachment, probable Basin and Range basalts that angularly truncate the tilted rhyolitic volcanics in the Vulture Mountains.

In the Superior region in the Teapot Mountain quadrangle, detachment related low-angle faults may be tightly bracketed between about 18 and 15 Ma. Here, low-angle normal faults cut rhyolitic volcanics as young as 18 to 16 Ma and are overlain positionally by rhyolitic tuffs (Keith, 1983b) that correlate with rhyolitic tuffs in the adjacent Mineral Mountain quadrangle that are dated at 16 to 15 Ma (Theodore and others, 1978). Farther to the southeast in the northern Tortilla Mountains, rhyolitic tuffs in the Ripsey Wash sequence of Schmidt (1971) have been dated at about 18 Ma. The Ripsey Wash sequence occurs in the upper plate of the Ripsey Wash detachment fault and, because it is cut by the Ripsey Wash detachment fault, the detachment fault must be younger than 18 Ma.

Termination of Galiuro Orogeny

Termination of Galiuro orogeny in the Basin and Range Province of Arizona is represented in general by a regional unconformity that is commonly angular and is of late mid-Miocene (15-11 Ma). Above the unconformity are basin-fill sediments in the sense of Scarborough and Peirce (1976) and Wilt and Scarborough (1981) or sediments of Unit II of Eberly and Stanley (1978). Below the unconformity are the sediments and volcanics of culminant Galiuro orogeny, which include Unit I of Eberly and Stanley (1978) or post-ignimbrite sediments of Wilt and Scarborough (1981). The unconformity at the end of the Galiuro orogeny is generally better displayed in horst blocks and is less obvious in the basin blocks.

One of the best indications of the termination of Galiuro orogeny is the dramatic change in the chemical nature of the magmatism from the culminant Galiuro orogeny to that of the succeeding San Andreas orogeny. The chemistry of the overlying San Andreas magmatism is of similar alkalinities to the Galiuro orogeny, but is distinctly more metaluminous. Also, magmatism of the San Andreas orogeny is distinctly more iron-rich, dramatically more anhydrous, less oxidized, and noticeably less siliceous than earlier Cretaceous-Cenozoic magmatism. The anhydrous nature of San Andreas magmatism is dramatically illustrated by the general lack of hydrous minerals such as amphibole or mica, whereas Galiuro orogenic magmatism generally contains noticeable hydrous minerals (greater than 1.5 volume percent). Strontium initial ratios for culminant Galiuro magmatism range from 0.706 to 0.7010, whereas strontium initial ratios for San Andreas basaltic magmatism are generally less than 0.705 and may be as low as 0.7022 (Keith and Dickinson, 1979). Galiuro orogeny magmatism features large volumes of siliceous ignimbrites having silica contents greater than 65 weight percent, whereas San Andreas magmatism features large volumes of basalt with silica contents between 42 to 50-52 weight percent.

The chemical and mineralogical switchover from Galiuro to San Andreas magmatism occurred between about 13 to 12 Ma in the Basin and Range Province south of Kingman and from about 11 to 9 Ma in

OROGENESIS, ARIZONA AND ADJACENT REGIONS

northwestern Arizona between Kingman and Las Vegas. Thus, magma chemistry indicates the switchover from Galiuro to San Andreas orogeny in Arizona and vicinity occupied a very narrow time interval of about 2 million years. The changeover is not represented by a broad transitional interval, such as the 'mid-Tertiary transition' of Shafiqullah and others (1980) or the Stage 2 transition of Damon and others (1984).

SAN ANDREAS OROGENY

The present physiography of the Basin and Range Province and of the Transverse Ranges was produced by the most recent orogenic event in the region. The event is herein named the San Andreas orogeny for very similar, modern day tectonics related to the San Andreas transform system in California, southwesternmost Arizona, and the Gulf of California region. As used in this paper, the term San Andreas orogeny is similar to the Basin and Range nomenclature widely used in the literature, for example, the Basin and Range disturbance of Scarborough and Peirce (1978). However, the term Basin and Range is not broad enough to include transverse physiographic components that probably developed at the same time as most of the Basin and Range physiography, for example, the spectacular Transverse Ranges of southern California and similar, transverse, physiographic mountain ranges in west-central Arizona. The term San Andreas orogeny is herein coined to include both physiographic elements. Consequently, San Andreas orogeny can be subdivided into two orogenic phases, which are also assemblages: the Transverse assemblage and the Basin and Range assemblage (Table 4).

Transverse Assemblage

The Transverse Assemblage is physiographically marked by mountain ranges that trend east-west to east-northeast--west-southwest. These trends are perpendicular to the trend of most of the ranges in the Basin and Range Province. The anomalous physiographic trend coincides with east-northeast-trending folds in Arizona and folds and thrusts in California.

Sedimentary rocks of the Transverse assemblage consist of coarse clastics near the mountain fronts that grade to braidplains and coastal plains away

from the range fronts and towards the center of the valleys. The facies changes are less abrupt than in the Basin and Range assemblage. Igneous rocks are generally absent, but when present consist mainly of basalt with local rhyolites. In Arizona one of the best candidates for Transverse assemblage strata is the Osborne Wash Formation northeast of Parker, which rests in a northeast-trending synclinal trough and thins away from the axis of the trough. Predominantly clastic sedimentary rocks in the Butler and McMullen valleys southeast of Parker are also assigned to the Transverse Assemblage.

In Arizona structures of the Transverse assemblage consist mainly of northeast-trending, broad to open anticlines and synclines, commonly arranged in an echelon patterns (Fig. 6). Where exposed, the folds typically have wavelengths of 4 to 12 km and amplitudes of 100 to 600 m (Spencer, 1982). These sharply contrast to earlier Galiuro orogeny folds, which have wavelengths of 50 to 100 km and amplitudes of 6 to 10 km. Structures assigned to the Transverse assemblage include the zone of an echelon folds from the Harquahala to Parker region in west-central Arizona, South Mountain south of Phoenix, and west-southwest-plunging folds in the Rincon Mountains southwest of Tucson. Another transverse structural element is northwest-trending faults with right slip movement in areas of northeast-southwest-trending folding. Examples of such faults are widespread in the Harquahala to Parker region, where some of these faults cut the 15 to 9 Ma Osborne Wash Formation. Also, throughout this region, the northeast-southwest-trending folds conspicuously deform the 18 to 15 Ma detachment faults and thus are at least as young as 15 Ma.

Basin and Range Assemblage

The Basin and Range assemblage is physiographically marked by mountain ranges that trend north-south to north-northwest. In non-pedimented areas, the mountain ranges are bounded by steep, northwest- to north-trending normal faults.

Sedimentary rocks of the Basin and Range assemblage include coarse clastics at the edges of the steep mountain fronts with local megabreccias near the range front faults. The coarse clastics undergo rapid facies changes to fine-grained and

ASSEMBLAGE	SEDIMENTATION	MAGMATISM	STRUCTURAL FEATURES	MINERAL RESOURCES	AGE (Ma)
Basin & Range	clastics & evaporites in grabens	alkaline anhydrous metaluminous basaltic volcanism	N-S trend horsts & grabens bounded by generally steep normal faults	sand and gravel salt, zeolites cinders, gypsum	0-13
Transverse	clastics	none or rare	NE-SW-trending folds, NW-striking, right-slip faults	petroleum, gas	0-12

Table 4. Summary of assemblages of the San Andreas orogeny in Arizona.

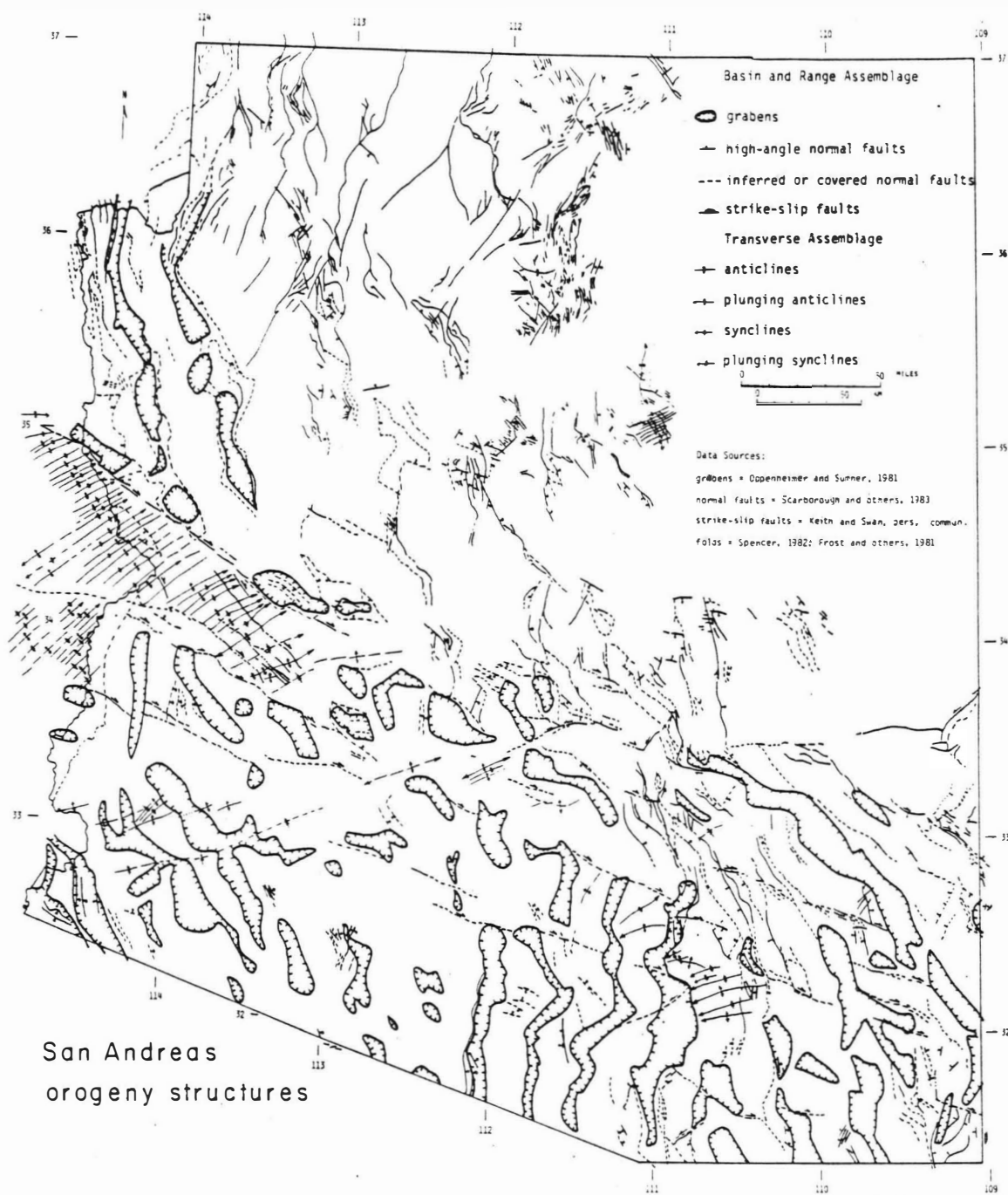


Figure 6. Map of structural features of the San Andreas orogeny in Arizona and vicinity.

evaporitic facies in the basin centers. Numerous sedimentary accumulations in Arizona have been documented by Peirce (1976), Eberly and Stanley (1978), Scarborough and Peirce (1978), Wilt and Scarborough (1981), Nations and others (1982), and Peirce (1984). Present basins include the Picacho

Basin in Pinal County, the Red Lake Basin in Mohave County, the Safford Basin in Greenlee County, the Wilcox playa of Cochise County, and the Tucson Basin. Sedimentary formations assigned to the Basin and Range assemblage include the St. David and Quiburis formation in the upper and lower San Pedro

OROGENESIS, ARIZONA AND ADJACENT REGIONS

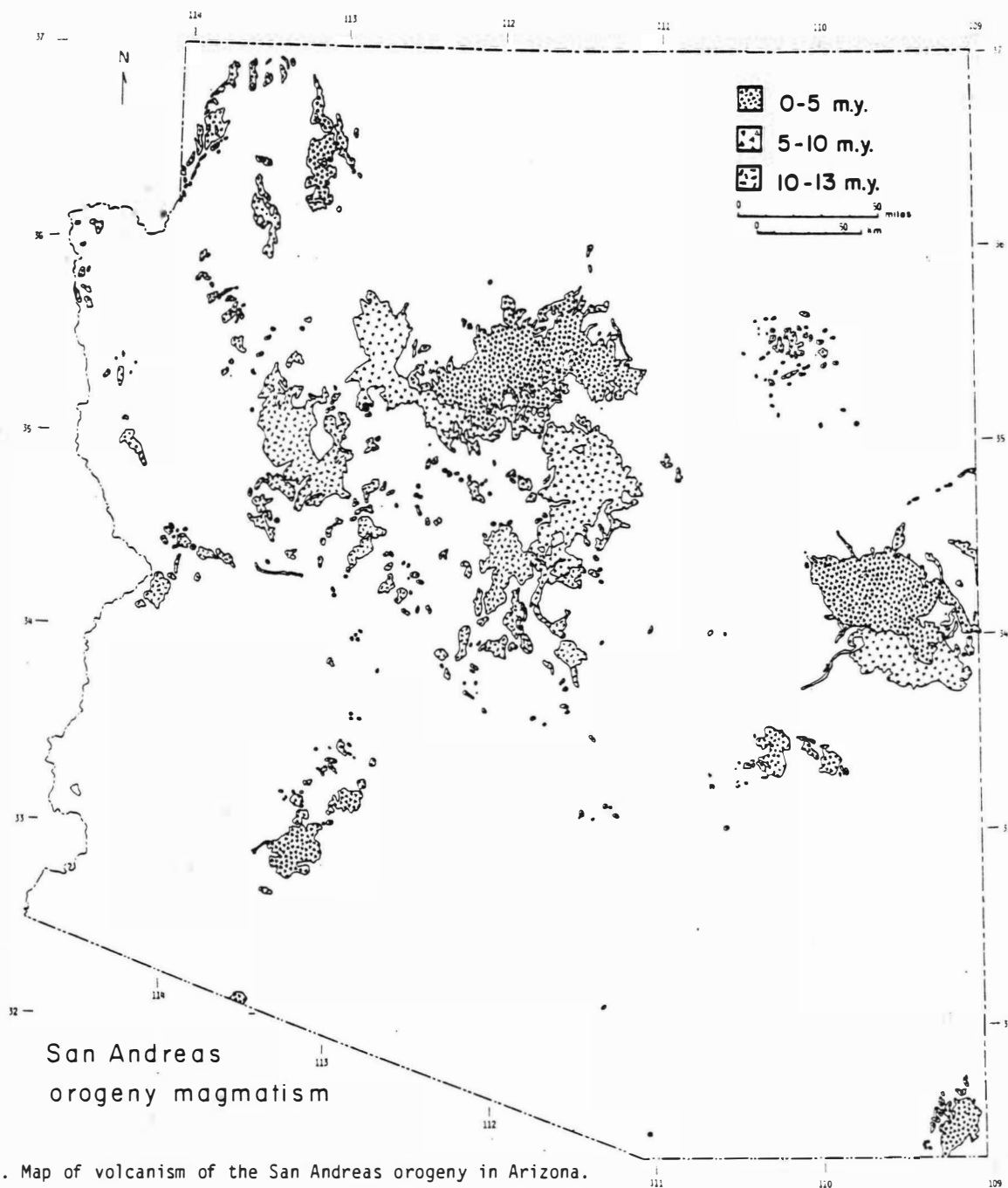


Figure 7. Map of volcanism of the San Andreas orogeny in Arizona.

valley of southeast Arizona, the Verde Formation in the Verde Valley of central Arizona, Bouse Formation, and the Muddy Creek Formation in northwestern Arizona.

In contrast to the Transverse assemblage, basaltic volcanism is widespread in the Basin and

Range assemblage. Examples of the main volcanic fields include the San Francisco Peaks near Flagstaff, the White Mountains volcanic field in eastern Arizona, the San Bernardino Volcanic field in southeastermost Arizona, the Pinacate volcanic field of southern Yuma and Pima Counties, the Sentinel volcanic field south and west of Gila Bend.

the Hickey basalts of northwestern Arizona and the Hopi Buttes volcanic field of northeastern Arizona (Fig. 7). Basaltic volcanism consistently migrated toward the Colorado Plateau from 13 to 0 Ma (Best and Brimhall, 1974; Luedke and Smith, 1978; Wilt and Scarborough, 1981). The earliest volcanics in the Basin and Range assemblage are the Hickey basalts in the central part of the state; they date from 13 to 9 Ma (Shafiqullah and others, 1980). Volcanism from 9 to 4 Ma occurred in the southern parts of the White Mountain field (Ratte and others, 1969), the San Francisco field (Damon and others, 1974), and the Cottonwood Basalt; volcanism during this time straddled the boundary between the Colorado Plateau and Basin and Range provinces. Volcanism from 3 to 0 Ma occurred in the northern parts of the White Mountain field and San Francisco field north of the Colorado Plateau boundary; volcanism also occurred in the San Bernardino valley in southeasternmost Arizona (Lynch, 1978), the Sentinel volcanic field of south central Arizona, and the Pinacate volcanic field (Gutmann and Sheridan, 1978) in southwestern Arizona. Chemistry of igneous rocks of the Basin and Range assemblage are markedly different from preceding Cretaceous-Cenozoic magmatism, as previously discussed.

Structures of the Basin and Range assemblage are shown in Figure 6. These structures generally consist of north-south to north-northwest trending grabens that are either symmetric or asymmetric. Many of the grabens exhibit pull-apart geometries with steep normal faults on their west and east margins and northwest- to west-northwest- trending faults with probable right slip motion on their north and south margins reminiscent of Death Valley. Structural relief developed in Basin and Range basins was locally impressive. For example, Scarborough and Peirce (1978) estimated as much as 2.5 to 3.7 km estimated stratigraphic separation for eight basins with drill hole control. The duration of Basin and Range faulting in any given area is less than 5 million years. In the Desert province of Arizona, Basin and Range faulting probably initiated about 13 Ma and terminated about 8 Ma; whereas in the mountain province, it probably initiated about 5 to 6 Ma and dramatically slowed about 2 Ma and continues at a much slower rate to the present.

CONCLUSION

Application of the strato-tectonic approach to late Cretaceous and Cenozoic orogenic development in Arizona has resulted in two fundamental, new insights. Firstly, a major, new, late Laramide, stratigraphic and tectonic event, previously unrecognized in Arizona was established. That is, the presence of intracrustal, peraluminous magmatism is accompanied by significant and possibly world class, gold mineralization (Mesquite, California) that developed in the presence of major, southwest-directed thrusting and crustal shortening of unprecedented magnitude. Secondly, structural development during Galiuro orogeny may well have been related to regional, crustal-scale warping that was accomplished by 2 to 4 percent crustal

shortening rather than crustal extension, in contrast to interpretations widely advocated in the literature.

Thirdly, it is impossible to overemphasize the importance of the strato-tectonic approach in understanding resource development and potential. In particular, Arizona may have much better gold potential than previously thought, if the peraluminous magmatism and its related gold metallogeny is fully explored. Also, because thrusting is of late Laramide age and is directed southwesterly rather than northeasterly as previously advocated in the literature, petroleum plays based on northeast-directed thrust models should be reevaluated.

REFERENCES CITED

- Anderson, R. E., Longwell, C. R., Armstrong, R. L., and Marvin, R. F., 1972, Significance of K-Ar ages of Tertiary rocks from the Lake Mead region, Nevada-Arizona: Geological Society of America Bulletin, v. 83, no. 2, p. 273-287.
- Anderson, J. L., and Rowley, M. C., 1981, Synkinematic intrusion of peraluminous and associated metaluminous granitic magmas, Whipple Mountains, California: Canadian Mineralogist, v. 19, p. 83-101.
- Armstrong, R. L., 1972, Low-angle (denudation) faults, hinterland of the Sevier orogenic belt, eastern Nevada and western Utah: Geological Society of America Bulletin, v. 83, p. 1729-1754.
- Baltz, E. H., 1967, Stratigraphy and regional tectonic implications of part of Upper Cretaceous and Tertiary rocks, east-central San Juan Basin, New Mexico: U. S. Geological Survey Professional Paper 552, 101 p.
- Best, M. G., and Brimhall, W. H., 1974, Late Cenozoic alkalic basaltic magmas in the western Colorado Plateaus and the Basin and Range Transition zone, U.S.A., and their bearing on mantle dynamics: Geological Society of America Bulletin, v. 85, no. 11, p. 1677-1690.
- Bornhorst, T. J., 1982, Major- and trace-element geochemistry and mineralogy of upper Eocene to Quaternary volcanic rocks of the Mogollon-Datil volcanic field, southwestern New Mexico: unpublished Ph.D. Thesis, University of New Mexico, Albuquerque, 1090 p.
- Brennan, D. J., 1962, Tertiary sedimentary rocks and structures of the Cienega Gap area, Pima County, Arizona: Arizona Geological Society Digest, v. 5, p. 45-58.
- Burnham, C. W., and Jahns, R. H., 1962, A method for determining the solubility of water in silicate melts: American Journal of Science, v. 260, p. 721-745.
- Carter, Bruce, and Silver, L. T., 1971, Post-emplacement structural history of the San Gabriel Anorthosite complex. (Abs.): Geological Society of America, Abstracts with Programs, v. 3, no. 2, p. 92-93.
- Chapin, C. E., and Cather, S. M., 1981, Eocene

OROGENESIS, ARIZONA AND ADJACENT REGIONS

- tectonics and sedimentation in the Colorado Plateau-Rocky Mountain area, in Dickinson, W. R., and Payne, W. D., eds., Relations of tectonics to ore deposits in the southern Cordillera: Arizona Geological Society Digest, v. 14, p. 173-198.
- Chew, R. T., 1952, Geology of the Mineta Ridge area, Pima and Cochise Counties, Arizona: unpublished M.S. Thesis, University of Arizona, Tucson, 53p.
- Clay, D. W., 1970, Stratigraphy and petrology of the Mineta Formation in Pima and eastern Cochise Counties, Arizona: unpublished Ph.D. thesis, University of Arizona, 187 p.
- Coney, P. J., 1972, Cordilleran tectonics and North America plate motions: American Journal of Science, v. 272, p. 603-628.
- Coney, P. J., 1976, Plate tectonics and the Laramide orogeny: New Mexico Geological Society Special Publication 6, p. 5-10.
- Coney, P. J., and Reynolds, S. J., 1977, Cordilleran Benioff zones: Nature, v. 270, p. 403-406.
- Cooley, M. E., and Davidson, E. S., 1963, The Mogollon Highlands - their influence on Mesozoic and Cenozoic erosion and sedimentation: Arizona Geological Society Digest, v. 6, p. 7-33.
- Couper, J. R., 1960, Some geologic features of the Pima mining district, Pima County, Arizona: U. S. Geological Survey Bulletin 1112-C, p. 63-103.
- Cornwall, H. R., Banks, N. G., and Phillips, C. H., 1971, Geologic map of the Sonora quadrangle, Pinal and Gila Counties, Arizona: U.S. Geological Survey Geological Quadrangle Map GQ-1021, scale 1:24,000.
- Creasey, S. C., Banks, N. G., Ashley, R. P., and Theodore, T. G., 1976, Middle Tertiary plutonism in the Santa Catalina and Tortolita Mountains, Arizona: U. S. Geological Survey Open-file Report 76-262, 20 p.
- Creasey, S. C., Jinks, J. E., Williams, F. E., and Meeves, H. C., 1981 [1982], Mineral resources of the Galiuro Wilderness and contiguous further planning areas, Arizona: U. S. Geological Survey Bulletin 1490, 94 p.
- Creasey, S. C., and Krieger, M. H., 1978, Galiuro volcanics, Pinal, Graham, and Cochise counties, Arizona: U. S. Geological Survey Journal of Research, v. 6, p. 115-131.
- Crowe, B. M., Crowell, J. C., and Krummenacher, D., 1979, Regional stratigraphy, K-Ar ages, and tectonic implications of Cenozoic volcanic rocks, southeastern California: American Journal of Science, v. 279, no. 2, p. 186-216.
- Crowell, J. C., 1981, An outline of the tectonic history of southeastern California, in Ernst, W. G., ed., The Geotectonic Development of California, Rubey Volume I: Prentice-Hall, New Jersey, p. 583-599.
- Damon, P. E., and Bikerman, Michael, 1964, Potassium-argon dating of post-Laramide plutonic and volcanic rocks within the Basin and Range province of southeastern Arizona and adjacent areas: Arizona Geological Society Digest, v. 7, p. 63-78.
- Damon, P. E., and Mauger, R. L., 1956, Epeirogeny-orogeny viewed from the Basin and Range province: Society of Metallurgical Engineers Transactions, v. 223, p. 99-112.
- Damon, P. E., Lynch, D. J., and Shafiqullah, M., 1984, Cenozoic landscape development in the Basin and Range Province of Arizona, in Smiley, T. L., Nations, J. U., Pewe, T. L., and Schafer, J. P., eds., Landscapes of Arizona, the Geological Story: University Press of America, New York, p. 175-206.
- Damon, P. E., Shafiqullah, M., and Leventhal, J. S., 1974, K-Ar chronology for the San Francisco volcanic field and rate of erosion of the Little Colorado River: Geology of Northern Arizona, Field Guide for Geological Society of America, Rocky Mountain Section Meeting, Northern Arizona University, p. 221-235.
- Davis, G. A., and Fleck, R. J., 1977, Chronology of Miocene volcanic and structural events, central Owlhead Mountains, eastern San Bernardino County, California (Abs.): Geological Society of America Abstracts with Programs, v. 9, no. 4, p. 409.
- Davis, G. A., Anderson, J. L., Frost, E. G., and Shackelford, T. J., 1980, Mylonitization and detachment faulting in the Whipple-Buckskin-Rawhide Mountains terrane, southeastern California and western Arizona, in Crittenden, M. D., Jr., Coney, P. J., and Davis, G. H., eds., Cordilleran Metamorphic Core Complexes: Geological Society of America Memoir 153, p. 79-129.
- Davis, G. A., Anderson, J. L., Martin, D. L., Krummenacher, D., Frost, E. G., and Armstrong, R. L., 1982, Geologic and geochronologic relations in the lower plate of the Whipple detachment fault, Whipple Mountains, southeastern California; a progress report, in Frost, E. G., and Martin, D. L., eds., Mesozoic-Cenozoic Tectonic Evolution of the Colorado River Region, California, Arizona, and Nevada: Cordilleran Publishers, San Diego, California, p. 408-432.
- Davis, G. H., 1980, Structural characteristics of metamorphic core complexes, southern Arizona, in Crittenden, M., Jr., Coney, P. J., and Davis, G. H., eds., Cordilleran metamorphic core complexes: Geol. Soc. America, Memoir 153, p. 35-77.
- Davis, G. H., 1983, Shear-zone model for the origin of metamorphic core complexes: Geology, v. 11, p. 342-347.
- Deal, E. G., Elston, W. E., Erb, E. E., Peterson, S. L., Reiter, D. E., Damon, P. E., and Shafiqullah, M., 1978, Cenozoic volcanic geology of the Basin and Range Province in Hidalgo County, southwestern New Mexico, in Callender, J. F., Wilt, J. C., Clemons, R. E., and James, H. L., eds., Land of Cochise, Southeastern Arizona: New Mexico Geological Society, 29th Field Conference, p. 219-230.
- Drewes, H., 1972, Cenozoic rocks of the Santa Rita Mountains, southeast of Tucson, Arizona: U. S. Geological Survey Professional Paper 746, 66 p.
- Drewes, H., 1974, Geologic map and sections of the Happy Valley quadrangle, Cochise County, Arizona: U. S. Geological Survey Miscellaneous Investigations Map I-832, scale 1:48,000.

- Drewes, H., 1977 [1978], Geologic map and sections of the Rincon Valley quadrangle, Pima County, Arizona: U. S. Geological Survey Miscellaneous Investigations Map I-997, scale 1:48,000.
- Drewes, H., 1981, Tectonics of southeastern Arizona: U. S. Geological Survey Professional Paper 1144, 96 p.
- Drewes, H., and Thorman, C. H., 1977, New evidence for multiphase development of the Rincon metamorphic core complex east of Tucson, Arizona (Abs.): Geological Society of America Abstracts with Programs, v. 10, no. 3, p. 103.
- Eastwood, R. L., 1970, A geochemical-petrological study of mid-Tertiary volcanism in parts of Pima and Pinal Counties, Arizona: unpublished Ph.D. Thesis, University of Arizona, Tucson, 212 p.
- Eberly, L. D., and Stanley, T. B., Jr., 1978, Cenozoic stratigraphy and geologic history of southwestern Arizona: Geological Society of America Bulletin, v. 89, no. 6, p. 921-940.
- Ehlig, P. L., 1968, Causes of distribution of Pelona, Rand, and Orocopia schists along the San Andreas and Garlock faults: Stanford University Publications in Geological Sciences, v. 11, p. 294-306.
- Elston, W. E., Damon, P. E., Coney, P. J., Rhodes, R. C., Smith, E. I., and Bickman, M., 1973, Tertiary volcanic rocks, Mogollon-Datil Province, New Mexico, and surrounding region: K-Ar dates, patterns of eruption, and periods of mineralization: Geological Society of America Bulletin, v. 84, p. 2259-2274.
- Epis, R. C., and Chapin, C. E., 1975, Geomorphic and tectonic implications of the post-Laramide, Late Eocene erosion surface in the Southern Rocky Mountains: Geological Society of America Memoir 144, p. 45-74.
- Finnell, T. L., 1970, Pantano Formation: U. S. Geological Survey Bulletin 1294-A, p. 35-36.
- Frost, Eric G., 1981, Structural style of detachment faulting in the Whipple Mountains, California, and Buckskin Mountains, Arizona: Ariz. Geol. Soc. Digest, v. 13, p. 25-29.
- Frost, E. G., and Martin, D. L., 1981, Comparison of Mesozoic compressional tectonics with mid-Tertiary detachment faulting in the Colorado River area, California, Arizona, and Nevada, in Cooper, J. D., compiler, Guidebook, Geological Excursions in the California Desert: Geological Society of America, Field Trip Numbers 2, 7, 13, April, 1982, p. 113-158.
- Frost, E. G., and Martin, D. L., eds., 1982, Mesozoic-Cenozoic tectonic evolution of the Colorado River region, California, Arizona, and Nevada: Cordilleran Publishers, San Diego, California, 608 p.
- Gardulski, A. F., 1980, A structural and petrologic analysis of a quartzite-pegmatite tectonite, Coyote Mountains, southern Arizona: unpublished M.S. Thesis, University of Arizona, Tucson, 69 p.
- Garner, W. E., Frost, E. G., Tanges, S. E., and Germinario, M. P., 1982, Mid-Tertiary detachment faulting and mineralization in the Trigo Mountains, Yuma County, Arizona, in Frost, E. G., and Martin, D. L., eds., Mesozoic-Cenozoic Tectonic Evolution of the Colorado River Region, California, Arizona, and Nevada: Cordilleran Publishers, San Diego, California, p. 158-172.
- Gilluly, James, 1956, General geology of central Cochise County, Arizona: U. S. Geological Survey Professional Paper 281, 196 p.
- Graham, C. M., and England, P. C., 1976, Thermal regimes and regional metamorphism in the vicinity of overthrust fault - an example of shear heating and inverted metamorphic zonation from southern California: Earth and Planetary Science Letters, v. 31, p. 142-152.
- Gross, W. W., and Hillemeier, F. L., 1982, Geometric analysis of upper-plate fault patterns in the Whipple-Buckskin detachment terrane, in Frost, E. G., and Martin, D. L., eds., Mesozoic-Cenozoic Tectonic Evolution of the Colorado River Region, California, Arizona, and Nevada: Cordilleran Publishers, San Diego, California, p. 256-266.
- Gutmann, J. T., and Sheridan, M. F., 1978, Geology of the Pinacate volcanic field, in Burt, D. M., and Pewe, T. L., eds., Guidebook to the Geology of Central Arizona: Arizona Bureau of Geology and Mineral Technology, Special Paper No. 2, p. 47-60.
- Hamilton, W., 1982, Structural evolution of the Big Maria Mountains, northeastern Riverside County, southeastern California, in Frost, E. G., and Martin, D. L., eds., Mesozoic-Cenozoic Tectonic Evolution of the Colorado River Region, California, Arizona, and Nevada: Cordilleran Publishers, San Diego, California, p. 1-27.
- Haxel, G. B., and Dillon, J., 1978, The Pelona-Orocopia Schist and Vincent-Chocolate Mountain thrust system, southern California, in Howell, D. G., and McDougall, K. A., Mesozoic Paleogeography of the western United States: Society of Economic Paleontologists and Mineralogists, Pacific Coast Paleogeography Symposium 2, p. 453-469.
- Haxel, G. B., and Grubensky, M. J., 1984, Tectonic significance of localization of middle Tertiary detachment faults along Mesozoic and early Tertiary thrust faults, southern Arizona region (Abs.): Geological Society of America, Abstracts with Programs, v. 15, no. 6, p. 533.
- Haxel, G. B., Tosdal, R. M., May, D. J., and Wright, J. E., 1984, Latest Cretaceous and early Tertiary orogenesis in south-central Arizona: thrust faulting, regional metamorphism, and granitic plutonism: Geological Society of America Bulletin, v. 95, p. 631-653.
- Hayes, P. T., and Raup, R. B., 1968, Geologic map of the Huachuca and Mustang Mountains, southeastern Arizona: U. S. Geological Survey Miscellaneous Investigations Map I-509, scale 1:48,000.
- Helmstaedt, H., and Doig, R., 1975, Eclogite nodules from kimberlite pipes of the Colorado Plateau - samples of subducted Franciscan-type oceanic lithosphere: Physics and Chemistry of the Earth, v. 9, p. 95-111.
- Heindel, L. A., 1962, Cenozoic geology of Arizona - a 1960 resume: Arizona Geological Society Digest, v. 5, p. 9-24.
- Holdaway, M. J., 1971, - kyanite stability = 12 km :

OROGENESIS, ARIZONA AND ADJACENT REGIONS

- American Journal of Science, v. 271, p. 97-131.
- Howard, K. A., Stone, P., Pernokas, M. A., and Marvin, R. F., 1982, Geologic and geochronologic reconnaissance of the Turtle mountains area, California: west border of the Whipple Mountains detachment terrane, in Frost, E. G., and Martin, D. L., eds., *Mesozoic-Cenozoic Tectonic Evolution of the Colorado River Region, California, Arizona, and Nevada*: Cordilleran Publishers, San Diego, California, p. 341-354.
- Keith, S. B., 1977, The Cenozoic Galiuro and Basin Range orogenies in southern Arizona (Abs.): Fifth Geoscience Daze, University of Arizona, Department of Geosciences, p. 18.
- Keith, S. B., 1978, Paleosubduction geometries inferred from Cretaceous and Tertiary magmatic patterns in southwestern North America: *Geology*, v. 6, p. 516-521.
- Keith, S. B., 1980, The great southwestern Arizona overthrust oil and gas play, drilling commences: Fieldnotes from the State of Arizona Bureau of Geology and Mineral Technology, v. 10, no. 1, p. 1-3, 6-8.
- Keith, S. B., 1982a, Evidence for late Laramide southwest vergent underthrusting in southeast California, southern Arizona, and northeast Sonora (Abs.): *Geological Society of America, Abstracts with Programs*, v. 14, no. 4, p. 177.
- Keith, S. B., 1983, Regional Eocene SW-directed thrusting, Santa Catalina - Rincon crystalline complex, SE Ariz. (Abs.): *Geological Society of America, Abstracts with Programs*, v. 15, no. 5, p. 425.
- Keith, S. B., 1983b, Results of mapping project near Ray, Pinal County, Arizona: Arizona Bureau of Geology and Mineral Technology, Open-file Report 83-14.
- Keith, S. B., 1984, Map of outcrops of Laramide (Cretaceous-Tertiary) rocks in Arizona and adjacent regions: Arizona Bureau of Geology and Mineral Technology, scale 1:1,000,000.
- Keith, S. B., and Dickinson, W. R., 1979, Transition from subduction to transform tectonics in southwestern North America (22-8 m.y. B.P.) (Abs.): *Geological Society of America, Abstracts with Programs*, v. 11, no. 7, p. 455.
- Keith, S. B., and Reynolds, S. J., 1981, Low-angle subduction origin for paired peraluminous-metaluminous belts of mid-Cretaceous to Early Tertiary Cordilleran granitoids (abs.): *Geological Society of America, Abstracts with Programs, Cordilleran Section Meeting*, p. 63.
- Keith, S. B., Reynolds, S. J., Damon, P. E., Shafiqullah, M., Livingston, D. E., and Pushkar, P. D., 1980, Evidence for multiple intrusion and deformation within the Santa Catalina-Rincon-Tortolita crystalline complex, southeastern Arizona: *Geological Society of America Memoir* 153, p. 217-267.
- Keith, S. B., and Wilt, J. C., in press for 1986, Laramide Orogeny in Arizona and surrounding regions: *Arizona Geological Society Digest*, v.
- Krieger, M., 1977, Large landslides, composed of megabreccia, interbedded in Miocene basin deposits, southeastern Arizona: U.S. Geological Survey Professional Paper 1008, 25 p.
- Krieger, M. H., Johnson, M. G., and Bigsby, P., 1979, Mineral resources of the Aravaipa Canyon Basinate Wilderness Area, Pinal and Graham Counties, Arizona: U.S. Geological Survey, Open-file Report 79-291, 183 p.
- Krieger, M. H., 1968, Geologic map of the Holy Joe Peak quadrangle, Pinal County, Arizona: U. S. Geological Survey, Geological Quadrangle Map GQ-669, scale 1:24,000.
- Lingrey, S. H., 1982, Structural geology and tectonic evolution of the northeastern Rincon Mountains, Cochise and Pima Counties, Arizona: unpublished M.S. Thesis, University of Arizona, Tucson, 202
- Lowell, J. D., 1968, Geology of the Kalamazoo ore body, San Manuel district, Arizona: *Economic Geology*, v. 63, no. 6, p. 645-654.
- Luedke, R. G., and Smith, R. L., 1978, Map showing distribution, composition, and age of late Cenozoic volcanic centers in Arizona and New Mexico: U. S. Geological Survey Miscellaneous Investigations Map I-1091 A.
- Lynch, D. J., 1978, The San Bernardino volcanic field of southeastern Arizona, in Callender, J. F., Wilt, J. C., and Clemons, R. E., eds., *Land of Cochise, Southeastern Arizona*: New Mexico Geological Society, 29th Field Conference Guidebook, p. 251-258.
- Martin, D. L., Kruppenacher, D., and Frost, E. G., 1982, K-Ar geochronologic record of Mesozoic and Tertiary tectonics of the Big Maria - Little Maria- Riverside Mountains terrane, in Frost, E. G., and Martin, D. L., eds., *Mesozoic-Cenozoic Tectonic Evolution of the Colorado River Region, California, Arizona, and Nevada*: Cordilleran Publishers, San Diego, California, p. 518-549.
- Marvin, R. F., and others, 1973, Radiometric ages of igneous rocks from Pima, Santa Cruz, and Cochise Counties, southeastern Arizona: U.S. Geological Survey Bulletin 1379, 27 p.
- Miller, C. F., and Bradfish, L. J., 1980, An inner Cordilleran belt of muscovite-bearing plutons: *Geology*, v. 8, p. 412-416.
- Miller, F. K., and Morton, D. M., 1980, Potassium-argon geochronology of the eastern Transverse Ranges and southern Mojave Desert, southern California: U.S. Geological Survey Professional Paper 1142, ? p.
- Mukasa, S. B., Dillon, J. T., and Tosdal, R. M., 1984, A Late Jurassic minimum age for the Pelona-Orocopia Schist protolith, southern California (abs.): *Geological Society of America, Abstracts with Programs*, v. 16, p. 323.
- Nations, J. D., Landye, J. J., and Hevly, R. H., 1982, Location and chronology of Tertiary sedimentary deposits in Arizona: a review, in Ingersoll, R. V., and Woodburne, M. O., eds., *Cenozoic Nonmarine Deposits of California and Arizona*: Society of Economic Paleontologists and Mineralogists, Pacific Section, p. 107-119.
- Olmsted, F. H., Loeltz, G. J., and Irelan, B., 1973 [1974], *Geohydrology of the Yuma area, Arizona and California*: U. S. Geological Survey Professional Paper 486-H, 227 p.

S.B. KEITH AND J.C. WILT

- Oppenheimer, J. S., and Sumner, J. S., 1981, Gravity modeling of the basins in the Basin and Range province, Arizona, in Stone, C., and Jenney, J. P., eds.: Arizona Geological Society Digest, v. 13, p. 111-115.
- Osburn, G. R., and Chapin, C. E., 1983, Ash flow tuffs in caldrons in northeastern Mogollon-Datil volcanic field, a summary, in Chapin, C. E., and Callender, J. F., eds., Socorro Region II: New Mexico Geological Society Guidebook, 34th Field Conference, p. 197-204.
- Otton, J. K., 1981, Late Mesozoic underthrusting of continental crust southwest of the Colorado Plateau (Abs.): Geological Society of America, Abstracts with Programs, Hermosillo, Mexico, p. 100.
- Otton, J. K., 1982, Tertiary extensional tectonics and associated volcanism in west-central Arizona, in Frost, E. G., and Martin, D. L., eds., Mesozoic-Cenozoic Tectonic Evolution of the Colorado River Region, California, Arizona, and Nevada: Cordilleran Publishers, San Diego, Calif., p. 143-157.
- Pashley, E. F., 1966, Structure and stratigraphy of the central, northern, and eastern parts of the Tucson Basin, Arizona: unpublished Ph.D. Thesis, University of Arizona, Tucson, 273 p.
- Peirce, H. W., 1976, Tectonic significance of Basin and Range thick evaporite deposits, in Wilt, J. C., and Jenney, J. P., Tectonic Digest: Arizona Geological Society Digest, v. 10, p. 325-339.
- Peirce, H. W., 1984, Some late Cenozoic basins and basin deposits of southern and western Arizona, in Smiley, T. L., Nations, J. D., Pewe, T. L., and Schafer, J. P., eds., Landscapes of Arizona: the Geological Story: University Press of America, New York, 505 p., p. 207-228.
- Peirce, H. W., Damon, P. E., and Shafiqullah, M., 1979, An Oligocene(?) Colorado Plateau edge in Arizona: Tectonophysics, v. 61, p. 1-24.
- Pridmore, C. L., and Craig, C., 1982, Upper-plate structure and sedimentation of the Baker Peaks area, Yuma County, Arizona, in Frost, E. G., and Martin, D. L., eds., Mesozoic-Cenozoic Tectonic Evolution of the Colorado River Region, California, Arizona, and Nevada: Cordilleran Publishers, San Diego, California, p. 356-376.
- Ransome, F. L., 1923, Geology of the Datman gold district, Arizona: U.S. Geological Survey Bulletin 743, 58 p.
- Ratte, J. C., Landis, E. R., Gaskill, D. L., and Raabe, R. G., 1969, Mineral resources of the Blue Range Primitive area, Greenlee County, Arizona, and Catron County, New Mexico: U.S. Geological Survey Bulletin 1261-E, 91 p.
- Rehrig, W. A., 1982, Metamorphic core complexes of the southwestern United States; an updated analysis, in Frost, E. G., and Martin, D. L., eds., Mesozoic-Cenozoic Tectonic Evolution of the Colorado River Region, California, Arizona, and Nevada: Cordilleran Publishers, San Diego, California, p. 551-559.
- Rehrig, W. A., and Heidrick, T. L., 1976, Regional tectonic stress during the Laramide and Late Tertiary intrusive periods, Basin and Range Province, Arizona, in Wilt, J. C., and Jenney, J. P., eds., Tectonic Digest: Arizona Geological Society Digest, v. 10, p. 205-228.
- Rehrig, W. A., and Reynolds, S. J., 1980, Geologic and geochronologic reconnaissance of a northwest-trending zone of metamorphic core complexes in southern and western Arizona: Geological Society of America, Memoir 153, p. 131-157.
- Rehrig, W. A., Shafiqullah, M., and Damon, P. E., 1980, Geochronology, geology, and listric normal faulting of the Vulture Mountains, Maricopa County, Arizona, in Jenney, J. P., and Stone, C., eds., Studies in Western Arizona: Arizona Geological Society Digest, v. 12, p. 89-110.
- Reif, D. M., and Robinson, J. P., 1981, Geophysical, geochemical, and petrographic data and regional correlation from the Arizona State A-1 well, Pinal County, Arizona, in Stone, C., and Jenney, J. P., eds.: Arizona Geological Society Digest, v. 13, p. 99-109.
- Reynolds, S. J., 1982, Geology and geochronology of the South Mountains, central Arizona: unpublished Ph.D. Thesis, University of Arizona, Tucson, 240
- Reynolds, S. J., Keith, S. B., and Coney, P. J., 1980, Stacked overthrusts of Precambrian crystalline basement and inverted Paleozoic sections emplaced over Mesozoic strata, west-central Arizona, in Jenney, J. P., and Stone, C., eds., Studies in Western Arizona: Arizona Geological Society Digest, v. 12, p. 45-52.
- Reynolds, S. J., and Rehrig, W. A., 1980, Mid-Tertiary plutonism and mylonitization, South Mountains, central Arizona, in Crittenden, M. D., Jr., Coney, P. J., and Davis, G. H., eds., Cordilleran Metamorphic Core Complexes: Geol. Soc. America Memoir 153, p. 159-175.
- Sabins, F. F., Jr., 1957, Geology of the Cochise Head and western part of the Vanar quadrangle, Arizona: Geological Society of America Bulletin, v. 68, no. 10, p. 1315-1342.
- Scarborough, R., 1981, Reconnaissance geology, Goldfield and northern Superstition Mountains: Fieldnotes, Ariz. Bur. Geology and Mineral Technology, v. 11, no. 4, p. 6-10.
- Scarborough, R., Menges, C., and Pearthree, C., 1983, Map of Basin and Range (post 15 m.y.a.) exposed faults, grabens, and basalt-dominated volcanism in Arizona: Ariz. Bureau of Geology and Mineral Technology, open-file report 83-21, scale 1:500,000.
- Scarborough, R. B., and Peirce, H. W., 1978, Late Cenozoic basins of Arizona, in Callender, J. F., Wilt, J. C., and Clemons, R., eds., Land of Cochise, Southeastern Arizona: New Mexico Geological Society, 29th Field Conference, p. 253-260.
- Scarborough, R., and Wilt, J. C., 1979, A study of uranium favorability of Cenozoic sedimentary rocks, Basin and Range Province, Arizona: U. S. Geological Survey, Open-file Report 79-1429, 101p.
- Schmidt, E. A., 1971, A structural investigation of the northern Tortilla Mountains, Pinal County, Arizona: unpublished Ph.D. Thesis, University of Arizona, Tucson, 248 p.
- Shackelford, T. J., 1980, Tertiary tectonic

OROGENESIS, ARIZONA AND ADJACENT REGIONS

- denudation of a Mesozoic-early Tertiary(?) gneiss complex, Rawhide Mountains, western Arizona: *Geology*, v. 8, p. 190-194.
- Shafiqullah, M., Lynch, D. J., Damon, P. E., and Peirce, H. W., 1976, Geology, geochronology and geochemistry of the Picacho Peak area, Pinal County, Arizona, in Wilt, J. C., and Jenney, J. P., eds., *Tectonic Digest: Arizona Geological Society Digest*, v. 10, p. 305-324.
- Shafiqullah, M., Damon, P. E., Lynch, D. J., and Kuck, P. H., 1978, Mid-Tertiary magmatism in southeastern Arizona, in Callendar, J. F., Wilt, J. C., and Clemons, R. E., eds., *Land of Cochise, Southeastern Arizona: New Mexico Geological Society, 29th Field Conf.*, p. 231-241.
- Shafiqullah, M., Damon, P. E., Lynch, D. J., Reynolds, S. J., Rehrig, W. A., and Raymond, R. H., 1980, K-Ar geochronology and geologic history of southwestern Arizona and adjacent areas, in Jenney, J. P. and Stone, C., eds., *Studies in Western Arizona: Arizona Geological Society Digest*, v. 12, p. 201-260.
- Silver, L. T., Sams, D. B., Bursik, M. I., Graymer, R. W., Nourse, J. A., Richards, M. A., and Salyards, S. L., 1984, Some observations on the tectonic history of the Rand Mountains, Mohave Desert, California (Abs.): *Geological Society of America, Abstracts with Programs*, v. 16, no. 5, p. 333.
- Simons, F. S., 1964, Geology of the Klondyke quadrangle, Graham and Pinal counties, Arizona: U. S. Geological Survey Professional Paper 461, 173 p.
- Simpson, Carol, 1984, Borrego Springs-Santa Rosa mylonite zone; a late Cretaceous, west-directed thrust in southern California: *Geology*, v. 12, p. 8-11.
- Snyder, W. S., Dickinson, W. R., and Silberman, M. L., 1976, Tectonic implications of space-time patterns of Cenozoic magmatism in the western United States: *Earth and Planetary Science Letters*, v. 32, p. 91-108.
- Spencer, J. E., 1982, Origin of folds of Tertiary low-angle fault surfaces, southeastern California and western Arizona, in Frost, E. G., and Martin, D. L., eds., *Mesozoic-Cenozoic Tectonic Evolution of the Colorado River Region, California, Arizona, and Nevada: Cordilleran Publishers, San Diego, California*, p. 123-134.
- Spencer, J. E., and Turner, R. D., 1982, Dike swarms and low-angle faults, Homer Mountain and the northwestern Sacramento Mountains, southeastern California, in Frost, E. G., and Martin, D. L., eds., *Mesozoic-Cenozoic Tectonic Evolution of the Colorado River Region, California, Arizona, and Nevada: Cordilleran Publishers, San Diego, California*, p. 97-108.
- Spittler, T. E., and Arthur, M. A., 1982, The lower Miocene Diligencia Formation of the Orocofia Mts., Southern California: stratigraphy, petrology, sedimentology and structure, in Ingersoll, R. V., and Woodburne, M. O., eds., *Cenozoic Nonmarine Deposits of California and Arizona: Society of Economic Paleontologists and Mineralogists*, p. 83-99.
- Stewart, J. H., 1980, Regional tilt patterns of late Cenozoic basin-range fault blocks, western United States: *Geological Society of America Bulletin*, pt. 1, v. 91, no. 8, p. 460-464.
- Stuckless, J. S., and Sheridan, M. F., 1971, Tertiary volcanic stratigraphy in the Goldfield and Sup[er]stition Mountains, Arizona: *Geological Society of America Bulletin*, v. 82, p. 3235-3240.
- Teel, D. B., and Frost, E. G., 1982, Synorogenic evolution of the Copper Basin Formation in the eastern Whipple Mountains, San Bernardino County, California, in Frost, E. G., and Martin, D. L., eds., *Mesozoic-Cenozoic Tectonic Evolution of the Colorado River Region, California, Arizona, and Nevada: Cordilleran Publishers, San Diego, California*, p. 275-285.
- Theodore, T. G., Blair, W. L., Nash, J. T., 1982, Preliminary report on the geology and gold mineralization of the Gold Basin - Lost Basin mining districts, Mohave County, Arizona: U. S. Geological Survey Open-file Report 82-1052, 352 p.
- Theodore, T. G., Keith, W. J., Till, A. B., Petersen, J. A., and Creasey, S. C., 1978, Preliminary geologic map of the Mineral Mountain quadrangle, Arizona: U.S. Geological Survey Open-file Report 78-468, scale 1:24,000.
- Thorman, C. H., 1980, Geology of the Pinaleno Mountains, Arizona: a preliminary report, in Stone, C., and Jenney, J. P., eds.: *Arizona Geological Society Digest*, v. 13, p. 5-12.
- Thorson, J. P., 1971, Igneous petrology of the Oatman district, Mohave County, Arizona: unpublished Ph.D. Thesis, University of California at Santa Barbara, Santa Barbara, California, 189 p.
- Vice, K. H., 1974, The geology and petrography of the Babocomari Ranch area, Santa Cruz-Cochise counties: unpublished M. S. thesis, Arizona State University, Tempe, 152 p.
- Weibel, W. L., 1981, Depositional history and geology of the Cloudburst Formation near Mammoth, Arizona: unpublished M. S. Thesis, University of Arizona, Tucson, 81 p.
- Wilson, E. D., 1962, A resume of the geology of Arizona: *Arizona Bureau of Mines Bulletin* 171, p. 71-86.
- Wilt, J. C., and Scarborough, R. B., 1981, Cenozoic sediments, volcanics, and related uranium in the Basin and Range Province of Arizona, in Goodell, P. C., and Waters, A. C., eds., *Uranium in Volcanic and Volcaniclastic Rocks: American Association of Petroleum Geologists, Studies in Geology No. 13*, p. 123-143.
- Wright, J. E., and Haxel, Gordon, 1982, A garnet-two-mica granite, Coyote Mountains, southern Arizona: Geologic setting, uranium-lead isotopic systematics of zircons, and nature of the granite source region: *Geological Society of America Bulletin*, v. 93, p. 1176-1188.
- Young, R. A., 1982, Paleogeomorphic evidence for the structural evolution of the Basin and Range-Colorado Plateau boundary in western Arizona, in Frost, E. G., and Martin, D. L., eds., *Mesozoic-Cenozoic Tectonic Evolution of the Colorado River Region, California, Arizona, and Nevada: Cordilleran Publishers, San Diego, California*, p. 29-40.

CENOZOIC PALEOGEOGRAPHY OF WEST-CENTRAL UNITED STATES

Maps and Cross-Sections
of
Areas to be Visited
on
Arizona Geological Society Field Trip
Fall 1985

